NATIONAL COOPERATIVE
HIGHWAY RESEARCH PROGRAM REPORT **315**

POTENTIAL BENEFITS OF GEOSYNTHETICS IN FLEXIBLE PAVEMENT SYSTEMS

TRANSPORTATION RESEARCH BOARD
NATIONAL RESEARCH COUNCIL

POTENTIAL BENEFITS OF GEOSYNTHETICS IN FLEXIBLE PAVEMENT SYSTEMS

RICHARD D. BARKSDALE
Georgia Institute of Technology
Atlanta, Georgia
STEPHEN F. BROWN and FRANCIS CHAN
University of Nottingham
Nottingham, England

AREAS OF INTEREST

    Pavement Design and Performance
    Construction
    General Materials
    (Highway Transportation)

NATIONAL COOPERATIVE HIGHWAY RESEARCH PROGRAM

Systematic, well-designed research provides the most effective approach to the solution of many problems facing highway administrators and engineers. Often, highway problems are of local interest and can best be studied by highway departments individually or in cooperation with their state universities and others. However, the accelerating growth of highway transportation develops increasingly complex problems of wide interest to highway authorities. These problems are best studied through a coordinated program of cooperative research.

In recognition of these needs, the highway administrators of the American Association of State Highway and Transportation Officials initiated in 1962 an objective national highway research program employing modern scientific techniques. This program is supported on a continuing basis by funds from participating member states of the Association and it receives the full cooperation and support of the Federal Highway Administration, United States Department of Transportation.

The Transportation Research Board of the National Research Council was requested by the Association to administer the research program because of the Board's recognized objectivity and understanding of modern research practices. The Board is uniquely suited for this purpose as: it maintains an extensive committee structure from which authorities on any highway transportation subject may be drawn; it possesses avenues of communications and cooperation with federal, state, and local governmental agencies, universities, and industry; its relationship to the National Research Council is an insurance of objectivity; it maintains a full-time research correlation staff of specialists in highway transportation matters to bring the findings of research directly to those who are in a position to use them.

The program is developed on the basis of research needs identified by chief administrators of the highway and transportation departments and by committees of AASHTO. Each year, specific areas of research needs to be included in the program are proposed to the National Research Council and the Board by the American Association of State Highway and Transportation Officials. Research projects to fulfill these needs are defined by the Board, and qualified research agencies are selected from those that have submitted proposals. Administration and surveillance of research contracts are the responsibilities of the National Research Council and the Transportation Research Board.

The needs for highway research are many, and the National Cooperative Highway Research Program can make significant contributions to the solution of highway transportation problems of mutual concern to many responsible groups. The program, however, is intended to complement rather than to substitute for or duplicate other highway research programs.

Published reports of the

NATIONAL COOPERATIVE HIGHWAY RESEARCH PROGRAM

are available from:

Transportation Research Board
National Research Council
2101 Constitution Avenue, N.W.
Washington, D.C. 20418

FOREWORD

By Staff
Transportation
Research Board

Based on findings from laboratory tests and computer modeling, this report documents the results of a feasibility study to determine the benefits of placing geosynthetics into the unbound aggregate layer of flexible pavement structures. The potential benefits under investigation included either increased performance or reduced costs for equal performance. The report also contains recommendations on full scale field studies for those interested in pursuing this research area and the potential of geosynthetics. Materials technologists, geotechnical engineers, construction engineers, pavement designers, and researchers will find the report to be an important contribution to the use of geosynthetics.

Previous test results had indicated that by developing tension in geosynthetics (used here to describe geotextiles and geogrids), the structural capacity and performance of aggregate-surfaced roads placed over very weak subgrades were improved. Geosynthetics were tensioned by either prestretching the geosynthetic or by loading and developing ruts in the geosynthetic-aggregate system before placing additional (leveling) aggregate base.

The applicability of geosynthetics to higher type pavement systems incorporating unbound aggregate layer(s) with an asphalt surface (flexible pavement systems) needed to be studied to determine whether the structural capacity and performance potential could be improved as was the case with aggregate-surfaced roads. Although geosynthetics had already been used to some extent in the unbound aggregate layers of higher type pavements, their behavior and influence on pavement performance were not well understood. Consequently, a number of questions needed to be answered before the feasibility and the potential for widespread use of geosynthetics in flexible pavement systems could be determined.

The Georgia Institute of Technology, Atlanta, Georgia, in cooperation with the University of Nottingham, Nottingham, England, undertook NCHRP Project 10-33 to determine the feasibility of placing geosynthetics on the subgrade or in the unbound aggregate layers to improve the performance of flexible pavement systems or to provide alternative designs for equal performance. Evaluations were based on laboratory experimentation and computer modeling. These evaluations have provided data on the behavior of geosynthetics and their effect on pavement performance. Although the data may not generally support the use of geosynthetics under present economic conditions, applications to certain site-specific situations may be appropriate. Consequently, field study designs were also developed for those interested in conducting additional studies and more fully exploring the potential use of geosynthetics in the aggregate layers of flexible pavement systems.

Readers should note that appendixes not published herein are contained in a separate agency report titled, "Potential Benefits of Geosynthetics in Flexible Pavements, Supplement to NCHRP Report 315." Copies of the agency-prepared supplemental report have been sent to all NCHRP sponsors, namely the state highway agencies. Others wishing to obtain the additional details found in the supplemental report (available for $7.00) should contact the Publications Office, Transportation Research Board, 2101 Constitution Avenue, N.W., Washington, D.C. 20418.

CONTENTS

POTENTIAL BENEFITS OF GEOSYNTHETICS IN FLEXIBLE PAVEMENTS

SUMMARY   This study was concerned primarily with the geosynthetic reinforcement of an aggregate base of a surfaced, flexible pavement. Specific methods of improvement evaluated included (1) geotextile and geogrid reinforcement placed within the base, (2) pretensioning a geosynthetic placed within the base, and (3) prerutting the aggregate base either with or without geosynthetic reinforcement. The term geosynthetic as used in this study refers to either geotextiles or geogrids manufactured from polymers.

Reinforcement

Both large-scale laboratory pavement tests and an analytical sensitivity study were conducted. The analytical sensitivity study considered a wide range of pavement structures, subgrade strengths, and geosynthetic stiffnesses. The large-scale pavement tests consisted of a 1.0-in. to 1.5-in. (25 to 38 mm) thick asphalt surfacing placed over a 6-in. or 8-in. (150 or 200 mm) thick aggregate base. The silty clay subgrade used had a CBR of about 2.5 percent. A 1,500-lb (6.7 kN) moving wheel load was employed in the laboratory experiments.

Analytical Modeling. Extensive measurements of pavement response from this study, and also from previous work, were employed to select the most appropriate analytical model for use in the sensitivity study. The accurate prediction of tensile strain in the bottom of the base was found to be of utmost importance in geosynthetic applications. Larger strains cause greater forces in the geosynthetic and more effective reinforcement performance. A linear elastic finite element model having a cross-anisotropic aggregate base was found to give a slightly better prediction of tensile strain and other response variables than a nonlinear finite element model having an isotropic base. The resilient modulus of the subgrade was found to rapidly increase with depth. The low resilient modulus existing at the top of the subgrade causes a relatively large tensile strain in the bottom of the aggregate base and, hence, much larger forces in the geosynthetic than does a subgrade whose resilient modulus is constant with depth.

The model assumed a membrane reinforcement with appropriate friction factors on the top and bottom and, thus, it models a membrane such as a woven geotextile. Geogrids, however, were found to perform differently from a woven geotextile. More analytical and experimental research is required to define the mechanisms of improvement associated with geogrids and develop suitable models.

Mechanisms of Reinforcement. The effects of geosynthetic reinforcement on stress, strain, and deflection are all relatively small for pavements designed to carry more than about 200,000 equivalent 18-kip (80 kN) single axle loads. As a result, geosynthetic reinforcement of an aggregate base, in general, will have relatively little effect on overall pavement stiffness. A modest improvement in fatigue life can be gained from geosynthetic reinforcement. The greatest beneficial effect of reinforcement appears to be due to small changes in radial stress and strain together with slight

reductions of vertical stress in the aggregate base and on top of the subgrade. Reinforcement of a thin pavement (SN $\leq$ 2.5 to 3) on a weak subgrade (CBR $\leq$ 3 percent) can potentially reduce the permanent deformations in the subgrade or the aggregate base by significant amounts. As the strength of the pavement section increases and the materials become stronger, the state of stress in the aggregate base and the subgrade moves away from failure. As a result, the improvement caused by reinforcement rapidly becomes small. Reductions in rutting due to reinforcement occur in only about the upper 12 in. (300 mm) of the subgrade. Forces developed in the geosynthetic are relatively small, typically being less than about 30 lb/in. (5 kN/m).

Type and Stiffness of Geosynthetic. The experimental results indicate that a geogrid having an open mesh has the reinforcing capability of a woven geotextile having a stiffness approximately 2.5 times as great as the geogrid. Hence, geogrid performance is different from that of woven geotextiles. Therefore, in determining the beneficial effects of geogrids, a reinforcement stiffness 2.5 times the actual one should be used in the figures and tables. From the experimental and analytical findings, the minimum stiffness to be used for aggregate base reinforcement applications should be about 1,500 lb/in. (260 kN/m) for geogrids and 4,000 lb/in. (700 kN/m) for woven geotextiles. Geosynthetic stiffness S_g is defined as the force in the geosynthetic per unit length at 5 percent strain divided by the corresponding strain.

Reinforcement Improvement. Light to moderate strength sections placed on weak subgrades having a CBR $\leq$ 3 percent (E_s = 3,500 psi; 24 MN/m^2) are most likely to be improved by geosynthetic reinforcement. The structural section, in general, should have AASHTO structural numbers (SN) no greater than about 2.5 to 3 if reduction in subgrade rutting is to be achieved by geosynthetic reinforcement. As the structural number and subgrade strength decrease below these values, the improvement in performance due to reinforcement should rapidly become greater. Strong pavement sections placed over good subgrades would not be expected to show any significant level of improvement due to geosynthetic reinforcement of the type studied. Also, sections with asphalt thicknesses much greater than about 2.5 in. to 3.5 in. (64 to 90 mm) would be expected to exhibit relatively little improvement even if placed on relatively weak subgrades. Some stronger sections having low quality bases or weak subgrades may be improved by reinforcement, but this needs to be established by field trials.

Improvement Levels. Light sections on weak subgrades reinforced with geosynthetics having woven geotextile stiffnesses of about 4,000 to 6,000 lb/in. (700 to 1,000 kN/m) can give reductions in base thickness on the order of 10 to 20 percent based on equal strain criteria in the subgrade and bottom of the asphalt surfacing. For light sections, this corresponds to actual reductions in base thickness of about 1 in. to 2 in. (25 to 50 mm). For weak subgrades or low quality bases, total rutting in the base and subgrade of light sections may, under ideal conditions, be reduced on the order of 20 to 40 percent. Considerably more reduction in rutting occurs for the thinner sections on weak subgrades than for heavier sections on strong subgrades.

Low Quality Base. Geosynthetic reinforcement of a low quality aggregate base can, under the proper conditions, reduce rutting. The asphalt surface should be less than about 2.5 in. to 3.5 in. (64 to 90 mm) in thickness for the reinforcement to be most effective. Field trials are required to establish the benefits of reinforcing heavier sections having low quality bases.

Geosynthetic Position. For light pavement sections constructed with low quality aggregate bases, the reinforcement should be in the middle of the base to minimize rutting, particularly if a good subgrade is present. For pavements constructed on soft subgrades, the reinforcement should be placed at or near the bottom of the base. This

would be particularly true if the subgrade is known to have rutting problems, and the base is of high quality and is well compacted.

Prerutting and Prestressing

The experimental results indicate that both prerutting and prestressing the geosynthetic significantly reduces permanent deformations within the base and subgrade. Stress relaxation over a long period of time, however, may considerably reduce the effectiveness of prestressing the geosynthetic. The laboratory experiments indicate that prerutting without reinforcement gives performance equal to that of prestressing, and notably better performance compared to the use of stiff to very stiff, nonprestressed reinforcement. The cost of prerutting an aggregate base at one level would be on the order of 50 to 100 percent of the in-place cost of a stiff geogrid ($S_g = 1,700$ lb/in.; 300 kN/m). The total expense associated with prestressing an aggregate base would be on the order of 5 or more times that of the base at one level when a geosynthetic reinforcement is not used. Full-scale field experiments should be conducted to more fully validate the concept of prerutting and develop appropriate prerutting techniques.

Separation and Filtration

Separation problems involve the mixing of an aggregate base/subbase with an underlying weak subgrade. They usually occur during construction of the first lift of the granular layer. Large, angular open-graded aggregates placed directly on a soft or very soft subgrade are most critical with respect to separation. Either a properly designed sand or geotextile filter can be used to maintain a reasonably clean interface. Both woven and nonwoven geotextiles have been found to adequately perform the separation function.

When an open-graded drainage layer is placed above the subgrade, the amount of contamination due to fines being washed into this layer must be minimized by use of a filter. A very severe environment with respect to subgrade erosion exists beneath a pavement which includes reversible, possibly turbulent, flow conditions. The severity of erosion is dependent on the structural thickness of the pavement, which determines the stress applied to the subgrade and also the number of load applications. Sand filters used for filtration, when properly designed, may perform better than geotextile filters, although satisfactorily performing geotextiles can usually be selected. Thick nonwoven geotextiles perform better than thin nonwovens or wovens, partly because of their three-dimensional effect.

Durability

Strength loss with time is highly variable and depends on many factors including material type, manufacturing details, stress level, and the local environment in which it is placed. Under favorable conditions the loss of strength of geosynthetics on the average is about 30 percent in the first 10 years; because of their greater thickness, geogrids may exhibit a lower strength loss. For separation, filtration, and pavement reinforcement applications, geosynthetics—if selected to fit the environmental conditions—should generally have at least a 20-year life. For reinforcement applications, geosynthetic stiffness is the most important structural consideration. Some geosynthetics become more brittle with time and actually increase in stiffness. Whether better reinforcement performance will result has not been demonstrated.

Additional Research

Geogrid reinforcement and prerutting the base of nonreinforced sections appear to be the most promising methods studied for the reinforcement of aggregate bases. Mechanistically, geogrids perform differently from the analytical model used in this study to develop most of the results. Therefore, the recommendation is made that full-scale field tests be conducted to further explore the benefits of these techniques. A proposed preliminary guide for conducting field tests is given in Appendix H. Additional research is needed to better define the durability of geosynthetics under varying stress and environmental conditions.

CHAPTER ONE

INTRODUCTION AND RESEARCH APPROACH

BACKGROUND

The geotextile industry in the United States at present distributes more than 1,000 million sq yd (0.85×10^9 m^2) of geotextiles annually. Growth rates in geotextile sales during the 1980s have averaged about 20 percent each year. Both nonwoven and woven geotextile fabrics are made from polypropylene, polyester, nylon, and polyethylene. These fabrics have widely varying material properties including stiffness, strength, and creep characteristics [1]. (Note: the numbers given in brackets throughout this report refer to the references presented in Appendix A.) More recently, polyethylene and polypropylene geogrids have been introduced in Canada and in the United States [2]. Geogrids are manufactured by a special process, and have an open mesh with typical rib spacings of about 1.5 in. to 4.5 in. (38 to 114 mm). The introduction of geogrids that are stiffer than the commonly used geotextiles has led to the use of the term "geosynthetic" which may include geotextiles, geogrids, geocomposites, geonets, and geomembranes. As used in this report, however, geosynthetics refer to geotextiles and geogrids.

Because of their great variation in type, composition, and resulting material properties, geotextiles have a very wide application in civil engineering, in general, and transportation engineering, in particular. Early civil engineering applications of geosynthetics were primarily for drainage, erosion control and haul road or railroad construction [3, 4]. With time many new uses for geosynthetics have developed including the reinforcement of earth structures such as retaining walls, slopes, and embankments [2, 5, 6].

The application of geosynthetics for reinforcement of many types of earth structures has gained reasonably good acceptance in recent years. Mitchell et al. [6] have recently presented an excellent state-of-the-art summary of the reinforcement of soil structures including the use of geosynthetics.

A number of studies have also been performed to evaluate the use of geosynthetics for overlays [7, 8, 9, 10, 11, 12]. Several investigations have also been conducted to determine the effect of placing a geogrid within the asphalt layer to prolong fatigue life and reduce rutting [12, 13]. The results of these studies appear to be encouraging, particularly with respect to the use of stiff geogrids as reinforcement in the asphalt surfacing.

Considerable interest presently exists among both highway engineers and manufacturers for using geosynthetics as reinforcement for flexible pavements. At the present time, however, relatively little factual information has been developed concerning the use of geosynthetics as reinforcement in the aggregate base. An important need exists for establishing the potential benefits that might be derived from the reinforcement of the aggregate base and the conditions necessary for geosynthetic reinforcement to be effective.

OBJECTIVES OF RESEARCH

One potential application of geosynthetics is the improvement in performance of flexible pavements by the placement of a geosynthetic either within or at the bottom of an unstabilized aggregate base. The overall objective of this research project was to evaluate, from both a theoretical and practical viewpoint, the potential structural and economic advantages of geosynthetic reinforcement within a granular base of a surfaced, flexible pavement structure. The specific objectives of the research were as follows:

1. Perform an analytical sensitivity study of the influence due to reinforcement of pertinent variables on pavement performance.

2. Verify, using laboratory tests, the most promising combination of variables.

3. Develop practical guidelines for the design of flexible pavements having granular bases reinforced with geosynthetics including economics, installation, and long-term durability aspects.

4. Develop a preliminary experimental plan including layout and instrumentation for conducting a full-scale field experiment to verify and extend to practice the most promising findings of this study.

RESEARCH APPROACH

To approach this problem in a systematic manner, consideration had to be given to a large number of factors potentially

affecting the overall long-term behavior of a geosynthetic rein-
forced, flexible pavement structure. Of these factors, the more
important ones were geosynthetic type, stiffness, and strength;
geosynthetic location within the aggregate base and overall
strength of the pavement structure; and finally, separation, fil-
tration, and durability aspects of the geosynthetic. Techniques
to potentially improve geosynthetic performance within a pave-
ment included (1) prestressing the geosynthetic, and (2) pre-
rutting the geosynthetic. The potential effects on performance
of geosynthetic slack, which might develop during construction,
and of slip between the geosynthetic and surrounding materials,
were also included in the study.

The import of all of the foregoing factors on pavement per-
formance leads to the conclusion that geosynthetic reinforce-
ment of a pavement is not a simple problem. Furthermore, it
is worth noting that the influence of the geosynthetic reinforce-
ment is relatively small in terms of its effect on the stresses and
strains within the pavement. Therefore, caution must be exer-
cised in a study of this type in distinguishing between conditions
that will and will not result in improved performance due to
reinforcement.

Figure 1 summarizes the general research approach. The most
important variables affecting geosynthetic performance were
first identified, including both design and construction-related
factors. An analytical sensitivity study was then conducted,
followed by large-scale laboratory tests. Emphasis in the inves-
tigation was placed on identifying the mechanisms associated
with reinforcement and their effects on the levels of improve-
ment.

The analytical sensitivity studies permitted careful investi-
gation of the influence on performance and design of all the
variables identified. The analytical studies were essential for
extending the findings to include practical pavement design
considerations.

The large-scale laboratory tests made possible verification of
the general concept and mechanisms of reinforcement. They
also permitted investigation, in an actual pavement, of such
factors as prerutting and prestressing of the geosynthetic, which
are difficult to model theoretically, and hence require verifica-
tion.

A nonlinear, isotropic finite element pavement idealization
was selected for use in the sensitivity study. This analytical
model permitted the inclusion of a geosynthetic reinforcing
membrane at any desired location within the aggregate layer.
As the analytical study progressed, feedback from the laboratory
test track study and previous investigations showed that ad-
justments in the analytical model were required to yield better
agreement with observed response. This important feedback loop
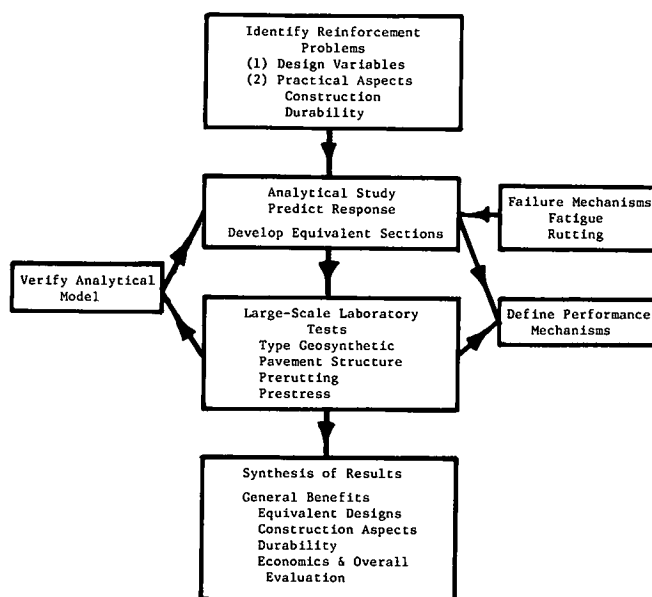
Figure 1. General approach used in evaluating geosynthetic re-
inforcement of aggregate bases for flexible pavements.

thus improved the accuracy and reliability of the analysis. As
a result, a linear elastic, cross-anisotropic model was used for
most of the sensitivity study which agreed reasonably well with
the observed experimental test section response. The lateral
tensile strain that developed in the bottom of the aggregate base
and the tensile strain in the geosynthetic were considered to be
two of the more important variables used to verify the cross-
anisotropic model.

The analytical model was used to develop equivalent pave-
ment structural designs for a range of conditions comparing
geosynthetic reinforced sections with similar nonreinforced sec-
tions. The equivalent designs were based on maintaining the
same strain in the bottom of the asphalt surfacing and at the
top of the subgrade. Permanent deformation in both the aggre-
gate base and the subgrade was also evaluated. The analytical
results were then carefully integrated together with the large-
scale laboratory test studies. Drawing on the findings of this
study and previous investigations, a detailed synthesis of the
results was assembled, which includes all important aspects of
reinforcement—the actual mechanism leading to improvement,
the role of geosynthetic stiffness, equivalent structural designs,
and practical considerations such as economics and construction
aspects.

CHAPTER TWO

FINDINGS—OVERVIEW

INTRODUCTION

The potential beneficial effects of applying a geosynthetic as
a reinforcement within a flexible pavement are investigated in

this chapter. The only position of the reinforcement considered
is within an unstabilized aggregate base. At present, the state
of the art in geosynthetic reinforcement of pavements is rapidly
expanding, perhaps, at least partially because of the emphasis
being placed in this area by the geosynthetics industry. Unfor-
tunately, relatively little factual information is available to assist
the designer with the proper use of geosynthetics for pavement
reinforcement applications.

The potential beneficial effects of aggregate base reinforce-
ments are investigated in this study using an analytical finite
element model and a large-scale laboratory test track study. The

analytical investigation permits a broad range of variables to be considered, including development of structural designs for reinforced pavement sections. The laboratory investigation was conducted to verify the general analytical approach and to also study selected aspects of reinforcement, using simulated field conditions including moving wheel loading.

The important general pavement variables considered in this investigation were as follows: (1) type and stiffness of the geosynthetic reinforcement; (2) location of the reinforcement within the aggregate base; (3) pavement thickness; (4) quality of subgrade and base materials as defined by their resilient moduli and permanent deformation characteristics; (5) slip at the interface between the geosynthetic and surrounding materials; (6) influence of slack left in the geosynthetic during field placement; (7) prerutting the geosynthetic as a simple means of removing slack and providing a prestretching effect; and (8) prestressing the geosynthetic.

Potential improvement in performance is evidenced by an overall reduction in permanent deformation and improvement in fatigue life of the asphalt surfacing. For the laboratory test track study, pavement performance was assessed primarily by permanent deformation, including the total amount of surface rutting and, also, the individual rutting in the base and subgrade. In the analytical studies, equivalent pavement designs were developed for geosynthetic reinforced structural sections and compared to similar sections without reinforcement. The equivalent sections were established by requiring equal tensile strain in the bottom of the asphalt layer for both sections; constant vertical subgrade strain criteria were also used to control subgrade rutting. Finally, an analytical procedure was used to evaluate the effects of geosynthetic reinforcement on permanent deformations.

The findings are introduced in the remainder of this chapter. A detailed synthesis, interpretation, and appraisal of the many results presented in this chapter is given in Chapter Three.

LITERATURE REVIEW—REINFORCEMENT OF ROADWAYS

Unsurfaced Roads

Geosynthetics are frequently used as a reinforcing element in unsurfaced haul roads. Tests involving the reinforcement of unsurfaced roads have almost always shown an improvement in performance. These tests have been conducted in test boxes at model scale [3, 13, 14], in large scale test pits [16, 18, 19,

20], and in full-scale field trials [21, 22, 23, 24, 25, 26, 42]. The economics of justifying the use of a geosynthetic must, however, be considered for each application [26]. Beneficial effects are greatest when construction is on soft cohesive soils, typically characterized by a CBR less than 2 percent. Although improved performance may still occur, it is usually not as great as when stronger and thicker subbases are involved [24].

Mechanisms of Behavior

Bender and Barenberg [3] studied the behavior of soil-aggregate and soil-fabric systems both analytically and in the laboratory. They identified the following four principal mechanisms of improvement when a geosynthetic is placed between a haul road fill and a soft subgrade: (1) confinement and reinforcement of the fill layer, (2) confinement of the subgrade, (3) separation of the subgrade and fill layer, and (4) prevention of contamination of the fill by fine particles. The reinforcement of the fill layer was attributed primarily to the high tensile modulus of the geotextile element. This finding, of course, would apply for either geotextile or geogrid reinforcement.

Bender and Barenberg [3] concluded, for relatively large movements, that a reinforcing element confines the subgrade by restraining the upheaval generally associated with a shear failure. Confinement, frequently referred to as the tension membrane effect, increases the bearing capacity of the soil as shown in Figures 2 and 3. The importance of developing large rut depths (and, hence, large fabric strain) was later confirmed by the work of Barenberg [27] and Sowers et al. [28]. The work of Bender and Barenberg [3] indicated that over ground of low bearing capacity having a CBR less than about 2 percent, the use of a geotextile could enable a 30 percent reduction in aggregate depth. Another 2-in. to 3-in. (50 to 70 mm) reduction in base thickness was also possible because aggregate loss did not occur during construction of coarse, uniform bases on very soft subgrades. Later work by Barenberg [27] and Lai and Robnett [29] emphasized the importance of the stiffness of the geotextile, with greater savings being achieved with the use of a stiffer reinforcement.

Structural Performance—Full-Scale Experimental Results

Relatively few full-scale field tests have been conducted to verify the specific mechanisms that account for the observed
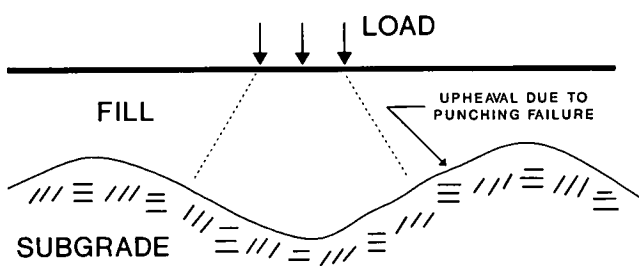
Figure 2. Effect of reinforcement on behavior of a subgrade-haul road section without reinforcement.
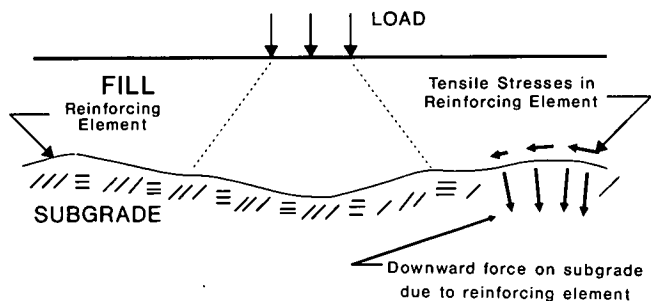
Figure 3. Effect of reinforcement on behavior of a subgrade-haul road section with reinforcement.

improvement in performance of geosynthetic reinforced haul roads. Ramalho-Ortigao and Palmeira [26] found, for a geotextile reinforced haul road constructed on a very soft subgrade, that approximately 10 to 24 percent less cohesive fill was required when reinforcement was used. Webster and Watkins [25] observed for a firm clay subgrade that one geotextile reinforcement increased the required repetitions to failure from 70 to 250 equivalent 18-kip (80 kN) axle loads; use of another geotextile increased failure to 10,000 repetitions. Ruddock et al. [21] found plastic strains in the subgrade to be reduced by the presence of a geotextile. Nevertheless, the conservative recommendation was made that no reduction in aggregate thickness should be allowed.

Surfaced Pavements

For surfaced pavements that undergo a small level of permanent deformation, the important reinforcing effects observed in unsurfaced haul roads are considerably less apparent. To be effective as a reinforcing element, the geosynthetic must undergo tensile strain due either to lateral stretching or to large permanent deformations. Theoretical studies by Thompson and Raad [32], Vokas and Stoll [33], and Barksdale and Brown [34] indicate that, for low deformation pavements, the resilient surface deflections and also transient stresses and strains within the pavement structure are only slightly reduced by the inclusion of a reinforcing element. Both a laboratory study by Barvashov et al. [35] and a theoretical study by Raad [36], however, have shown that prestressing the aggregate layer using a membrane greatly alters the stress state and potentially could result in improved pavement performance.

A full-scale field study by Ruddock et al. [21, 30] on a reasonably heavy pavement section with a moderately thick bituminous surfacing has shown reinforcement to have little measurable effect on resilient pavement response. Further, a large-scale laboratory study by Brown et al. [37] not only agreed with this finding, but even indicated that greater permanent deformations could occur as a result of geotextile inclusion. These results are supported by the work of Barker [38] and Forsyth et al. [39] whose findings indicate no measurable increase in pavement stiffness due to reinforcement.

In apparent conflict with these findings, several studies have shown that under the proper conditions, geosynthetic reinforcement can result in improved performance. Pappin [23] has reported a pavement reinforcing experiment carried out in New South Wales. A stiff geogrid was placed at the bottom of an aggregate base of a pavement surfaced with a 0.4-in. (10 mm) thick asphalt seal. The road experienced considerably reduced permanent surface deformation, but dynamic response was unchanged by the presence of the geogrid. A field investigation by Barker [38] and a laboratory study by Penner et al [40] have also shown that geogrid reinforcement can result in reduced permanent deformations. A recent study by van Grup and van Hulst [41] involved placing a steel mesh at the interface between the asphalt and the aggregate base. The primary effect on pavement response was an important reduction in tensile strain in the bottom of the asphalt and, hence, the potential for improvement in fatigue performance. Of significance is the fact that all of the studies which showed encouraging results involved the use of geogrids. This suggests, as will be verified later by the laboratory tests, that geogrids do perform differently from geotextiles.

The foregoing findings appear to be somewhat conflicting and clearly demonstrate that additional study is required to define the mechanisms and level of improvement associated with geosynthetic reinforced flexible pavements. A more detailed literature review of the experimental findings concerning geosynthetic reinforcement of pavements is given in Appendix B.

ANALYTICAL STUDY

The analytical study was performed using a comprehensive finite element program called GAPPS7. The GAPPS7 finite element program was developed previously to predict the response of surfaced or unsurfaced pavements reinforced with a geosynthetic [16, 43]. Both a nonlinear elastoplastic model and a linear, cross-anisotropic model were used to idealize selected pavement sections reinforced with a geosynthetic. The cross-anisotropic model was found, in general, to give better agreement with observed pavement response than the isotropic, nonlinear model. As a result, the cross-anisotropic formulation was selected after considerable study as the primary model.

The stiffness of a geosynthetic used for pavement reinforcement applications is an important, but often underrated or overlooked, aspect that has a considerable effect on the ability of reinforcement to improve performance. The stiffness of the geosynthetic, S_g, can be determined by stretching it and dividing the applied force per unit length by the corresponding induced strain. Most geosynthetics suitable for pavement reinforcement can, for practical purposes, be assumed to perform in a linear manner for the small strains in the geosynthetic that should develop within pavements designed for small levels of permanent deformation.

Analytical Sensitivity Study Results

Sensitivity Study Parameters

The results of the analytical sensitivity study are summarized in this section including predicted response for a range of geosynthetic stiffnesses, pavement geometries, and subgrade stiffnesses. The material properties and finite element model used in the theoretical analyses together with verification of the model are covered in Appendix C. The general effect on response of placing a geosynthetic within the aggregate layer is demonstrated, including its influence on vertical and lateral stresses, tensile strain in the bottom of the asphalt layer, and vertical strain on top of the subgrade. The effect of prestressing the geosynthetic is also considered for geosynthetic positions at the middle and bottom of the aggregate layer. The potential beneficial effects of geosynthetic reinforcement are also more clearly quantified in terms of the reduction in aggregate base thickness and the relative tendency to undergo rutting in both the base and the upper portion of the subgrade. Both linear, cross-anisotropic and nonlinear finite element sensitivity analyses were performed during the study.

Pavement Geometries. Pavement geometries and subgrade stiffnesses used in the primary sensitivity investigations are shown in Figure 4. The basic pavement condition investigated (Fig. 4(a)) consisted of light to moderate strength pavements resting on a subgrade having stiffnesses varying from 2,000 to

8
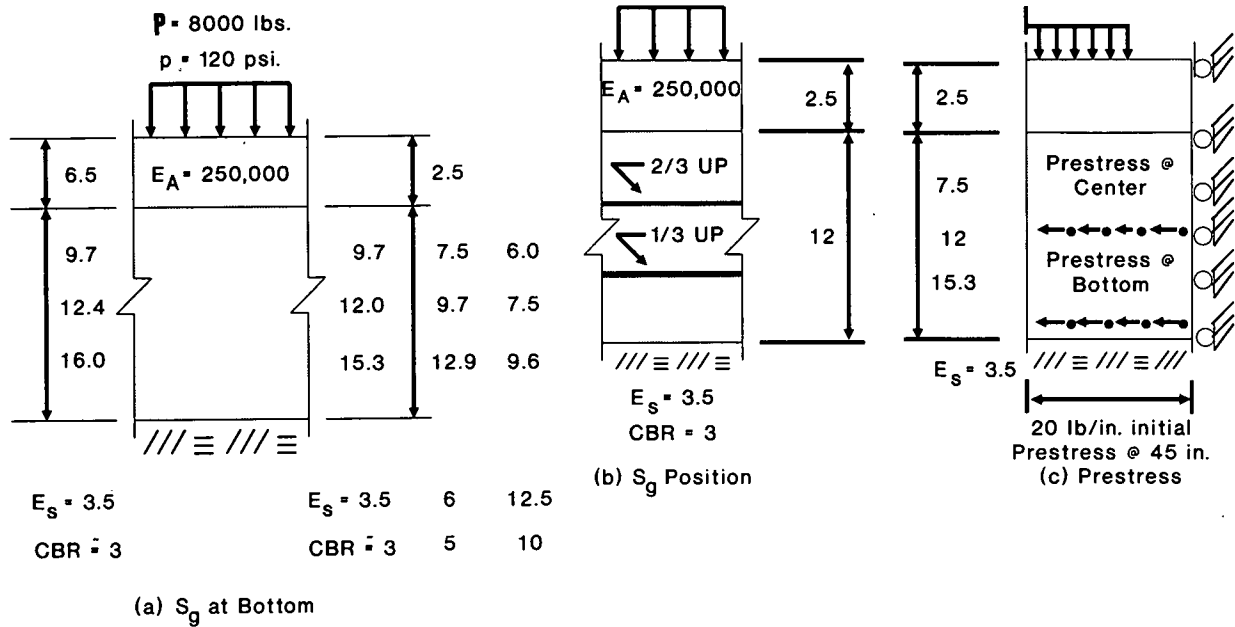
Figure 4. Pavement geometries, resilient moduli and thicknesses used in primary sensitivity studies. (Note: units of inches and kips used unless shown)

12,500 psi (14 to 86 MN/m^2); the geosynthetic was located in the bottom of the base. Sensitivity studies were also conducted to determine the effect of geosynthetic position (Fig. 4(b)) and the potential beneficial effect of prestressing the aggregate base and subgrade using a geosynthetic (Fig. 4(c)). Aggregate base quality was also investigated. Other supplementary sensitivity studies were performed to evaluate various effects including slip at the geosynthetic interfaces, slack in the geosynthetic, and the value of Poisson's ratio of the geosynthetic.

Geosynthetic Stiffness. Three levels of geosynthetic reinforcement stiffness S_g were used in the sensitivity study, $S_g = 1,000$, 4,000, and 6,000 lb/in. (170, 700, 1,050 kN/m). To reduce the number of computer runs to a manageable level, all three levels of geosynthetic stiffness were only included in selected studies. Because small values of stress and strain were found to develop in the geosynthetic, their response was taken to be linear. Poisson's ratio was assumed to be 0.30, except in a limited sensitivity study to investigate its effect on reinforcement behavior.

Equivalent AASHTO Design Sections. Preliminary analyses indicated that the geosynthetic reinforcement of heavy sections (or lighter sections on very good subgrades) would probably have relatively small beneficial effects. Therefore, structural pavement sections were selected for use in the study having light-to-moderate load-carrying capacity. Table 1 shows selected pavement thickness designs for 200,000, 500,000, and 2,000,000 equivalent 18 kip (80 kN) single axle loadings (ESALs). Also given in the table are subgrade support values and other constants used in the 1972 AASHTO design method. The equivalent axle loads which these sections can withstand serve as a convenient reference for assessing the strength of the sections used in the sensitivity study.

Subgrades having CBR values of 3, 5, and 10 were selected for use. A CBR value of 10 was considered to be a realistic upperbound on the strength of subgrade that might possibly be suitable for geosynthetic reinforcement. Average subgrade re-

silient moduli of 3.5, 6, and 12.5 ksi (24, 41, 86 kN/m^2) were selected from Figure 5 for use in the cross-anisotropic sensitivity studies to characterize subgrades having CBR values of 3, 5, and 10, respectively.

An important objective of the sensitivity study was to establish pavement sections reinforced with a geosynthetic that structurally have the same strength as similar nonreinforced sections. The beneficial effect was accounted for by establishing the reduction in base thickness due to reinforcement. Equivalent pavement sections with and without reinforcement are hence identical except for the thickness of the aggregate base.

Almost all mechanistic design procedures currently used are based on (1) limiting the tensile strain in the bottom of the asphaltic concrete surfacing as a means of controlling fatigue and (2) limiting the vertical compressive strain at the top of the subgrade to control subgrade rutting [44, 45]. In keeping with these accepted design concepts, the procedure followed in this study was to determine the required aggregate base thickness for a reinforced section that gives the same critical tensile and compressive strains as calculated for similar sections without reinforcement. Separate reductions in base thickness are presented based on equal resistance to fatigue and rutting as defined by this method. Limiting the vertical compressive strain on the subgrade is an indirect method for controlling permanent deformation of only the subgrade. Therefore, the effect of geosynthetic reinforcement on permanent deformation in the aggregate base and upper part of the subgrade was independently considered using the previously discussed layer strain approach and hyperbolic permanent strain model. These results are presented in Chapter Three.

Cross-Anisotropic Sensitivity Study Results

Geosynthetic at Bottom of Aggregate Layer. Structural pavement sections for the primary sensitivity study were analyzed using the previously discussed cross-anisotropic finite element

Table 1. AASHTO design for pavement sections used in sensitivity study.

SECTION	TRAFFIC LOADING[2] (x10^3)	SUBGRADE CBR (%)	SUBGRADE E_S (ksi)	SOIL SUPPORT, S	STRUCT. NO. (SN)	SURFACE THICKNESS,T_S (in.)	AGG. BASE THICKNESS, T_B (in.)
1	200	3	3.5	3.2		2.5	11.9
2	200	5	6.0	3.9	2.85	2.5	9.7
3	200	10	12.5	5.0	2.45	2.5	7.5
4	500	3	3.5	3.2	3.62	2.5	15.3
5	500	5	6.0	3.9	3.30	2.5	12.8
6	500	10	12.5	5.0	2.80	2.5	9.6
7	2000	3	3.5	3.2	4.55	6.5	12.4

1. Design Assumptions:

        Present Serviceability Index = 2.5
        Regional Factor = 1.5

           Asphalt Surfacing: a_1 = 0.44 $T_{AC} \leq 3.5$ in.
                               a_2 = 0.35 $T_{AC} > 3.5$ in. for T in excess of 3.5 in.
           Aggregate Base: a_3 = 0.18 $T_{AC} + T_B \leq 12$ in.
                               a_4 = 0.14 $T_{AC} + T_B > 12$ in.

2. Equivalent 18 kip, single axle loadings.

model. Tables 2 through 5 give a detailed summary of the effect of reinforcement on the stress, strain, and deflection response of each pavement layer. The force developed in the geosynthetic reinforcement is also shown. The percent difference is given between the particular response variable for a reinforced section compared to the corresponding nonreinforced section of equal thickness.

All response variables given in the tables are those calculated by the finite element model at a distance of 0.7 in. (18mm) horizontally outward from the center of the load. The pavement response under the exact center of the loading can not easily be determined using a finite element representation. In these tables a positive stress or strain indicates tension and a negative value compression. Downward deflections are negative. Also refer to the notes given at the bottom of the tables for other appropriate comments concerning these data.

An examination of the results given in Tables 2 through 5 shows that the effect of the geosynthetic reinforcement is, in general, relatively small in terms of the percent change it causes in the response variables usually considered to be of most significance. These variables include tensile strain in the bottom of the asphalt, vertical subgrade stress and strain, and vertical deflections. The force mobilized in the geosynthetic is also small, varying from less than 1 lb/in. to a maximum of about 18 lb/in. (0.2 to 3.1 N/m), depending on the structural section and subgrade strength. The force developed in the geosynthetic increases as the thickness of the structural section decreases, and as the subgrade becomes softer.

The presence of the geosynthetic can have a small, but potentially important, beneficial effect on the radial and tangential stresses and strains developed in the aggregate base and upper portion of the subgrade because of the externally applied loading. The variation in radial stress that can occur within the upper part of the subgrade is shown in Figure 6. The change in both radial stress and radial strain expressed as a percentage of that developed in a similar section without reinforcement can be significant (Fig. 6). The radial stresses caused by loading a
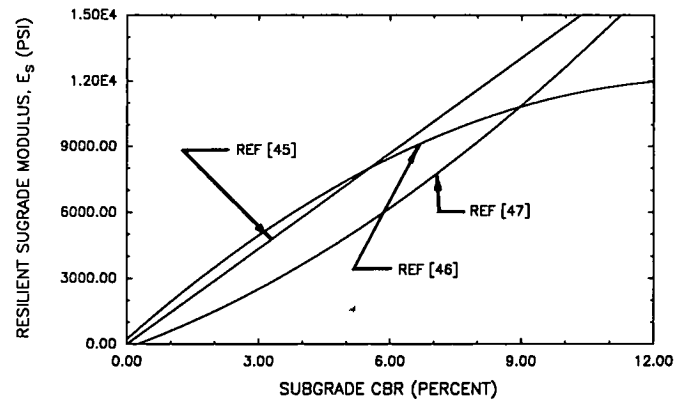
Figure 5. Typical variations of resilient moduli with CBR.

heavier section having a 6.5-in. (165 mm) AC surfacing are very small. Thus, the change in stress resulting from the geosynthetic has a negligible effect on performance. This is especially true considering the magnitude of the initial stress that would exist in the layer because of overburden and compaction effects. Even when lighter sections are placed on a stiff subgrade having a CBR of about 10 percent (E_s = 12,500 psi; 86 kN/m²), small radial stresses occur regardless of the presence of geosynthetic reinforcement (Fig. 6).

General Response. Figures 7 through 9 summarize the effect of geosynthetic reinforcement on the tensile strain in the bottom of the asphalt and the vertical compressive strain on top of the subgrade. Equivalent structural sections can be readily estimated as shown in Figures 7 and 8 by selecting a reduced aggregate base thickness for a reinforced section that has the same level of strain as in the corresponding unreinforced section. To develop a set of design curves for the three levels of geosynthetic stiffnesses requires a total of 12 finite element computer analyses.

Table 2. Effect of geosynthetic reinforcement on pavement response: 2.5-in. AC, E_s = 3,500 psi.

GEOSYN. STIFF. S_g (lbs/in)	VERT. SURFACE DEFLECTION		SUBGRADE				TENSILE STRAIN BOTTOM OF AC		TOP 1/3 OF AGGREGATE BASE								GEOSYN. FORCE (lbs/in)
			VERT. DEFLECTION		VERTICAL STRESS				VERTICAL STRESS		RADIAL STRESS		RADIAL STRAIN		VERTICAL STRAIN		
	δ_z(in.)	% Diff.	δ_z(in.)	% Diff.	σ_z(psi)	% Diff.	$\epsilon_r(10^{-6})$	% Diff.	σ_z(psi)	% Diff.	$\epsilon_r(10^{-6})$	% Diff.	$\epsilon_r(10^{-6})$	% Diff.	$\epsilon_r(10^{-6})$	% Diff.	
							2.5 IN. AC/9.72 IN. AGGREGATE BASE		SUBGRADE E_s = 3500 PSI								
0	-0.0770	-	-0.0497	-	-11.41	-	1210	-	-37.29	-	2.258	-	1566	-	-3268	-	-
1500	-0.0765	0.6	-0.0492	1.0	-11.15	2.3	1210	0	-37.51	-0.6	2.037	-9.8	1551	1.0	-3270	-0.06	4.087
6000	-0.0754	2.1	-0.0482	3.0	-10.59	7.2	1190	-1.7	-37.94	-1.7	1.552	-31.3	1516	3.2	-3271	-0.09	13.177
9000	-0.0748	2.9	-0.0477	4.0	-10.32	9.6	1180	-2.5	-38.12	-2.2	1.321	-41.5	1498	4.3	-3269	-0.03	17.637
							2.5 IN. AC/12.0 IN. AGGREGATE BASE		SUBGRADE E_s = 3500 PSI								
0	-0.07323	-	-0.04267	-	-9.082	-	1170	-	-36.48	-	1.693	-	1478	-	-3159	-	-
1500	-0.07283	0.6	-0.04230	0.9	-8.874	2.29	1170	0.0	-36.63	-0.4	1.537	9.2	1468	-0.7	-3161	-0.06	3.476
6000	-0.07185	1.9	-0.04144	2.9	-8.421	7.28	1160	0.9	-36.94	-1.3	1.189	29.8	1442	-2.4	-3161	-0.06	11.279
9000	-0.07132	2.6	-0.04100	3.9	-8.203	9.68	1150	1.7	-37.07	-1.6	1.020	39.8	1429	-3.3	-3160	-0.03	15.131
							2.5 IN. AC/15.3 IN. AGGREGATE BASE		SUBGRADE E_s = 3500 PSI								
0	-0.0697	-	-0.0356	-	-6.078	-	1130	-	-34.95	-	1.149	-	1367	-	-2992	-	-
1500	-0.0694	0.4	-0.0353	0.84	-6.558	2.2	1120	-0.9	-35.04	-0.3	1.053	-8.4	1360	-0.5	-2993	-0.03	2.746
6000	-0.0686	1.3	-0.0347	2.53	-6.227	7.2	1120	-0.9	-35.23	-0.8	0.831	-27.7	1344	-1.7	-2993	-0.03	9.006
9000	-0.0682	2.2	-0.0343	3.65	-6.066	9.6	1110	-1.8	-35.31	-1.0	0.719	-37.4	1335	-2.3	-2992	0.00	12.130

Note: 1. Sign Convention: Tension is Positive; 2. Resilient Modulus of Subgrade = E_s; 3. "Diff." is the percent difference between a reinforced and non-reinforced section.

Table 2. Continued.

GEOSYN. STIFF. S_g (lbs/in)	BOTTOM 1/3 OF AGGREGATE BASE								SUBGRADE							
	VERTICAL STRESS		RADIAL STRESS		RADIAL STRAIN		VERTICAL STRAIN		VERTICAL STRESS		RADIAL STRESS		RADIAL STRAIN		VERTICAL STRAIN	
	σ_z(psi)	% Diff.	σ_r(psi)	% Diff.	$\epsilon_r(10^{-6})$	% Diff.	$\epsilon_r(10^{-6})$	% Diff.	σ_z(psi)	% Diff.	σ_r(psi)	% Diff.	$\epsilon_r(10^{-6})$	% Diff.	$\epsilon_r(10^{-6})$	% Diff.
				2.5 IN. AC/9.72 AGGREGATE BASE			SUBGRADE E_s = 3500 PSI									
0	-14.94	-	0.573	-	2219	-	-2141	-	-8.567	-	0.654	-	1089	-	-2600	-
1500	-14.84	0.7	0.517	-9.77	2086	-6.0	-2121	0.9	-8.446	1.4	0.423	-35.3	1035	-5.0	-2512	3.38
6000	-14.61	2.2	0.401	-30.0	1812	-18.3	-2074	3.1	-8.172	4.6	-0.083	-112.7	917.8	-15.7	-2318	10.85
9000	-1448	3.1	0.349	-39.1	1687	-24.0	-2050	4.2	-8.034	6.2	-0.323	-149.4	861.1	+20.9	-2223	14.5
				2.5 IN. AC/12.0 AGGREGATE BASE			SUBGRADE E_s = 3500 PSI									
0	-1250	-	0.524	-	1956	-	-1797	-	-6.909	-	0.802	-	925.4	-	-2159	-
1500	-1242	0.6	0.478	-8.8	1849	5.5	-1781	0.9	-6.820	1.3	0.583	-27.3	877.6	-5.2	-2083	3.5
6000	-1224	2.1	0.383	-26.9	1624	17.0	-1743	3.0	-6.612	4.3	0.102	-87.3	771.8	-16.6	-1914	11.4
9000	-1214	2.9	0.340	-35.1	1521	22.2	-1797	4.1	-6.506	5.8	-0.126	-115.7	720.6	-22.1	-1831	15.2
				2.5 IN. AC/15.3 AGGREGATE BASE			SUBGRADE E_s = 3500 PSI									
0	-9.784	-	0.448	-	1616	-	-1411	-	-5.207	-	0.871	-	743.2	-	-1688	-
1500	-9.731	0.5	0.414	-7.6	1538	-4.8	-1400	0.8	-5.148	1.1	0.677	-22.3	703.4	-5.4	-1627	3.6
6000	-9.599	1.9	0.343	-23.4	1370	-15.2	-1373	2.7	-5.007	3.8	0.250	-71.3	614.2	-17.4	-1489	11.8
9000	-9.528	2.6	0.310	-30.8	1291	-20.1	-1359	3.7	-4.933	5.3	0.045	-94.8	570.6	-23.2	-1420	15.9

Table 3. Effect of geosynthetic reinforcement on pavement response: 6.5-in. AC, E_s = 3,500 psi.

GEOSYN. STIFF. S_g (lbs/in)	VERTICAL SURFACE DEFLECTION δ_z(in.)	% Diff.	SUBGRADE VERT. DEFLECTION δ_z(in.)	% Diff.	VERTICAL STRESS σ_z(psi)	% Diff.	TENSILE STRAIN BOTTOM OF AC $\varepsilon_r(10^{-6})$	% Diff.	TOP 1/3 OF AGGREGATE BASE VERTICAL STRESS σ_z(psi)	% Diff.	RADIAL STRESS $\varepsilon_r(10^{-6})$	% Diff.	RADIAL STRAIN $\varepsilon_r(10^{-6})$	% Diff.	VERTICAL STRAIN $\varepsilon_r(10^{-6})$	% Diff.	GEOSYN. FORCE (lbs/in)
							6.5 IN. AC/9.72 IN. AGGREGATE BASE SUBGRADE E_s = 3500 PSI									
0	-.011129	-	-.007987	-	-1.297	-	160	-	-2.826	-	0.626	-	166.5	-	-279.9	-	-
1500	-.011105	0.2	-.007960	0.3	-1.282	1.2	160	0	-2.854	1.0	0.607	3.0	165.5	0.6	-280.9	0.4	0.375
6000	-.0111042	0.8	-.007891	1.2	-1.248	3.8	159	0.6	-2.915	3.2	0.562	10.2	163.0	2.1	-282.7	1.0	1.278
9000	-.0011006	1.1	-.007853	1.7	-1.231	5.1	158	1.25	-2943	4.1	0.539	13.9	161.6	2.9	-283.4	1.2	1.760
							6.5 IN. AC/12.42 IN. AGGREGATE BASE SUBGRADE E_s = 3500 PSI									
0	-.01074	-	-.00683	-	-1.005	-	155	-	-2.871	-	0.445	-	149.2	-	-270.7	-	-
1500	-.01071	0.3	-.00680	0.4	-0.994	1.1	155	0.0	-2.888	0.6	0.433	2.7	148.6	0.4	-271.2	0.2	0.305
6000	-.01066	0.7	-.00674	1.3	-0.967	3.8	154	0.6	-2.926	1.9	0.403	9.4	146.8	1.6	-272.3	0.6	1.048
9000	-.01062	1.1	-.00671	1.8	-0.953	5.2	153	1.3	-2.945	2.6	0.445	13.0	145.7	2.4	-272.7	0.7	1.445
							6.5 IN. AC/16.0 IN. AGGREGATE BASE SUBGRADE E_s = 3500 PSI									
0	-.01047	-	-.00606	-	-0.842	-	152	-	-2.846	-	0.337	-	136.9	-	-260.8	-	-
1500	-.01045	0.2	-.00604	0.3	-0.833	1.1	152	0.0	-2.858	0.4	0.328	2.7	136.4	0.4	-261.2	0.2	0.259
6000	-.01040	0.7	-.00599	1.2	-0.811	3.7	151	0.7	-2.885	1.4	0.305	9.5	135.0	1.4	-261.8	0.4	0.895
9000	-.01037	1.0	-.00596	1.6	-0.800	5.0	151	0.7	-2.889	1.5	0.293	13.1	134.2	2.0	-262.1	0.5	1.237

Note: 1. Sign Convention: Tension is Positive; 2. Resilient Modulus of Subgrade = E_s; 3. "Diff." is the percent difference between a reinforced and non-reinforced section.

Table 3. Continued.

GEOSYN. STIFF. S_g (lbs/in)	BOTTOM 1/3 OF AGGREGATE BASE VERTICAL STRESS σ_z(psi)	% Diff.	RADIAL STRESS σ_r(psi)	% Diff.	RADIAL STRAIN $\varepsilon_r(10^{-6})$	% Diff.	VERTICAL STRAIN $\varepsilon_r(10^{-6})$	% Diff.	SUBGRADE VERTICAL STRESS σ_z(psi)	% Diff.	RADIAL STRESS σ_r(psi)	% Diff.	RADIAL STRAIN $\varepsilon_r(10^{-6})$	% Diff.	VERTICAL STRAIN $\varepsilon_r(10^{-6})$	% Diff.
					6.5 IN. AC/8.0 IN. AGGREGATE IN BASE SUBGRADE E_s = 3500 PSI											
0	-1.523	-	0.045	-	196.5	-	-216.6	-	-1.063	-	-0.053	-	112.4	-	-291.9	-
1500	-1.521	0.1	0.041	8.9	187.4	4.6	-215.8	0.4	-1.057	0.6	-0.071	34.0	108.6	3.4	-285.9	2.1
6000	-1.513	0.7	0.033	26.67	167.8	14.6	-213.7	1.3	-1.042	2.0	-0.114	115.0	99.5	11.5	-711.9	6.8
9000	-1.507	1.1	0.029	35.6	158.4	19.4	-212.4	1.9	-1.034	2.7	-0.136	156.6	94.9	15.6	-264.5	9.4
					6.5 IN. AC/12.42 IN. AGGREGATE BASE SUBGRADE E_s = 3500 PSI											
0	-1.234	-	0.0392	-	165.0	-	-175.9	-	-0.842	--	-0.009	-	94.7	-	-238.6	-
1500	-1.231	0.2	0.0363	7.4	158.3	4.1	-171.1	0.4	-0.838	0.5	-0.028	211.1	91.0	3.9	-233.1	2.3
6000	-1.223	0.9	0.0298	24.0	143.2	13.2	-173.2	1.5	-0.823	2.3	-0.072	700.0	82.2	13.2	-220.0	7.8
9000	-1.218	1.3	0.0266	32.1	135.7	17.8	-172.1	2.2	-0.822	2.4	-0.095	955.6	77.6	18.1	-213.2	10.6
					6.5 IN. AC/16.0 IN. AGGREGATE BASE SUBGRADE E_s = 3500 PSI											
0	-1.062	-	0.033	-	141.5	-	-151.3	-	-0.714	-	0.002	-	81.9	-	-204.5	-
1500	-1.060	0.2	0.031	6.1	136.2	3.8	-150.7	0.4	-0.711	0.4	-0.016	900.0	78.6	4.0	-199.6	2.4
6000	-1.053	0.8	0.026	21.2	123.9	12.4	-149.1	1.4	-0.704	1.4	-0.057	2950.0	70.5	13.9	-187.9	8.1
9000	-1.049	1.2	0.023	30.3	117.7	16.8	-148.2	2.0	-0.699	2.1	-0.079	4050.0	66.4	18.9	-181.8	11.1

12

Table 4. Effect of geosynthetic reinforcement on pavement response: 2.5-in. AC, E_s = 6,000 psi.

GEOSYN. STIFF. S_g (lbs/in)	VERTICAL SURFACE DEFLECTION		SUBGRADE				TENSILE STRAIN BOTTOM OF AC		TOP 1/3 OF AGGREGATE BASE								GEOSYN. FORCE (lbs/in)
			VERT. DEFLECTION		VERTICAL STRESS				VERTICAL STRESS		RADIAL STRESS		RADIAL STRAIN		VERTICAL STRAIN		
	δ_z(in.)	% Diff.	δ_z(in)	% Diff.	σ_z(psi)	% Diff.	ε_r(10^-6)	% Diff.	σ_z(psi)	% Diff.	σ_r(psi)	% Diff.	ε_r(10^-6)	% diff.	ε_r(10^-6)	% Diff.	
2.5 IN. AC/7.5 IN. AGGREGATE BASE SUBGRADE E_s = 6000 PSI																	
0	-0.0529	-	-0.0363	-	-16.71	-	936	-	-46.83	-	3.909	-	1213	-	-2439	-	-
1500	-0.0527	-0.4	-0.0361	-0.6	-16.46	-1.5	931	-0.5	-47.04	+0.45	3.669	-6.1	1202	-0.9	-2440	-0.04	3.461
6000	-0.0521	-1.5	-0.0355	-2.2	-15.86	-5.1	919	-1.8	-47.51	+1.45	3.094	-20.8	1177	-3.0	-2438	-0.04	11.844
9000	-0.0517	-2.3	-0.0352	-3.0	-15.55	-6.9	913	-2.5	-47.73	+1.92	2.795	-28.5	1163	-4.1	-2436	-0.12	16.288
2.5 IN. AC/9.75 IN. AGGREGATE BASE SUBGRADE E_s = 6000 PSI																	
0	-.04955	-	-.03068	-	-12.79	-	886	-	-45.85	-	2.855	-	1128	-	-2348	-	-
1500	-0.0498	-0.5	-.03050	-0.6	-12.59	-1.6	874	-1.4	-46.00	+0.3	2.695	-5.6	1121	-0.6	-2348	0	2.896
6000	-0.4923	-1.4	-.03004	-2.1	-12.12	-5.2	875	-1.2	-46.32	+1.03	2.305	-19.3	1104	-2.1	-2347	-0.04	9.961
9000	-.04894	-2.0	-.02979	-2.9	-11.87	-7.2	871	-1.7	-46.48	+1.37	2.099	-26.5	1095	-2.9	-2346	-0.09	13.728
2.5 IN. AC/12.85 IN. AGGREGATE BASE SUBGRADE E_s = 6000 PSI																	
0	-0.0468	-	-0.0249	-	-9.143	-	842	-	-43.93	-	1.912	-	1031	-	-2214	-	-
1500	-0.0467	-0.2	-0.0248	-0.4	-9.004	-1.5	840	-0.24	-44.02	+0.2	1.818	- 4.9	1027	-0.4	-2215	-0.05	2.254
6000	-0.0463	-1.1	-0.0244	-2.0	-8.666	-5.2	836	-0.71	-44.21	+0.6	1.584	-17.2	1016	-1.4	-2214	-0.00	7.824
9000	-0.0460	-1.7	-0.0242	-2.8	-8.487	-7.2	833	-1.07	-44.31	+0.9	1.457	-23.8	1011	-1.9	-2214	-0.00	10.827

Note: 1. Sign Convention: Tension is Positive;   2. Resilient Modulus of Subgrade = E_s;
3. "Diff." is the percent difference between a reinforced and non-reinforced section.

Table 4. Continued

GEOSYN. STIFF. S_g (lbs/in)	BOTTOM 1/3 AGGREGATE BASE								SUBGRADE							
	VERTICAL STRESS		RADIAL STRESS		RADIAL STRAIN		VERTICAL STRAIN		VERTICAL STRESS		RADIAL STRESS		RADIAL STRAIN		VERTICAL STRAIN	
	σ_z(psi)	% Diff.	σ_r(psi)	% Diff.	ε_r(10^-6)	% Diff.	ε_r(10^-6)	% Diff.	σ_z(psi)	% Diff.	σ_r(psi)	% Diff.	ε_r(10^-6)	% Diff.	ε_r(10^-6)	% Diff.
2.5 IN. AC/7.5 IN. AGGREGATE BASE SURFACE E_s = 6000 PSI																
0	-21.10	-	0.768	-	1772	-	-1761	-	-12.18	-	0.406	-	850.3	-	-2087	-
1500	-21.01	-0.4	0.713	- 7.2	1697	- 4.2	-1750	-0.6	-12.05	-1.1	0.247	-39.2	825.8	-2.9	-2044	-2.1
6000	-20.76	-1.6	0.588	-23.4	1524	-14.0	-1721	-2.3	-11.74	-3.6	-0.145	-135.7	765.9	-9.9	-1939	-7.1
9000	-20.62	-2.3	0.526	-31.5	1438	-18.8	-1705	-3.2	-11.57	-5.0	-0.352	-186.7	734.2	-13.6	-1883	-9.8
2.5 IN. AC/9.75 IN. AGGREGATE BASE SURFACE E_s = 6000 PSI																
0	-17.16	-	0.705	-	1547	-	-1438	-	-9.490	--	0.788	-	709.7	-	-1688	-
1500	-17.09	-0.4	0.6612	- 6.2	1487	- 3.9	-1429	-0.6	-9.395	-1.0	0.628	-20.3	687.5	- 3.1	-1651	-2.0
6000	-16.90	-1.5	0.561	-20.4	1349	-12.8	-1407	-2.1	-9.164	-3.4	0.237	-69.9	633.2	-10.8	-1560	-7.6
9000	-16.79	-2.2	0.511	-27.5	1279	-17.3	-1394	-3.1	-9.039	-4.75	0.031	-96.1	604.4	-14.8	-1512	-10.4
2.5 IN. AC/12.85 IN. AGGREGATE BASE SURFACE E_s = 6000 PSI																
0	-13.15	-	0.604	-	1270	-	-1107	-	-6.933	-	0.986	-	559.8	-	-1288	-
1500	-13.10	-0.4	0.573	- 5.1	1228	- 3.3	-1101	-0.5	-6.873	-0.9	0.840	-14.8	541.2	- 3.3	-1259	-2.2
6000	-12.98	-1.3	0.501	-17.0	1127	-11.3	-1085	-2.0	-6.723	-3.0	0.483	-51.0	495.6	-11.5	-1186	-7.9
9000	-12.50	-4.9	0.463	-23.3	1076	-15.3	-1076	-2.8	-6.641	-4.2	0.294	-70.2	471.2	-15.8	-1147	-11.0

Table 5. Effect of geosynthetic reinforcement on pavement response: 2.5-in. AC, $E_s = 12{,}500$ psi.

GEOSYN. STIFF. S_g (lbs/in)	VERTICAL SURFACE DEFLECTION		SUBGRADE				TENSILE STRAIN BOTTOM OF AC		TOP 1/3 OF AGGREGATE BASE								GEOSYN. FORCE (lbs/in)
			VERT. DEFLECTION		VERTICAL STRESS				VERTICAL STRESS		RADIAL STRESS		RADIAL STRAIN		VERTICAL STRAIN		
	σ_z(in.)	% Diff.	δ_z(in.)	% Diff.	σ_z(psi)	% Diff.	$\epsilon_r(10^{-6})$	% Diff.	σ_z(psi)	% Diff.	$\epsilon_r(10^{-6})$	% Diff.	$\epsilon_r(10^{-6})$	% Diff.	$\epsilon_r(10^{-6})$	% Diff.	
2.5 IN. AC/6.0 IN. AGGREGATE BASE SUBGRADE E_s = 12,500 PSI																	
0	-0.010369	-	-0.006379	-	-7.378	-	378	-	-27.42	-	3.998	-	390.3	-	-721.2	-	-
1500	-0.010344	-0.2	-0.006353	-0.4	-7.666	-0.9	377	-0.3	-27.49	+0.3	3.924	-1.9	388.9	-0.4	-721.3	-0.01	0.877
6000	-0.010275	-0.9	-0.006285	-1.5	-7.477	-3.4	375	-0.8	-27.67	+0.9	3.732	-6.7	385.0	-1.4	-721.6	-0.06	3.141
9000	-0.010233	-1.3	-0.006245	-2.1	-7.370	-4.8	374	-1.1	-27.76	+1.2	3.622	-9.4	382.7	-2.0	-721.6	-0.06	4.416
2.5 IN. AC/7.5 IN. AGGREGATE BASE SUBGRADE E_s = 12,500 PSI																	
0	-.00991	-	-.00550	-	-6.096	-	.365	-	-26.51	-	3.148	-	356.4	-	-682.7	-	-
1500	-.00988	-0.3	-.00548	-0.4	-6.036	-1.0	364	-0.3	-26.56	+0.2	3.098	-1.6	355.4	-0.2	-682.8	-0.01	0.739
6000	-.00983	-0.8	-.00542	-1.4	-5.879	-3.6	363	-0.6	-26.68	+0.6	2.966	-5.8	352.8	-1.0	-683.0	-0.04	2.656
9000	-.00979	-1.2	-.00539	-2.0	-5.790	-5.0	362	-0.8	-26.75	+0.9	2.890	-8.2	351.2	-1.5	-683.0	-0.04	3.742
2.5 IN. AC/9.62 IN. AGGREGATE BASE SUBGRADE E_s = 12,500 PSI																	
0	-.00939	-	-.00455	-	-4.453	-	353	-	-25.15	-	2.308	-	318.4	-	-633.8	-	-
1500	-.00937	-0.2	-.00453	-0.4	-4.408	-1.0	352	-0.3	-25.18	+0.1	2.278	-1.3	317.8	-0.2	-633.9	-0.02	0.582
6000	-.00932	-0.8	-.00449	-1.3	-4.290	-3.7	351	-0.6	-25.25	+0.4	2.198	-4.8	316.1	-0.7	-634.0	-0.03	2.104
9000	-.00929	-1.1	-.00446	-2.0	-4.223	-5.2	351	-0.6	-25.29	+0.6	2.151	-6.8	315.2	-1.0	-634.0	-0.03	2.976

Note: 1. Sign Convention: Tension is Positive; 2. Resilient Modulus of Subgrade = E_s; 3. "Diff." is the percent difference between a reinforced and a non-reinforced section.

Table 5. Continued.

GEOSYN. STIFF. S_g (lbs/in)	BOTTOM 1/3 OF AGGREGATE BASE								SUBGRADE							
	VERTICAL STRESS		RADIAL STRESS		RADIAL STRAIN		VERTICAL STRAIN		VERTICAL STRESS		RADIAL STRESS		RADIAL STRAIN		VERTICAL STRAIN	
	σ_z(psi)	% Diff.	σ_r(psi)	% Diff.	$\epsilon_r(10^{-6})$	% Diff.	$\epsilon_r(10^{-6})$	% Diff.	σ_z(psi)	% Diff.	σ_r(psi)	% Diff.	$\epsilon_r(10^{-6})$	% Diff.	$\epsilon_r(10^{-6})$	% Diff.
2.5 IN. AC/6.0 IN. AGGREGATE BASE SUBGRADE E_s = 12,500 PSI																
0	-10.18	-	0.440	-	454.0	-	-410.2	-	-5.482	-	-0.171	-	166.8	-	-428.1	-
1500	-10.16	-0.2	0.421	-4.3	442.0	-2.6	-409.1	0.3	-5.431	0.9	-0.184	7.6	164.5	-1.4	-423.2	-1.1
6000	-10.12	-0.6	0.374	-15.0	411.9	-9.3	-405.8	1.1	-5.300	3.3	-0.225	31.6	158.4	-5.0	-410.1	-4.2
9000	-10.09	-0.9	0.349	-20.7	395.4	-12.9	-403.8	1.6	-5.228	4.6	-0.251	46.8	154.8	-7.2	-402.6	-6.0
2.5 IN. AC/7.5 IN. AGGREGATE BASE SUBGRADE E_s = 12,500 PSI																
0	-8.44	-	0.398	-	397.6	-	-341.5	-	-4.420	-	+0.005	-	141.3	-	-354.2	-
1500	-8.43	-1.2	0.383	-3.8	388.0	-2.4	-340.6	0.3	-4.380	0.9	-0.014	-380	139.2	-1.5	-349.9	-1.2
6000	-8.40	-4.7	0.346	-13.1	363.8	-8.5	-337.9	1.1	-4.4281	3.1	-0.068	-1460	133.4	-5.6	-338.4	-4.5
9000	-8.37	-8.3	0.325	-18.3	350.5	-11.9	-336.2	1.6	-4.225	4.4	-0.101	-2120	141.3	-7.9	-331.8	-6.3
2.5 IN. AC/9.62 IN. AGGREGATE BASE SUBGRADE E_s = 12,500 PSI																
0	-6.57	-	0.342	-	329.5	-	-266.7	-	-3.323	-	0.169	-	114.2	-	-276.9	-
1500	-6.56	-0.2	0.331	-3.2	322.5	-2.1	-266.0	0.3	-3.297	0.8	0.147	-13.0	112.3	-1.7	-273.3	-1.3
6000	-6.53	-0.6	0.304	-11.1	304.8	-7.5	-263.9	1.1	-3.229	2.8	0.085	-49.7	107.2	-6.1	-264.0	-4.7
9000	-6.51	-0.9	0.289	-15.5	295.0	-10.5	-262.7	1.5	-3.191	4.0	0.048	-71.6	104.2	-8.8	-258.5	-6.6
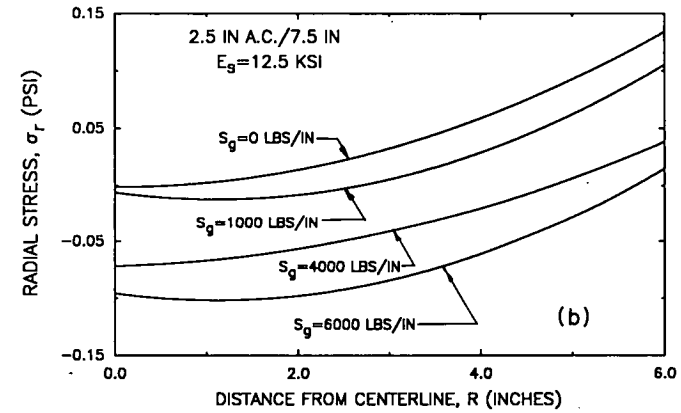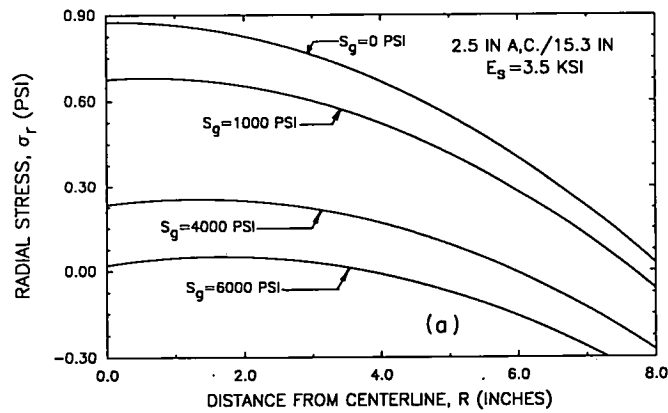
Figure 6. Variation of radial stress at top of subgrade with radial distance from centerline (tension is positive): (a) subgrade E_s = 3,500 psi; (b) subgrade E_s = 12,500 psi.
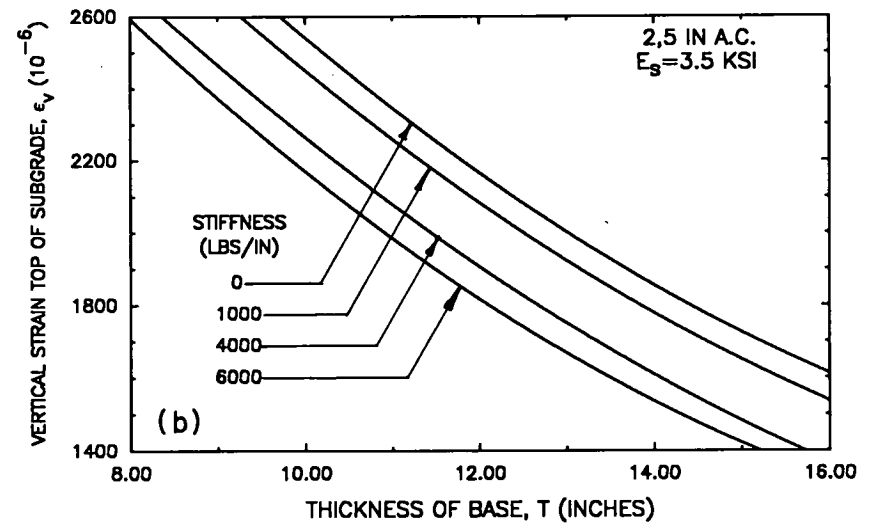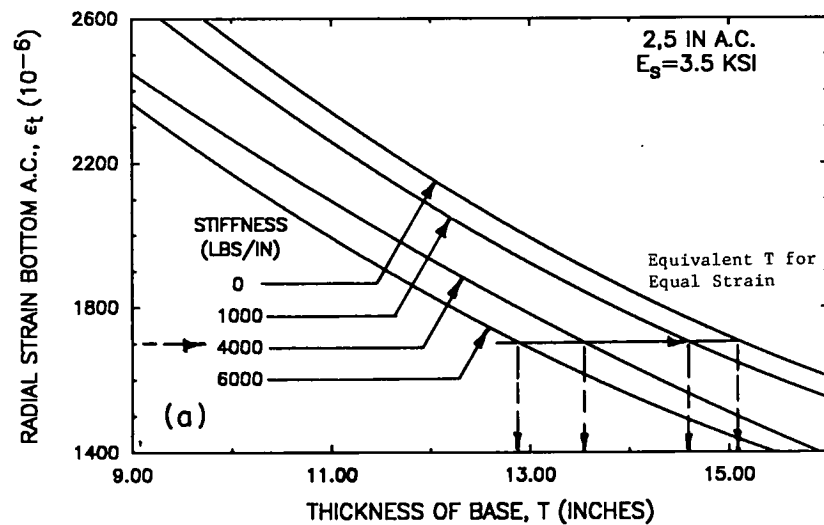
Figure 7. Equivalent base thickness for equal strain: 2.5 in. AC/E_s = 3.5 ksi: (a) radical ϵ_v in AC; (b) vertical ϵ_v on subgrade.
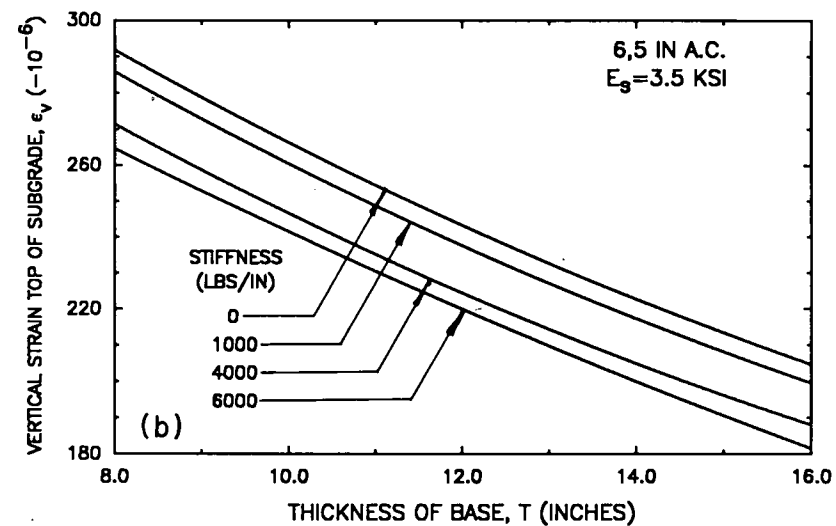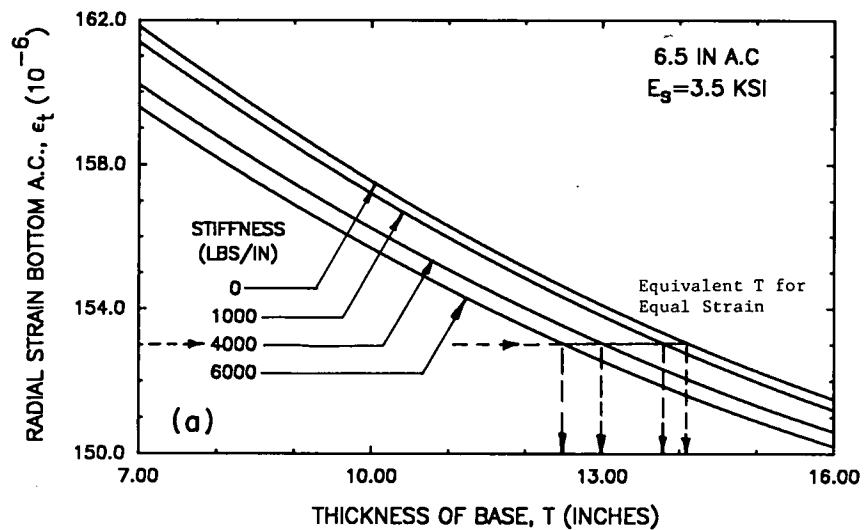
Figure 8. Equivalent base thickness for equal strain: 6.5 in. AC/E_s = 3.5 ksi: (a) radial ϵ_v in AC; (b) vertical ϵ_v on subgrade.

Figure 9. Equivalent base thickness for equal strain: 2.5 in. AC/E_s = 12.5 ksi: (a) radial ϵ_r in AC; (b) vertical ϵ_v on subgrade.

15

16

Figure 10 shows for the same sections, as compared in Figure 7, the reduction in radial tensile stress caused in the bottom of the aggregate base due to reinforcement. The actual magnitude of the change in radial stress in the bottom of the aggregate base is about 10 to 20 percent of that occurring in the subgrade. An exception is the section having the stiff subgrade where the difference was much less, with the stresses being very small.

Geosynthetic Position. The pavement response was also determined for geosynthetic reinforcement locations at the lower $\frac{1}{3}$ and upper $\frac{2}{3}$ positions within the aggregate base in addition to the bottom of the base. The theoretical effect of reinforcement position on the major response variables is summarized in Table 6 for the three levels of geosynthetic stiffness used in the study. The effect of position was only studied for sections having a subgrade stiffness $E_s = 3,500$ psi (24 MN/m²).

The influence of reinforcement position on horizontal tensile strain in the bottom of the asphalt and vertical compressive strain on top of the subgrade is shown in Figures 11 and 12 for the $\frac{1}{3}$ up from the bottom of the aggregate base position.

Slack. To determine the effect of slack on performance, three different levels of slack in the geosynthetic were analyzed using the nonlinear finite element model. Slack levels 0.25, 0.75, and 1.4 percent strain were chosen for the analysis. As wheel load is applied in the field, the geosynthetic will gradually start to deform and begin picking up some of this load. The force on the geosynthetic should increase slowly at first, with the rate at which it is picked up becoming greater with the applied strain level. This type of geosynthetic load-strain behavior was modeled using a smoothly varying interpolation function as shown in Figure 13 for the 0.25 and 0.75 percent slack level. The results of the slack sensitivity study for the stronger subgrade are given in Table 7. The relative effects of slack on force in the geosynthetic were found to be similar for the stiff subgrade shown in Table 7 and also a weaker subgrade having $E_s = 3.5$ ksi (24 MN/m²).

Poisson's Ratio. The literature was found to contain little information on the value of Poisson's ratio of geosynthetics, or its effect on the response of a reinforced pavement. A limited
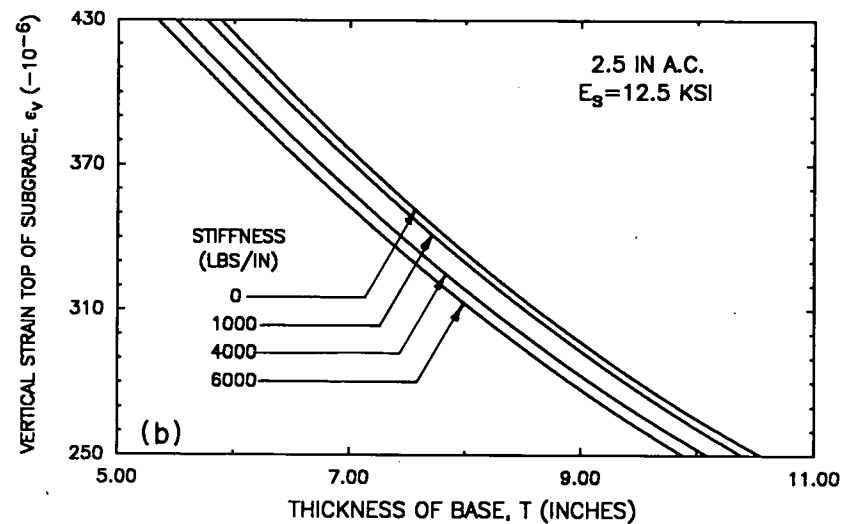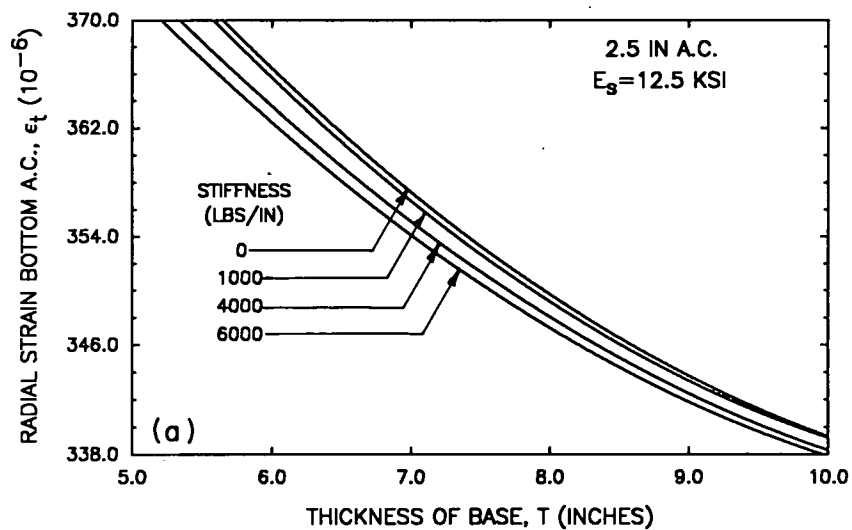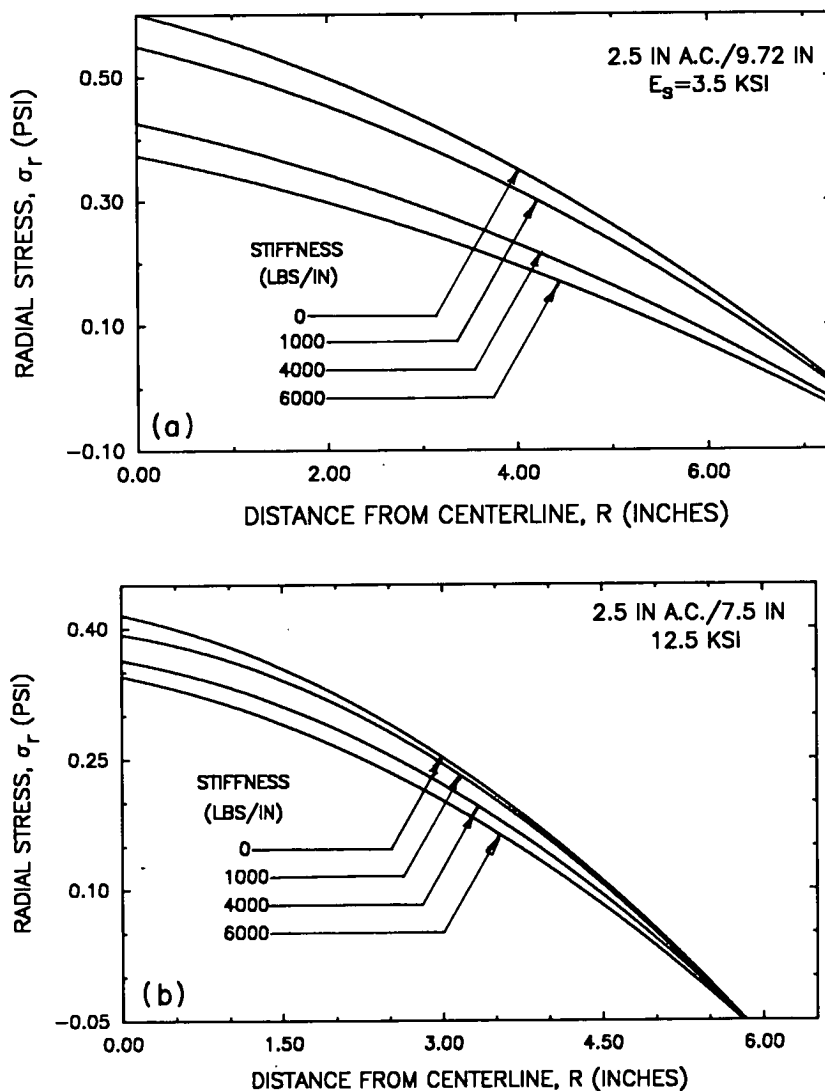

Figure 10. Variation in radial strain in bottom of aggregate base (tension is positive): (a) subgrade $E_s = 3.5$ *ksi; (b) subgrade* $E_s = 12.5$ *ksi.*

Table 6. Effect of geosynthetic reinforcement position on pavement response: 2.5-in. AC, E_s = 3,500 psi.

GEOSYN. STIFF. S_g (lbs/in)	VERT. SURFACE DEFLECTION		SUBGRADE				TENSILE STRAIN BOTTOM OF AC		TOP 1/3 OF AGGREGATE BASE								GEOSYN. FORCE S_g (lbs/in)
			VERT. DEFLECTION		VERTICAL STRESS				VERTICAL STRESS		RADIAL STRESS		RADIAL STRAIN		VERTICAL STRAIN		
	δ_z (in.)	% Diff.	δ_z (in.)	% Diff.	σ_z(psi)	% Diff.	$\epsilon_r(10^{-6})$	% Diff.	σ_z(psi)	% Diff.	$\epsilon_r(10^{-6})$	% Diff.	$\epsilon_r(10^{-6})$	% Diff.	$\epsilon_r(10^{-6})$	% Diff.	
GEOSYNTHETIC @ BOTTOM 2.5 IN. AC/12.0 IN. AGGREGATE BASE SUBGRADE E_s = 3500 PSI																	
0	-0.07323	-	-0.04267	-	-9.082	-	1170	-	-36.48	-	1.693	-	1478	-	-3159	-	-
1500	-0.07283	0.6	-0.04230	0.9	-8.874	2.29	1170	0.0	-36.63	-0.4	1.537	9.2	1468	-0.7	-3161	-0.06	3.476
6000	-0.07185	1.9	-0.04144	2.9	-8.421	7.28	1160	0.9	-36.94	-1.3	1.189	29.8	1442	-2.4	-3161	-0.06	11.279
9000	-0.07132	2.6	-0.04100	3.9	-8.203	9.68	1150	1.7	-37.07	-1.6	1.020	39.8	1429	-3.3	-3160	-0.03	15.131
GEOSYNTHETIC 1/3 UP 2.5 IN. AC/12.0 IN. AGGREGATE BASE SUBGRADE E_s = 3500 PSI																	
0	-.07267	-	-.04209	-	-	-	1170	-	-36.47	-	1.712	-	1480	-	-3160	-	-
1500	-.07227	0.6	-.04201	0.2	-	-	1160	-0.9	-36.69	-0.6	1.443	-15.7	1460	-1.35	-3159	0.0	4.041
6000	-.07130	1.9	-.04173	0.9	-	-	1150	-1.7	-37.07	-1.6	0.859	-49.8	1412	-4.82	-3148	0.4	12.925
9000	-.07079	2.6	-.04155	1.3	-	-	1140	-2.6	-37.21	-2.0	0.582	-66.0	1388	-6.22	-3141	0.6	17.289
GEOSYNTHETIC 2/3 UP 2.5 IN. AC/12.0 IN. AGGREGATE BASE SUBGRADE E_s = 3500 PSI																	
0	-.07627	-	-.04209	-	-	-	1170	-	-36.47	-	1.713	-	1480	-	-3160	-	-
1500	-.07241	0.4	-.04208	0.0	-	-	1160	-0.8	-36.49	-0.1	1.341	-21.7	1442	-2.6	-3135	0.8	3.722
6000	-.07175	1.3	-.04203	0.1	-	-	1150	-1.7	-36.48	-0.0	0.475	-72.3	1351	-8.72	-3072	2.6	12.458
9000	-.07137	1.8	-.04198	0.3	-	-	1140	-2.6	-36.45	0.1	0.038	-97.8	1304	-11.9	-3038	3.9	17.955

Note: 1. Sign Convention: Tension is Positive;   2. Resilient Modulus of Subgrade = E_s;   3. "Diff". is the percent difference between a reinforced and non-reinforced section.

Table 6. Continued.

| GEOSYN. STIFF. S_g (lbs/in)	BOTTOM 1/3 OF AGGREGATE BASE								SUBGRADE							
	VERTICAL STRESS		RADIAL STRESS		RADIAL STRAIN		VERTICAL STRAIN		VERTICAL STRESS		RADIAL STRESS		RADIAL STRAIN		VERTICAL STRAIN	
	σ_z(psi)	% Diff.	σ_r(psi)	% Diff.	$\epsilon_r(10^{-6})$	% Diff.	$\epsilon_r(10^{-6})$	% Diff.	σ_z(psi)	% Diff.	σ_r(psi)	% Diff.	$\epsilon_r(10^{-6})$	% Diff.	$\epsilon_r(10^{-6})$	% Diff.
GEOSYNTHETIC AT BOTTOM 2.5 IN. AC/12.0 AGGREGATE BASE SUBGRADE E_s = 3500 PSI																
0	-1250	-	0.524	-	1956	-	-1797	-	-6.909	-	0.802	-	925.4	-	-2159	-
1500	-1242	0.6	0.478	-8.8	1849	5.5	-1781	0.9	-6.820	1.3	0.583	-27.3	877.6	-5.2	-2083	3.5
6000	-1224	2.1	0.383	-26.9	1624	17.0	-1743	3.0	-6.612	4.3	0.102	-87.3	771.8	-16.6	-1914	11.4
9000	-1214	2.9	0.340	-35.1	1521	22.2	-1797	4.1	-6.506	5.8	-0.126	-115.7	720.6	-22.1	-1831	15.2
GEOSYNTHETIC 1/3 UP 2.5 IN. AC/12.0 IN. AGGREGATE BASE SUBGRADE E_s = 3500 PSI																
0	-12.50	-	1.399	-	1998	-	-1798	-	-6.951	-	0.8767	-	942.9	-	-2188	-
1500	-12.25	2.0	1.232	-11.9	1873	-6.3	-1755	2.4	-6.925	0.4	0.7690	-12.3	921.6	-2.3	-2156	1.5
6000	-11.70	6.4	0.920	-34.2	1637	-18.1	-1665	7.4	-6.856	1.4	0.5075	-42.1	869.1	-7.8	-2076	5.1
9000	-11.44	8.5	0.785	-43.9	1534	-23.2	-1624	9.7	-6.816	1.9	0.3707	-57.7	841.1	-10.8	-2034	7.0
GEOSYNTHETIC 2/3 UP 2.5 IN. AC/12.0 IN. AGGREGATE BASE SUBGRADE E_s = 3500 PSI																
0	-12.50	-	0.527	-	1964	-	-1798	-	-6.951	-	0.8767	-	942.9	-	-2188	-
1500	-12.47	0.2	0.513	-2.7	1929	-1.8	-1792	0.3	-6.955	-0.1	0.8411	-4.1	937.3	-0.6	-2181	0.3
6000	-12.38	1.0	0.476	-4.7	1841	-6.3	-1774	1.3	-6.959	-0.1	0.747	-14.8	921.7	-2.2	-2161	1.2
9000	-12.32	1.4	0.456	-13.5	1793	-8.7	-1764	1.9	-6.958	-0.1	0.693	-21.0	912.2	-3.3	-2148	1.8
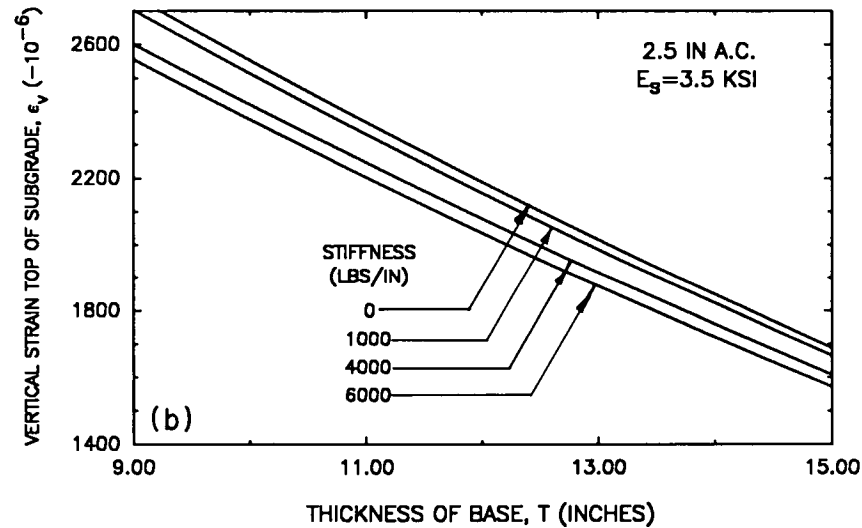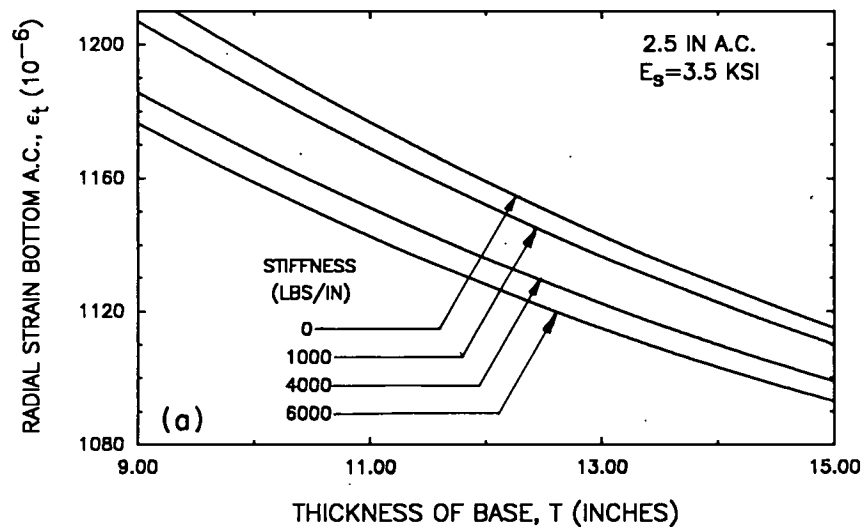
Figure 11. Equivalent base thicknesses for equal strain: $S_g = \frac{1}{3}$ *up: (a) radial* ϵ_r *in AC; (b) vertical* ϵ_v *on subgrade.*

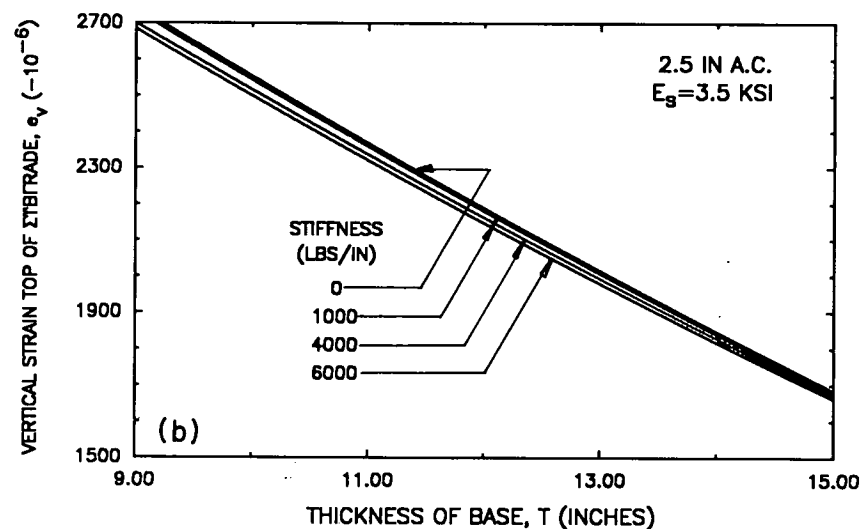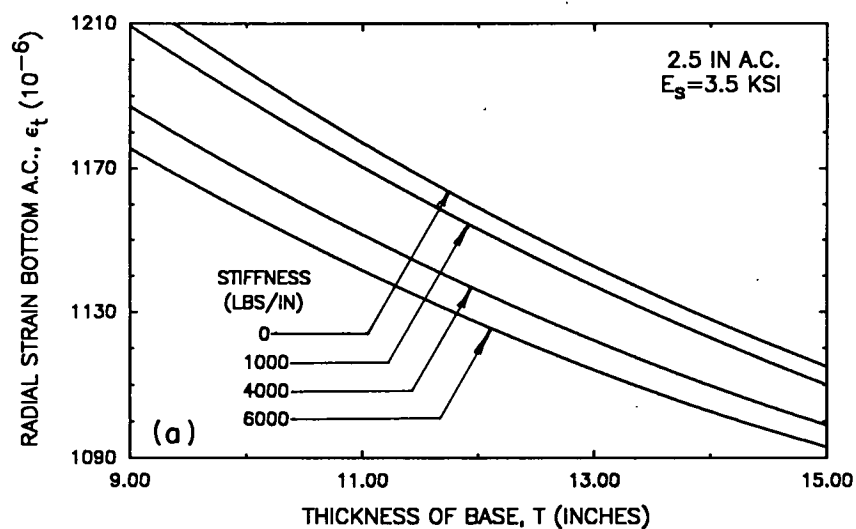*Figure 12. Equivalent base thicknesses for equal strain:* $S_g = \frac{2}{3}$ *up: (a) radial* ϵ_r *in AC; (b) vertical* ϵ_v *on subgrade.*

sensitivity study was therefore conducted for Poisson's ratios of $v = 0.2, 0.3,$ and 0.4. A geosynthetic was used having an actual stiffness of 6,000 lb/in. (1 MN/m). The resulting radial stress in the top of the subgrade as a function of Poisson's ratio of the geosynthetic is shown in Figure 14.

Base Quality. A supplementary sensitivity study was conducted to determine the effect of base quality on the performance of geosynthetic reinforced pavements. For this study the subgrade used had a resilient modulus $E_s = 3,500$ psi (24 MN/m²). A nonlinear finite element analysis indicated that a low quality base has a modular ratio between the aggregate base, E_b, and the subgrade, E_s, of about $E_b/E_s = 1$ to 1.8 as compared to the average $E_b/E_s = 2.5$ used as the standard modular ratio in the cross-anisotropic analyses. The results of this study, which employed a modular ratio of 1.45, are summarized in Table 8.

Figure 13. Geosynthetic slack force = strain relations used in nonlinear model.

Prestressed Geosynthetic

An interesting possibility consists of prestressing the aggregate base using a geosynthetic to apply the prestressing force [*35, 36*]. The prestressing effect was simulated in the finite element model at both the bottom and the middle of the aggregate base. Once again, the same light reference pavement section was used consisting of a 2.5-in. (64 mm) asphalt surfacing, a variable thickness aggregate base, and a homogenous subgrade having a resilient modulus $E_s = 3,500$ psi (24 MN/m²). The cross-anisotropic, axisymmetric finite element formulation was once again used for the prestress analysis. A net prestress force on the geosynthetic of either 10, 20, or 40 lb/in. (2, 4, 7 kN/m) was applied in the model at a distance of 45 in. (1140 mm) from the center of loading.
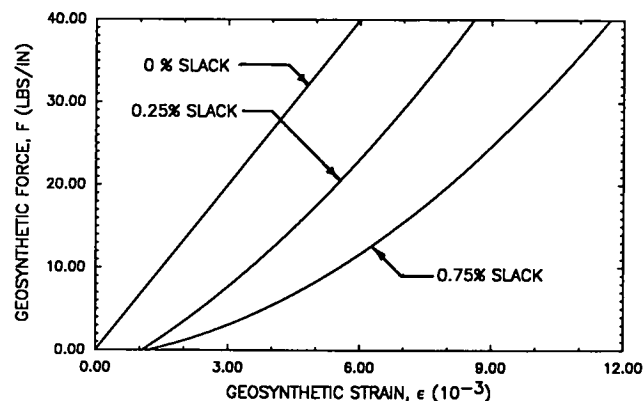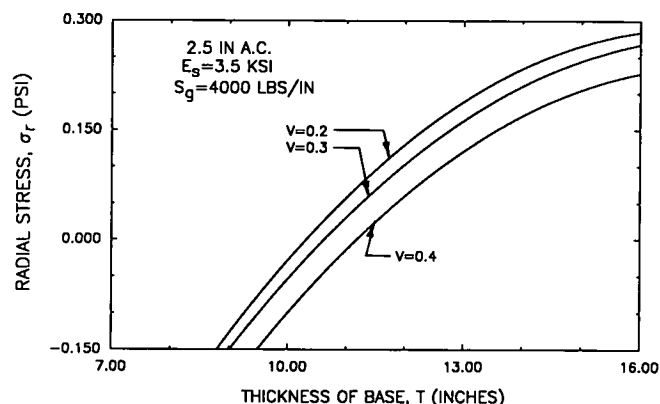
Figure 14. Variation of radial stress σ_r with Poisson's ratio (tension is positive).

Table 7. Effect of initial slack on geosynthetic performance—force in geosynthetic.

Design[3]	$E_{subg.}$ (avg) (ksi)	Stiffness[1] S_g (lbs/in.)	Slack (Percent)			
			None	0.25	0.75	1.4
2.5/9.72	12.3	6000	10.4	1.9	0.9	0[2]
		9000	13.3	–	–	0
2.5/12.0	12.4	6000	8.3	1.34	–	0[2]
		9000	10.6	–	–	0
2.5/15.3	12.4	6000	6.3	0.4	–	0[2]
		9000	8.5	–	–	0.4

Notes:
1. The initial stiffness of each geosynthetic was assumed to be $S_g = 300$ lbs/in. rather than zero. The stiffnesses shown are the limiting stiffnesses at the strain level where all the slack has been taken out; this strain level corresponds to the slack indicated.

2. Zero stress is inferred from the results obtained from the results for $S_g = 9000$ lbs/in.

3. The numbers 2.5/9.72, for example, indicate a 2.5 in. asphalt surfacing and a 9.72 in. aggregate base.

4. Base characterized using high quality properties (Table C-5, Appendix C).

5. Subgrade characterized by bilinear properties (Table C-5, Appendix C).

Table 8. Effect of base quality on geosynthetic reinforcement performance.[1]

BASE THICK. T (in.)	REDUCTION IN BASE THICKNESS				REDUCTION IN RUTTING			
	Vert. Subg. ϵ_v		AC Radial ϵ_r		Total Rutting[2]		Base Rutting	
	Poor Base Diff. (%)	Good Base Diff. (%)	Poor Base Diff. (%)	Good Base Diff. (%)	Poor Base Diff. (%)	Good Base Diff. (%)	Poor Base Diff. (%)	Good Base Diff. (%)
2.5 IN. AC SURFACING 3500 PSI SUBGRADE								
15.3	-11	-12	-8	-6.5	-11	-22	-2.0	-4
12.0	-11	-12	-10	- 8	-4.1	-30	-2.6	-6
9.75	-11	-14	-15	-12	-19.8	-39	-3.7	-10

Note: 1. Cross-anisotropic analysis; 2.5 in. AC surfacing; 3.5 ksi subgrade; Modular ratio $E_b/E_s = 1.45$.

2. Reduction in permanent deformation of the aggregate base and subgrade.

Theory shows that the force in a stretched axisymmetric membrane should vary linearly from zero at the center to maximum value along the edges. Upon releasing the pretensioning force on the geosynthetic, shear stresses are developed along the length of the geosynthetic as soon as it tries to return to its unstretched position. These shear stresses vary approximately linearly from a maximum at the edge to zero at the center, provided slip of the geosynthetic does not occur. The shear stresses transferred from the geosynthetic to the pavement can be simulated by applying statically equivalent concentrated horizontal forces at the node points located along the horizontal plane where the geosynthetic is located.

In the analytical model the effect of the prestretched geosynthetic was simulated entirely by applying appropriately concentrated forces at node points. The external wheel load, which was applied, will cause a tensile strain in the geosynthetic and hence affect performance of the prestressed system. Therefore, the tensile strain in the geosynthetic caused by the load was neglected in the prestress analysis; other effects due to the wheel loading were not neglected. The geosynthetic membrane effect due to the external loading that was neglected will reduce the prestress force, but improve performance because of the reinforcing effect of the membrane.

In the prestress model the outer edge of the finite element mesh used to represent the pavement was assumed to be restrained in the horizontal directions. This was accomplished by placing rollers along the exterior vertical boundary of the finite element grid. Edge restraint gives conservative modeling with respect to the level of improvement caused by the geosynthetic. The benefits derived from prestressing should actually fall somewhere between a fixed and free exterior boundary condition.

The important effect of prestressing either the middle or the bottom of the aggregate base on selected stresses, strains, and deflections within each layer of the pavement is given in Table 9. Comparisons of tensile strain in the asphalt layer and vertical compressive strain in the top of the subgrade are shown in Figure 15 for a geosynthetic stretching force of 20 lb/in. (3.5 kN/m). To reduce tensile strain in the asphalt surface or reduce rutting of the base, prestressing the middle of the layer is more effective than prestressing the bottom. On the other hand, if subgrade deformation is of concern, prestressing the bottom of the layer is most effective.
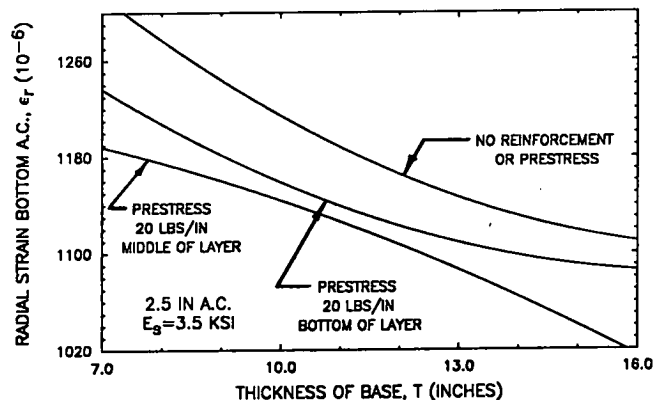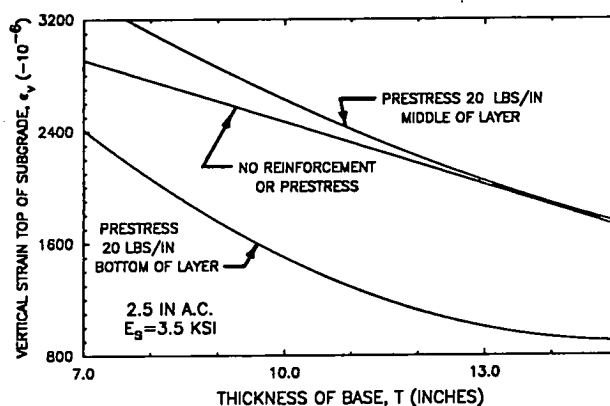

(a) Radial Strain ϵ_r in AC

(b) Vertical Strain ϵ_v on Subgrade

Figure 15. Theoretical influence of prestress on equivalent base thickness: ϵ_r and ϵ_v strain criteria.

Table 9. Effect of prestressing on pavement response: 2.5-in. AC, E_s = 3,500 psi.

PRE-STRESS FORCE (lbs/in)	VERT. SURFACE DEFLECTION		SUBGRADE				TENSILE STRAIN BOTTOM OF AC		TOP 1/3 OF AGGREGATE BASE								GEOSYN. FORCE (lbs/in)
			VERT. DEFLECTION		VERTICAL STRESS				VERTICAL STRESS		RADIAL STRESS		RADIAL STRAIN		VERTICAL STRAIN		
	σ_z(in.)	% Diff.	δ_z(in.)	% Diff.	σ_z(psi)	% Diff.	$\epsilon_r(10^{-6})$	% Diff.	σ_z(psi)	% Diff.	$\epsilon_r(10^{-6})$	% Diff.	$\epsilon_r(10^{-6})$	% Diff.	$\epsilon_r(10^{-6})$	% Diff.	
PRESTRESS @ BOTTOM: 2.5 IN. AC/7.5 IN. AGGREGATE BASE SUBGRADE E_s = 3500 PSI																	
0	-.08127	-	-.054916	-			1284		-29.96	-	-1786	-	1942	-	-3520	-	-
10	-	-	-		-	-	-	-	-	-	-	-	-	-	-	-	-
20	-.07672	+5.6	-.05093	-7.3	-	-	1222	-4.8	-30.81	-2.8	-1898	-6.3	1705	12.2	-3579	-	-
40																	
PRESTRESS @ BOTTOM: 2.5 IN. AC/12.0 IN. AGGREGATE BASE SUBGRADE E_s = 3500 PSI																	
0	-.07342	-	-.04278	-	-	-	1164	-	-36.41	-	-3.495	-	-1485	-	-3176	-	-
10	-.00241	96.7	-.000520	-98.7	-	-	210.7	-81.9	1.942	-94.7	-5.225	49.5	-120.3	91.9	179.4	94.4	-
20	-.06920	5.7	-.03754	-12.2	-	-	1125	-3.4	-37.91	-4.1	-3.617	-3.5	1408	-5.2	-3213	-1.2	-
40	-.06497	11.5	-.02999	-29.9	-	-	1085	-6.8	-39.54	8.6	-3.787	-8.4	-1334	-10.2	-3257	-2.6	-
PRESTRESS @ BOTTOM: 2.5 IN. AC/15.3 IN. AGGREGATE BASE SUBGRADE E_s = 3500 PSI																	
0	-.06937	-	-.03503	-	-	-	1119	-	-34.87	-	-3.230	-	-1371	-	-3004	-	-
10	-	-	-	-	-	-	-	-	-	-	-	-	-	-	-	-	-
20	-.06558	5.5	-.03032	-13.4	-	-	1089	-2.7	-35.94	-3.1	-3.334	-3.2	-1309	-4.5	-3026	0.7	-
40	-	-	-	-	-	-	-	-	-	-	-	-	-	-	-	-	-

Note: 1. Sign Convention: Tension is Positive;   2. Resilient Modulus of Subgrade = E_s;   3. "Diff." is the percent difference between a reinforced and a non-reinforced section.

Table 9. Continued.

PRE-STRESS FORCE (lbs/in)	BOTTOM 1/3 OF AGGREGATE BASE								SUBGRADE							
	VERTICAL STRESS		RADIAL STRESS		RADIAL STRAIN		VERTICAL STRAIN		VERTICAL STRESS		RADIAL STRESS		RADIAL STRAIN		VERTICAL STRAIN	
	σ_z(psi)	% Diff.	σ_r(psi)	% Diff.	$\epsilon_r(10^{-6})$	% Diff.	$\epsilon_r(10^{-6})$	% Diff.	σ_z(psi)	% Diff.	σ_r(psi)	% Diff.	$\epsilon_r(10^{-6})$	% Diff.	$\epsilon_r(10^{-6})$	% Diff.
PRESTRESS @ BOTTOM: 2.5 IN. AC/7.5 IN. AGGREGATE BASE SUBGRADE E_s = 3500 PSI																
0	-10.36	-	3.023	-	-1686	-	-3716	-	-9.410	-	.6086	-	1189	-	-2838	-
10	-	-	-	-	-	-	-	-	-	-	-	-	-	-	-	-
20	-10.90	5.2	.2438	91.9	1281	24.0	-3222	13.3	-8.054	14.4	-.1260	79.3	952.6	19.9	-2235	21.2
40	-	-	-	-	-	-	-	-	-	-	-	-	-	-	-	-
PRESTRESS @ BOTTOM: 2.5 IN. AC/12.0 IN. AGGREGATE BASE SUBGRADE E_s = 3500 PSI																
0	-12.54	-	.5169	-	1963	-	-1819	-	-7.012	-	.7704	-	935.6	-	-2189	-
10	-2.517	79.9	-.5531	207.0	-1054	153.7	-294.3	77.7	-.1578	97.7	-.5288	168.6	-40.87	104.4	95.99	104.4
20	-12.87	2.6	-.2492	148.2	283.7	85.5	-1765	3.0	-4.853	30.8	.00289	100.0	611.7	34.6	-1339	38.8
40	-14.92	19.0	-1.093	311.5	-1331	167.8	-1923	5.7	-5.310	24.2	-4.475	680.9	143.0	84.7	-1923	12.2
PRESTRESS @ BOTTOM: 2.5 IN. AC/15.3 IN. AGGREGATE BASE SUBGRADE E_s = 3500 PSI																
0	-9.781	-	.4400	-	161.1	-	-1420	-	-5.246	-	.8337	-	743.8	-	-1695	-
10	-	-	-	-	-	-	-	-	-	-	≙	-	-	-	-	-
20	-10.23	4.6	-.2520	157.3	107.8	93.3	-1392	2.0	-3.146	40.0	-.07175	108.6	402.9	45.8	-831.6	50.9
40	-	-	-	-	-	-	-	-	-	-	-	-	-	-	-	-

LARGE-SCALE LABORATORY EXPERIMENTS

Large-scale laboratory experiments were conducted to explore specific aspects of aggregate base reinforcement behavior, and to supplement and assist in verifying the analytical results previously presented. These large-scale tests were performed in a test facility 16 ft by 8 ft (4.9 by 2.4 m) in plan using a 1.5-kip (7kN) wheel loading moving at a speed of 3 mph (4.8 km/hr). Up to 70,000 repetitions of wheel loading were applied to the sections in a constant temperature environment.

Four series of experiments were carried out, each consisting of three pavement sections. The pavement sections included a thin asphalt surfacing, an aggregate base (with or without geosynthetic reinforcement), and a soft silty clay subgrade. A large number of potentially important variables exist which can influence the performance of an asphalt pavement having a geosynthetic reinforced aggregate base. Therefore, several compromises were made in selecting the variables included in the 12 sections tested.

Those variables included in the investigation were (1) geosynthetic type, (2) location of geosynthetic within the aggregate base, (3) prerutting the reinforced and unreinforced sections, (4) prestressing the aggregate base using a geosynthetic, and (5) pavement material quality. The test sections included in this study and their designations are given in Table 10. A knowledge of the notation used to designate the sections is helpful later when the observed results are presented. A section name is generally preceded by the letters PR (prerutted) or PS (prestressed) if prerutting or prestressing is involved. This designation is then followed by the letters GX (geotextile) or GD (geogrid) which indicates the type of geosynthetic used. The location of the geosynthetic, which follows, is represented by either M (middle of base) or B (bottom of base). Following this notation, the section PR-GD-B indicates that it is a prerutted section having a geogrid located at the bottom of the aggregate base.

Materials, instrumentation, and construction procedures used in the laboratory tests are described in Appendix D. A summary of the material properties is presented in Appendix E.

Pavement Test Procedures

Load Application

The pavement tests were conducted at the University of Nottingham in the Pavement Test Facility (PTF), as shown in Figure 16. This facility has been described in detail by Brown et al. [66]. Loading was applied to the surface of the pavement by a 22-in. (560 mm) diameter, 6-in. (150 mm) wide loading wheel fitted to a support carriage. The carriage moves on bearings between two support beams which span the long side of the rectangular test pit. The beams, in turn, are mounted on end bogies that allow the whole assembly to traverse across the pavement. Two ultra-low friction rams controlled by a servohydraulic system are used to apply load to the wheel and lift and lower it. A load feedback servomechanism is incorporated in the system to maintain a constant wheel loading. The maximum wheel load that can be achieved by the PTF is about 3.4 kip (15 kN), with a speed range of 0 to 10 mph (0 to 16 km/hr). The whole assembly is housed in an insulated room having temperature control.

Multiple Track Tests

The moving wheel in the PTF can be programmed to traverse, in a random sequence, across the pavement to nine specified positions (four on each side of the centerline). At each position a predetermined number of wheel passes is applied. The spacing
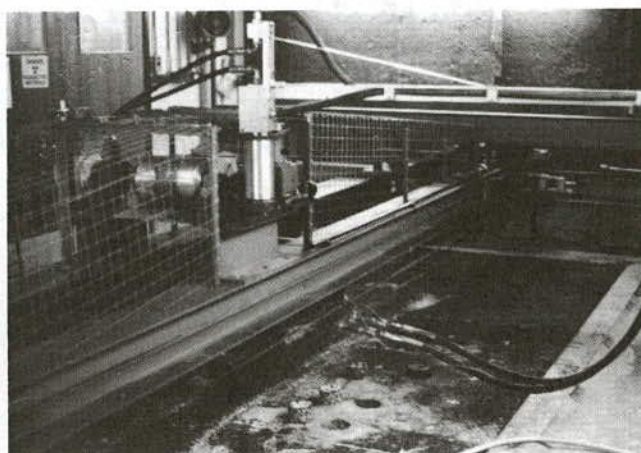
Table 10. Summary of test sections.

Test Series	Proposed Geometry	Section Designation	Details of Geosynthetic and Section Specification
1	1 in. A.C. 6 in. Sand & Gravel Base	PR-GX-B	Geotextile placed at bottom of Base; Subgrade prerutted by 0.75 in.
		CONTROL	Control Section; no geosynthetics and no prerutting
		GX-B	Same as PR-GX-B; no prerutting
2	1.5 in. A.C. 8 in. Crushed Limestone	PR-GD-B	Geogrid placed at bottom of Base; Subgrade prerutted by 0.4 in.
		CONTROL	Control Section
		GD-B	Same as PR-GD-B; no prerutting
3		GX-B	Geotextile placed at bottom of Base
		CONTROL	Control Section; Prerutting carried out at single track test location
		GX-M	Geotextile placed at middle of Base
4		GX-M	Same as GX-M (Series 3); Prerutting carried out at single track test location
		GD-M	Same as GX-M but use geogrid
		PS-GD-M	Prestressed Geogrid placed at middle of base

Notes for section designation: PR = Prerutted PS = Prestress
GX = Geotextile GD = Geogrid
B = Bottom of Base
M = Middle of Base

Figure 16. Pavement test facility.

between wheel positions was set at a constant step of 3 in. (75 mm). A realistic simulation can be obtained of actual loading where traffic wander exists. Table 11 gives the loading sequence adopted for the last three series of tests. It consisted of a 250-pass cycle, starting with 55 passes along the center of the section (position 5), followed by 15 passes at position 8, then 7 passes at position 9 until it finished back at the center-line where the cycle was repeated. During the scheduled recording of output from the instrumentation, the center-line track was given an additional 100 passes of wheel load before actual recording began. This procedure ensured that consistent and compatible outputs were recorded from the instruments installed below the center-line of the pavement. The total number of passes in the multiple track tests for the second to fourth series were 69,690, 100,070, and 106,300, respectively. The distribution of these passes across each loading position is shown in Figure 17. Note that the width of the tire is larger than the distance between each track position. Therefore, during the test, the wheel constantly overlapped two tracks at any one time. Hence, the numbers shown in Table 11 and Figure 17 apply only to the center of each track position.

In the first series of tests, because of the rapid deterioration and very early failure of the pavement sections, the loading program described previously could not be executed. The total number of wheel load passes for this test series was 1,690, and their distribution is shown in Figure 17.

Single-Track Tests

On completion of the main multitrack tests, single-track tests were carried out along one or both sides of the main test area where the pavement had not been previously loaded. These special tests normally involved the use of a much higher wheel load, so that the deterioration of the pavement structure would be greatly accelerated. Stress and strain data were not obtained for these single-track tests, because instruments were not located beneath the loading path. Only surface rut depth was measured. Nonetheless, these tests helped greatly to confirm trends observed in the development of permanent deformation during the multitrack tests. The single-track tests also made possible extra comparisons of the performance of pavement sections tested in the prerutted and nonprerutted condition. Three additional single-track tests were performed during the second to fourth test series. Details of these tests and their purposes are given in Table 12. The designations of the test sections follow those for the multitrack tests previously described.

Wheel Loads

Bidirectional wheel loading was used in all tests. Bidirectional loading means that load was applied on the wheel while it moved in each direction. The load exerted by the rolling wheel on the pavement during test series 2 through 4 of the multitrack tests was 1.5 kip (6.6 kN). In the first series of tests, because of rapid deterioration of the pavement and hence large surface deformations, difficulties were encountered at an early stage of the test in maintaining a uniform load across the three pavement sections that underwent different amounts of deflection. Therefore, while the average load was 1.5 kip (6.6 kN), the actual load varied from 0.7 to 2.5 kip (3 to 11 kN). In subsequent test

Table 11. Transverse loading sequence used in multiple track test series 2 through 4. Note: Each load position is separated by a 3-in. (75 mm) distance.

SEQUENCE NUMBER	1	2	3	4	5	6	7	8	9
POSITION NUMBER	5	8	9	7	6	4	1	2	3
DISTANCE FROM CENTRE LINE (IN)	0	9	12	6	3	3	12	9	6
NUMBER OF PASSES	55	15	7	30	45	45	8	15	30
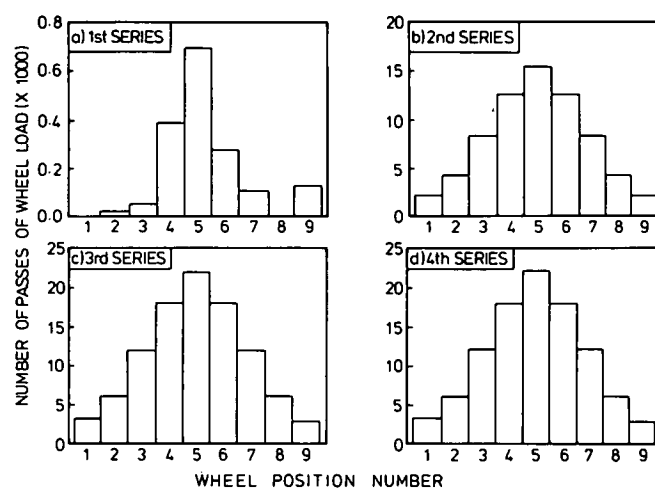
Figure 17. Distribution of the number of passes of wheel load in multiple track tests.

series, however, much stronger pavement sections were constructed, and refinements were made in the servosystem which controlled the load. As a result, only minor variations of load occurred, generally less than 10 percent of the average value. This load variation was probably also due to the unevenness in the longitudinal profile of the pavement. In the single-track tests, a wheel load of 1.8 kip (8 kN) was used for the first test series. For all other test series a 2-kip (9 kN) load was applied. With the exception of the single-track test carried out during the first series, all of these supplementary tests employed bidirectional loading.

The tire pressure was maintained at 80 psi (550 kN/m²). Based on a previous investigation of the effect of wheel tread, tire wall strength, tire pressure and load, the contact pressures acting on the pavement from a 1.5-kip and 2-kip (6.6 and 9 kN) wheel load were estimated to be 67 psi and 73 psi (460 and 500 kN/m²), respectively. These gave radii of contact areas, assuming them to be circular, of 2.7 in. and 3 in. (68 and 76 mm), respectively.

The wheel moved at a speed of about 2 to 3 mph (3.2 to 4.8 km/hr) with slight variations between forward and reversed directions. Near the end of the test when the pavement surface became uneven, a slower speed was sometimes necessary to maintain constant loading.

The temperature inside the PTF was maintained at 68°F ± 3.6°F (20 ± 2°C) throughout the testing. Temperatures at the

Table 12. Description of test sections used in laboratory experiment and purpose of the supplementary single-track tests.

Test Series	Section Geometry	Section Designation	Details of Geosynthetic and Section Specification	Purpose of Test
2	8 in. Crushed Limestone	GD-B	Geogrid at bottom of Base	To compare performance of reinforced and un-reinforced un-bound pavement sections
		CONTROL	Control Section	
		GD-B	Same as the 1st GD-B·	
3	1.5 in. A.C. 8 in. Crushed Limestone	GX-B	Geotextile at bottom of base	To compare performance of non-prerut-reinforced and prerut-unreinforced sections
		PR-CONTROL	Control section;base prerutted by 2 in.	
		GX-M	Geotextile at middle of Base	
4		PR-GX-M	Same as GX-M; base prerutted by 2 in.	To determine performance of reinforced-and-prerutted and pre-stressed but non-pre-rutted sections
		PR-GD-M	Same as PR-GX-M; use geogrid	
		PS-GD-M	Prestressed Geogrid at middle of non-prerutted base	

```
* PR= Prerutted    GX= Geotextile  M= Middle of Base
  PS= Prestressed  GD= Geogrid     B= Bottom of Base
```

asphalt surface and within the aggregate base and the subgrade were found to be about 2°F to 4°F (1 to 2°C) lower than that of the air. However, it was previously observed that during long continuous runs of the PTF, the temperature of the asphalt in the wheel track could increase by as much as 9°F (5°C) because of the repeated loading by the wheel.

Data Recording Procedure

The transverse profile and permanent strain readings from the aggregate base and silty clay subgrade were taken at appropriate intervals during testing of all pavement sections to establish their deformation characteristics under loading. In addition, elevations of all the reference points at the surface of the sections along the centerline were measured and checked. During the actual loading, resilient strains and transient stresses were recorded on an ultraviolet oscillograph, which also recorded wheel load, position, and speed. All pressure cells could be recorded continuously, but it was only possible to record one strain coil pair at a time. Therefore, it normally required about 100 to 200 wheel load passes at the centerline to obtain a complete set of strain coil readings. A "peak hold" data acquisition system was later used to record the peak values of the stress and strain pulses. The outputs from the thermocouples, which measured temperature at selected depths in the pavement structure, were monitored regularly by means of a readout device. Air temperature of the PTF was obtained from a thermometer placed inside the facility.

Test Results

A summary of important measured pavement response variables recorded at both an early stage of loading, and also near the end of each test series, is given in Table 13. Unless indicated, all the results were obtained from multitrack tests. Most of the results presented show variation of test data either with time

(i.e., number of load cycles) or with depth in the pavement structure at a particular time. The permanent strain results were obtained near the end of the test, after relatively large permanent deformations had developed. Vertical resilient strains are given at early stages of the test when the pavement structure was still undamaged; usually only relatively small changes of this variable occurred with time.

Direct comparisons can be made between each test section within a given series. In addition, comparisons can be made between test series if appropriate adjustments are made in observed responses, based on the relative behavior of the similar control section in each test series. Whenever there is more than one value of data available (e.g., permanent vertical deformation, permanent vertical strain, subgrade stress), an average value is reported in the tables and figures. Erratic data, however, are excluded from the averaging process.

Permanent Vertical Deformation

In this study the permanent vertical surface deformation of the pavement is taken as the primary indicator of performance. The accumulation of surface rutting measured by the profilometer is shown in Figure 18. Profiles showing the permanent deflection basin at the end of the tests are given in Figure 19. The permanent deformation occurring in the base and subgrade is shown in Figures 20 and 21, respectively, and also in Table 13. Permanent vertical deformation in both layers was calculated from the changes in distance between the pairs of strain coils.

Figure 18 clearly shows that the pavement sections used in the first test series are very weak, with large deformations developing in less than 2,000 passes of wheel load. These results indicate that the inclusion of a stiff to very stiff geotextile at the bottom of the very weak sand-gravel base reduces the amount of rut by about 44 percent for a rut depth of 0.43 in. (11 mm) in the control section. Furthermore, prerutting does not appear to improve the overall rutting performance of the weak pave-

Table 13. Summary of measured pavement response data near the beginning and end of the tests for all test series.

Test Series 1											
		Data at 150 passes of 1.5 kips wheel load					Data at 1262 passes of 1.5 kips wheel load				
Section	Section	Permanent Deformation (in)			Subgrade	Asphalt	Permanent Deformation (in)			Subgrade	Asphalt
Designation[1]	Geometry[2]	Total	Base	Subgd	σ_v(psi)[3]	ϵ_t (με)[4]	Total	Base	Subgd	σ_v (psi)[3]	ϵ_t (με)[4]
PR-GX-B	1.2/6.3	0.30	0.28	0.02	6.3	/	0.63	0.59	0.04	6.5	/
CONTROL	1.4/5.8	0.43	0.31	0.12	7.5	3047	0.94	0.69	0.25	10.2	3929
GX-B	1.3/6.1	0.24	0.15	0.09	8.0	/	0.55	0.35	0.20	11.6	/

Test Series 2											
		Data at 10000 passes of 1.5 kips wheel load.					Data at 70000 passes of 1.5 kips wheel load				
PR-GD-B	1.2/8.5	0.28	0.21	0.03	7.8	3738	0.56	0.45	0.03	8.0	2676
CONTROL	1.2/8.3	0.83	0.57	0.21	7.5	3761	1.55	1.07	0.37	8.6	2941
GD-B	1.1/8.1	0.76	0.60	0.10	5.5	4433	1.36	1.10	0.15	6.0	3788

Test Series 3											
GX-B	1.2/8.1	0.34	0.28	0.03	6.9	2355*	0.98	0.77	0.13	6.3	4090**
CONTROL	1.2/8.3	0.39	0.29	0.07	6.0	2983*	0.90	0.62	0.13	5.9	/
GX-M	1.3/7.7	0.28	0.20	0.06	6.2	2198*	0.70	0.51	0.15	6.5	2917**

Test Series 4											
GX-M	1.5/8.3	0.26	0.17	0.03	8.0	3450	0.68	0.46	0.07	7.7	2850
GD-M	1.4/8.5	0.18	0.09	0.04	9.1	/	0.42	0.25	0.07	8.5	/
PS-GD-M	1.6/8.6	0.10	0.06	0.01	8.2	2350	0.26	0.17	0.03	7.8	2700

Notes: 1. PR=Prerutted;PS=Prestressed;GX=Geotextile;GD=Geogrid;M=Middle of Base;B=Bottom of base.
2. Thickness of asphaltic/granular base layer. In 1st series, HRA and sand & gravel used. In other series, AC and dolomitic limestone were used.
3. Vertical transient stress at the top of subgrade.
4. Longitudinal resilient strain at the bottom of the asphaltic layer.
* measured at beginning of test at 400 passes of wheel load.
** measured at 10,000 passes of wheel load.
/ data not available.

NOTE: PR = Prerutted   GX = Geotextile   M=Middle of Base
PS = Prestressed   GD = Geogrid   B= Bottom of Base
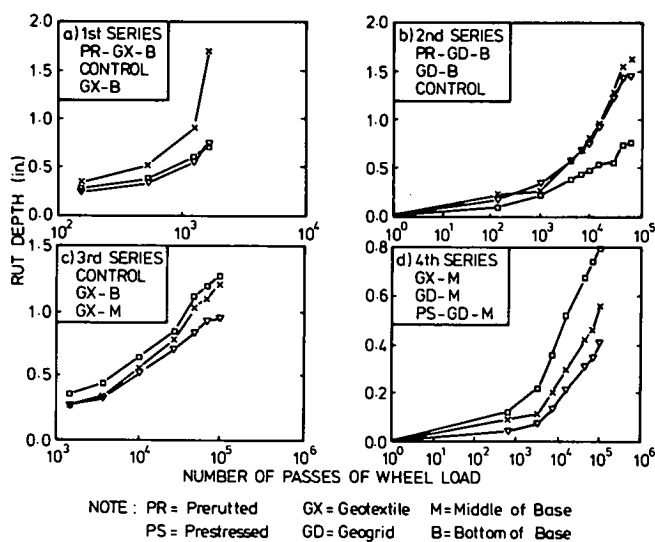
Figure 18. Variation of rut depth measured by profilometer with the number of passes of 1.5-kip wheel load—all test series.

Note: PR = Prerutted   GX= Geotextile   M= Middle of Base
PS = Prestressed   GD= Geogrid   M= Middle of Base
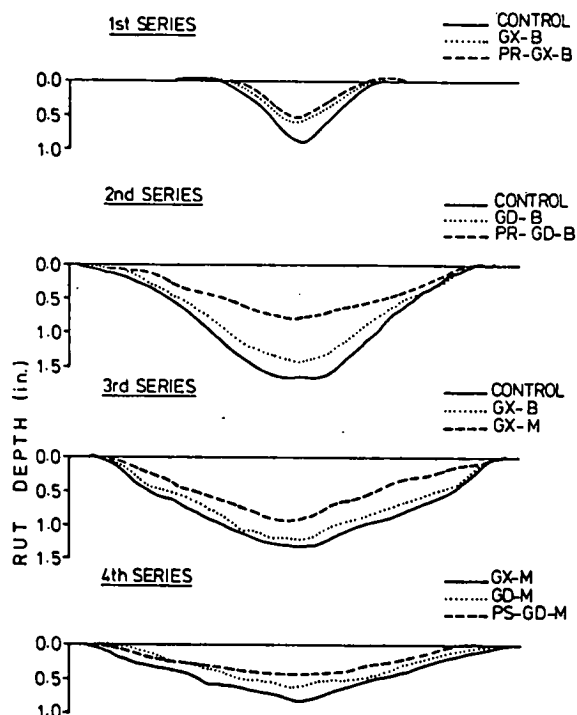
Figure 19. Pavement surface profiles measured by profilometer at end of tests—all test series.
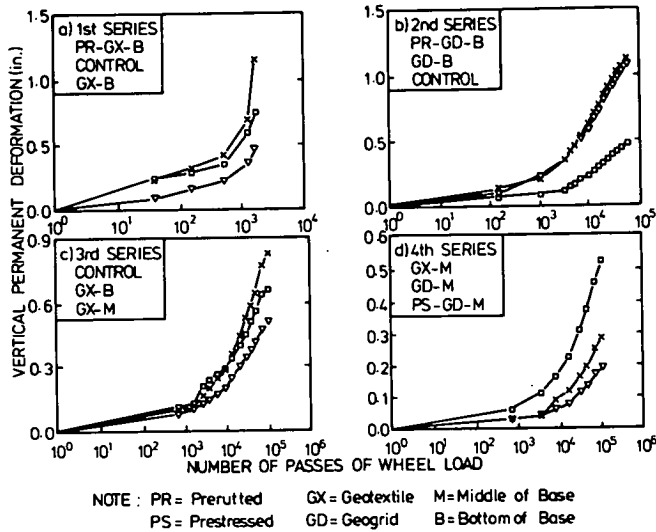
Figure 20. Variation of vertical permanent deformation in the aggregate base with number of passes of 1.5-kip wheel load—all four test series.
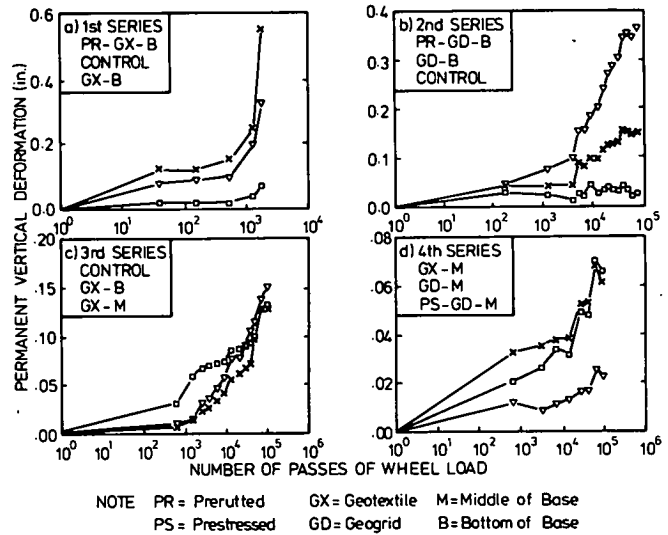

Figure 21. Variation of vertical permanent deformation in the subgrade with number of passes of 1.5-kip wheel load—all four test series.

ment section compared to the geotextile reinforced section that was not prerutted.

Because of the use of a higher quality aggregate base and thicker base and surfacing, the life for the pavement sections of the other three series of tests was considerably longer, as shown in Figure 18. However, in contrast to the results of the first test series, the prerutted section in the second series performed best. This section was reinforced with a geogrid at the bottom of the base and resulted in a 66 percent reduction in total rutting of the base and subgrade. Thus, prerutting of the reinforced section was quite effective. This finding by itself is misleading, as will be discussed subsequently for the single test track results, because similar, very good performance was also observed for prerutted sections that were not reinforced.

Only an 8 percent reduction in rutting was observed for the geogrid reinforced section used in test series 2 which was not prerutted (Fig. 18(b)). A similar, relatively low level of improvement with respect to rutting (13 percent reduction) was observed for the section in test series 3 that was reinforced with a stiff to very stiff geosynthetic (S_g = 4,300 lb/in.; 750 kN/m) located at the bottom of the layer (Table 13; Fig. 18(c)). This section was not prerutted. When the location of the geotextile was raised to the middle of the aggregate base in test series 3, the amount of rutting was reduced by a total of 28 percent; most of this improvement occurred within the aggregate layer (Table 13; Fig. 18(c)).

Results from the last series of tests indicate that prestressing the geosynthetic appears to improve performance compared with a nonprestressed section having the same geogrid reinforcement (Table 13; Fig. 18(d)). Further, use of geogrid reinforcement, despite its lower stiffness (S_g = 1,600 lb/in.; 280 kN/m) resulted in better performance than a higher stiffness, woven geotextile when both were placed at the middle of the granular layer (Fig. 18(d)).

A large portion of the total permanent deformation occurred within the aggregate base. Therefore, it follows that the pattern of permanent deformation as a function of load repetitions observed in the base was very similar to that observed at the pavement surface, as can be seen by comparing Figure 18 with Figure 20. Permanent vertical deformation in the subgrade was relatively small compared to that occurring in the base, particularly for the prerutted sections. An important reduction in subgrade deformation was evident when a geosynthetic was placed directly on top of the subgrade, as shown in Table 13 and Figure 21. Reductions in subgrade rutting of 25 to 57 percent were observed for this condition.

The trend in the development of total permanent deformation in all 12 sections of the four test series in the multitrack loading tests was generally confirmed by the single track studies (Fig. 22).

Permanent Vertical Strain

The variation of permanent vertical strain with depth for all the sections at the end of testing is shown in Figure 23. The average values of strain are plotted at the mid-point between the two strain coils which measure the corresponding vertical movement. In general, the pattern of results is very similar for all test series, with large permanent strain at the top of the granular base, decreasing rapidly with depth towards the subgrade. Other interesting results that can be obtained from these figures reveal the following differences between pavement sections:

1. When comparing results from the geosynthetic reinforced and control sections, a redistribution of vertical permanent strain is seen to occur because of the presence of the reinforcement. For sections with the geosynthetic reinforcement placed at the bottom of the granular base, a decrease of strain is generally observed near the top of the subgrade. At the same time (with the exception of the first series results), an increase in permanent
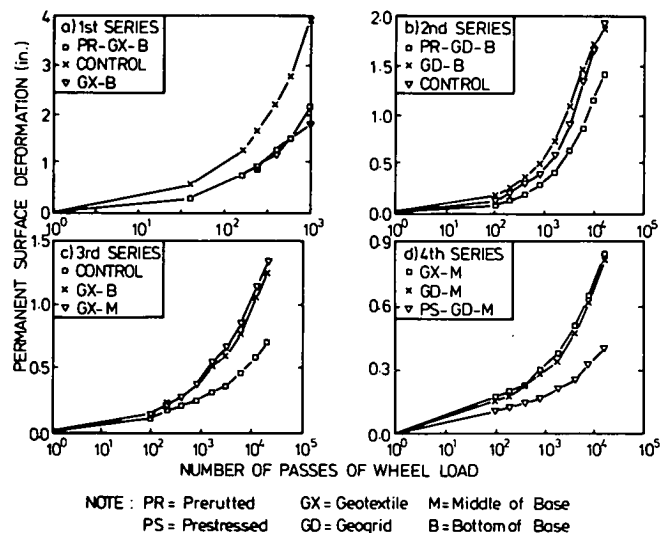
Figure 22. Variation of permanent surface deformation with number of passes of wheel load in single track tests—all four test series.

strain occurred in the top of the granular base.

2. Figure 23 shows that as a result of placing the geotextile at the middle of the aggregate base, a substantial decrease in permanent vertical strain occurs immediately below the geotextile, while permanent strain at the top of the subgrade increased.

3. The vertical permanent strains for the two prerutted sections are, in general, smaller than those in the nonprerutted sections with or without reinforcement, as shown in Figures 23(a) and 23(b). The only exception is the permanent strain developed within the prerutted sand-gravel base, which shows a greater value than its nonprerutted counterparts.

4. Prestressing of the geogrid appears to reduce the development of permanent vertical strain in both the granular base and the subgrade layer.

Vertical Resilient Strain

The variations of vertical resilient strain with depth for all the pavement sections are shown in Figure 24. The results for the first series of tests are considered unreliable because the pavement structure deteriorated rapidly at quite an early stage of the experiment. As a result, uniform conditions across all the three sections could not be maintained while the resilient response of all the sections was being measured. Nevertheless, it
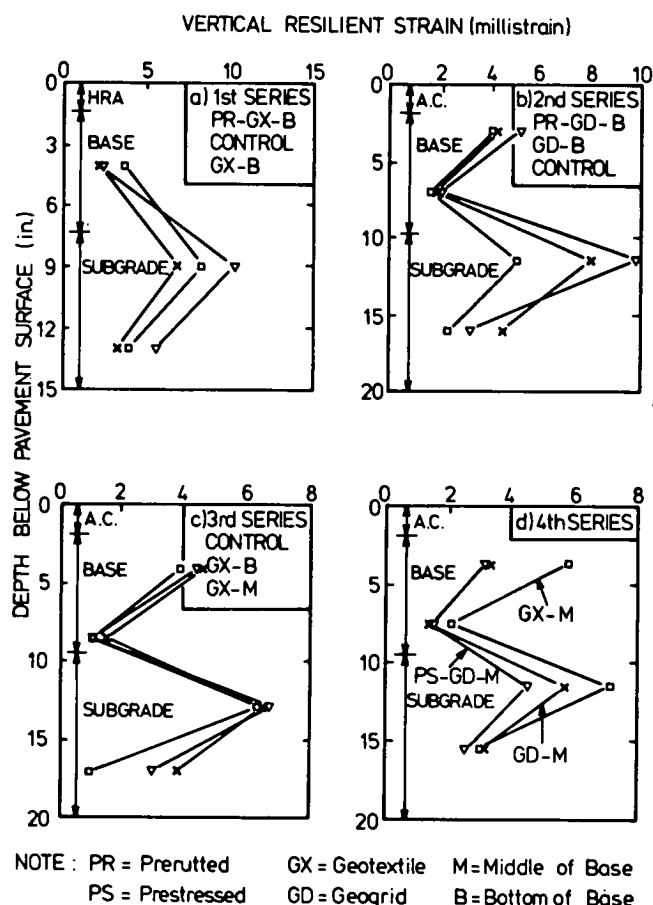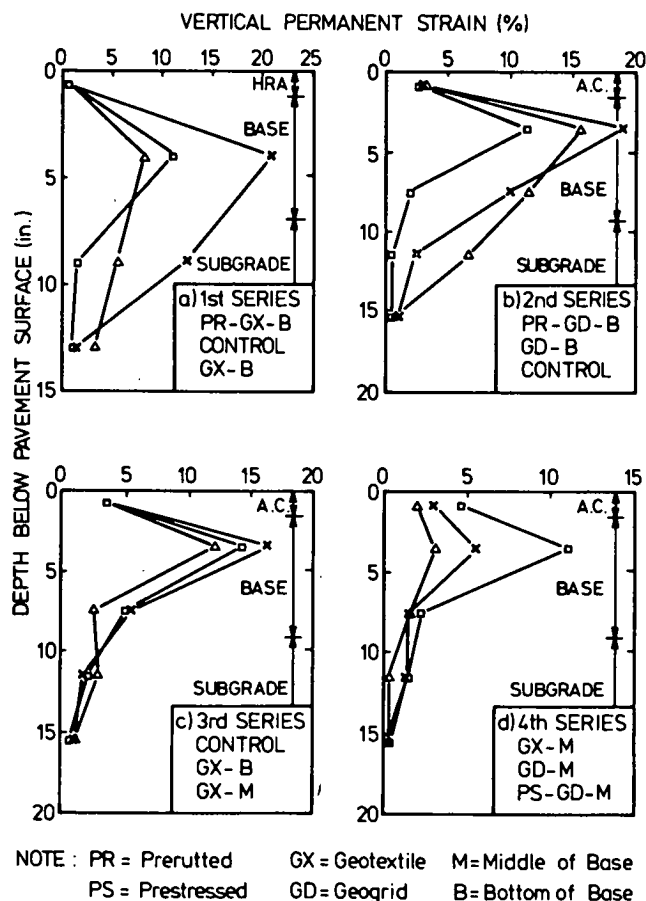
Figure 23. Variation of vertical permanent strain with depth of pavement for all four test series.

Figure 24. Variation of vertical resilient strain with depth of pavement for all test series.

is believed that the recorded strains shown in Figure 24(a) at least show the correct trends. For other series of tests, however, the 100 to 200 passes of wheel load required to complete the recording procedure did not have a significant influence on the consistency of the results.

Figure 24 shows that the resilient strain profile for all the sections has a similar shape and, within one series of tests, a similar magnitude of strain. In general, large strains were obtained at the top of both the aggregate base and subgrade. The nonreinforced control sections (with the exception of the first series of tests) normally exhibited slightly higher resilient strains than the reinforced sections. However, overall resilient response of the pavement sections does not seem to be significantly influenced by the geosynthetic reinforcement, regardless of its location within the pavement structure. Both prestressing and prerutting appear to reduce significantly the resilient strain at the top of the subgrade.

Lateral Resilient Strain

Lateral resilient strains were only recorded from the strain coils installed on the geosynthetics and in the complementary location of the control sections. The lateral resilient strains recorded during the four test series are given in Tables 14 and 15. In general, for a given test series the magnitude of the resilient lateral strain in the geosynthetic reinforcement of both sections is quite similar, but that in the nonreinforced control section tends to be considerably higher. No consistent trend emerged regarding the effect of geosynthetic stiffness and location of the reinforcement on the measured resilient lateral strain.

Longitudinal Resilient Strain

The results of the resilient longitudinal strain for the asphalt surfacing and the aggregate base are given in Tables 14 and 15 and Figure 25, respectively. Longitudinal resilient strains at the bottom of the asphalt surfacing were measured for all the sections. Beginning with the third test series they were also measured in two of the three sections at both the top and bottom of the aggregate layer. Unlike the vertical resilient strain, the longitudinal resilient strain varied greatly throughout the test. Generally, longitudinal resilient strain increased in the top and bottom of the aggregate base as the pavement started to deteriorate. Only resilient strains at the beginning of the test are given in Tables 14 and 15. For resilient longitudinal strains measured within the aggregate base, there did not appear to be a consistent development trend. Longitudinal strain at the bottom of the asphalt surfacing also varied from one series of tests to another. This could be at least partly due to the slight differences in the finished thickness of the surfacing and base and small differences in material properties.

Transient Stresses

The variation of transient vertical stress at the top of the subgrade during each test for all the pavement sections is shown in Figure 26. Transient stress is that change in stress caused by the moving wheel load. The subgrade stress for the last three

test series remained reasonably constant throughout the test, with the magnitude of vertical stress typically varying from about 6 psi to 9 psi (42 to 63 kN/m²). For the first series of tests, however, the subgrade stress rapidly increased as the pavement developed large permanent deformations early in the experiment. A consistent influence of geosynthetic reinforcement on vertical subgrade stress was not observed in any of the test series.

Longitudinal, horizontal transient stress (in the direction of wheel traffic) at both the top and bottom of the aggregate base was measured in the third and fourth test series. The results, shown in Figure 27, indicate that the horizontal stress at the top of the granular layer increased throughout each test. Figure 27(a) also suggests that the inclusion of geosynthetic reinforcement at the middle of the aggregate base may result in a slower rate of increase in horizontal stress at the top of the layer. The horizontal stress at the bottom of the aggregate base, on the other hand, did not appear to be influenced either by the progress of the test nor by the presence of a geosynthetic at the center of the layer.
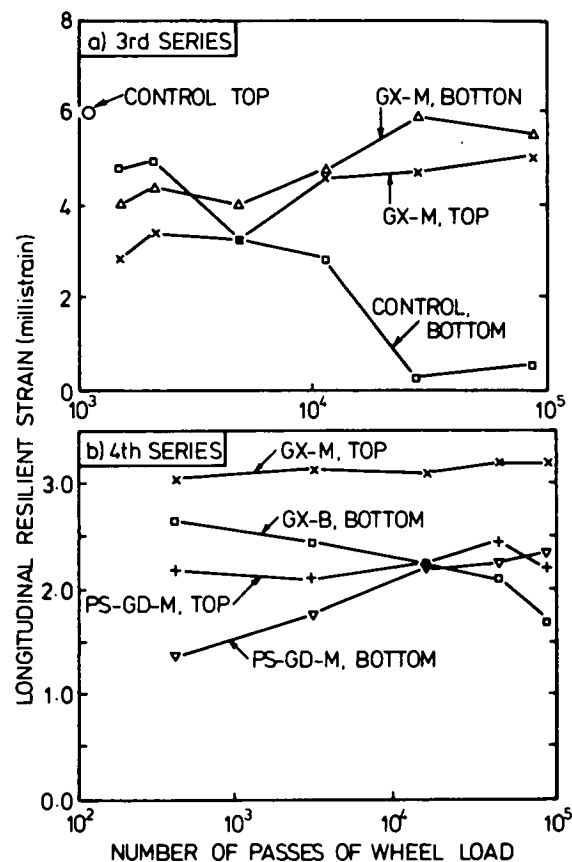
Note: 1. For section designation—
      PS = Prestressed GX = Geotextile GD = Geogrid
      M, B = Geosynthetics placed at middle, bottom of base

      2. For location of strain measurement—
      TOP, BOTTOM = strain measured at top, bottom of base

Figure 25. Variation of longitudinal resilient strain at top and bottom of granular base with number of passes of 1.5-kip wheel load—third and fourth series.

Table 14. Summary of lateral resilient strain in geosynthetics and longitudinal resilient strain at bottom of asphalt—test series 1 and 2.

Test Series	No. of Passes	Section Designation*	Lateral Resilient Strain in Geosynthetic** (με)	Longitudinal Resilient Strain at bottom of asphalt (με)
1	50	PR-GX-B CONTROL GX-B	1480 4740 1200	/ 2047 /
	1675	PR-GX-B CONTROL GX-B	2317 11340 2561	
2	250	PR-GD-B CONTROL GD-B	1585 3130 2616	3725 3860 4121
	40000	PR-GD-B CONTROL GD-B	1730 3410 2852	

Note: * PR= Prerutted   GX= Geotextile M= Middle of Base
.PS= Prestressed GD= Geogrid   B= Bottom of base
** In the control sections, the measured strain is that of the soil.

Table 15. Summary of lateral resilient strain in geosynthetics and longitudinal resilient strain at bottom of asphalt—test series 3 and 4.

Test Series	No. of Passes	Section Designation	Lateral Resilient Strain in Geosynthetic	Longitudinal Resilient Strain at bottom of asphalt
3	400	GX-B CONTROL GX-M	1413 6871 2103	2355 2983 2198
	70000	GX-B CONTROL GX-M	1609 4765 2242	
4	400	GX-M GD-M PS-GD-M	2550 1500 1500	2800 / 1800
	46000	GX-M GD-M PS-GD-M	1650 1800 2050	

Note: * PR= Prerutted   GX= Geotextile M= Middle of Base
.PS= Prestressed GD= Geogrid   . B= Bottom of base
** In the control sections, the measured strain is that of the soil.

Single-Track Supplementary Tests

After performing the multiple track tests in test series 2 through 4, single-track tests were conducted along the side of the test pavements. These tests were carried out where wheel loads had not been previously applied during the multiple track tests. The single-track tests consisted of passing the moving wheel load back and forth in a single wheel path. These special supplementary tests contributed important additional pavement response information for very little additional effort. The single-track tests performed are described in Table 12, and the results of these tests are shown in Figure 28. The following observations,

which are valid for the conditions existing in these tests, can be drawn from these experimental findings:

1. Placement of a geogrid at the bottom of the aggregate base did not have any beneficial influence on the performance of the unsurfaced pavement in test series 2 (Fig. 28(a)). This test series was conducted during the excavation of test series 2 pavement after the surfacing was removed. For these tests the permanent vertical deformation in the two reinforced sections and the unreinforced control section were all very similar; permanent deflections in the reinforced sections were actually slightly greater throughout most of the test. A significant part of the
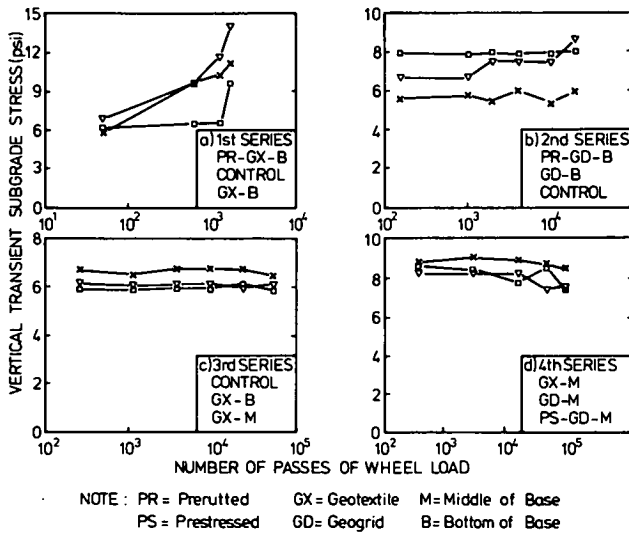
Figure 26. Variation of transient vertical stress at top of subgrade with number of passes of 1.5-kip wheel load—all test series.
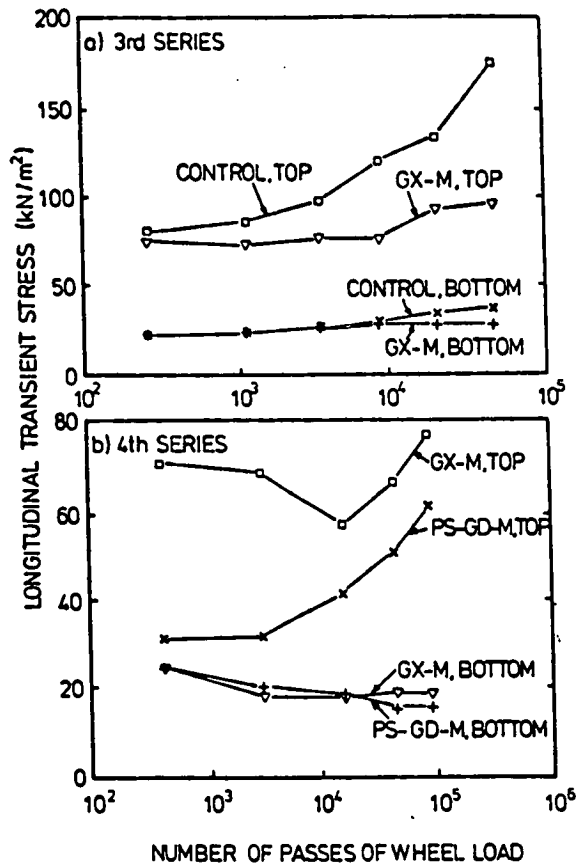
Figure 27. Variation of transient longitudinal stress at top and bottom of granular base with number of passes of 1.5-kip wheel loads—third and fourth series.

permanent deformation probably occurred in the granular base above the location of the grid; other tests indicate that a higher grid location should give an improvement in performance.

2. A surfaced pavement section that has been prerutted during construction, but is not reinforced, can perform better than a similar section that has been reinforced with a very stiff geotextile at the middle of the aggregate base, but has not been prerutted (Fig. 28(b)).

Placement of the very stiff geotextile at the middle of the layer did result, for the conditions of the test, in important reductions in rutting compared to placing the same reinforcement at the bottom of the layer.

3. The improvement in performance is greater because of a combination of prerutting and geosynthetic reinforcement at the middle of the aggregate base than it is because of prestressing the same geogrid at the same location within the aggregate base (Fig. 28(c)).

Surface Condition and Soil Contamination

Surface Condition at End of Test. The surface condition of the pavement sections at the end of the tests is shown in Figure 29. With the exception of the first test series, no Class 2 cracks developed within the wheel track during the multitrack tests. Class 2 cracking is defined as the stage where cracks have connected together to form a grid-type pattern.

During the single-track tests, however, surface cracks were observed along the shoulder of the deeper ruts. Heaving outside of the rut was generally not observed for the sections with crushed limestone base. However, heaving along the edge was evident for the three sections of test series 1 using the sand-gravel base.

Soil Contamination. Contamination of the aggregate base by the silty clay subgrade was evident in most sections except those where a geotextile was placed directly on top of the subgrade.
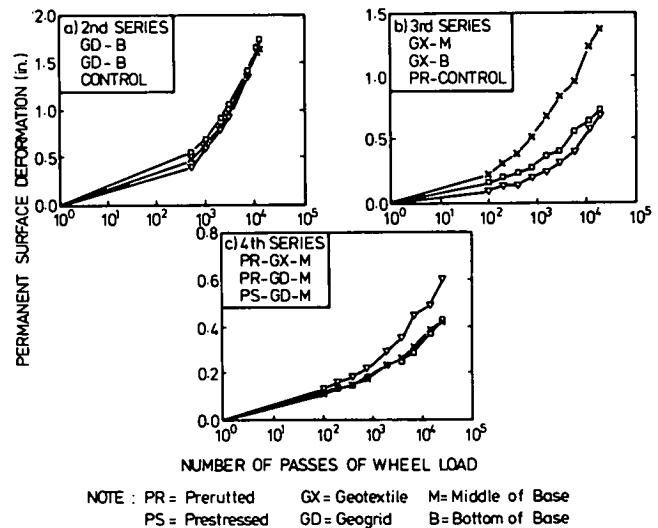
Figure 28. Variation of permanent surface deformation with number of passes of wheel load in supplementary single track tests—second to fourth test series.
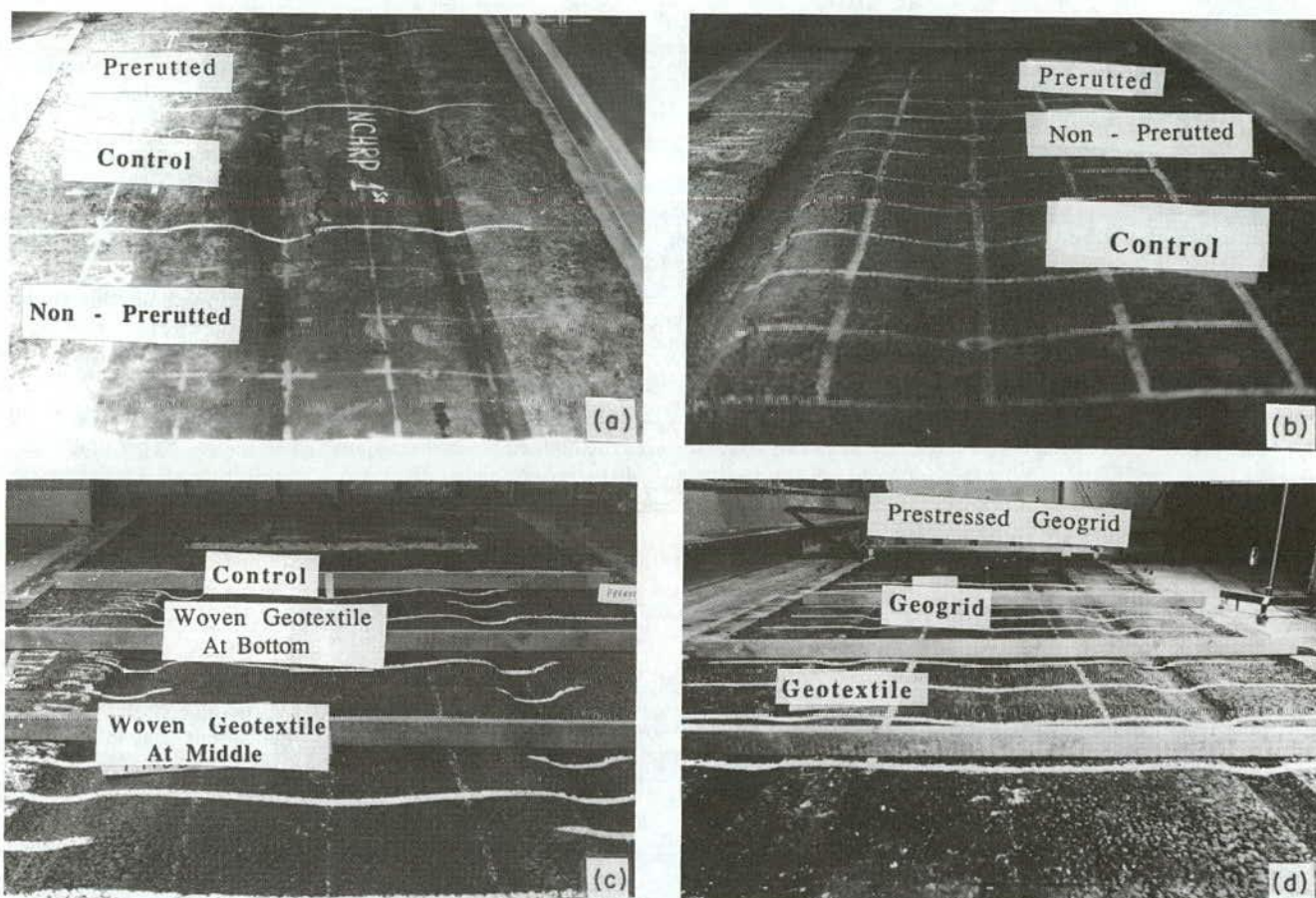
Figure 29. Pavement surface condition at the end of the multitrack tests—all test sections: (a) first test series, (b) second test series, (c) third test series, and (d) fourth test series.

Contamination occurred as a result of both stone penetration into the subgrade and the subgrade soil migrating upward into the base. When a geogrid was placed on the subgrade, upward soil migration appeared to be the dominant mechanism of contamination. Depth of soil contamination of the base was found to be in the range of 1 in. to 1.5 in. (25 to 38 mm).

CHAPTER THREE

SYNTHESIS OF RESULTS—INTERPRETATION, APPRAISAL, AND APPLICATION

INTRODUCTION

The present study is concerned with the use of a geosynthetic within the unstabilized aggregate base of a surfaced, flexible pavement. Geosynthetics may be included within the aggregate base of a flexible pavement structure to perform the following important functions: (1) *reinforcement:* to structurally strengthen the pavement section by changing the response of the pavement to loading; (2) *separation:* to prevent contamination of an aggregate layer by the underlying subgrade and hence maintain a clean interface; and (3) *filtration:* to aid in improving subsurface drainage and allow the rapid dissipation of excess subgrade pore pressures caused by traffic loading; at the same time, the geosynthetic must minimize the possibility of erosion of soil into the drainage layer and resist clogging of the filter over the design life of the pavement.

The emphasis of this study was placed on the reinforcement aspects of surfaced pavements. Relatively little is presently known about the influence of geosynthetic reinforcement on pavement response. This influence can be expressed as changes

in stress, strain, and deflection within the pavement and how these changes influence overall structural fatigue and rutting performance. Importance is also placed on developing an understanding of the fundamental mechanisms of geosynthetic reinforcement. These mechanisms are of considerable value because of the many new innovations in reinforcement that will have to be evaluated in the future. (As an example, the use of steel reinforcement in the base has been introduced as an alternative to geosynthetics as the present project was being carried out.)

Both the separation and filtration mechanisms of geosynthetics are considered as a part of the general synthesis of the use of geosynthetics within aggregate base layers; the existing literature was heavily relied upon for this portion of the study. For reinforcement to be effective, it must be sufficiently durable to serve its intended function for the design life of the facility. Therefore, because of its significance, the present state of the art of durability aspects are considered and put in perspective. (Appendixes F and G cover these aspects in detail.)

GEOSYNTHETIC REINFORCEMENT

The response of a surfaced pavement having an aggregate base reinforced with a geosynthetic is a complicated engineering mechanics problem. However, analyses can be performed on pavement structures of this type using theoretical approaches similar to those employed for nonreinforced pavements but adapted to the problem of reinforcement. As will be demonstrated subsequently, a linear elastic, cross-anisotropic finite element formulation can be successfully used to model geosynthetic reinforcement of a pavement structure.

The advantage of using a simplified linear elastic model of this type is the relative ease with which an analysis can be performed of a pavement structure. Where a higher degree of modeling accuracy is required, a more sophisticated, but time consuming, nonlinear finite element analysis was employed in the study. Use of a finite element analysis gives reasonable accuracy in modeling a number of important aspects of the problem including slack in the geosynthetic, slip between the geosynthetic and the surrounding material, accumulation of permanent deformation, and the effect of prestressing the geosynthetic.

Geosynthetic Stiffness

The stiffness of the geosynthetic is the most important variable associated with base reinforcement that can be readily controlled. In evaluating potential benefits of reinforcing an aggregate base, the first step should be to establish the stiffness of the geosynthetic to be used. Geosynthetic stiffness S_g, as defined here, is equivalent to the modulus of elasticity of the geosynthetic times its average thickness. Geosynthetic stiffness should be used because the modulus of elasticity of a thin geosynthetic has relatively little meaning unless its thickness is taken into consideration. The ultimate strength of a geosynthetic plays, at most, a very minor role in determining reinforcement effectiveness of a geosynthetic. This does not imply that the strength of the geosynthetic is not of concern. Under certain conditions it is an important consideration in ensuring the success of an installation. For example, as will be discussed later, the geo-

synthetic strength and ductility are important factors when the geosynthetic is used as a filter layer between a soft subgrade and an open-graded drainage layer consisting of large, angular aggregate.

The stiffness of a relatively thin geotextile can be determined in the laboratory by a uniaxial extension test. The wide width tension test as specified by ASTM Test Method D-4595 is the most suitable test at the present time to evaluate stiffness. Note that ASTM Test Method D-4595 uses the term "modulus" rather than stiffness S_g which is used throughout this study; both the ASTM "modulus" and the stiffness as used here have the same physical meaning. Use of the grab-type tension test to evaluate geotextile stiffness is not recommended.

The secant geosynthetic stiffness S_g is defined in Figure 30 as the uniformly applied axial stretching force F (per unit width of the geosynthetic) divided by the resulting axial strain in the geosynthetic. Because many geosynthetics give a nonlinear load-deformation response, the stiffness of the geosynthetic must be presented for a specific value of strain. For most, but not all, geosynthetics the stiffness decreases as the strain level increases. A strain level of 5 percent has gained some degree of acceptance. This value of strain has been employed, for example, by the U.S. Army Corps of Engineers in reinforcement specifications. Use of a 5 percent strain level is generally conservative for flexible pavement reinforcement applications that involve low permanent deformations.

A geosynthetic classification based on stiffness for reinforcement of aggregate bases is given in Table 16. This table includes typical ranges of other properties and also approximate 1988 cost. A very low stiffness geosynthetic has a secant modulus at 5 percent strain of less than 800 lb/in. (140 kN/m) and costs about \$0.30 to \$0.50/yd^2 (0.36 to 0.59/m^2). As discussed later, for low deformation conditions, a low stiffness geosynthetic does not have the ability to cause any significant change in stress or strain within the pavement, and hence is not suitable for use as a reinforcement. For low deformation pavement reinforcement applications, the geosynthetic should, in general, have a stiffness exceeding 1,500 lb/in. (260 kN/m). Several selected geosynthetic stress-strain curves are shown in Figure 31 for comparison.

Reinforcement Modeling

Changes in response of the pavement are for the most part determined by the tensile strain developed in the geosynthetic. A surfaced flexible pavement of low-to-moderate structural strength (AASHTO structural number SN $\cong$ 2.5 to 3.0) resting on a soft subgrade (CBR = 3 percent), however, develops relatively low tensile strain in the aggregate base and hence low geosynthetic forces. The many problems associated with modeling the behavior of a nonreinforced aggregate base that can take only tension are well known [16, 44, 48, 49]. A reinforced aggregate base presents an even more challenging problem.

Cross-Anisotropic Model

Measured vertical and horizontal strains from two well-instrumented laboratory studies described in Chapter Two and Appendix C clearly indicate that the aggregate base exhibits much higher stiffness in the vertical direction than in the hor-
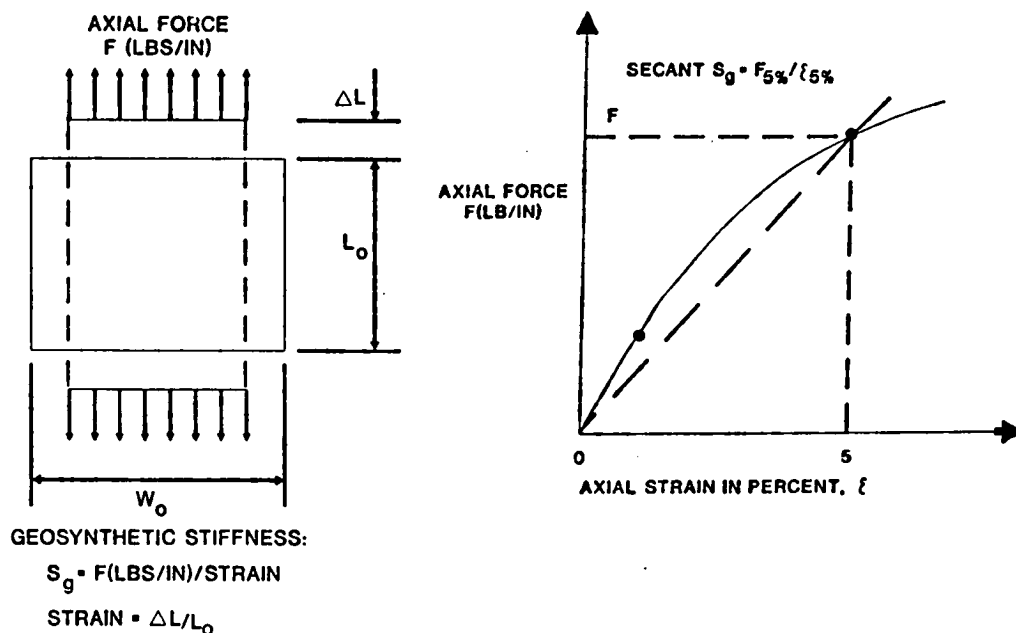
AXIAL FORCE
F (LBS/IN)

ΔL

L$_o$

W$_o$

GEOSYNTHETIC STIFFNESS:

S$_g$ = F(LBS/IN)/STRAIN

STRAIN = ΔL/L$_o$

SECANT S$_g$ = F$_{5\%}$/$\ell_{5\%}$

F

AXIAL FORCE
F(LB/IN)

0   5

AXIAL STRAIN IN PERCENT, ℓ

Figure 30. Basic idealized definitions of geosynthetic stiffness.

izontal direction. These results can only be explained if the aggregate base behaves as a cross-anisotropic solid. As a result, a linear elastic, cross-anisotropic finite element model appears to give the best overall predictions of pavement response (Tables C-1 and C-3 in Appendix C).

The best agreement with observed response was found for a cross-anisotropic model where vertical stiffness of the base became about 40 percent smaller in going from the upper one-third to the lower one-third of the aggregate base, and the model

became progressively more cross-anisotropic with depth (refer to Tables C-2 and C-4).

Use of a subgrade where the resilient modulus increases significantly with depth greatly increases calculated tensile strains in the aggregate base and shows much better agreement with observed pavement response (Table C-1). This was true for either the cross-anisotropic model or the nonlinear finite element models. For the micaceous silty sand and silty clay subgrades used in the two validation studies, the resilient subgrade modulus

Table 16. Tentative stiffness classification of geosynthetic for base reinforcement of surfaced pavements.[1]

Stiffness Description	Secant Stiffness @ 5% Strain, S$_g$ (lbs./in.)	Elastic Limit (lbs./in.)	Tensile Strength (lbs./in.)	Failure Elongation (% Initial Length)	Typical Cost Range ($/yd^2)
Very Low	< 800	10-30	50-150	10-100	0.30-0.50
Low	800-1500	15-50	60-200	10-60	0.40-0.50
Stiff	1500-4000	20-400	85-1000	10-35	0.50-3.00
Very Stiff	4000-6500	≥ 300	350-500 (or more)	5-15	$3.00-$7.00

NOTES: 1. The properties given in addition to stiffness are typical ranges of manufacturers properties and do not indicate a material specification.
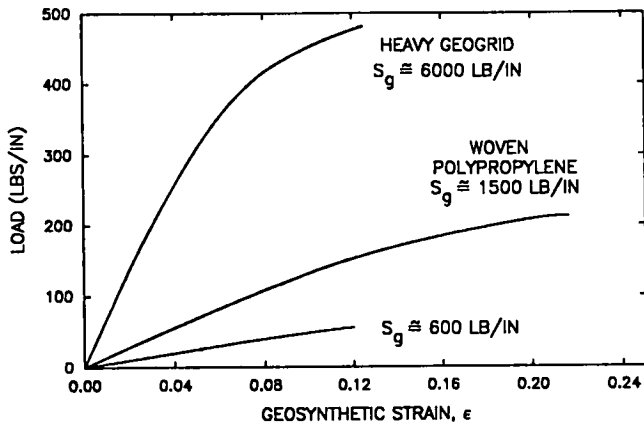
Figure 31. Selected geosynthetic stress-strain relationships.

Figure 32. Variation of subgrade resilient modulus with depth estimated from test results.

near the surface appeared to be about 10 and 20 percent, respectively, of the average resilient subgrade modulus, as shown in Figure 32. As expected, the resilient modulus of the soft silty clay subgrade apparently did not increase as much as that of the micaceous silty sand subgrade. The rigid layer, which was located below the subgrade in the instrumented pavement studies, may have had some influence on performance, but should not have been a dominant factor. A discussion of the increase in resilient modulus with depth has been given by Brown and Dawson [50].

Nonlinear Isotropic Model

A nonlinear isotropic model was used in the sensitivity study primarily to investigate the effect of special variables such as geosynthetic slip, aggregate base quality, and permanent deformation. The nonlinear, isotropic finite element model which was used can, upon proper selection of material parameters, predict reasonably well the tensile strain in the aggregate base and also the other commonly used response parameters. The isotropic nonlinear analysis can not, however, predict at the same time both the large tensile strain measured in the bottom of the aggregate base and the small measured vertical resilient strain observed throughout the aggregate layer. Use of a simplified contour model for aggregate bases [51, 52] appeared to give better results than the often used K-θ type of model.

When the nonlinear properties originally selected for the subgrade were employed, the nonlinear analysis underpredicted vertical strain in the subgrade. The nonlinear resilient modulus was therefore adjusted to approximately agree with the variation of modulus with depth shown in Figure 32.

Summary

Reasonably good response was obtained using both the linear cross-anisotropic model and the nonlinear, simplified contour model. The cross-anisotropic model appears to give slightly better results and was more economical to use. Therefore, it was the primary method of analysis employed in the sensitivity study. Considerable progress was made in this study in developing appropriate techniques to model both reinforced and nonreinforced aggregate bases.
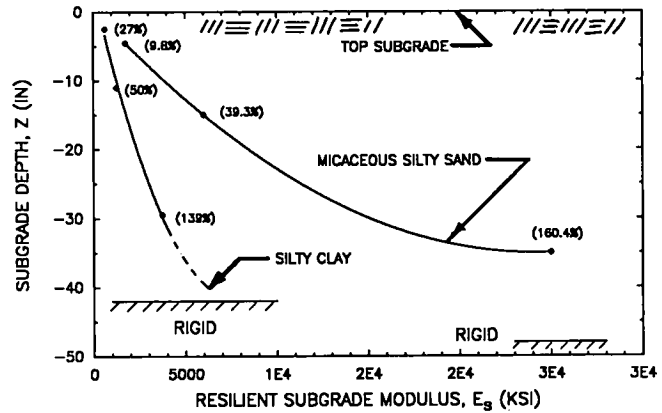
Improvement Mechanisms

The analytical and experimental results show that placement of a high stiffness geosynthetic in the aggregate base of a surfaced pavement designed for more than about 200,000 equivalent 18-kip (80 kN) single axle loads results in relatively small changes in the resilient response of the pavement. Field measurements by Ruddock et al. [21, 30] confirm this finding. Pavement response is defined in terms of the transient stresses, resilient strains, and displacements caused by the applied loadings.

The analytical results shown in Figure 33 (see also Tables 2 through 4 of Chapter Two) indicate that radial strain in the asphalt surfacing and surface deflection are generally changed by less than 5 percent; and vertical subgrade strain, by less than 10 percent when the geosynthetic is present. This level of change applies even for relatively light structural sections placed on a soft subgrade and reinforced with a very stiff geosynthetic having $S_g = 4,000$ lb/in. (700 kN/m).

Even though the changes in response are relatively small, some modest improvement can usually be derived from reinforcement following the commonly employed design approaches of limiting vertical subgrade strain and radial tensile strain in the asphalt. Specific benefits resulting from reinforcement using these criteria are discussed later.
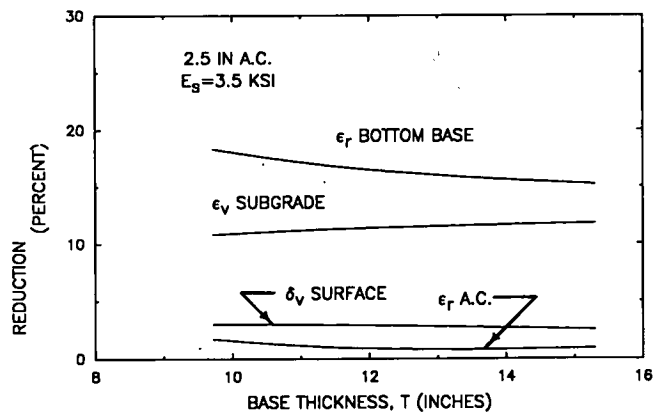
Figure 33. Reduction in response variable as a function of base thickness.

Pavement Stiffness

The structural strength of a pavement section is frequently evaluated using the falling weight deflectometer (FWD) or Dynaflect devices. These devices measure the deflection basin from which the overall stiffness of the pavement and of its constituent layers can be determined [49]. The overall stiffness of a structural section can be defined as the force applied from a loading device, such as the FWD, divided by the resulting deflection. The analytical results of this study indicate that the overall increase in stiffness of the pavement will be less than about 3 percent, even when a very stiff geosynthetic is used as reinforcement. The laboratory test results also indicate no observable improvement in pavement stiffness.

The improvement in stiffness resulting from geosynthetic reinforcement is, therefore, too small to be reliably measured in either a full-scale or laboratory pavement. The results of several field studies also tend to substantiate this finding [21, 30, 38, 39]. Dynaflect measurements in Texas described by Scullion and Chou [53] showed one section to be stiffened when a geosynthetic was added, while another indicated no observable difference. Variations in pavement thickness or material quality including subgrade stiffness could account for the difference in overall pavement stiffness observed for the one series of tests in Texas. These findings therefore indicate that stiffness is a poor indicator of the potential benefit of geosynthetic reinforcement on performance.

Radial Stress and Strain. Both the laboratory and analytical results indicate the change in radial stress and strain as a result of base reinforcement probably to be the most important single factor contributing to improved pavement performance. The experimental measurements show the strain in the geosynthetic to be about 50 percent of the corresponding strain in a non-reinforced aggregate base (Table 15). The analytical studies performed on stronger sections indicate changes in radial strain in the bottom of the base to be about 4 to 20 percent for sections having low to moderate structural numbers.

Changes in radial stress determined from the analytical study typically vary from about 10 percent to more than 100 percent of the corresponding radial stress developed in an unreinforced section (Fig. 34). Recall that tension is positive so the decrease in stress shown in Figure 34 actually means an increase in confinement.

Considering just the large percent change in radial stress, however, does not give the full picture of the potential beneficial effect of reinforcement. First, the actual value of change in radial stress is relatively small, typically being less than about 0.5 psi to 1.0 psi (3 to 7 kN/m²) for relatively light sections. As the pavement section becomes moderately strong (structural number SN $\cong$ 4.5), however, the changes in radial stress usually become less than about 0.1 psi (0.7 kN/m²), as shown in Table 3. Secondly, the radial stresses, including the relatively small changes resulting from reinforcement, must be superimposed on the initial stresses resulting from body weight and compaction effects as illustrated in Figure 35. The initial stress in the base due to body weight and compaction is likely to be at least twice as large as the radial stress caused by the external loading. Consequently, the beneficial effects of changes in radial stress caused by reinforcement are reduced but are not eliminated.

As the resilient modulus of the subgrade and the ratio between the base modulus and subgrade modulus decreases, the strain in the geosynthetic becomes greater. As a result improvement also becomes more pronounced.
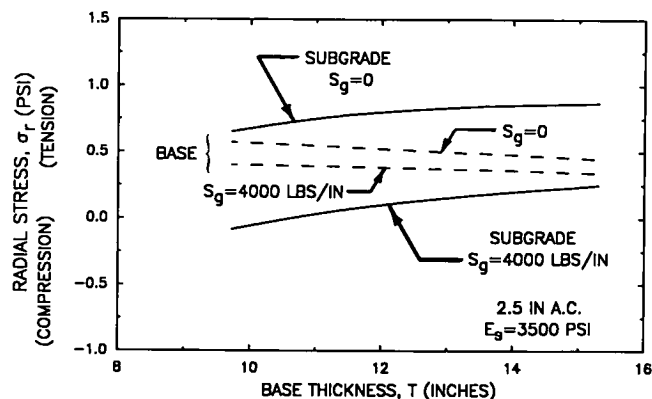
Figure 34. Variation of radial stress in base and subgrade with base thickness.
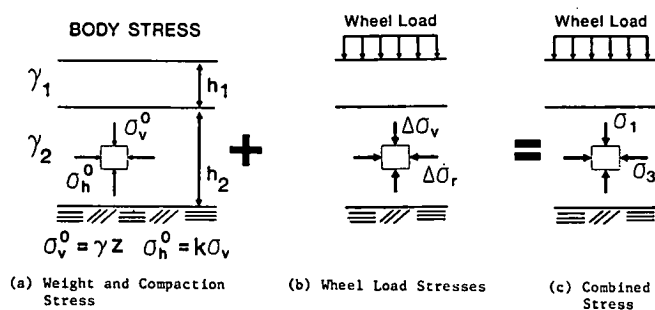
Figure 35. Superposition of initial stress and stress change due to loading.

Permanent Deformation. The small beneficial changes in radial stress due to reinforcement can have important effects on permanent deformation under the proper conditions. By far the largest beneficial effects are realized when the stress state is close to failure on an element of material in, for example, the top of the subgrade. The addition of reinforcement under the proper conditions causes a small, but potentially important, increase in compressive radial stress and a slight reduction in vertical stress. As a result, the deviator stress on an element of subgrade soil is decreased slightly. If the section is weak and hence the initial stress state is near failure, significant reductions in permanent deformation may occur as shown in Figure 36. When examining Figure 36 it must be kept in mind that permanent deformation is proportional to the permanent strain developed in a thin sublayer of material. Because of the highly nonlinear stress-permanent strain response of the subgrade or base (Fig. 36), a small increase in compressive confining pressure and decrease in deviator stress can lead to a significant reduction in permanent deformation when the element of material is near failure. The reduction in permanent deformation becomes disproportionately larger as the stress state in the top of the subgrade (or bottom of the base) moves closer to failure. Conversely, as the stress state becomes less severe, the beneficial effect of reinforcement becomes significantly less.

Depth of Subgrade Improvement. The large-scale laboratory tests indicate that both resilient and permanent strains in the subgrade, when reduced, were only changed to a depth of about 6 in. to 7 in. (150 to 180 mm) below the surface of the subgrade.

36
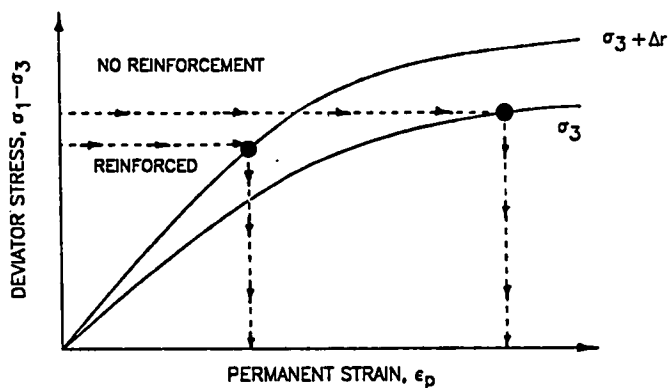
Note: $\Delta\sigma_r$ = change in radial stress due to reinforcement

Figure 36. Reduction in permanent deformation due to geosynthetic for soil near failure.

The tire loading in this case, however, was relatively light. For the heavy load used in the analytical study, the depth of reduction in permanent strain in the subgrade was about 12 in. (300 mm). Findings by Barksdale et al. [16] on unsurfaced pavements tend to verify that the depth of improvement in the subgrade due to reinforcement is relatively shallow. The changes in radial stresses due to reinforcement appear to be caused by the reduction in tensile strain in the lower part of the aggregate base. The increase in confining pressure caused by the geosynthetic would make the upper portion of the subgrade more resistant to liquefaction.

Tensile Strain Variation with Load Repetitions. Strain measurements made in the third test series of the experimental study show a very large reduction in tensile strain in the bottom of the aggregate base due to reinforcement at low load repetitions. With increasing numbers of repetitions, however, the difference in tensile strain resulting from reinforcement appeared to disappear and, eventually, the tensile strain in the nonreinforced sections was less than in the reinforced section. In this comparison a geotextile reinforcement was located in the middle of the base.

Summary

The effects of geosynthetic reinforcement on stress, strain, and deflection are all relatively small for pavements designed to carry more than about 200,000 equivalent 18-kip (80 kN) single axle loads. As a result, geosynthetic reinforcement of an aggregate base will have relatively little effect on overall pavement stiffness. A modest improvement in fatigue life can be gained from reinforcement as discussed subsequently.

The greatest beneficial effect of reinforcement appears to be due to changes in radial stress and strain together with small reductions of vertical stress in the aggregate base and on top of the subgrade. Reinforcement of a thin pavement (SN $\leq$ 2.5 to 3) on a weak subgrade (CBR < 3 percent) can potentially reduce the permanent deformations in the subgrade and/or the aggregate base by significant amounts. As the strength of the pavement section increases, or the materials become stronger, the states of stress in the aggregate base and the subgrade move

away from failure. As a result, the improvement caused by reinforcement would be expected to rapidly become small.

Reinforcement Effects

In this section the primary factors associated with aggregate base reinforcement are discussed including their interaction with each other and the overall pavement response. Geosynthetic reinforcement levels included in the analytical sensitivity study varied from low to high stiffness (S_g = 1,000 to 6,000 lb/in.; 170 to 1,000 kN/m). The influence of reinforcement on the required pavement thickness was studied considering both fatigue and permanent deformation (rutting) mechanisms. Alternate thicknesses are given from the analytical sensitivity study for subgrade strengths varying from a resilient modulus of 3,500 psi (24 kN/m^2) to 12,500 psi (86 MN/m^2). This range of subgrade stiffness approximately corresponds to a variation of CBR from 3 to 10 percent. Effects of reinforcement on permanent deformations that may occur in the base are also considered, and a number of practical aspects are examined such as slack and slip of the geosynthetic.

In the analytical sensitivity study, the reduction in aggregate base thickness as a result of geosynthetic reinforcement was determined using an equal strain approach for controlling fatigue and rutting. A reduction in base thickness due to reinforcement was established by requiring the reinforced section to have the same tensile strain in the bottom of the asphalt surfacing as the nonreinforced section. A similar procedure was employed to determine the reduction in base thickness for equal vertical strain near the top of the subgrade. An estimate of reduction in rutting in the aggregate base and subgrade was also made using the layer strain method. The layer strain method and the permanent strain materials properties employed in the analysis are described in Appendix C.

Optimum Geosynthetic Position

The laboratory pavement tests together with the results of the analytical sensitivity study can be used to establish the optimum positions for placement of geosynthetic reinforcement within an aggregate base. The experimental findings of test series 3 demonstrate the effect of geosynthetic position on performance with respect to permanent deformation.

Permanent Deformation—Experimental Findings. Test series 3 was constructed using a stiff asphalt surfacing mix 1.2 in. (30 mm) thick, and an 8-in. (200 mm) crushed limestone base. A stiff to very stiff woven geotextile was used (S_g = 4,300 lb/in.; 750 kN/m). The geotextile was placed at the bottom of the base in one section and at the center of the base in another section. A control section without reinforcement was also present. A total of 100,070 load repetitions were applied by a 1.5-kip (6.7 kN) wheel. This test series was terminated when the total permanent deformation reached about 1 in. (25 mm).

When placed in the bottom of the aggregate base, the stiff to very stiff geotextile caused a 57 percent reduction in permanent deformation in the subgrade, but only a 3 percent reduction of permanent deformation in the aggregate base (Table 13). In contrast, when the same geotextile was placed in the middle of the aggregate base, permanent deformation in the base was reduced by 31 percent. Subgrade permanent deformations, however, were reduced by only 14 percent.

The results of test series 2 also tend to verify these findings. A geogrid, when placed in the bottom of the base, did not decrease the permanent deformation in the base (measurements suggested an increase of 5 percent). A 52 percent reduction in permanent subgrade deformation was observed in this test series.

Permanent Deformation—Analytical Results. An analytical study was also performed to establish the effect of geosynthetic position on the reduction in rutting in the base and subgrade (Tables 17 and 18). Improvements due to reinforcement in terms of a reduction in base thickness are apparent from the data in Tables 17 and 18 and other tables and figures in this chapter. The actual reduction in base thickness is equal to the base thickness without reinforcement indicated in the table or figure multiplied by the percent reduction, expressed as a decimal.

The results of this analytical study for the standard reference section having a 2.5-in. (64 mm) thick asphalt surfacing and a relatively soft subgrade (E_s = 3,500 psi; 24 MN/m^2) are summarized in Figures 37 and 38. The reduction in subgrade deformation gradually goes from about 45 percent to 10 percent as the geosynthetic location moves from the bottom of the base to a location ⅔ up from the bottom. Conversely, the reduction of permanent deformation in the base becomes much greater as the reinforcement is moved upward in the base (Fig. 38).

In Figures 37 and 38 the solid symbols indicate observed reductions in rutting from the previously described test series 3 experiment. Geotextile reinforcement positions were at the bottom and center of the layer. Agreement between the observed

and calculated reductions in rutting is reasonably good. The maximum measured reductions are greater than calculated values for similar pavement base thicknesses. Material properties of the test sections were, however, poorer than for standard reference sections. Also, the asphalt thickness of the experimental sections was only 1.2 in. (30 mm) compared to 2.5 in. (64 mm) for the analytically developed relations shown in the figures.

Fatigue. The analytical results (Table 17) show for increasing fatigue life that placing the reinforcement ⅓ to ⅔ up in the base is better than placing it at the bottom. The maximum calculated changes in tensile strain in the asphalt were less than about 3 percent. These small changes in tensile strain, however, cause reductions in required base thickness of up to about 20 percent (Table 17) for light pavements on a subgrade having a low resilient modulus E_s = 3,500 psi (24 MN/m^2). The analytically calculated reductions in strain in the bottom of the asphalt surfacing were not validated by the experimental results which were inconsistent. Strain measurements from test series 3 indicate that placement of a stiff to very stiff geotextile in the middle of the aggregate base reduced the tensile strain by about 26 percent. In contrast, the measurements from test series 2 showed the strain in the bottom of the asphalt layer to be higher because of the placement of a stiff geogrid at the bottom of the layer.

Full-scale measurements made by van Grup et al. [41] did point out that an extremely stiff steel mesh reinforcement placed

Table 17. Influence of geosynthetic position on potential fatigue and rutting performance.

GEOSYN. POSITION	BASE THICK,T w/o GEOSYN. (in.)	CHANGE IN BASE THICKNESS (%)						CHANGE IN RUTTING OF BASE AND SUBGRADE (%)					
		CONSTANT VERTICAL SUBGRADE STRAIN,ε_v			CONSTANT TENSILE STRAIN AC, ε_t			GOOD BASE/FAIR SUBG.			POOR BASE/FAIR SUBG.		
		GEOSYNTHETIC STIFFNESS, S_g (lbs/in.)											
		1000	4000	6000	1000	4000	6000	1000	4000	6000	1000	4000	6000
2.5 IN. AC SURFACING 3500 PSI SUBGRADE													
GEOSYN @ BOTTOM	15.3	-3.9	-12	-16	-1.8	-6.5	-9	-9	-22	-27	-4	-11	-15
	11.92	-3.3	-12	-16	- 2	- 8	-12	-12	-30	-36	-7	-19	-23
	9.75	-4.9	-14	-18	-2.6	-12	-18	-18	-39	-46	-12	-28	-33
2.5 IN. AC SURFACING 3500 PSI SUBGRADE													
GEOSYN @ 1/3 UP	15.3	-0.7	-3.6	- 5	-2.5	- 9	-13	-2.7	- 9	-15	-4	-11	-14
	11.92	-1.4	-5.5	-7.5	-3.5	-12	-17	-	-	-	-	-	-
	9.75	-2.1	-7.3	-7.7	-4.8	-17	-23.3	-	-	-	-8	-22	-28
2.5 IN. AC SURFACING 3500 PSI SUBGRADE													
GEOSYN @ 2/3 UP	15.3	-0.2	-0.5	-0.8	-2.8	-10	-14	-2.6	- 9	-12	-4	-11	-15
	11.92	-0.3	-1.1	-1.8	-2.5	-12	-17	-	-	-	-7	-	-
	9.75	-0.3	-1.7	-2.9	-3.8	-15	-22	-	-	-	-6	-17	-22

Note: 1. Permanent deformation (rutting) calculated by Layer Strain Method.

38

Table 18. Influence of asphalt thickness and subgrade stiffness on geosynthetic effectiveness.

GEOSYN. POSITION	BASE THICK,T w/o GEOSYN. (in.)	CHANGE IN BASE THICKNESS (%)						CHANGE IN RUTTING OF BASE AND SUBGRADE (%)[2]					
		CONSTANT VERTICAL SUBGRADE STRAIN,ϵ_v			CONSTANT TENSILE STRAIN AC, ϵ_t			GOOD BASE/FAIR SUBG.			POOR BASE/FAIR SUBG.		
		GEOSYNTHETIC STIFFNESS, S_g (lbs/in.)											
		1000	4000	6000	1000	4000	6000	1000	4000	6000	1000	4000	6000
6.5 IN. AC SURFACING 3500 PSI SUBGRADE													
GEOSYN @ BOTTOM	15.3	-4	-12	-17	-2	-8	-12	-	-	-	+0.1	+0.5	+0.7
	12.42	-4	-14	-19	-2	-8	-12	+0.4	+1	-14	+0.6[1]	.+ 2	+0.6
	9.75	-5	-17	-23	-3	-11	-17	-	-	-	+0.3	-2.2	+1.7
2.5 IN. AC SURFACING 6000 PSI SUBGRADE													
GEOSYN @ BOTTOM	12.85	-2	-7	-10	-1	-4	-7	-	-	-	-	-	-
	9.72	-3	-9	-12	-2	-7	-9	-16	-38	-88	-13.7	-31	-37
	7.50	-3	8	-11	-2	-9	-11	-	-	-	-	-	-
2.5 IN. AC SURFACING 12,500 PSI SUBGRADE													
GEOSYN. @ BOTTOM	9.62	1	5	6	0.6	2	4	-	-	-	-	-	-
	7.5	1	6	8	1	4	5	-1	-5	-7	-0.5	-3	-2
	6.0	2	5	7	1	4	6	-	-	-	-	-	-

Note: (1) Good Base/Poor Subgrade;   (2) Permanent deformation (rutting) calculated by Layer Strain Method.
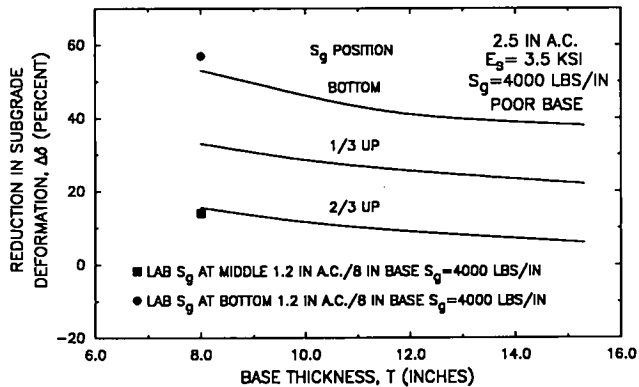
Figure 37. Reduction in subgrade permanent deformation.
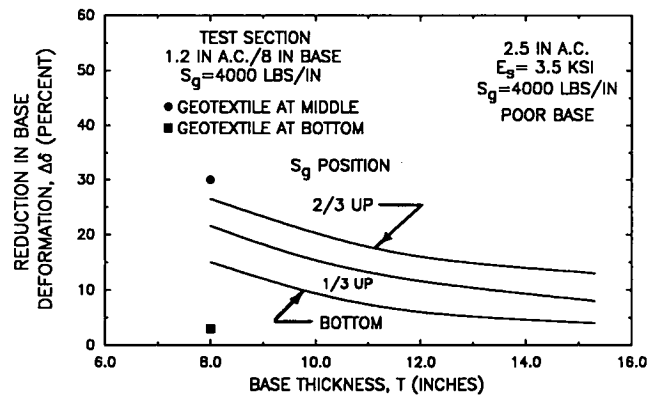
Figure 38. Reduction in base permanent deformation.

at the top of the aggregate base can reduce tensile strains by about 18 percent under certain conditions. If only fatigue is of concern, the reinforcement should be placed at the top of the base.

Summary. The optimum position of the geosynthetic with respect to minimizing permanent deformation depends on the strength of the section, the specific material properties, and the loading conditions. The optimum depth might also be dependent on the width of wheel load, although this variable was not investigated. To minimize rutting in the aggregate base, the optimum reinforcement position is near the middle of the base, or perhaps as high as $\frac{2}{3}$ up, as indicated by the analytical study. Consideration should be given to placing the reinforcement near the middle of the base when low quality aggregate bases are used which are known to be susceptible to rutting. A greater beneficial effect will also be realized for this higher location of reinforcement with respect to fatigue of the asphalt surfacing.

The analytical results show that when high quality base materials and good construction practices are employed, reinforcement, when used, should be placed in the bottom of the base.

The purpose of this reinforcement would be to reduce rutting within a soft subgrade typically having a CBR < 3 percent. Both the laboratory tests and the analytical study reveal that placement of the reinforcement at the bottom of the layer should be most effective where a soft subgrade is encountered, particularly if it is known to be susceptible to rutting.

The analytical results demonstrate that to minimize fatigue cracking of the asphalt surfacing, the reinforcement should be placed somewhere between the middle and the top of the layer. Reductions in tensile strain due to reinforcement, as indicated by the analytical theory, may not be as great as actually occur in the pavement. The reduction in tensile strain, in general, should be considerably less for full-size sections than the 26 percent reduction observed for test series 3. Nevertheless, even small reductions in tensile strain in the bottom of the asphalt can give, for equal fatigue performance, large reductions in required aggregate base thickness. The experimental results of van Grup and van Hulst [41], which used steel mesh reinforcement, are quite promising for the reduction of fatigue cracking.

Base Quality

Use of a low quality base can result in a significant reduction in the level of pavement performance because of increased permanent deformation and asphalt fatigue as a result of a lower resilient modulus. A low quality base may be caused by achieving a compaction level less than 100 percent of AASHTO T-180 density, or by using low quality materials. Low quality aggregate bases would include those having a fines content greater than about 8 percent and also gravels, sand-gravels, and soil-aggregate mixtures. A high fines content base may also be frost susceptible [54].

Observed Test Section Improvements. The pavement used in test series 1 had a 1.4-in. (36 mm) bituminous surfacing and 6-in. (150 mm) thick sand-gravel base. The pavement failed after about 1,262 wheel repetitions (Table 13). At this time the base of the control section without reinforcement had a permanent deformation of 0.69 in. (18 mm). The companion section having a very stiff geotextile (S_g = 4,300 lb/in.; 750 kN/m) at the bottom of the base had a corresponding permanent deformation of only 0.35 in. (9 mm). Thus, for underdesigned sections having low quality bases, geosynthetic reinforcement can reduce base rutting up to about 50 percent, as observed in test series 1. Of interest is the finding that at about one-half of the termination rut depth, the reduction in base rutting was also about 50 percent.

The same very stiff geotextile was used in test series 3 as for test series 1. As previously discussed, the sections included in test series 3 were considerably stronger than the first series. Test series 3 sections had a thicker 8-in. (200 mm) crushed limestone base and an asphalt surfacing rather than the rolled asphalt used in the first series. The pavement in test series 3 withstood about 100,000 load repetitions, confirming it was a higher quality pavement than that used in the first series.

When the very stiff geosynthetic reinforcement was placed at the bottom of the base, permanent deformation within the base was reduced by only 3 percent compared to 50 percent for the lower quality pavement in test series 1. In contrast, placement of the same reinforcement at the center of the base resulted in a 31 percent reduction of permanent deformation within the base.

Analytical Results. Results of a nonlinear finite element analysis indicate that for low quality bases, the ratio of the average resilient modulus of the base to that of the subgrade (E_b/E_s) averages about 1.45 compared to about 2.5 for high quality materials for the sections studied. Therefore, reductions in rutting in the light reference pavement, previously described, were developed for both of the above values of modular ratios (Table 19). The stress state within the pavement was first calculated using the cross-anisotropic analysis and these modular ratios. The layer strain approach was then employed together with appropriate permanent strain properties to calculate permanent deformations.

Both a high quality base (indicated in the tables as a "good" base) and a low quality base (indicated as a "poor" base) were included in the layer-strain analyses (Table 19). A complete description of the layer strain approach and the permanent strain material properties are given in Appendix C.

Calculated permanent deformations are given in Tables 17 and 18 for both the poor and good bases for a modular ratio E_b/E_s = 2.5. This was done to extend the results and develop a better understanding of the influence of reinforcement on permanent deformation. To be precise, the lower quality base properties should probably not have been used with the stress states obtained from analyses for E_b/E_s = 2.5. The results for a lower modular ratio E_b/E_s = 1.45, which are more suitable for lower quality base pavements, are given in Table 19.

Use of a geosynthetic-reinforced low-quality aggregate base, rather than a high quality base, causes about 3 times greater reduction in actual permanent displacement in the base. The analytical results show that little change occurs in permanent deformation in the base as the position of the geosynthetic is varied. The experimental findings, however, indicate that reinforcement at the middle of the base is most effective and is preferred to reduce base rutting.

Geosynthetic Stiffness

The analytical results point out that geosynthetic stiffness has an important effect on the level of improvement, as shown in Figures 39 and 40 (refer also to Tables 17 and 18). For stiffnesses greater than about 4,000 lb/in. (700 kN/m), the rate of change in improvement with increasing stiffness appears to decrease.

The pavement sections shown in Figures 39 and 40 have an asphalt surface thickness of 2.5 in. (64 mm) and a subgrade with a resilient modulus of 3,500 psi (24 MN/m²), corresponding to a CBR of about 3 percent. Base thicknesses varied from 9.75 in. to 15.3 in. (250 to 390 mm).

For these conditions, an AASHTO design for 200,000 equivalent 18-kip (80 kN) single axle loads (ESALs) has a base thickness of about 12 in. (300 mm). The equal vertical subgrade strain analytical approach (Fig. 39) indicates that allowable reductions in base thickness for this design increase from about 3 to 16 percent as the geosynthetic stiffness increases from 1,000 to 6,000 lb/in. (170 to 1,000 kN/m). Permanent deformations as determined by layer strain theory are reduced from 12 percent to 36 percent for a similar variation in geosynthetic stiffness (Fig. 40(a)). The experimental results suggest that the levels of improvement in rutting shown in Figure 40 may be too high for the pavement section used in the comparison. From a practical viewpoint, these results point out that very low stiffness geosynthetics (S_g < 800 lb/in.; 140 kN/m) would be expected

Table 19. Influence of aggregate base quality on effectiveness of geosynthetic reinforcement.

BASE QUALITY	BASE THICK T (in.)	REDUCTION IN RUTTING (PERCENT)						E_b/E_s	TOTAL DEF. (in.)	BASE DEF. (in.)	SUBG. DEF. (in.)
		S_g = 1000 lbs/in.		S_g = 4000 lbs/in.		S_g = 6000 lbs/in.					
		Base	Subgrade	Base	Subgrade	Base	Subgrade				
GEOSYNTHETIC AT BOTTOM OF AGGREGATE BASE											
Poor	9.75	–	–	–7	–34	–	–	1.45	0.2	0.13	0.07
Poor	9.75	–3.3	–20	–10	–47	–13	–55	2.5	0.23	0.12	0.11
Good	0.75	–10	–20	–15	–47	–17	–55	2.5	0.14	0.03	0.11
Poor	12.0	–	–	–	–	–	–	1.45	–	–	–
Poor	12.0	–2	–16	–6	–41	–9	–50	2.5	0.18	0.12	0.06
Good	12.0	–2	–17	–6	–42	–8	–36	2.5	.09	0.03	0.06
Poor	15.3							1.45			
Poor	15.3	–1	–15	–3.7	–38	–5	–48	2.5	0.14	0.105	0.035
Good	15.3	–1.4	–15	–4	–38	–6	–48	2.5	0.06	0.03	0.03
GEOSYNTHETIC 1/3 UP FROM BOTTOM											
Poor	9.75	–5.8	–10	–16	–29	–36	–36	2.5	0.23	0.12	0.11
Poor	15.3	–2.5	–8.5	–8	–22	–10	–28	2.5	0.14	0.11	0.03
Good	15.3	–2.7	–8.4	–9	–22	–11	–28	2.5	0.06	0.03	0.03
GEOSYNTHETIC 2/3 UP FROM BOTTOM											
Poor	9.75	–8	–3.3	–21	–12	–26	–16	2.5	0.23	0.12	0.11
Poor	15.3	–4	–1.6	–13	–6	–16	–9	2.5	0.14	0.11	0.03

to have no noticeable effect on pavement performance. This would be true even for the relatively light structural sections shown in Figures 39 and 40.

Structural Strength

The beneficial effect of reinforcement in terms of reduction in base thickness and rutting decreases as the overall base thickness becomes greater when all other variables are held constant. Consider the light reference pavement described in the previous section (2.5-in. AC, E_s = 3,500 psi; 64 mm, 24 MN/m^2), with reinforcement in the bottom having an S_g = 4,000 lb/in. (700 kN/m). Increasing the base thickness from 9.75 in. (250 mm) to 15.3 in. (400 mm) results in a very small reduction in base thickness decreasing from 14 to 12 percent based on the subgrade strain criteria (Fig. 39(a)). Reductions in rutting of the base and subgrade computed by layer strain theory were from 39 percent to 22 percent. The total reduction in permanent deformation increases from about 10 percent to 55 percent as the thickness of the pavement decreases from 15 in. to 6 in. (381 to 150 mm), as shown in Figure 41.

The results of test series 2 and 3 suggest that actual levels of improvement in permanent deformation for the sections shown in Figures 39 and 40 may not be as great as indicated by layer strain theory. However, for the first series of laboratory pavement tests, the observed reduction in rutting due to reinforcement was about 44 percent. These sections were thin and very weak and were placed on a poor subgrade ($E_s \cong 2,000$ psi; 13.8 MN/m^2). Thus, both the laboratory and analytical results show that if the system is weak enough so that stresses are close to

failure, important reductions in permanent deformations can be achieved by base reinforcement.

Now consider the effect of significantly increasing the load carrying capacity of the pavement from the 200,000 ESALs of the previous example to perhaps a more typical value of 2,000,000 ESALs. The subgrade resilient modulus will remain the same with E_s = 3,500 psi (24 MN/m^2). Let the asphalt surfacing increase from 2.5 in. to 6.5 in. (54 to 165 mm), with an aggregate base thickness of about 12.4 in. (315 mm). For a section having this structural strength, relatively small changes in stress result from the applied loading either with or without reinforcement (Table 3). For example, the total change in radial stress due to loading near the top of the subgrade is less than 0.1 psi (0.7 kN/m^2). Hence, as shown in Table 18, very little reduction in rutting occurs as a result of reinforcement. This conclusion is in agreement with the previous observations of Brown et al. [37] for large-scale laboratory pavements and Ruddock et al. [21, 30] for a full-scale pavement having a comparable bituminous thickness to the section above.

Subgrade Strength

A decrease in the strength of the subgrade, as defined by the subgrade stiffness E_s, has a very dramatic beneficial effect on the level of improvement due to reinforcement that can be expected based on the fatigue and rutting equal strain comparisons. Consider a pavement having an asphalt surface thickness of 2.5 in. (64 mm) and a base thickness of 9.7 in. (250 mm). Figure 42 shows that a reduction in subgrade stiffness from E_s = 12,500 psi (86 MN/m^2) to 3,500 psi (24 MN/m^2) causes
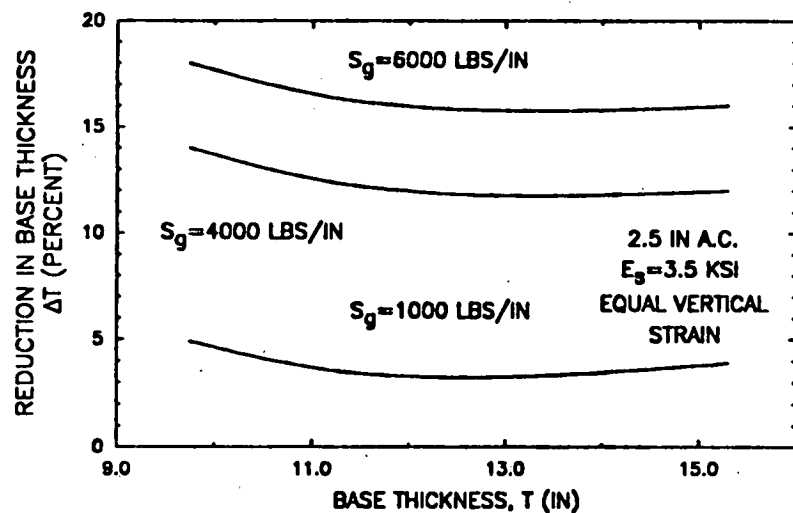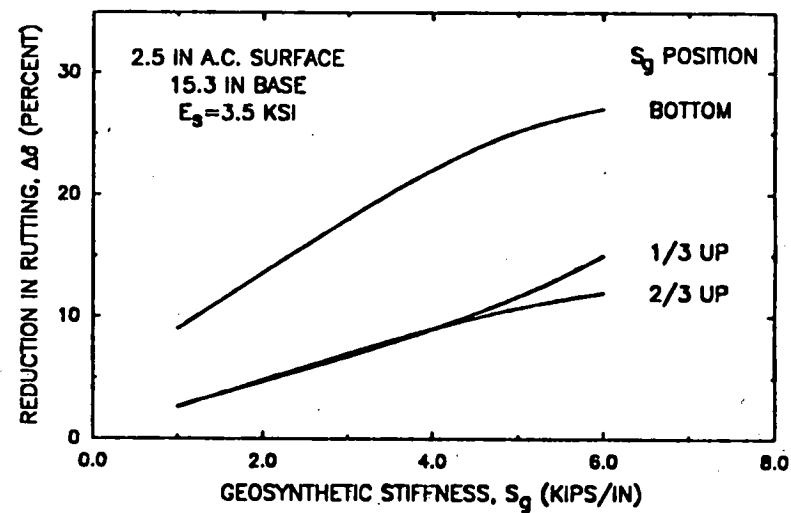
(a) Reduction in Base Thickness (b) Position

Figure 39. Improvement in performance with geosynthetic stiffness.
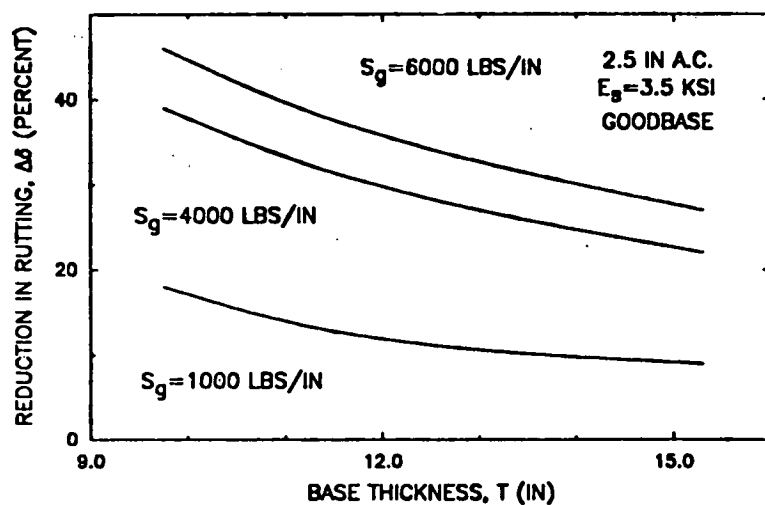
(a) Total Deformation (b) Subgrade Deformation
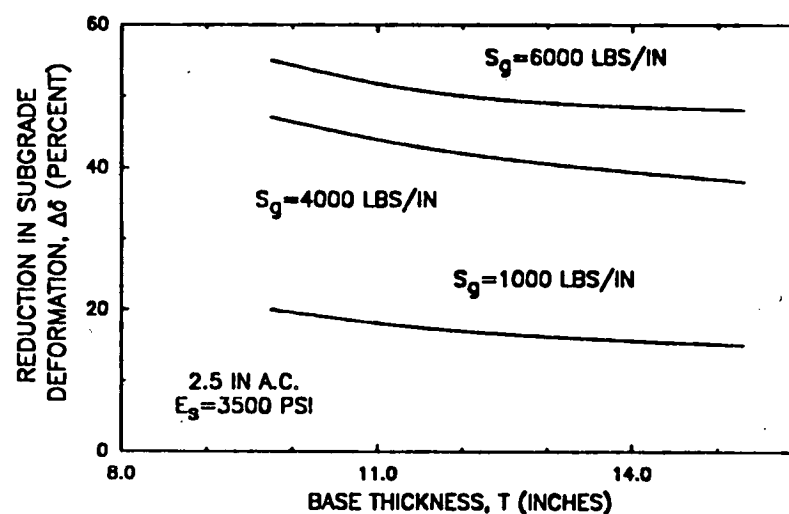
Figure 40. Improvement in performance with geosynthetic stiffness.
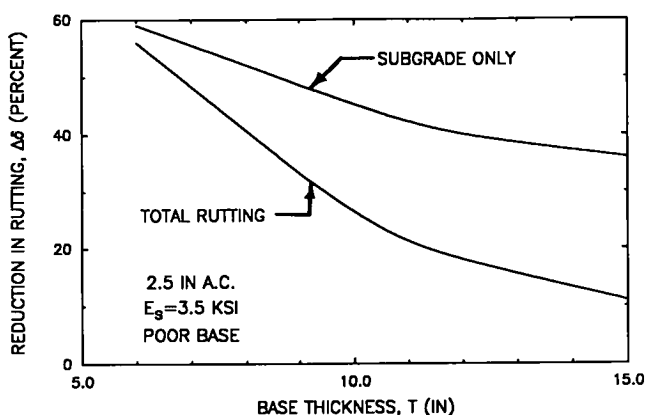
Figure 41. Influence of base thickness on permanent deformation: $S_g = 4,000 \, lb/in.$
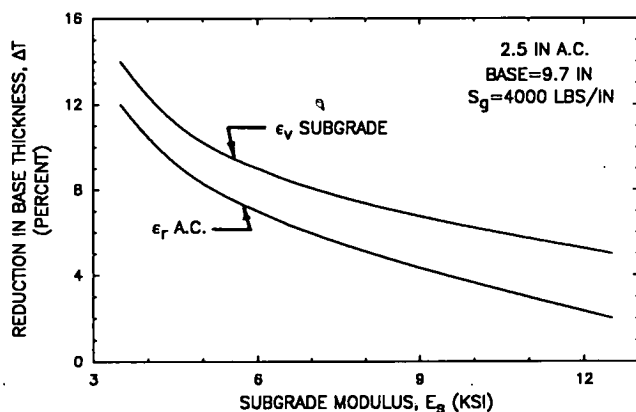
Figure 42. Influence of subgrade modulus on permanent deformation: $S_g = 4,000 \, lb/in.$
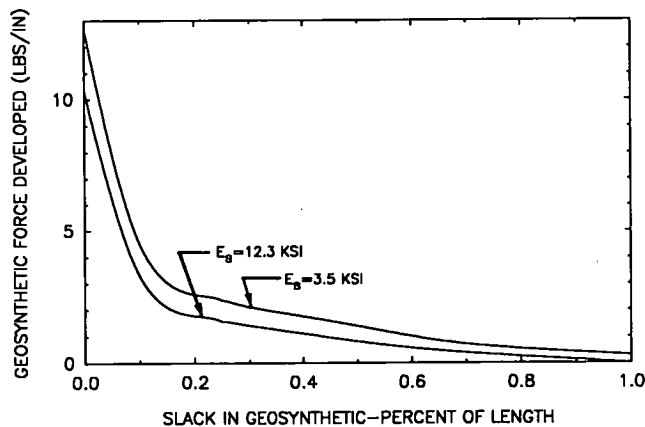
Figure 43. Theoretical effect of slack on force in geosynthetic: 2.5-in. AC/9.72-in. base: $S_g = 6,000 \, lb/in.$

the decrease in base thickness due to reinforcement to increase from about 5 percent to 14 percent, for a stiff geosynthetic having $S_g = 4,000 \, lb/in.$ (700 kN/m). For a similar section having a reinforcement stiffness $S_g = 6,000 \, lb/in.$ (1,000 kN/m), the corresponding decrease in base thickness is from 6 percent to 16 percent as the stiffness of the subgrade decreases. These comparisons both are for equal vertical subgrade strain; this criterion gives the greatest reductions in base thickness.

For a given structural section, the layer strain theory would also show a significant increase in beneficial effect with regard to rutting as the strength of the subgrade decreases. For all computations of permanent deformation using the layer strain approach, however, the same subgrade permanent strain properties were used, regardless of the resilient modulus employed in the analysis. Suitable permanent deformation properties for other subgrades were not available.

Slack

During installation of a geosynthetic, slack in the form of wrinkles and irregularities may develop in the reinforcement. As a result, its effectiveness as a reinforcement may be significantly reduced, as indicated by a supplementary nonlinear finite element sensitivity study. Figure 43 shows that even a small amount of slack in a geosynthetic theoretically can result in a very significant reduction in the force developed in the reinforcement. The rate of reduction in geosynthetic force becomes less as the amount of slack increases.

For the purposes of this study, slack was defined in terms of strain in the geosynthetic. Hence, slack expressed as a displacement equals a geosynthetic length, such as its width, times the slack expressed as a decimal. A slack of 0.1 percent corresponds to 0.14 in. (3.6 mm) in a distance of 12 ft (3.6 m). Slack in a geosynthetic as small as about 0.1 percent of its width reduces the geosynthetic force by about 60 percent, and a slack of 0.4 percent causes a 90 percent reduction in force (Fig. 43).

In an actual installation, the effect of slack may not be quite as great as indicated by theory. This would be because the geosynthetic generally is in full contact with the surrounding materials after construction has been completed. In laboratory tests, such as those performed for this study, slack can easily be removed by hand stretching the small pieces of geosynthetic required in these tests. In full-scale field installations, slack is an important practical consideration which must be minimized through proper construction practices, as discussed later.

Poisson's Ratio

The value of Poisson's ratio of the geosynthetic was found to have a moderate effect on the force developed in the geosynthetic. As the value of Poisson's ratio increases, the force developed in the geosynthetic also becomes larger, and hence the effectiveness of the reinforcement increases. For light pavement sections on a weak subgrade, increasing Poisson's ratio ν from 0.2 to 0.4 results in a 29 percent increase in the force developed in the geosynthetic; corresponding reductions in tensile strain in the asphalt surfacing and vertical compressive strain on the subgrade are less than 0.2 and 1 percent, respectively. Further, the compressive increase in radial stress is only about 0.075 psi (0.5 MN/m²) as shown in Figure 14. A Poisson's ratio of 0.3 was used in all other sensitivity analyses.

In summary, if all other factors are equal, the geosynthetic having the greatest value of Poisson's ratio should perform best. The improvement in performance for moderate increases in Poisson's ratio should be reasonably small. Such improvements would be very hard to detect experimentally because of variability in the results. Practically no information is presently available concerning the value of Poisson's ratio for geosynthetics.

Geosynthetic Slip

A slip failure can occur along the interfaces between the geosynthetic and the materials above and below. The occurrence of interface slip reduces the effectiveness of the geosynthetic reinforcement. As the rutting beneath the geosynthetic increases, the tendency to slip also increases. Whether or not slip occurs depends on (1) the shear strength, τ, that can be developed between the geosynthetic and the materials in contact with it, and (2) the level of shear stress developed along the interface due to the external load applied to a particular pavement structure. The level of applied shear stress is related to both the resilient and permanent deformations in the pavement, including the shape of the deflection basin.

Slip may occur directly at the interface between the geosynthetic and the adjacent soil, or by sliding of soil on soil immediately adjacent to the interface. The resulting ultimate interface shear stress, τ, for sliding at the interface can be predicted by the expression:

$$\tau = c_a + \sigma_n \tan\delta \qquad (1)$$

where: τ = ultimate shearing resistance along the interface, σ_n = stress acting normal to the geosynthetic, c_a = adhesion, and δ = friction angle.

The contact efficiency e between the geosynthetic and the surrounding material is defined as $e = \delta/\phi$ and is expressed as either a percent of ϕ or in decimal form [55]. Angular, well-graded sands and silty sands have been found to exhibit high efficiencies when in contact with most geotextiles. Angular soil grains exhibit better friction performance than rounded grains.

Testing Methods. The interface friction characteristics of a geosynthetic to be used for aggregate base reinforcement can best be evaluated using a direct shear test [55, 56, 57, 58, 59] as compared to a pullout-type test [55, 60, 61]. Either a free-type or a fixed-type direct shear test can be used. The free-type direct shear test appears, however, to be preferable to the fixed test. In the free-type direct shear test, one end of the geosynthetic is left free as shown in Figure 44. The same materials to be used in the field should be placed below and above the geosynthetic, and carefully compacted to the densities expected in the field. When large-size base course aggregates are used, the apparatus should be at least 8 in. and preferably 12 in. (200 to 300 mm) on a side. Frequently the materials are saturated before performing the test.

In the fixed shear test, development of strain in the geosynthetic is prevented and this can have an important effect on the interface friction developed [61], particularly if it has a relatively low in-plane stiffness. Bonding the geosynthetic to a rigid block is another technique that has been used, but this hampers natural soil grain penetration and interaction with the underlying material. Nevertheless, Ingold [61] found relatively small differences in results between fixed and free-type tests.
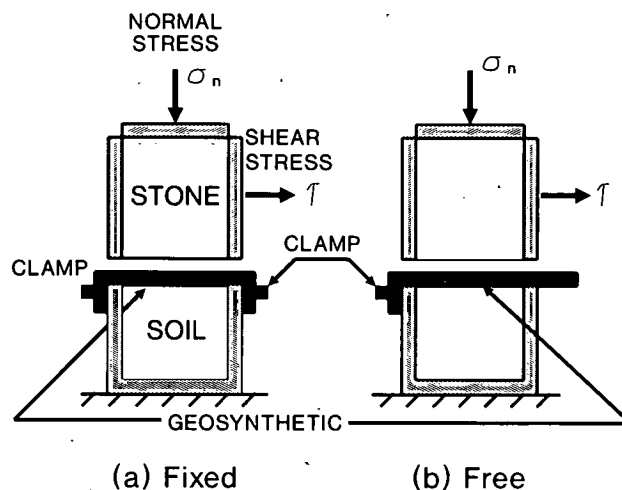
Figure 44. Free and fixed direct shear apparatus for evaluating interface friction.
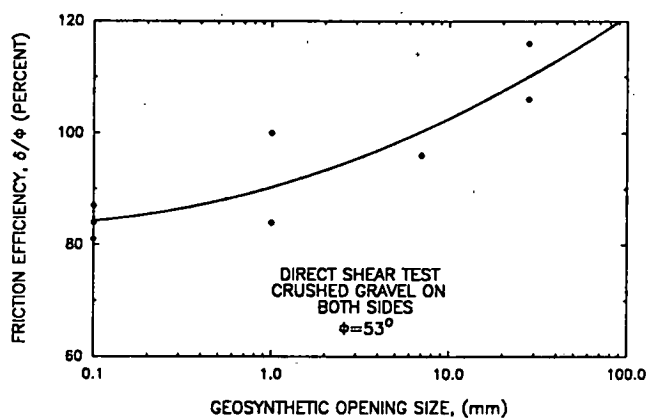
Figure 45. Influence of geosynthetic pore opening size on friction efficiency (data from Collios et al., Ref. 55).

Interface Behavior. A slip type failure tends to develop under low confining stress and for smooth, stiff geosynthetics that resist penetration of soil grains into the surface [56]. For conditions where soil grains penetrate into the surface, failure develops a small distance from the geosynthetic within the soil. Failure occurs in this case by adhesion and rolling, sliding, dilation, and interlock of soil grains [56]. Cohesive soils require less surface roughness than cohesionless materials for development of a "soil on soil" failure immediately adjacent to the geotextile.

The contact efficiency for loose sands in contact with a wide range of geotextiles is close to the angle of internal friction, with the range in contact efficiency typically varying from about 90 percent to 100 percent of ϕ [62]. For dense sands the contact efficiency is lower, typically varying from about 75 percent to 90 percent, but it can be as great as 100 percent [57, 62].

When the effective grain size of the soil on the side that has relative movement is smaller than the pore openings of the geosynthetic, contact efficiency is high. Factors that otherwise would be important generally have only minor influence on the friction behavior. As pore openings of the geosynthetic increase (or the grain size of the soil decreases), better penetration of the grains into the pores of the geosynthetic occurs, and hence the friction angle, δ, becomes greater, as shown in Figure 45

Table 20. Typical friction and adhesion values found for geosynthetics placed between aggregate base and clay subgrade.

GEOSYNTHETIC CLASSIFICATION	INTERFACE	RANGE OF VALUES		TYPICAL VALUES	
		ADHESION	FRICTION ANGLE, δ (DEGREES)	ADHESION	FRICTION ANGLE, δ (DEGREES)
High Friction	Soil Geosyn. Stone-Geosyn.	(0.6-0.8)c (0.4-0.7)c	0-12 19-23	0.8c 0.5c	6 20
Low Friction	Soil-Geosyn. Stone-Geosyn.	(0.2-0.3)c (-0.3-+0.3)c	6-13 11-30	0.2c 0.2c	9 20

for a crushed gravel. When the material particle size is less than the openings of the reinforcement, the contact efficiency may be greater than 100 percent (i.e., $\delta/\phi > 1$). A high contact efficiency is, therefore, achieved for most materials placed against very open reinforcement such as geogrids. Clays also have a high contact efficiency [55].

A geotextile that is compressible in the direction perpendicular to the plane of the fabric allows better penetration of particles. This has been observed for nonwoven, needle-punched geotextiles by Martin et al. [57]. The in-plane stiffness of the geotextile also affects interface friction behavior. Consider two geotextiles having the same size pore openings. The geotextile having the higher in-plane stiffness reaches the peak interface shear stress at a much lower deformation than the lower modulus geosynthetic. The lower stiffness geosynthetic, however, eventually reaches a higher peak shear stress [55].

Aggregate Bases. Collios et al. [55] found for tests involving stone on stone that the contact efficiencies of three different large stones were 86 percent for crushed gravel and 66 percent for rounded gravel compared to 84 percent for sand. These friction test results are applicable when a geotextile is placed within a granular layer, because stone was located both above and below the geosynthetic.

Usually the geosynthetic has been placed at the interface between the granular base or subbase and the subgrade. To simulate field conditions, the subgrade soil should be compacted in the bottom of the shear box, and the coarse base or subbase aggregate in the top [59, 63].

The relative displacement required to develop full shear strength at a ballast-geosynthetic interface was found by Saxena and Budiman [59] to be about 1.6 in. (41 mm). This large displacement was about three times that required at the soil-geosynthetic interface on the other side. Upon cycling the shear stress, up to 40 percent loss of interface shear strength was observed. The loss of shear strength appeared to be due to the ballast pulling the fibers and causing severe deterioration of the geotextile.

The deflection required to reach peak shear stress is a function of the particle size and the normal stress. Typically, displacements of 0.1 in. to 0.4 in. (3 to 10 mm) are required [56]. However, for large base coarse aggregate or very rough geosynthetics, as much as 1 in. to 2 in. (25 to 50 mm) of displacement may be necessary to mobilize full interface strength [59]. Hence, for the pavement problem where deformations are small, full interface strength will probably not be mobilized.

Robnett and Lai [63] have determined typical values of adhesion and friction angle for geotextiles exhibiting both good and poor friction characteristics. These results changed into a slightly different form are given in Table 20. The occurrence of relatively large adhesion for slippage at both the soil and the stone-geotextile interface is in agreement with the findings of Saxena and Budiman [59].

Grid Reinforcement. Both metallic and polymer-type grid reinforcements have large openings. As a result well-graded base coarse aggregates protrude through the openings and, hence, exhibit a high contact efficiency. The high contact efficiency has in the past been attributed, for granular materials, to aggregate interlock. Jewell et al. [64] have presented an excellent discussion of the interaction between a geogrid and soil and give contact efficiencies for seven aggregates. In addition to the mechanisms previously discussed, a bearing capacity type failure may occur in front of the transverse members of a grid.

Ingold [61] has found the contact efficiency of a geogrid for the free, direct shear test to be about 106 percent, compared to 88 percent for the fixed shear test. A medium to coarse sand with some gravel was used in the comparison.

Slip in Reinforced Pavements. The shear stresses developed at the geosynthetic interface become larger and, hence, a greater tendency to slip occurs as the total deflection of the geosynthetic increases. The laboratory shear test results show that a relative movement of up to 2 in. (50 mm) between a geosynthetic and a soft cohesive soil is required to mobilize full friction. Nonlinear finite element analyses indicate that slip is not likely to occur for sections of moderate strength or subgrades with a CBR $\geq$ 3 percent.

For lighter sections or lower strength subgrades, slip does appear to become a problem. Problems with slip and also separation can occur at deformations less than 0.25 in. (6 mm) if the full friction in the geosynthetic is not mobilized. These results indicate that only geosynthetics with good friction characteristics should be used for reinforcement. The experimental results showing that a stiff geogrid performed better than a very stiff woven geotextile supports this finding. From the previous discussion of friction, a nonwoven needle-punched geosynthetic should have better frictional characteristics than a woven geotextile, but probably not as high a friction as a geogrid.

Type of Geosynthetic Reinforcement

Reinforcement. A geogrid and a woven geotextile were placed at the center of the base in two different sections in test series 4. The geogrid, despite its lower stiffness, gave better performance than the much stiffer woven geotextile (refer, for example,

to Table 13 and Figs. 18(d) and 19). The stiffness of the geogrid was about 1,700 lb/in. (300 kN/m) compared to about 4,300 lb/in. (750 kN/m) for the very stiff geotextile. The better performance of the geogrid under the relatively light wheel loading might be caused by better interface friction characteristics because of interlocking between the geosynthetic and the aggregate base.

Results of the two supplementary single track test studies (Figs. 22(c) and 28(c)) appear to suggest that the stiff woven geotextile used in this project required a much higher deformation to mobilize an equal level of reinforcing potential. This seems to indicate that the strengthening observed in the tests was not due to membrane effects but rather to local reinforcement, probably caused by small increases in lateral confining pressure. This conclusion is supported by the work of Penner, Haas and Walls [40]. These results show that special consideration must be given in an analytical study of sections having geogrid compared to geotextile reinforcement.

Separation. The woven geotextile performed better than the very open mesh geogrid in acting as a separator between subgrade and base. The amount of subgrade soil contamination of the base in sections having the geotextile was negligible, while in geogrid sections it was as great as 1.5 in. (38 mm). Geogrids, of course, were not developed to perform the function of separation. The separation effect is not considered to be significant for this study in regard to improvement in pavement performance.

Prerutting

As previously discussed, slack in the geosynthetic can significantly reduce its effectiveness as a reinforcement. One efficient method of removing slack and even applying some pretensioning to the geosynthetic is by means of prerutting as demonstrated by Barenberg [65]. The performance of a number of prerutted sections both reinforced and nonreinforced was evaluated during the laboratory phase of this investigation. A geotextile and a geogrid were placed at both the bottom and middle of the aggregate base of different sections. Prerutting was carried out in both a sand-gravel base and a crushed dolomitic limestone base.

Prerutting was performed by applying applications of a wheel load to the top of the aggregate base before the asphalt surfacing was applied. The loading was carried out along a single wheel path until the desired level of rutting was developed. When loading was conducted above instrumentation, prerutting was continued until a rut depth was developed on the subgrade of about 0.75 in. (19 mm) for the first test series which involved very weak sections. For the subsequent stronger test series where instrumentation was present a subgrade rut depth of 0.4 in. (10 mm) was developed. If instrumentation was not present, prerutting was continued until a surface rut of about 2 in. (50 mm) was achieved in the sections having an 8-in. (200 mm) thick aggregate base. This level of rutting was approximately equivalent to a 0.4-in. (10 mm) subgrade rut. The number of load repetitions required to accomplish prerutting was between 5,000 and 10,000.

The experimental results of test series 2 (Fig. 22(b)) indicate that prerutting an aggregate base reinforced with a geosynthetic results in an important overall reduction in surface rutting of the completed pavement. Reinforced sections that have been

prerutted can reduce surface rutting by 30 percent or more compared to nonprerutted sections. Prerutting appears to reduce vertical resilient and permanent strains in the base and subgrade (Figs. 23(a) and 23(b) and Figs. 24(a) and 24(b)). The vertical stress on the subgrade appears to remain relatively constant with number of load repetitions until the pavement has been severely damaged (Fig. 26(a)). The vertical subgrade stress developed in nonprerutted sections tended to increase at a gradually increasing rate throughout the test.

Supplementary tests showed, however, that prerutting a nonreinforced section is just as effective as prerutting one which is reinforced (Fig. 28(b)). Therefore, prerutting alone is the mechanism which explains the observed improvement in performance. The presence of a geosynthetic reinforcement appears not to affect the efficiency of prerutting. The results from test series 2 (Table 13) indicate an 85 percent reduction in subgrade rutting and a 60 percent reduction in base rutting, apparently due to prerutting. Prerutting, therefore, appears to be most effective in reducing the permanent deformation in the soft subgrade, but it can also significantly reduce rutting in an aggregate base.

Prerutting is beneficial because of the additional compactive effect applied to the aggregate base, similar to that from a pneumatic-tired roller. Prerutting normally results in the formation of a denser, stiffer zone at the top of the aggregate layer. Improved resistance to permanent deformation and less rutting are thus achieved. Prerutting alone has more benefit than placing a geosynthetic at an effective location (Fig. 28(b)). Care must be taken, however, in prerutting a weak granular base which tends to shear rather than densify under a concentrated wheel load. The formation of shear planes or a weakened zone within the aggregate layer as a result of prerutting can have a detrimental effect on pavement performance. This mechanism was indicated by a high permanent deformation in the weak aggregate layer of the prerutted section in the first test series (Fig. 20(a)).

Prestressed Geosynthetic

Basic Prestressing Concepts

One potential approach for improving pavement performance is to prestress the geosynthetic [35, 36]. This can be achieved by the following procedure: (1) stretch the geosynthetic to a desired load level, (2) hold the geosynthetic in the stretched position until sufficient material is above it to prevent slip, and (3) then release the prestress force. On release, the geosynthetic prestressing element tries to return to its original, unstretched condition. The friction developed between the geosynthetic and the surrounding soils restrains the geosynthetic from moving. As a result, the force from the geosynthetic is transferred to the surrounding soil as a compressive lateral stress.

The mechanism of load transfer to the aggregate base and subgrade is through the shear stress developed along the sides of the geosynthetic. If sufficient friction can not be developed to hold the geosynthetic in place, part of the beneficial effect of prestressing is lost through slippage along the interface of the geosynthetic. The shear stress distribution developed along the geosynthetic is approximately as shown in Figure 46. Important losses of prestress force are also developed through stress relaxation. Stress relaxation is a loss of force in the geosynthetic occurring when it is prevented from undergoing any deforma-

SHEAR STRESS T

F_O ← → F_O

Initial Prestress
Force (lbs/in.)
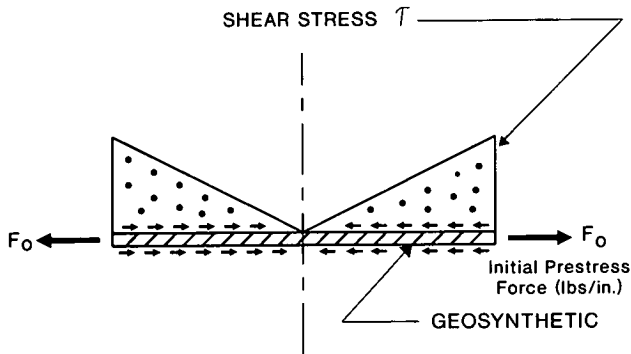
GEOSYNTHETIC

Figure 46. Variation of shear stress along geosynthetic due to initial prestress force on edge.

tion; stress relaxation can be visualized as the inverse of creep. The loss of prestressing effect through stress relaxation is unavoidable. Stress relaxation in geosynthetics can be quite large and is highly dependent on the material type with less stress relaxation occurring in polyester geosynthetics.

Experimental Findings

A stiff polypropylene geogrid was used for the prestressing experiments. The geogrid was initially stretched to a force of 40 lb/in. (7 kN/m) and, then, the sides were rigidly clamped against the walls of the test facility during construction of the aggregate base and asphalt surfacing. After construction, the clamps were removed. Prestress loss due to stress relaxation probably reduced the effective applied prestress force to perhaps 20 lb/in. (3.5 kN/m), which was the prestress level used in the analytical study. The improvement of pavement performance was clearly indicated by the results of the fourth test series as shown in Figures 18 and 19 (refer also to Table 15). The pavement with prestressed geogrid performed better than both a nonprestressed section reinforced with a stiff geogrid (S_g = 1,700 lb/in.; 300 kN/m), and a very stiff woven geotextile (S_g = 4,300 lb/in.; 750 kN/m) reinforced section. At 10,000 load repetitions the prestressed geogrid pavement had about 30 percent less permanent deformation than the corresponding nonprestressed geogrid section, which was the next most satisfactory one.

The measured strain in the bottom of the asphalt surfacing of the prestressed section at 10,000 load repetitions was about 30 percent less than in a geotextile reinforced section not prestressed (Table 13). By 70,000 repetitions, however, the difference in measured strain was only about 5 percent. An important unknown is whether the apparent loss of the beneficial effect of prestressing on strain was due to general deterioration of the pavement as a result of reaching the end of its life, or loss of prestress with increase in lapsed time from construction. If the beneficial effect of prestressing on tensile strain was a result of general pavement deterioration, prestressing should be quite effective in increasing fatigue life. On the other hand, if the loss of prestress was due to stress relaxation with time, prestressing would probably not be effective in a field installation for a pavement having a life of 10 to 20 years or more.

Of considerable practical importance is the finding that the prerutted section having a very stiff geotextile in the middle

performed equally well compared to the prestressed section. It then follows from the other results of the experimental study that prerutting a section without a geosynthetic should be just as effective in terms of reducing permanent deformation as prestressing (Figs. 28(c) and 28(d)). This conclusion is valid for the conditions of the study including using a polypropylene geogrid with S_g = 1,700 lb/in. (300 kN/m) initially stressed to 40 lb/in. (7 kN/m).

Analytical Results

In the analytical study of prestress effects, an effective prestress force of 20 lb/in. (3.5 kN/m) was applied. This represents the net force existing after all losses including stress relaxation. The standard reference section was used consisting of a 2.5-in. (64 mm) asphalt surfacing, a variable thickness base, and a subgrade with E_s = 3,500 psi (24 MN/m²). Prestressing the center of the aggregate base, based on tensile strain in the asphalt surfacing, resulted in large reductions in base thickness varying from about 25 to 44 percent (Table 21). For a base thickness of 11.9 in. (300 mm), expected reductions in total permanent deformation are on the order of 20 to 45 percent. For general comparison, the observed reductions in total rutting of the lighter prestressed experimental section was about 60 percent compared to the nonprestressed, geotextile reinforced section with reinforcement at the center.

The analytical results indicate that prestressing the center of the layer would have little effect on the vertical subgrade strain and may even increase it by a small amount; reduction in rutting of the subgrade would also be small. The experimental results, however, demonstrate that prestressing the center of the layer can, for very light sections, also lead to important reductions in permanent deformation of both the base and subgrade. With this exception, the analytical results tend to support the experimental finding that prestressing the middle of the aggregate base should greatly improve rutting of the base and fatigue performance.

The analytical study points out that prestressing the bottom of the layer is quite effective in reducing permanent deformation, particularly in the subgrade. For the reference section, reductions in permanent deformation were obtained varying from 30 to 47 percent, and reductions in base thickness, based on vertical subgrade strain of about 35 percent (Table 21). The analytical results indicate that prestressing the bottom of the base is not as effective, however, as prestressing the middle with respect to reducing tensile strain in the asphalt surfacing.

Pretensioning—Practical Field Considerations

To achieve the demonstrated potential for a significant improvement in performance, the geosynthetic should be prestressed in the direction transverse to that of the vehicle movement. Proper allowance should be made for prestress loss due to stress relaxation, which would depend on the type and composition of the geosynthetic and the initial applied stress level. Allowance must also be made for all other prestress losses resulting between the time pretensioning is carried out and the prestress force is transferred to the aggregate base. These losses would be related to the method used to apply and maintain the prestress force and the skill and care of the crew performing the work. Probably an initial pretensioning force on the order

Table 21. Beneficial effect on performance of prestressing the aggregate base.

GEOSYN. POSITION	BASE THICK,T w/o GEOSYN. (in.)	CHANGE IN BASE THICKNESS (%)						CHANGE IN RUTTING OF BASE AND SUBGRADE (%),					
		CONSTANT VERTICAL SUBGRADE STRAIN,ε_v			CONSTANT TENSILE STRAIN AC, ε_t			GOOD BASE/FAIR SUBG.			POOR BASE/FAIR SUBG.		
		GEOSYNTHETIC STIFFNESS OR PRESTRESS FORCE (lbs/in.)											
		1000 (10)	4000 (20)	6000 (40)	1000 (10)	4000 (20)	6000 (40)	1000 (10)	4000 (20)	6000 (40)	1000 (10)	4000 (20)	6000 (40)
2.5 IN. SURFACING 3500 PSI SUBGRADE (REINFORCED)													
GEOSYN @ BOTTOM	15.3	-3.9	-12	-16	-1.8	-6.5	-9	-9	-22	-27	-4	-11	-15
	11.92	-3.3	-12	-16	- 2	- 8	-12	-12	-30	-36	- 7	-19	-23
	9.75	-4.9	-14	-18	-2.6	-12	-18	-18	-39	-46	-7	-28	-33
2.5 IN. AC SURFACING 3500 PSI SUBGRADE (PRESTRESSED SECTION)													
PRESTRESS @ BOT.	15.3	-	-34	-	-	-19	-	-	-	-	-	-	-
	11.92	-	-35	-	-	-17	-	-30	-47	-	-16	-22	-
	9.75	-	-37	-	-	-22	-	-	-	-	-	-	-
	7.5	-	-	-	-	-	-	-	-	-	-	-52	-
2.5 IN. AC SURFACING 3500 PSI SUBGRADE (PRESTRESSED SECTION)													
PRESTRESS @ CENTER	15.3	-	-1.2	-	-	-26	-						
	11.92	-	+2.3	-	-	-25	-						
	9.75	-	+9.0	-	-	-44	-						

of 40 lb/in. (7 kN/m), which is the force used in the laboratory tests, would be a reasonable starting point for additional field studies.

One approach that could be employed for applying the pretensioning force would be to place sufficient stakes through loops into the ground along one side of the geosynthetic to firmly anchor it. An alternate approach would be to use a dead weight anchor such as a loaded vehicle.

Probably the most efficient method would be to apply the pretensioning force to the side opposite the anchored side of the geosynthetic using an electrically powered winch attached to a loaded truck. The truck would supply the dead weight reaction necessary to develop the pretensioning force. A rigid longitudinal rod or bar would be attached along this same side of the geosynthetic to distribute the pretensioning force uniformly. The pretensioning force could be applied by one winch to about a 10 ft to 15 ft (3 to 4.6 m) length of geosynthetic. To minimize bending in the rod or bar attached to the geosynthetic, the cable leading to the winch would be attached to the bar at two (or more) locations to form a "V" shape. It might be desirable to pretension two or more lengths of geosynthetic at a time.

The pretensioning force could then be maintained on the geosynthetic until sufficient aggregate base is placed and compacted over it to provide the necessary friction force to prevent slippage. If base construction was not progressing rapidly, as would likely be the case, it would be necessary to anchor the side of the geosynthetic being pretensioned probably using stakes. The winch and cable system could then be removed and used to pretension other segments of the geosynthetic.

Prestressing the base would most likely be carried out where the subgrade has a CBR less than 3 to 4 percent, or where a low quality aggregate base is used. For conditions where a soft subgrade exists, temporary anchorage of the geosynthetic becomes a serious problem. For example, consider a soft subgrade having an undrained shear strength of about 500 psf (24 kN/m^2). Wood stakes 2 in. by 2 in. (50 by 50 mm) by 3 ft (0.9 m) in length, having a spacing of about 2 ft to 3 ft (0.5 to 0.9 m), would be required to hold a light initial pretensioning load of only about 20 lb/in. (3.5 kN/m). The cost to just apply this light level of pretensioning to a geogrid by an experienced contractor would probably be about 1 to 1.5 times the geogrid cost.

Thus, the practicality of applying even a light pretensioning force to pavements constructed on soft subgrades having undrained shear strengths less than about 500 psf (24 kN/m^2] is questionable. Even moving equipment over very soft soils to provide temporary dead weight anchorage would probably not be practical.

SUMMARY

The presence of geosynthetic reinforcement causes a small but potentially important increase in the confining stress and reduction in vertical stress in the base and upper 6 in. to 12 in. (150 to 300 mm) of the subgrade. The stiffness of the geosynthetic is an important factor, and should be greater than 1,500 lb/in. (260 kN/m) for base reinforcement to start to become effective. A geogrid performs differently from a woven geotextile

reinforcement. The laboratory tests indicate that a geogrid having a stiffness of about 1,500 lb/in. (260 kN/m) performs about the same as a woven geotextile having a stiffness of about 4,000 lb/in. (700 kN/m).

For light pavement sections (SN ≅ 2.5 to 3) where stresses are high, reinforcement can have an important effect on reducing rutting in the base and upper part of the subgrade. For heavier sections the potential beneficial effect of reinforcement tends to decrease rapidly. In heavier sections, however, reinforcement may be beneficial where low quality bases or weak subgrades are present; this aspect needs to be established using full-scale field tests.

The experimental and analytical results indicate that significant reductions in rutting can, at least under idealized conditions, be achieved through prestressing the aggregate base. The experimental results indicate that prerutting the base without the use of a geosynthetic is equally effective, at least with respect to reducing permanent deformations. Prerutting would very likely be less expensive than prestressing and should be effective over an extended period of time.

The experimental results on the prestressed sections were obtained for short-term tests performed under idealized conditions. Loss of prestress effect in the field and prestress loss due to long-term stress relaxation effects are certainly important practical considerations that can only be fully evaluated through full-scale field studies. Limited strain measurements made in the bottom of the asphalt surfacing of the prestressed section show that a loss of benefit occurs with either time or deterioration of the pavement.

CHAPTER FOUR

CONCLUSIONS AND SUGGESTED RESEARCH

OVERALL EVALUATION OF AGGREGATE BASE REINFORCEMENT

The conclusions developed in this chapter are based on the geosynthetic reinforcement of an aggregate base of a flexible pavement. To evaluate the use of geosynthetics as reinforcement, an analytical sensitivity study and large-scale laboratory experiments were performed on selected pavement sections. A geotextile reinforcement may, at the same time, serve the functions of separation and/or filtration; therefore, these aspects were considered. The important question of durability of geosynthetics when buried for a long period of time is also addressed.

In studying new methods for improving pavement performance, all important factors must be carefully integrated together to develop a realistic overall evaluation. In this study methods were investigated involving the reinforcement of an unstabilized aggregate base to be used beneath a surfaced flexible pavement. Specific methods of improvement evaluated included: (1) geotextile and geogrid reinforcement placed within the base, (2) prestressing the geosynthetic, and (3) prerutting the aggregate base either with or without geosynthetic reinforcement. In the remainder of this chapter a general assessment of the foregoing improvement techniques is made including their overall benefits and relative potential, economic considerations, and construction and durability aspects. It is noted that the term geosynthetic as used herein means either geotextiles or geogrids.

Geosynthetic Reinforcement Benefits

The laboratory and analytical results indicate that geosynthetic reinforcement of an aggregate base can, under the proper conditions, improve pavement performance with respect to both permanent deformation and fatigue. In general, the analytical results indicate that important levels of improvement will only be derived for relatively light sections that are placed on weak subgrades or have low quality aggregate bases. Field tests need to be performed to verify whether reinforcement is effective for heavier sections that have low quality bases or very weak subgrades. Specific conclusions drawn from the study are as follows.

Type and Stiffness of Geosynthetic. The experimental results suggest that a geogrid having an open mesh has the reinforcing capability of a woven geotextile having a stiffness approximately 2.5 times as great as the geogrid. Hence, a geogrid performs differently from a woven geotextile. Comparative tests were not conducted on nonwoven geotextiles which might have better reinforcing characteristics than woven geotextiles because of improved friction characteristics. From the experimental and analytical findings, it appears that the minimum stiffness to be used for aggregate base reinforcement applications should be about 1,500 lb/in. (260 kN/m) for geogrids and 4,000 lb/in. (700 kN/m) for woven geotextiles. Geosynthetics having stiffnesses much less than the foregoing values would not have the ability to effectively perform as reinforcement even on weak pavements.

Placing geosynthetics having the above stiffnesses within pavements would not be expected to increase the overall stiffness of the system as indicated, for example, by falling weight deflectometer (FWD) or Dynaflect testing.

Geosynthetic Position. The experimental results show that placing the reinforcement in the middle of a thin aggregate base can reduce total permanent deformations. For light pavement sections constructed with low quality aggregate bases, the preferred position for the reinforcement should be in the middle of the base, particularly if a good subgrade is present. Placement of the reinforcement at the middle of the base, rather than at the bottom of the layer, will also result in better fatigue performance.

For pavements constructed on soft subgrades, the reinforcement should probably be placed at or near the bottom of the base. This would be particularly true if the subgrade is known to have rutting problems and the base is of high quality and is well compacted. The analytical approach indicated that the reinforcement should be placed at the bottom of the base to be most effective in minimizing permanent deformations in the subgrade. The experimental study verified this finding, showing that important improvements to subgrade rutting could be achieved when a very stiff geotextile is placed at the bottom of an extremely weak section. Almost no improvement was observed, however, for a stronger section having a stiff geogrid at the bottom. In these tests most of the rutting occurred in the base and, hence, reduction of rutting in the subgrade would be harder to validate. The possibility does exist that the geogrid may be more effective when it is surrounded by aggregate as compared to when it has a soft subgrade in contact with it on one side.

For improvement of fatigue performance of the asphalt surfacing, the optimum position appears to be at the interface between the asphalt and granular base. Where a good subgrade is present and a high quality base is used, consideration can be given to this reinforcement application.

Subgrade Rutting. Light to moderate strength sections placed on weak subgrades having a CBR < 3 percent (E_s = 3,500 psi; 24 MN/m^2) are most susceptible to significant improvement by geosynthetic reinforcement in the upper 6 in. to 12 in. (150 to 300 mm). The structural section should probably have AASHTO structural numbers no greater than 2.5 to 3 if reduction in subgrade rutting is to be achieved by geosynthetic reinforcement. As the structural section becomes stronger, the actual amount of reduction in rutting will, in general, become small even though the percent reduction in rutting may still be relatively large. Where weak subgrades are present the level of improvement will be greater, but the actual amount needs to be established by full-scale field tests.

Pavement Strength. As the structural number and subgrade strength of the pavement decreases below the above values, the improvement in performance due to reinforcement should rapidly become greater. Strong pavement sections placed over good subgrades would not be expected to show any significant level of improvement due to geosynthetic reinforcement of the type studied. Sections with asphalt surface thicknesses greater than about 2.5 in. to 3.5 in. (64 to 90 mm) would be expected to exhibit relatively little improvement even if placed on weak subgrades. Field verification of this finding is required.

Low Quality Base. Geosynthetic reinforcement of a low quality aggregate base can, under the proper conditions, reduce rutting. The asphalt surface should be less than 2.5 in. to 3.5 in. (64 to 90 mm) in thickness for the reinforcement to be most effective. Very weak bases, however, may show some improvement for even greater thicknesses of asphalt.

Improvement Levels. Light sections on weak subgrades reinforced with geosynthetics having effective stiffnesses of about 4,000 to 6,000 lb/in. (700 to 1,050 kN/m) can give reductions in base thickness of 10 percent to 20 percent based on equal strain levels in the subgrade and bottom of the asphalt surfacing. The equivalent stiffness of a geogrid would be about 2.5 times its actual stiffness. For light sections, this corresponds to actual reductions in base thickness of about 1 in. to 2 in. (25 to 50 mm). For weak subgrades and/or low quality bases, total rutting in the base and subgrade may, under ideal conditions, be

reduced by 20 to 40 percent. Considerably greater reductions in rutting occur, however, for the thinner sections on weak subgrades than for heavier sections on strong subgrades.

Fatigue. The analytical results indicate that improvements in permanent base and subgrade deformations may be greater than the improvement in fatigue life, when these improvements are expressed as a percent reduction of required base thickness. This is true for reinforcement locations at the center and bottom of the base. The experimental results are inconclusive as to whether fatigue is actually affected less by reinforcement than by rutting. Improvement in fatigue performance perhaps might be greater than indicated by the analytical analyses. The optimum position of geosynthetic reinforcement from the standpoint of fatigue appears to be at the top of the base.

Finally, geosynthetic reinforcement should not be used as a substitute for good construction and quality control practices. Good construction practices would include proper subgrade preparation including proof-rolling and undercutting when necessary and compacting aggregate bases to a minimum of 100 percent of AASHTO T-180 density. The fines content of aggregate bases should be kept as low as practical, preferably less than 8 percent.

Prerutting and Prestressing Potential

Both prerutting the aggregate base and prestressing the geosynthetic were found, experimentally, to significantly reduce permanent deformations within the base and subgrade. The analytical results also show prestressing to be quite effective; fatigue life being significantly improved if the center of the layer is prestressed. Stress relaxation over a long period, however, could significantly reduce the effectiveness of prestressing the geosynthetic in the aggregate base. The experimental findings of this study demonstrate that prerutting is equally effective with or without the presence of geosynthetic reinforcement. Prerutting required 5,000 to 10,000 wheel passes; heavier loads could be used in the field to reduce the required number of passes.

Prerutting without a geosynthetic provides the potential for a quick, permanent and cost-effective method for significantly improving performance of light pavements constructed on weak subgrades. Prerutting may also be found effective where low quality aggregate bases are used, or where reasonably strong pavement sections are placed on weak subgrades.

Economic Considerations

Prerutting and Prestressing. The most promising potential method of improvement appears to be prerutting a nonreinforced aggregate base. Prerutting without reinforcement should give performance equal to that of prestressing and significantly better performance compared to the use of stiff to very stiff nonprestressed reinforcement. Further, prerutting is a more positive treatment than prestressing.

The cost of prerutting an aggregate base at one level might be as small as 50 percent of the in-place cost of a stiff geogrid (S_g = 1,700 lb/in.; 300 kN/m). Further, prestressing the same geogrid would result in a total cost equal to about 2 times the actual cost of the geogrid. Therefore, the total expense associated with prestressing may be as great as 5 times that of prerutting
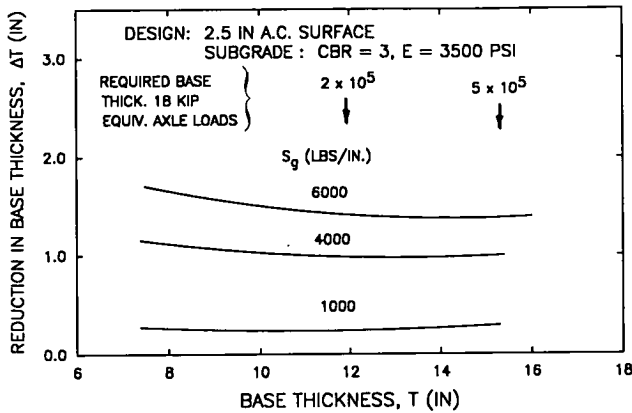
Figure 47. Approximate reduction in granular base thickness as a function of geosynthetic stiffness for constant radial strain in AC: 2.5-in. AC, subgrade CBR = 3.
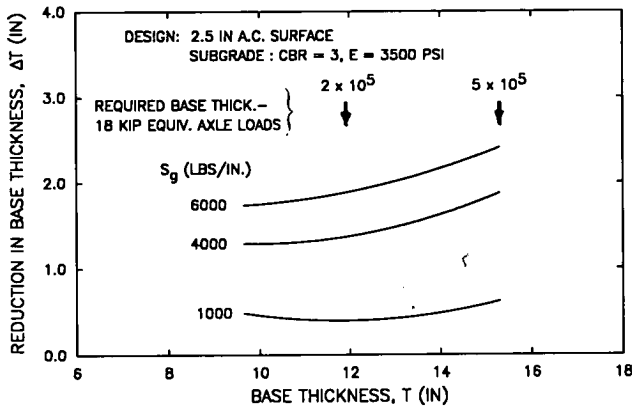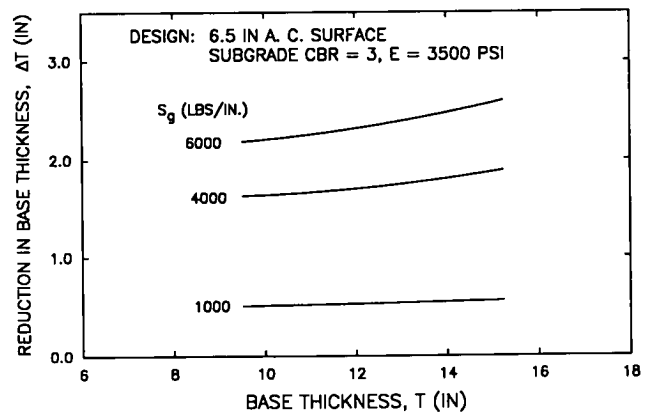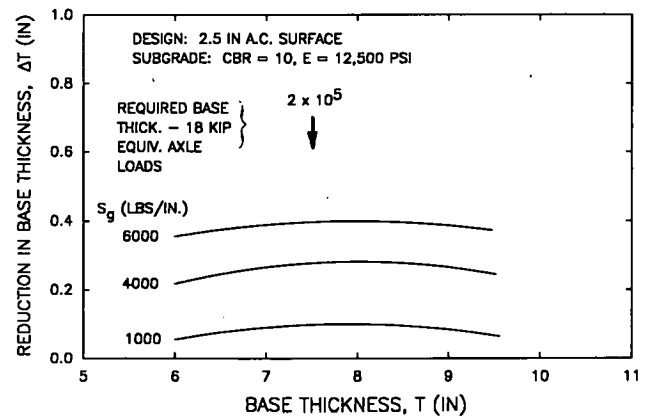

Figure 48. Approximate reduction in granular base thickness as a function of geosynthetic stiffness for constant vertical subgrade strain: 2.5-in. AC, subgrade CBR = 3.
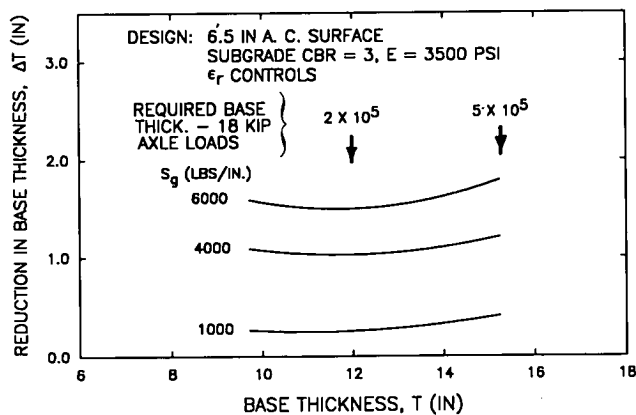
the base at one level when a geosynthetic reinforcement is not used. Prerutting without reinforcement is relatively cheap and appears to be quite effective, at least with regard to reducing permanent deformations. Full-scale field experiments should, therefore, be conducted to more fully validate the concept of prerutting and develop appropriate prerutting techniques.

Geosynthetic Reinforcement. The use of geosynthetic reinforcement is considered to be economically feasible when employed in light pavements constructed on soft subgrades, or where low quality bases are used beneath relatively thin asphalt surfacings. Geosynthetic reinforcement may also be economically feasible for other combinations of structural designs and material properties where rutting is a known problem.

General guidance concerning the level of improvement that can be achieved using geosynthetic reinforcement of the aggregate base is given in Figures 47 to 51 (refer also to Tables 17, 18, and 21). The results presented in this study were developed for specific conditions including material properties and methodology. Full-scale field studies are needed to validate the findings of this research. In estimating potential levels of improvement for a specific pavement, the results of the entire study, including the uncertainties associated with it, should be integrated together considering the specific unique conditions and features associated with each design.

Figure 52 gives the relationship between the in-place geosynthetic cost (or the cost of some other type of improvement), the local in-place cost of aggregate base, and the corresponding reduction in aggregate base thickness that would be required for the reinforcement to be comparable in cost to a nonreinforced aggregate base. This figure serves as an aid in evaluating the economics of using aggregate base reinforcement, particularly for subgrade rutting problems.

Consider as a hypothetical example, the economics of reinforcing a pavement having a light to moderate structural section constructed on a relatively weak subgrade (AC = 2.5 in., base = 10 in., CBR = 3 percent, E_s = 3,500 psi; 64 mm, 250 mm, 24 MN/m²) using a geogrid having a stiffness of about 1,700 lb/in. (300 kN/m). The geogrid should perform equal to, or somewhat better than, a very stiff woven geotextile based on the experimental results of test series 4. Assume the geogrid

Figure 49. Approximate reduction in granular base thickness as a function of geosynthetic stiffness for constant radial strain in AC: 6.5-in. AC, subgrade CBR = 3.

Figure 50. Approximate reduction in granular base thickness as a function of geosynthetic stiffness for constant vertical subgrade strain: 6.5-in. AC, subgrade CBR = 3.

costs $1/yd² ($1.19/m²) in-place and performs about the same as a geotextile having a stiffness of 4,000 lb/in. (700 kN/m). From Figures 47 and 48, the reduction in base thickness should be about 1.0 in. to 1.3 in. (25 to 33 mm). Considering fatigue may be improved more than the analytical approach indicates, assume the allowable reduction in base thickness is 1.3 in. (33 mm). From Figure 52, the required in-place cost of stone base to make the geosynthetic economically comparable to an aggregate base would be about $15 per ton. The use of a grid reinforcement could help to decrease rutting, particularly if poorer materials were involved, so this aspect should not be overlooked in making the final decision concerning reinforcement.

Construction and Durability Aspects

Stretching Geosynthetic in the Field. The results of this study show that the geosynthetic must develop significant strain to be effective as a reinforcement. The amount of strain required depends on the desired level of improvement and the stiffness of the geosynthetic. If the geosynthetic is placed in the field with slack or wrinkles, considerable deformation is required in the form of rutting before adequate strain is developed to mobilize sufficient tensile force in the geosynthetic. Theory indicates that even a small amount of slack (0.2 percent of the width of the geotextile) can render it essentially ineffective.

Wrinkles and irregularities can be removed by stretching the geosynthetic as tight as practical by hand during placement [42]. Then, a special fork, or other device, should be used to stretch the geosynthetic. To give the best performance and most uniform strain distribution within the geosynthetic [26, 42], it should be fastened down with wood or metal stakes. Use of a top plate on the stake is recommended to prevent a geogrid from lifting off the stake, particularly when a soft cohesive subgrade is present. If sufficient fill is to be placed, it may be possible to fold the reinforcement over at the edges to give anchorage [26].

For wide geosynthetic widths, for example, a roadway or embankment about 60 ft (18 m) in width and requiring several feet of fill (Fig. 53), a simple, but relatively effective method for stretching the geosynthetic involves first spreading out the geosynthetic over an area of about 200 ft to 300 ft (60 to 90 m) in length. The material is rolled out in the short direction and any necessary seams are made. Fingers of fill are then pushed out along the edges of the geosynthetic covered area in the direction perpendicular to the roll. Usually the fingers are extended out about 40 ft to 100 ft (12 to 30 m) ahead of the main area of fill placement between the fingers. The fingers of fill pushed out are typically 15 ft to 20 ft (5 to 8 m) in width, and serve to anchor the two ends of the geosynthetic. When fill is placed in the center area, the resulting settlement stretches the geosynthetic. This technique was found to be particularly effective in eliminating most of the slack in the geosynthetic where soft subgrade soils are encountered, and may even place a little initial stretch in the material.

Pretensioning. If the geosynthetic is to be pretensioned, a suitable technique must be developed. Suggestions were made in Chapter Three involving application of the pretensioning force by means of winches and cables. Effective methods of pretensioning, however, can only be developed and refined through studies including field trials.

Prerutting. Appropriate techniques for prerutting the aggre-

Figure 51. Approximate reduction in granular base thickness as a function of geosynthetic stiffness for constant radial strain in AC: 2.5-in. AC, subgrade CBR = 10.
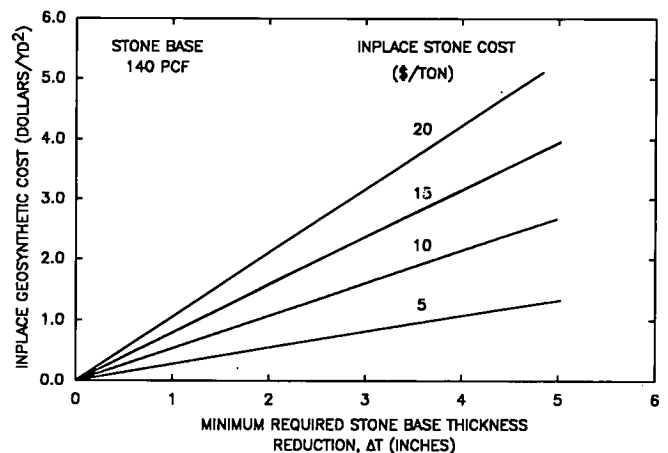
Figure 52. Break-even cost of geosynthetic for given savings in stone base thickness and stone cost.
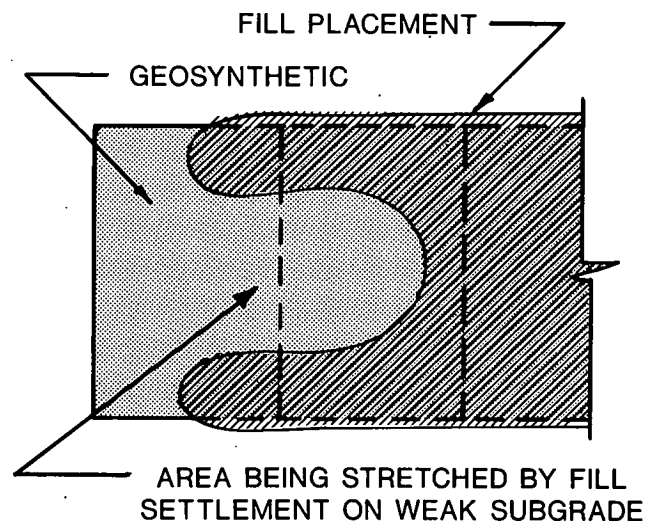
Figure 53. Placement of wide fill to take slack out of geosynthetic.

gate base in the field need to be established. Prerutting is just an extension of proof-rolling and should probably be carried out with a reasonably heavy loading. Prerutting in the laboratory was carried out in a single rut path for a base thickness of 8 in. (200 mm). Development of a total rut depth of about 2 in. (50 mm) was found to be effective in reducing rutting in both the 8-in. (200 mm) aggregate base and also the subgrade. For full-scale pavements, it may be desirable to prerut along two or three wheel paths, perhaps spaced about 12 in. (300 mm) apart. The actual rut spacing used would be dependent on the wheel configuration selected to perform the prerutting. Prerutting an 8-in. (200 mm) base lift thickness in the field would be a good starting point. Caution should be exercised to avoid excessive prerutting. Prerutting could be performed at more than one level within the aggregate base.

Wind Effects. Wind can complicate the proper placement of a geotextile. A moderate wind will readily lift or "kite" a geotextile. It is, therefore, generally not practical to place geotextiles on windy days. If geotextiles are placed during even moderate winds, additional wrinkling and slack may occur in the material. On the other hand, geogrids are not lifted up by the wind because of their open mesh structure and, hence, can be readily placed on windy days [42].

Separation and Filtration. The level of severity of separation and filtration problems varies significantly depending on many factors, as discussed in Appendix F, including the type of subgrade, moisture conditions, applied stress level, and the size, angularity and grading of the aggregate to be placed above the subgrade. Separation problems involve the mixing of an aggregate base or subbase with the underlying subgrade. Separation problems are most likely to occur during construction of the first aggregate lift or, perhaps, during construction before the asphalt surfacing has been placed. Large, angular open-graded aggregates placed directly on a soft or very soft subgrade result in a particularly harsh environment with respect to separation. When separation is a potential problem either a sand or a geotextile filter can be used to maintain a reasonably clean interface. Both woven and nonwoven geotextiles have been found to adequately perform the separation function.

When an open-graded drainage layer is placed above the subgrade, the amount of contamination due to fines moving into this layer must be minimized by use of a filter to ensure adequate flow capacity and also strength. A very severe environment with respect to subgrade erosion exists beneath a pavement which includes reversible, possibly turbulent flow conditions. The severity of erosion is greatly dependent on the thickness of the pavements which determines the stress applied to the subgrade. Low cohesion silts and clays, dispersive clays, and silty fine sands are quite susceptible to erosion. Sand filters, when properly designed, should perform better than geotextile filters with regard to filtration, although satisfactorily performing geotextiles can usually be selected. Thick nonwoven geotextiles perform better than thin nonwoven or woven geotextiles, partly because of their three-dimensional structure.

Semirational procedures are presented in Appendix F for determining when filters are needed for the separation and filtration functions. Guidance is also given in selecting suitable geotextiles for use beneath pavements. These procedures and specifications should be considered tentative until further work is conducted in these areas. Whether a sand filter or a geotextile filter is used would be a matter of economics for most applications.

Durability. Relatively little information is available concerning the durability of geosynthetics when buried in the ground for long periods of time. However, several studies are currently underway which should contribute to an understanding of durability.

Consideration should be given to the environment in which they will be used. Polypropylenes and polyethylenes are susceptible to degradation in oxidizing environments catalyzed by the presence of heavy minerals such as iron, copper, zinc, and manganese. Polyesters are attacked by strong alkaline and, to a lesser extent, strong acid environments; they are also susceptible to hydrolysis.

Under favorable conditions the loss of strength of typical geosynthetics should be on the average about 30 percent in the first 10 years. Because of their greater thickness, geogrids may exhibit a lower strength loss—although this has not been verified. For separation and filtration applications, geosynthetics should have at least a 20-year life. For reinforcement applications, geosynthetic stiffness is the most important structural consideration. Limited observations indicate that some geosynthetics will become more brittle with time and actually increase in stiffness. Whether better reinforcement performance will result has not been demonstrated. The typical force developed in a geosynthetic used for aggregate base reinforcement of surfaced pavements should be less than about 40 lb/in. (7 kN/m). Most geosynthetics would initially be strong enough to undergo significant strength loss for at least 20 years before a tensile failure of the geosynthetic might become a problem for pavement reinforcement applications. Whether geosynthetics used for separation, filtration, or reinforcement can last for 40 or 50 years has not been clearly demonstrated. A more detailed discussion of "Durability" is given in Appendix G.

SUGGESTED RESEARCH

Reinforcement

The laboratory investigation and the sensitivity analyses indicate that further research is needed in the following specific areas of base reinforcement: (1) *Prerutting:* Prerutting a non-reinforced aggregate base appears to have the best overall potential of the methods studied for improving pavement performance. Prerutting in the large-scale experiments was found to be both effective and is also inexpensive. (2) *Low quality aggregate base:* The geosynthetic reinforcement of an unstabilized, low quality aggregate base appears to offer promise as one method for reducing permanent pavement deformation of pavements having thin asphalt surfacings. (3) *Weak Subgrade:* Geosynthetic reinforcement of light pavement sections constructed on weak subgrades shows promise for reducing permanent deformations particularly in the subgrade; whether reinforcement of heavier sections will reduce permanent deformations needs to be further studied in the field.

The recommendation is therefore made that an additional experimental investigation should be conducted to further evaluate these three techniques for potentially improving pavement performance. This investigation should consist of carefully instrumented, full-scale field test sections. Geogrid reinforcement was found to perform better than a much stiffer woven geotextile. Therefore geogrid reinforcement is recommended as the primary reinforcement for use in this study. A description of a

proposed experimental plan for the study is given in Appendix H.

Separation and Filtration

Important areas involving separation and filtration deserving further research are:

1. *Geosynthetic Durability.* A very important need presently exists for conducting long-term durability tests on selected geosynthetics known to have good reinforcing properties. Such a study would be applicable to mechanically stabilized earth reinforcement applications in general. The geosynthetics used should be subjected to varying levels of stress and buried in several different carefully selected soil environments. Tests should run for at least 5 years and preferably 10 years. Soil environments to include in the experiment should be selected considering the degradation susceptibility of the polymers used in the study to specific environments. Properties to be evaluated as a function of time should include changes in geosynthetic strength, stiffness, ductility, and chemical composition.

Each geosynthetic product has a different susceptibility to environmental degradation, and a considerable amount of valuable information could be obtained from a long-term durability study of this type.

2. *Filtration.* A formal study should be undertaken to evaluate the filtration characteristics of a range of geotextiles when subjected to dynamic load and flowing water conditions likely to be encountered both beneath a pavement and also at lateral edge drains. The tests should probably be performed in a triaxial cell by applying cyclic loads as water is passed through the sample. At least 10^6 load repetitions should be applied during the test to simulate long-term conditions.

APPENDIX A

REFERENCES

1. BELL, J. R., ET AL., "Test Methods and Use Criteria for Filter Fabrics." *Report FHWA-RD-80-021,* Federal Highway Administration, U.S. Department of Transportation (1980).

2. BONAPARTE, R., KAMEL, N. I., DIXON, J. H., "Use of Geogrids in Soil Reinforcement." Paper submitted to Transportation Research Board Annual Meeting, Washington, D.C. (Jan. 1984).

3. BENDER, D. A., and BARENBERG, E. J., "Design and Behavior of Soil-Fabric-Aggregate Systems." TRB, *Transportation Research Record 671* (1978) pp. 64–75.

4. ROBNETT, Q. L., and LAI, J. S., "Fabric-Reinforced Aggregate Roads—Overview." TRB, *Transportation Research Record 875* (1982).

5. BELL, J. R., BARRET, R. K., RUCKMAN, A. C., "Geotextile Earth Reinforced Retaining Wall Tests: Glenwood Canyon, Colorado." For presentation at the 62nd Annual Meeting, Transportation Research Board, Washington, D.C., January, 1983.

6. MITCHELL, J. K., and VILLET, C. B., "Reinforcement of Earth Slopes and Embankments." Transportation Research Board, *NCHRP Report 290* (June 1987) 323 pp.

7. GULDEN, W., and BROWN, D., "Treatment for Reduction of Reflective Cracking of Asphalt Overlays of Jointed-Concrete Pavements in Georgia." Transportation Research Board, *Transportation Research Record 916* (1983) pp. 1–6.

8. BUTTON, J. W., and EPPS, J. A., "Field Evaluation of Fabric Interlayers." *Texas Transportation Research,* Vol. 19, No. 2 (Apr. 1983) pp. 4–5.

9. SMITH, R. D., "Laboratory Testing of Fabric Interlayers for Asphalt Concrete Paving: Interim Report." Transportation Research Board, *Transportation Research Record 916* (1983) pp. 6–18.

10. FREDERICK, D. A., "Stress Relieving Interlayers for Bituminous Resurfacing." New York State Department of Transportation Engineering, *Research and Development Bureau, Report 113,* (Apr. 1984) 37 pp.

11. KNIGHT, N. E., "Heavy Duty Membranes for the Reduction of Reflective Cracking in Bituminous Concrete Overlays." Pennsylvania Department of Transportation, Bureau of Bridge and Roadway Technology, Research Project 79-6 (Aug. 1985).

12. BROWN, S. F., HUGHES, D. A. B., and BRODRICK, B. V., "Grid Reinforcement for Asphalt Pavements." University of Nottingham, Report submitted to Netlon Ltd and SERC (Nov. 1983) 45 pp.

13. HALIM, A. O. H., HAAS, R., and PHANG, W. A., "Geogrid Reinforcement of Asphalt Pavements and Verification of Elastic Theory." Transportation Research Board, *Transportation Research Record 949,* (1983) pp. 55–65.

14. MILLIGAN, G. W. E., and LOVE, J. P., "Model Testing of Geogrids Under an Aggregate Layer on Soft Ground." *Polymer Grid Reinforcement: Proc.,* Conference sponsored by Science and Engineering Research Council and Netlon Ltd., London, 22–23 March 1984.

15. GOURC, J. P., PERRIER, H., RIONDY, G., RIGO, J. M., and PEFETTI, J., "Chargement Cyclic d'un Bicouche Renforce par Geotextile." *Polymer Grid Reinforcement: Proc.,* Conference sponsored by Science and Engineering Research Council and Netlon Ltd., London, 22–23 March 1984.

16. BARKSDALE, R. D., ROBNETT, Q. L., LAI, J. S., and ZEEVAERT-WOLF, A., "Experimental and Theoretical Behavior of Geotextile Reinforced Aggregate Soil Systems." *Proc.,*

54

Second International Conference on Geotextiles, Vol. II, Las Vegas (1982) pp. 375–380.

17. SOWERS, G. F., *Introductory Soil Mechanics and Foundations.* Fourth Edition, Macmillan, New York (1979).

18. PETRIX, P. M., "Development of Stresses in Reinforcement and Subgrade of a Reinforced Soil Slab." *Proc.,* First International Conference on Use of Fabrics in Geotechnics, Vol. I (1977) pp. 151–154.

19. POTTER, J. F. and CURRER, E. W. H., "The Effect of a Fabric Membrane on the Structural Behavior of a Granular Road Pavement." *Transport and Road Research Laboratory, Report LR 996* (1981).

20. RAUMANN, G., "Geotextiles in Unpaved Roads: Design Considerations." *Proc.,* Second International Conference on Geotextiles, Vol. II (1982) pp. 417–422.

21. RUDDOCK, E. C., POTTER, J. F., and MCAVOY, A. R., "Report on the Construction and Performance of a Full-Scale Experimental Road at Sandleheath, Hants." *CIRCIA, Project Record 245,* London (1982).

22. BELL, J. R., GREENWAY, D. R., and VISCHERM, W., "Construction and Analysis of a Fabric Reinforced Low Embankment on Muskeg." *Proc.,* First International Conference on Use of Fabrics in Geotechnics, Vol. 1 (1977) pp. 71–76.

23. PAPPIN, J. W., "Pavement Evaluation Project, Griffith, NSW." *CSIRO,* Division of Applied Geomechanics, *Project Report 2,* Melbourne (1975).

24. CHADDOCK, B. C. J., "Deformation of a Haul Road Reinforced with a Geomesh." *Proc.,* Second Symposium on Unbound Aggregates in Roads, Part 1 (1985) pp. 93–98.

25. WEBSTER, S. L., and WATKINS, J. E., "Investigation of Construction Techniques for Tactical Bridge Approach Roads Across Soft Ground." *Technical Report S-77-1,* U.S. Army Engineering Waterways Experiment Station, Vicksburg, Mississippi (Feb. 1977).

26. RAMALHO-ORTIGAO, J. A. and PALMEIRA, E. M., "Geotextile Performance at an Access Road on Soft Ground Near Rio de Janeiro." *Proc.,* Second International Conference on Geotextiles, Vol. II, Las Vegas, Nevada (Aug. 1982).

27. BARENBERG, E. J., "Design Procedures for Soil Fabric–Aggregate Systems with Mirafi 500X Fabric." University of Illinois, *UIL-ENG-80-2019* (Oct. 1980).

28. SOWERS, G. F., COLLINS, S. A., and MILLER, D.G., "Mechanisms of Geotextile-Aggregate Support in Low Cost Roads." *Proc.,* Second International Conference on Geotextiles, Vol. II (Aug. 1982) pp. 341–346.

29. LAI, J. S., and ROBNETT, Q.L., "Design and Use of Geotextiles in Road Construction." *Proc.,* Third Conference on Road Engineering Association of Asia and Australia, Taiwan (1981).

30. RUDDOCK, E. C., POTTER, J. F., and MCAVOY, A. R., "A Full-Scale Experience on Granular and Bituminous Road Pavements Laid on Fabrics." *Proc.,* Second International Conference on Geotextiles, Las Vegas, Vol. II (1982), pp. 365–370.

31. HALLIDAY, A. R., and POTTER, J. F., "The Performance of a Flexible Pavement Constructed on a Strong Fabric." *Transport and Road Research Laboratory, Report LR1123* (1984).

32. THOMPSON, M. R., and RAAD, L., "Fabric Used in Low-Deformation Transportation Support Systems." Transportation Research Board, *Transportation Research Record 810* (1981) pp. 57–60.

33. VOKAS, C. A., and STOLL, R. D., "Reinforced Elastic Layered Systems." Paper presented at the 66th Annual TRB Meeting (Jan. 1987).

34. BARKSDALE, R. D., and BROWN, S. F., "Geosynthetic Reinforcement of Aggregate Bases of Surfaced Pavements." Paper presented at the 66th Annual TRB Meeting (Jan. 1987).

35. BARVASHOV, V. A., BUDANOV, V. G., FOMIN, A. N., PERKOV, J. R., and PUSHKIN, V.I., "Deformation of Soil Foundations Reinforced with Prestressed Synthetic Fabric." *Proc.,* First International Conference on Use of Fabrics in Geotechnics, Vol. 1 (1977) pp. 67–70.

36. RAAD, L., "Reinforcement of Transportation Support Systems through Fabric Prestressing." Transportation Research Board, *Transportation Research Record 755* (1980) pp. 49–51.

37. BROWN, S. F., JONES, C. P. D., and BRODRICK, B. V., "Use of Nonwoven Fabrics in Permanent Road Pavements." *Proc.,* Constitution of Civil Engineers, Part 2, Vol. 73 (Sept. 1982) pp. 541–563.

38. BARKER, W. R., "Open-Graded Bases for Airfield Pavements." Waterways Experiment Station, *Misc. Paper GL-86* (July 1986).

39. FORSYTH, R. A., HANNON, J. B., NOKES, W. A., "Incremental Design of Flexible Pavements." Paper presented at the 67th Annual Meeting, Transportation Research Board (Jan. 1988).

40. PENNER, R., HAAS, R., WALLS, J., "Geogrid Reinforcement of Granular Bases." Presented to Roads and Transportation Association of Canada Annual Conference, Vancouver (Sept. 1985).

41. VAN GRUP, CHRIST, A. P. M., and VAN HULST, R. L. M., "Reinforcement at Asphalt-Granular Base Interface." Paper submitted to *J. Geotextiles and Geomembranes* (Feb. 1988).

42. BARKSDALE, R. D., and PRENDERGAST, J. E., "A Field Study of the Performance of a Tensar Reinforced Haul Road." Final Report, School of Civil Engineering, Georgia Institute of Technology (1985) 173 pp.

43. ZEEVAERT, A. E., "Finite Element Formulations for the Analysis of Interfaces, Nonlinear and Large Displacement Problems in Geotechnical Engineering." PhD Thesis, School of Civil Engineering, Georgia Institute of Technology, Atlanta (1980) 267 pp.

44. BROWN, S. F., and BARKSDALE, R. D., "Theme Lecture: Pavement Design and Materials." *Proc.,* Sixth International Conference on the Structural Design of Asphalt Pavements, Ann Arbor (Aug. 1987).

45. BROWN, S. F., and BRUNTON, J. M., "Developments to the Nottingham Analytical Design Method for Asphalt Pavements." *Proc.,* Sixth International Conference on the Structural Design of Asphalt Pavements, Ann Arbor (Aug. 1987) pp. 366–377.

46. LISTER, N. W., and POWELL, W. D., "Design Practice for Bituminous Pavements in the United Kingdom." *Proc.,* Sixth International Conference on the Structural Design of Asphalt Pavements, Ann Arbor (Aug. 1987) pp. 220–231.

47. LOFTI, H. A., SCHWARTZ, C. W., and WITCZAK, M. W., "Compaction Specification for the Control of Pavement

Subgrade Rutting." Submitted to Transportation Research Board (Jan. 1987).

48. BROWN, S. F., and PAPPIN, J. W., "The Modeling of Granular Materials in Pavements." Transportation Research Board, *Transportation Research Record 1011* (1985) pp. 45–51.

49. BARKSDALE, R. D., GREENE, R., BUSH, A. D., and MACHEMEHL, C. M., "Performance of a Thin-Surfaced Crushed Stone Base Pavement." ASTM Symposium on the Implication of Aggregate, New Orleans (1987).

50. BROWN, S. F., and DAWSON, A. R., "The Effects of Groundwater on Pavement Foundations." 9th European Conference on Soil Mechanics and Foundation Engineering, Vol. 2 (1987) pp. 657–660.

51. MAYHEW, H. C., "Resilient Properties of Unbound Roadbase Under Repeated Loading," *Transport and Road Research Laboratory, Report LR 1088* (1983).

52. JOUVE, P., MARTINEZ, J., PAUTE, J. S., and RAGNEAU, E., "Rational Model for the Flexible Pavements Deformations." *Proc.,* Sixth International Conference on the Structural Design of Asphalt Pavements, Ann Arbor (Aug. 1987) pp. 50–64.

53. SCULLION, T., and CHOU, E., "Field Evaluation of Geotextiles Under Base Courses—Supplement." Texas Transportation Institute, *Research Report 414-IF* (Supplement) (1986).

54. BARKSDALE, R. D., "Thickness Design for Effective Crushed Stone Use." *Proc.,* Conference on Crushed Stone, National Crushed Stone Assoc., Arlington, pp. VII-1 through VII-32 (June 1, 1984).

55. COLLIOS, A., DELMAS, P., GOORE, J. P., and GIROUD, J.P., "The Use of Geotextiles for Soil Improvement." 80-177, ASCE National Convention, Portland, Oregon (Apr. 17, 1980) pp. 53–73.

56. WILLIAMS, N. D., and HOULIHAN, M. F., "Evaluation of Interface Friction Properties Between Geosynthetics and Soil." Geosynthetic '87 Conference, New Orleans (1987) pp. 616–627.

57. MARTIN, J. P., KOERNER, R. M., and WHITTY, J. E., "Experimental Friction Evaluation of Slippage Between Geomembranes, Geotextiles and Soil," *Proc.,* International Conference on Geomembranes, Denver (1984) pp. 191–196.

58. FORMAZIN, J., and BATEREAU, C., "The Shear Strength Behavior of Certain Materials on the Surface of Geotextiles." *Proc.,* Eleventh International Conference on Soil Mechanics and Foundation Engineering, Vol. 3, San Francisco (Aug. 1985) pp. 1773–1775.

59. SAXENA, S. K., and BUDIMAN, J. S., "Interface Response of Geotextiles." *Proc.,* Eleventh International Conference on Soil Mechanics and Foundation Engineering, Vol. 3, San Francisco (Aug. 1985) pp. 1801–1804.

60. INGOLD, T. S., "Laboratory Pull-Out Testing of Grid Reinforcement in Sand." *Geotechnical Testing Journal,* GTJODJ, Vol. 6, No. 3 (Sept. 1983) pp. 100–111.

61. INGOLD, T. S., "A Laboratory Investigation of Soil-Geotextile Friction." *Ground Engineering* (Nov. 1984) pp. 21–112.

62. BELL, J. A., "Soil Fabric Friction Testing." ASCE National Convention, Portland, Oregon (Apr. 17, 1980).

63. ROBNETT, Q. L., and LAI, J. S., "A Study of Typar Non-Woven and Other Fabrics in Ground Stabilization Applications." School of Civil Engineering, Georgia Institute of Technology (Oct. 1982).

64. JEWELL, R. A., MILLIGAN, G. W. E., SARSBY, R. W., and DUBOIS, D., "Interaction Between Soil and Geogrids." Polymer Grid Reinforcement, Thomas Telford (1984) pp. 18–29.

65. BARENBERG, E. J., and BROWN, D., "Modeling of Effects of Moisture and Drainage of NJDOT Flexible Pavement Systems." University of Illinois, Dept. of Civil Engineering, Research Report, (Apr. 1981).

66. BROWN, S. F., BRODRICK, B. V., and PAPPIN, J. W., "Permanent Deformation of Flexible Pavements." University of Nottingham, Final Technical Report to ERO U.S. Army (1980).

APPENDIXES B THROUGH H

CONTENTS OF APPENDIX ITEMS NOT PUBLISHED

Appendixes B, C, D, E, F, G, and H of the final report are not published herewith. They are included under separate binding in the agency-prepared report entitled, "Potential Benefits of Geosynthetics in Flexible Pavements—Supplement to NCHRP Report 315." A limited number of copies of that report are available for purchase at a cost of $7.00, from the NCHRP, Transportation Research Board, 2101 Constitution Avenue, N.W., Washington, D.C. 20418.

The "Contents" pages appearing in the Supplement are reproduced here for the convenience of those interested in the subject area.

56

TRANSPORTATION RESEARCH BOARD

National Research Council

2101 Constitution Avenue, N.W.

Washington, D.C. 20418

ADDRESS CORRECTION REQUESTED

000015M014
STATE AERONAUTICS ADMINSTR

ITD DIV AERONAUTICS&PUBTRANSP
3483 RICKENBACKER
BOISE   ID 83705

POTENTIAL BENEFITS OF GEOSYNTHETICS
IN
FLEXIBLE PAVEMENTS

**Supplement
to
NCHRP Report 315**

Prepared for
National Cooperative Highway Research Program
Transportation Research Board
National Research Council

Richard D. Barksdale
Georgia Institute of Technology
Atlanta, Georgia

Stephen F. Brown
University of Nottingham
Nottingham, England

Supplement

to

NCHRP Report 315

POTENTIAL BENEFITS OF GEOSYNTHETICS IN FLEXIBLE PAVEMENTS

APPENDICES B-H

TABLE OF CONTENTS

TABLE OF CONTENTS (continued)

LIST OF FIGURES

LIST OF FIGURES (continued)

LIST OF TABLES

APPENDIX B

EXPERIMENTAL STUDIES OF SURFACED PAVEMENTS
REINFORCED WITH A GEOSYNTHETIC

APPENDIX B

EXPERIMENTAL STUDIES OF SURFACED PAVEMENTS
REINFORCED WITH A GEOSYNTHETIC

Field Tests - Thick Bituminous Surfacing

Full-scale experiments conducted by Ruddock, Potter and McAvoy [B-1,B-2] included two sections having a 6.3 in. (160 mm) thick bituminous surfacing and a 12 in. (300 mm) thick crushed granite base. One of these sections had a woven multi-filament polyester geotextile reinforcement in the bottom of the granular base. The woven geotextile had a strength of about 474 lb./in. (83 kN/m) in each direction, and an elongation at failure of 14.8 percent. The geotextile used was stiff (S_g @ 5 percent = 3400 lbs/in., 600 kN/m) and had an elastic modulus of about 72,000 lbs/in.^{2} (500 kN/m^2). The geosynthetic stiffness S_g is defined as the force applied per unit width of geosynthetic divided by the resulting strain.

The sections were constructed on a London clay subgrade having a CBR increasing with depth from about 0.7 percent at the top to 3.5 percent at a depth of 11.8 in. (300 mm). Loading was applied by a two-axle truck having dual rear wheels. A rear axle load of 21.9 kips (97.5 kN) was applied for 4600 repetitions, with the axle loading being increased to 30 kips (133 kN) for an additional 7700 passes.

Measurements made included surface deformations, transient stress and strain in the subgrade, permanent strain in the geotextile, and transient tensile strain in the bottom of the bituminous layer. For the conditions of the test which included a 6.3 in.(160 mm) bituminous surfacing, no difference in structural performance was observed between the geotexile reinforced sections and the control section. Ruddock et al. found that resilient vertical subgrade stresses and strains were not significantly

changed by fabric inclusions, although transverse resilient strains were somewhat reduced. To demonstrate if some improvement in permanent deformation could be achieved due to reinforcement, the pavement should have been loaded sufficiently to cause rutting to develop. Because of the use of a thick bituminous surfacing, however, it is doubtful that the conclusions reached would have been significantly changed.

Field Tests - Geogrid and Heavy Loading

Recently, Barker [B-3] has studied the performance of a pavement having an open-graded, unstabilized aggregate base reinforced by a stiff to very stiff geogrid. The geogrid was placed at the center of the aggregate base. The test sections consisted of a 3 in. (75 mm) asphalt surfacing overlying a 6 in. (150 mm) thick, very open-graded base consisting of No. 57 crushed limestone. A 6 in. (150 mm) cement stabilized clay-gravel subbase was constructed to provide a strong working platform for the open-graded base. The subgrade was a sandy silt having a CBR of 27 percent.

The granular base, even after compaction, was loose and unstable to most traffic [B-3]. An unstable base of this type would appear to be a good candidate for reinforcing with a stiff geogrid. The geogrid used had a secant stiffness at 5 percent strain of about 4,000 lbs./in. (700 kN/m).

The pavement was subjected to 1,000 repetitions of a heavy moving aircraft load. The 27-kip (120 kN) load applied to the pavement consisted of a single tire inflated to 265 psi (1.8 MN/m^2). The pavement was trafficked over a 60 in. (1.5 m) width. Falling Weight Deflectometer (FWD) tests showed the stiff to very stiff reinforcement did not affect the measured deflection basins throughout the experiment. This finding indicates similar stiffnesses and effective layer moduli for the reinforced and unreinforced sections. The general condition of the two pavements

appeared similar after 1,000 load repetitions. Maximum observed rutting of the reinforced section was about 8 percent less than the unreinforced section at a rut depth of 1 in. (25 mm), and about 21 percent less at a rut depth of 2 in. (50 mm) as shown in Figure B-1. Subsequent trench studies indicated that most of the permanent deformation occurred in the subgrade and not the base.

The non-conventional pavement section studied at WES had a very open-graded granular base, a cement stabilized supporting layer and was subjected to a very high wheel load and tire pressure. The reinforcement was placed in the middle of the granular base. These factors greatly complicate translating the test results to conventional pavements. For this well constructed pavement, important reductions in permanent deformation occurred due to reinforcement only after the development of relatively large deformations. The reinforcement was placed at the center of the aggregate base to improve its performance. Rutting, however, primarily occurred in the subgrade. Better performance might have been obtained had the reinforcement been placed at the bottom of the base.

Steel Mesh Reinforcement

A hexagonal wire netting of steel was placed at the interface between a crushed rubble aggregate base and the asphalt surfacing in a large scale test track experiment described by van Grup and van Hulst [B-4]. The asphalt surfacing was 2.4 in. (60 mm) thick, and the aggregate base varied in thickness from 8 to 16 in. (200-400 mm). The subgrade consisted of a compacted, coarse sand. A summary of the test conditions is given in Table B-1, and the rutting which developed as a function of load repetitions is given in Figure B-2.
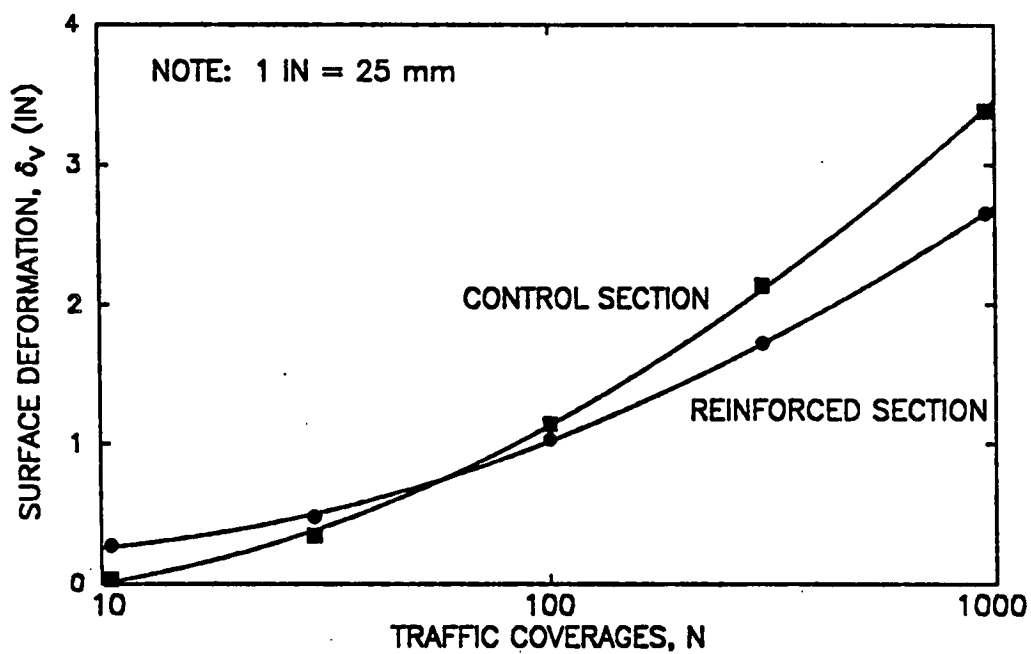
Figure B-1. Maximum Surface Deformation as a Function of Traffic
(After Barker, Ref. B-3).

Table B-1

Summary of Permanent Deformation in Full-Scale
Pavement Sections on a Compacted Sand Subgrade

| LAYER | LAYER THICKNESSES AND PERMANENT DEFORMATION OF SECTIONS (in.) | | | | | |
	1	2	3	4	5	6
Dense Asphaltic Concrete	2.4	2.4	2.4	2.4	2.4	2.4
Steel Mesh Reinf./ @ Top of Base	NO	NO	NO	NO	YES	YES
Crushed Rubble	0	7.9	11.8	15.7	11.8	0
Sand	47.2	39.3	35.4	31.5	47.2	35.4
Clayey Sand	-	-	-	-	-	-
Permanent Surface Deformation (in.) @ 140,000 Reps.	1.3	0.55	0.44	0.55	0.49	0.98

Note: 1. The steel mesh reinforcement was placed at the aggregate
base/asphalt surfacing interface.
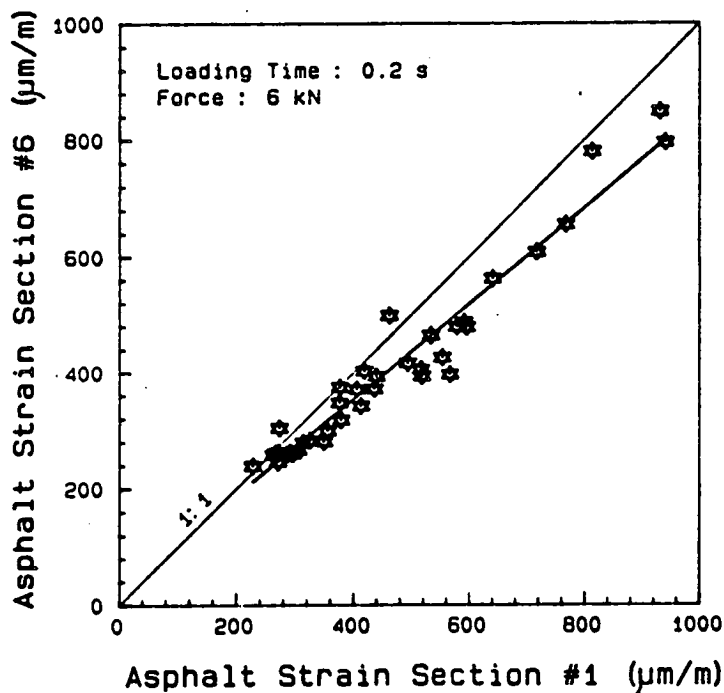
Figure B-2. Comparison of Strain at Bottom of Asphalt Surfacing With
and Without Mesh Reinforcement (After Van Grup and Van
Hulst, Ref. B-4).

B-6

Reinforcement of a weak section, which did not have an aggregate base, resulted in a 40 percent reduction in rutting at about 0.5 in (12 mm) rut depth. Reinforcement made little difference in rutting performance for the stronger sections having rubble aggregate bases. A reduction in tensile strain of about 18 percent was, however, observed in the bottom of the asphalt surfacing. This large level of reduction in strain, if maintained, would have a very significant beneficial effect on fatigue performance.

Large-Scale Laboratory Tests - Low Stiffness, Nonwoven Geotextiles

Brown, et al. [B-5] investigated the effect of the placement of a nonwoven geotextile within and at the bottom of the aggregate base of bituminous surfaced pavements. Seven different reinforced sections were studied; for each condition a similar control section was also tested without reinforcement. A moving wheel load was used having a magnitude of up to 3.4 kip (15 kN). The bituminous surfacing of the seven test sections varied in thickness from 1.5 to 2.1 in. (37-53 mm). The crushed limestone base was varied in thickness from 4.2 to 6.9 in. (107-175 mm). The pavements rested on a silty clay subgrade having a CBR that was varied from 2 to 8 percent.

Two very low to low stiffness, nonwoven, melt bonded geotextiles were used in the study. These geotextiles had a secant stiffness at one percent strain of about 1270 lbs./in. (220 kN/m) and 445 lbs/in. (78 kN/m).

The inclusion of the nonwoven geotextiles in the aggregate base in most tests appeared to cause a small increase in rutting (Figure B-3a), and no increase in effective elastic stiffness of the granular layer. Both vertical and lateral resilient and permanent strains were also found to be greater in the base and subgrade of all of the reinforced sections (Figure B-3b). The experiments included placing the geotextiles within the granular

RADIAL OFFSET DISTANCE (mm)

(A) SURFACE DEFLECTION

Lateral Resilient Strain
(millistrain)

LEGEND
● Unreinforced
■ Reinforced

(b) Lateral Strains

Permanent Lateral Strain, %

Note: 1 in. = 25 mm
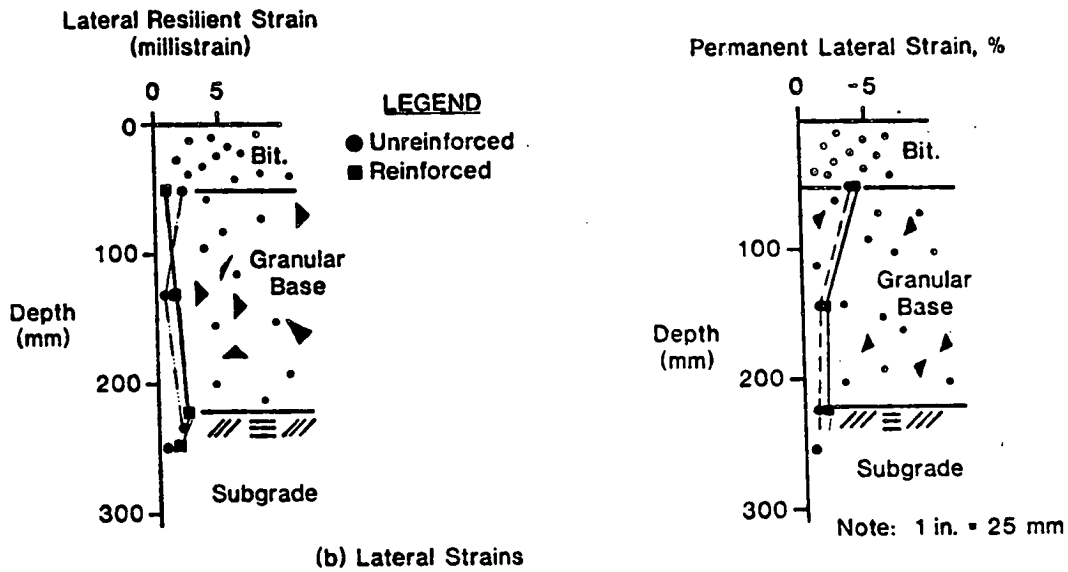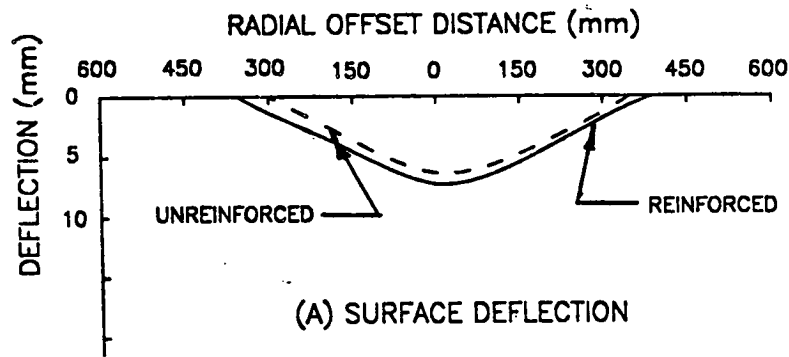
Figure B-3. Surface Deformation and Lateral Strain Measured in
            Nottingham Test Facility (After Brown, et al.,
            Ref. B-5).

B-8

layer and using geotextiles strengthened by stitching. Two layers of reinforcement were also employed in some tests.

The poor performance of the reinforced sections was attributed to a lack of adequate aggregate interlock between the base and the geotextiles. In the light of more recent findings, the relatively low geosynthetic stiffness probably also helps to explain the results. Maximum surface rutting was less than about 1 in. (25 mm), which resulted in relatively small strains in the geosynthetic. Finally, several factors suggest compaction of the aggregate above the geosynthetic may not have been as effective when the geotextile was present.

Large-Scale Laboratory Tests Using Stiff Geogrids

Penner, et al. [B-6] studied the behavior of geogrid reinforced granular bases in the laboratory using a shallow plywood box 3 ft. (0.9 m) deep. The secant stiffness, S_g of the geogrid at 5 percent strain was about 1780 lb/in. (312 kN/m). A stationary, 9 kip (40 kN) cyclic load was applied through a 12 in. (300 mm) diameter plate. The asphalt surface thickness was either 3 or 4 in. (75 or 100 mm).

The aggregate base was well-graded and was varied in thickness from 4 to 12 in. (100-300 mm). The base had a reported insitu CBR value of 18 percent but laboratory CBR testing indicated a value of 100 percent or more. The subgrade was a fine beach sand having a CBR of typically 4 to 8 percent before the tests. After testing, the CBR of Loop 3 was found to have increased by a factor of at least 2. An increase in CBR might also have occurred in other sections, although the researchers assumed for analyzing test results an increase did not occur. In one series of tests, peat was mixed with the fine sand at a high water content to give a very weak subgrade having an initial CBR of only 0.8 to 1.2 percent.

Placement of the geogrid within the granular base was found to result in a significant reduction in pavement deformation when placed in the middle or near the bottom of the base. Little improvement was observed when the reinforcement was located at the top of the base.

For one section having an 8 in. (200 mm) granular base and 3 in. (75 mm) asphalt surfacing, sections having geogrid reinforcement at the bottom and mid-height exhibited only about 32 percent of the 0.6 in. (15 mm) deformation observed in the unreinforced section. Important improvements in performance were found in this test for deformations of the reinforced section as small as 0.2 in. (5 mm). In contrast with the above findings, use of geogrid reinforcement in under-designed sections on weak subgrades showed no apparent improvement until permanent deformations became greater than about 1 in. (25 mm).

APPENDIX B

REFERENCES

B-1 Ruddock, E.C., Potter, J.F., and McAvoy, A.R., "Report on the Construction and Performance of a Full-Scale Experimental Road at Sandleheath, Hants", CIRCIA, Project Record 245, London, 1982.

B-2 Ruddock, E.C., Potter, J.F., and McAvoy, A.R., "A Full-Scale Experience on Granular and Bituminous Road Pavements Laid on Fabrics", Proceedings, Second International Conference on Geotextiles, Las Vegas, Vol. II, 1982, pp. 365-370.

B-3 Barker, W.R., "Open-Graded Bases for Airfield Pavements", Waterways Experiment Station, Misc. Paper GL-86, July, 1986.

B-4 van Grup, Christ, A.P.M., and van Hulst, R.L.M., "Reinforcement at Asphalt-Granular Base Interface", paper submitted to Journal of Geotextiles and Geomembranes, February, 1988.

B-5 Brown, S.F., Jones, C.P.D., and Brodrick, B. V., "Use of Nonwoven Fabrics in Permanent Road Pavements", Proceedings, Institution of Civil Engineers, Part 2, Vol. 73, Sept., 1982, pp. 541-563.

B-6 Penner, R., Haas, R., Walls, J., "Geogrid Reinforcement of
     Granular Bases", presented to Roads and Transportation Association
     of Canada Annual Conference, Vancouver, September, 1985.

APPENDIX C

DEVELOPMENT OF ANALYTICAL MODELS USED TO PREDICT
REINFORCED PAVEMENT RESPONSE

APPENDIX C

DEVELOPMENT OF ANALYTICAL MODELS USED TO PREDICT
REINFORCED PAVEMENT RESPONSE

The GAPPS7 finite element model has been described in detail elsewhere [C-1]. Therefore, the capabilities of this comprehensive program are only briefly summarized in this section. The GAPPS7 program models a general layered continuum reinforced with a geosynthetic and subjected to single or multiple load applications.

Important features of the GAPPS7 program include:

1. A two dimensional flexible fabric membrane element which can not take either bending or compression loading.

2. The ability to model materials exhibiting stress dependent behavior including elastic, plastic and failure response.

3. Modeling of the fabric interfaces including provisions to detect slip or separation.

4. The ability to consider either small or large displacements which might, for example, occur under multiple wheel loadings in a haul road.

5. A no-tension analysis that can be used for granular materials, and

6. Provision for solving either plane strain or axisymmetric problems.

The GAPPS7 program does not consider either inertia forces or creep, and repetitive loadings, when used, are applied at a stationary position (i.e. the load does not move across the continuum). Material properties can, however, be changed for each loading cycle to allow considering time and/or load dependent changes in properties to be considered. Only

axisymmetric, small displacement analyses were performed for this study using a single loading.

GAPPS7 consists of a main program and twelve subroutines. The main program handles the input, performs the needed initializations, and calls the appropriate subroutines. The twelve subroutines perform the actual computations. An automatic finite element mesh generation program MESHG4 is used to make the GAPPS7 program practical for routine use. In addition to handling material properties, MESHG4 completely generates the finite element mesh from a minimum of input data. A plotting program called PTMESH can be used to check the generated mesh and assist in interpreting the large quantity of data resulting from the application of the program. These supplementary programs greatly facilitate performing finite element analyses and checking for errors in the data.

Resilient Properties

Three different models can be utilized in the GAPPS7 program to represent the stress dependent elastic properties of the layers. The stress dependent resilient modulus E_r of the subgrade is frequently given for cohesive soils as a bi-linear function of the deviator stress $\sigma_1 - \sigma_3$ as shown in Figure C-1. For this model the resilient modulus is usually considered to very rapidly decrease linearly as the deviator stress increases a small amount above zero. After a small threshold stress is exceeded, the resilient modulus stops decreasing and may even very slightly increase in a linear manner. When a nonlinear model was used the subgrade was characterized following this approach.

The most commonly used nonlinear model for the resilient modulus of cohesionless granular base materials is often referred to as the k-θ model (Figure C-1b) which is represented as

C-3
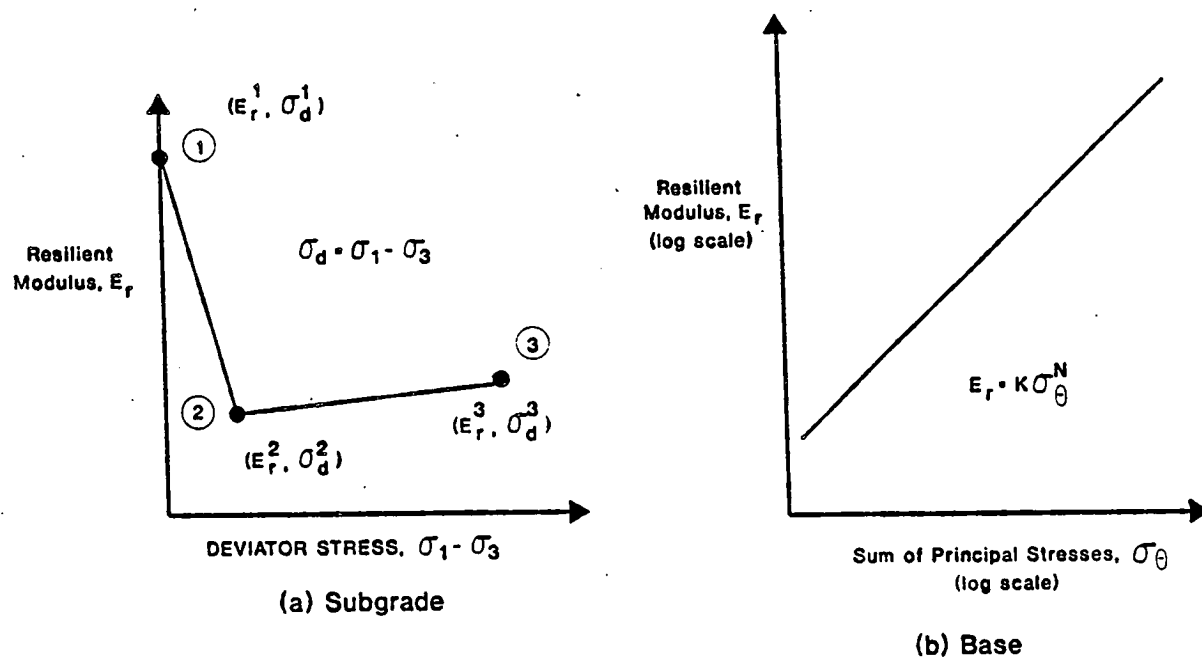
Figure C-1. Resilient Modulus Relationships Typically Used for a Cohesive Subgrade and Aggregate Base.

$$E_r = K \sigma_\theta{}^N \qquad \text{(C-1)}$$

where E_r = resilient modulus of elasticity, sometimes called M_r, determined from laboratory testing

k and θ = material constants determined from laboratory testing

σ_θ = sum of principle stresses, $\sigma_1 + \sigma_2 + \sigma_3$

In recent years several improved models, often referred to as contour models, have been developed by Brown and his co-workers [C-3,C-4] to more accurately characterize granular base materials. The contour model as simplified for routine use by Mayhew [C-5] and Jouve, et al. [C-6] was employed in this study. Following their approach the bulk modulus (K) and shear modulus (G) of the base can be calculated from the simplified relations

$$K = K_1 \, p^{(1-n)}\{1 + \gamma \, (\tfrac{q}{p})^2\} \qquad \text{(C-2)}$$

$$G = G_1 \, p^{(1-m)} \qquad \text{(C-3)}$$

where: K = bulk modulus

G = shear modulus

p = average principal stress, $(\sigma_1 + \sigma_2 + \sigma_3)/3$

q = shear stress

K_1, G_1, n, m = material properties evaluated in the laboratory from special cyclic loading stress path tests

The model described by Equations (C-2) and (C-3) is referred to throughout this study as the simplified contour model.

For a general state of stress, the deviator stress q can be defined as

$$q = 0.707 \sqrt{J_2} \qquad \text{(C-4)}$$

where $J_2 = (\sigma_1 - \sigma_2)^2 + (\sigma_2 - \sigma_3)^2 + (\sigma_3 - \sigma_1)^2$

Laboratory tests by Jouve et al. [C-6] have shown that the material constants n and m are approximately related to G_1 as follows:

$$n = 0.03 \ G_1^{0.31} \tag{C-5}$$

$$m = 0.028 \ G_1^{0.31} \tag{C-6}$$

The bulk modulus (K) as given by equation (C-2) is always greater than zero which neglects the dilation phenomenon which can cause computational difficulties. All three of the above nonlinear models for representing resilient moduli were employed in the present study and their use will be discussed subsequently.

MODEL VERIFICATION - PREDICTED PAVEMENT RESPONSE

Little work has been carried out to verify the ability of theoretical models to accurately predict at the same time a large number of measured stress, strain and deflection response variables. To be able to reliably predict the tensile strain in an unstabilized granular base is quite important in a study involving granular base reinforcement. An accurate prediction of tensile strain is required since the level of tensile strain developed in the base determines to a large extent the force developed in the geosynthetic and hence its effectiveness. The importance of the role which tensile strain developed in the reinforcing layer plays became very apparent as the analytical study progressed.

The presence of a tensile reinforcement and relatively thick granular layers which have different properties in tension compared to compression greatly complicate the problem of accurately predicting strain in the aggregate layer. Partway through this study it became apparent that the usual assumption of material isotropy, and the usually used subgrade and base properties, including the k-θ type model, were in general not

indicating the level of improvement due to reinforcement observed in the weak section used in the first laboratory test series. Therefore, a supplementary investigation was undertaken to develop modified models that could more accurately predict the tensile strain and hence the response of geosynthetic reinforced pavements.

Two independent comparison studies were performed to both verify the analytical model selected for use and to assist in developing appropriate material parameters. The first study involved theoretically predicting the response, including tensile strain in the aggregate base, of a high quality, well instrumented test section without geosynthetic reinforcement tested previously by Barksdale and Todres [C-7,C-8]. The second study used the extensive measured response data collected from Test Series 3 of the large scale laboratory pavement tests conducted as a part of the present study.

Unreinforced, High Quality Aggregate Base Pavement

As a part of an earlier comprehensive investigation to evaluate aggregate bases, several pavement sections having a 3.5 in. (90 mm) asphalt surfacing and an 8 in. (200 mm) thick granular base were cyclically loaded to failure [C-7,C-8]. High quality materials were used including the asphalt and the crushed stone base which was compacted to 100 percent of AASHTO T-180 density.

These sections were placed on a micaceous silty sand subgrade compacted to 98 percent of AASHTO T-99 density at a water content 1.9 percent above optimum. A total of about 2.4 million applications of a 6.5 kip (29 kN) uniform, circular loading were applied at a primary and six secondary positions.

In the verification study a number of models were tried including the nonlinear finite element k-θ and contour models. The simplified, nonlinear

C-7

contour model and a linear elastic, cross anisotropic model were selected as having the most promise. A manual trial and error procedure was used to select material properties that gave the best overall fit to all of the measured response quantities.

A cross-anisotropic representation has different elastic material properties in the horizontal and vertical directions. The usually used isotropic model has the same material properties such as stiffness in all directions. A homogeneous material has the same properties at every point in the layer.

A comparison of the observed and measured pavement response variables for each model is given in Table C-1. These results indicate that a cross anisotropic model is at least equal to, and perhaps better than the simplified contour model for predicting general pavement response. The cross-anisotropic model using an isotropic, homogeneous subgrade was able to predict measured variables to within about ± 20 percent; the one exception was the tensile strain in the bottom of the base which was about 30 percent too low. At the time this comparison was made a homogeneous, isotropic subgrade resilient modulus was used.

Later, after the sensitivity study was under way, it was discovered that the tensile strain in the base greatly increased if the subgrade modulus increases with depth. The cross-anisotropic material properties employed in the sensitivity study are summarized in Table C-2. They are similar to those used for the homogeneous subgrade comparison in Table C-1. Thus the important finding was made that the resilient modulus of the subgrade near the surface had to be quite low as indicated by the very large measured vertical strains on the subgrade. Since the total measured surface deflections were relatively small, the average stiffness of the subgrade was

Table C-1

Comparison of Measured and Calculated Response for a Strong Pavement
Section: 3.5 in. Asphalt Surfacing; 8 in. Crushed Stone Base

CONDITION	VERTICAL SUBGRADE STRESS/STRAIN		STRAIN BOTTOM AC	STRAIN BOTTOM OF BASE		VERT. STRAIN TOP OF BASE	VERTICAL SURF. DEF.	$E^{(avg.)}_{base}$	$E^{(avg.)}_{subg.}$	$\dfrac{E_b}{E_s}$
	σ_z(psi)	ε_v(x10^{-6})	ε_r(x10^{-6})	ε_r(x10^{-6})	ε_v(x10^{-6})	ε_v(x10^{-6})	δ_v(in.)	(ksi)	(ksi)	
Measured	9.9	2000	330	936	280	580	0.017	-	-	-
Cross-Anisotropic E_s Constant	7.8	721	275	593	348	556	0.016	38.0[1]	8.0	4.75
E_s Variable	6.2	1400	318	951	278	567	0.0216	38.0	8.0	4.75
Finite Element Model[2]	5.9	1708	394	527	1242	1120	0.025	18.1	10.7	1.7

Notes: 1. Average vertical resilient modulus of base: E_b varied from 50 ksi at the top to 28 ksi at the bottom; horizontal resilient modulus varied from 40 ksi at the top to 0.8 ksi at the bottom.

2. Nonlinear model used the resilient properties given in Table C-5; in the lower third of the base the modulus was taken as 40% of these properties.

3. Resilient modulus of base is E_b; that of subgrade is E_s.

Table C-2
Anisotropic Material Properties Used for Final
Georgia Tech Test Study

Location in Pavement	Resilient Modulus		Poisson's Ratio	
	Vertical	Horizontal	Vertical	Horizontal
Aggregate Base (Anisotropic)				
Top	$1.420E_b$	$1.136E_b$	0.43	0.15
Middle	$1E_b$	$0.0852E_b$	0.43	0.15
Bottom	$0.818E_b$	$0.0227E_b$	0.45	0.10
Subgrade (Isotropic)				
Top	$0.375E_s$	$0.375E_s$	0.4	0.4
Middle	$0.75E_s$	$0.75E_s$	0.4	0.4
Bottom	$1.875E_s$	$1.875E_s$	0.4	0.4

Note: 1. E_s = average resilient modulus of elasticity of subgrade; E_b = resilient modulus of base as shown in Table C-1.

2. Modular ratio $E_b(avg)/E_s$ = 4.75 where E_s = 8000 psi and $E_b(avg)$ = 35,200 psi; the numerical average of the three vertical resilient moduli of base = 38,000 psi.

quite high. Therefore, the stiffness of the silty sand subgrade underwent a significant increase with depth, probably much larger than generally believed at the present time. The significant decrease in strain and increase in confinement with depth probably account for most of this observed increase in stiffness with depth [C-10]. The better agreement with measured pavement response when using a subgrade resilient modulus that rapidly increases with depth is shown in Table C-1.

The isotropic, nonlinear finite element method could not predict at the same time large tensile strain in the bottom of the aggregate base and the small observed vertical strains in the bottom and upper part of that layer. This important difference in measured strain is readily explained if the actual stiffness of the aggregate base is considerably greater in the vertical than the horizontal directions. The cross-anisotropic model gave a much better estimate of the vertical stress on the subgrade and the vertical surface deflection than did the nonlinear model.

Response of Geosynthetic Reinforced Sections

A total of 12 well-instrumented laboratory test sections were tested as a part of this study. These comprehensive experiments, which included the measurement of tensile strain in the aggregate base and also in the geosynthetic, are described in detail in the last section of this chapter. The measured pavement response obtained from the three sections included in Test Series 3 of these laboratory tests provide an excellent opportunity to verify the theory. A cross-anisotropic model was used to predict the response of the two geotextile reinforced sections and the non-reinforced control section included in the study. These test sections had an average asphalt surface thickness of about 1.2 in. (30 mm), and a crushed stone base thickness of about 8.2 in (208 mm). The wheel loading was 1.5 kips (6.7 kN)

at a tire pressure of 80 psi (0.6 MN/m^2). A soft clay subgrade (CL) was used having an average inplace CBR before trafficking of about 2.8 percent.

The comparison between the anisotropic model using the best fit material properties and the measured response is shown in Table C-3 for each section. These sections were constructed over a subgrade having a very low average resilient modulus that was back-calculated to be about 2000 psi (15 MN/m^2). Once again, based on the measured strains, the conclusion was reached that the resilient modulus of subgrade was quite low near the surface but rapidly increased with depth. Overall, the theory predicted observed response reasonably well. The strain in the geosynthetic was over predicted by about 33 percent when the geosynthetic was located in the bottom of base. It was under predicted by about 14 percent when located in the middle of the layer. Of considerable interest is the fact that the largest calculated geosynthetic stress was about 10 lbs/in (17 N/m), only strain was measured in the geosynthetic. The vertical stress on the top of the subgrade was about 50 percent too small. As a result, the computed vertical strain at the top of the subgrade was too small by about the same amount. Larger radial strains were measured in the bottom of the aggregate base than calculated by about 50 percent.

In summary, these pavement sections, as originally planned, were quite weak and exhibited very large resilient deflections, strains and stresses. The postulation is presented that, under repetitive loading, perhaps due to a build up of pore pressures, the subgrade used in Test Series 3 probably performed like one having a CBR less than the measured value of 2.7 to 2.9 percent. The cross anisotropic model was less satisfactory in predicting the pavement response of the weak Test Series 3 sections compared to the stronger sections previously described. These sections only withstood about

Table C-3

Comparison of Measured and Calculated Response for
Nottingham Series 3 Test Sections

Condition	Vert. Subg. Stress/Strain		Strain Bottom A.C. $\varepsilon_r(10^{-6})$	Strain Bottom of Base		Strain Top of Base		Geosynthetic		Def. δ_v(in.) (2)	$E_{subg.}$ (avg.) (ksi)	E_b/E_s
	Stress σ_z (psi)	Strain ε_v (10^{-6})		Radial $\varepsilon_r(10^{-6})$	Vert. $\varepsilon_v(10^{-6})$	Radial $\varepsilon_r(10^{-6})$	Vert. ε_v (10^{-6})	Strain ε(lbs/in)	Stress σ(lbs/in)			
CONTROL SECTION - NO GEOSYNTHETIC												
Measured	-6.0	-8200	2983	6400[1]	-2000	6000	6600	-	-	0.076	-	-
Model 1	-4.6	-4357	1818	4334	-2033	2620	5300	-	-	0.066	2080	2.12
Model 2	-4.6	-4674	1950	4670	-2078	2810	5553	-	-	0.070	1800	2.63
GEOSYNTHETIC IN BOTTOM OF BASE												
Measured	-6.6	-7400	2355	-	-1500	-	-5400	1413-1609	-	0.08	-	-
Model 1	-3.6	-3260	1800	2599	-1930	2530	-5278	2065	10.3	0.060	2080	2.12
Model 2	-3.6	-3450	1880	2753	-1973	2610	-5533	2165	10.8	0.065	1800	2.63
GEOSYNTHETIC IN MIDDLE OF BASE												
Measured	-6.1	-7300	2198	5900	-1500	5000	-5600	2103-2242	-	0.064	-	-
Model 1	-3.2	-3963	1730	3167	-1660	2080	-4377	1862	9.3	0.060	2080	2.12
Model 2	-3.1	-3748	1790	1600	-1280	2260	-4800	1579	7.9	0.063	1800	2.63

Notes: 1. Radial strain in base was originally 15,000μ and decreased to 6400μ at 70,000 repetitions.
2. Resilient vertical deflections measured after 3500 passes.

70,000 load repetitions with permanent deflections of 1.5 to 2 in. (38-50 mm) as compared to about 2.4 million heavier load repetitions for the stronger sections on a better subgrade used in the first comparison. A reasonably strong section would in general be more commonly used in the field. Nevertheless, the calculated relative changes in observed response between the three sections did appear to indicate correct trends. This finding suggests relative comparisons should be reasonably good, and indicate correct relative trends of performance. Undoubtedly the analytical studies are susceptible to greater errors as the strength of the pavement sections decrease toward the level of those used in the laboratory studies involving the very weak subgrade.

MODEL PROPERTIES USED IN SENSITIVITY STUDY

The cross-anisotropic model was selected as the primary approach used in the sensitivity studies to investigate potential beneficial effects of geosynthetic reinforcement. The nonlinear, simplified contour model was also employed as the secondary method for general comparison purposes and to extend the analytical results to include slack in the geosynthetic and slip between the geosynthetic and the base and subgrade.

The measured strain in the bottom of the aggregate base in the test section study that withstood 2.4 million load repetitions (Table C-1) was about 1.6 times the value calculated using the cross-anisotropic base model. The subgrade used was isotropic and homogeneous. In an actual pavement the development of larger tensile strains in the granular base than predicted by theory would result in the reinforcing element developing a greater force and hence being more effective than indicated by the theory. To approximately account for this difference in strain, the stiffness of the

geosynthetics actually used in the analytical sensitivity studies was 1.5 times the value reported.

Tensile strains in the aggregate base and geosynthetic can be calculated directly by assuming a subgrade stiffness that increases with depth. Unfortunately, this important finding was not made until the sensitivity study was almost complete. A supplementary analytical study using a higher geosynthetic stiffness with a homogeneous subgrade gave comparable results to a model having a subgrade stiffness increasing with depth.

Using the above engineering approximation, actual geosynthetic stiffnesses, S_g = 1500, 6000 and 9000 lbs/in. (260, 1000, 1600 kN/m) were used in the theoretical analyses. Therefore, the corresponding stiffnesses reported as those of the sections would, using the 1.5 scaling factor, be 1000, 4000 and 6000 lbs/in (170, 700, 1000 kN/m). Because of the small stresses and strains developed within the geosynthetics, they remain well within their linear range. Hence nonlinear geosynthetic material properties are not required for the present study.

Cross-Anisotropic Model Material Properties. The relative values of cross-anisotropic elastic moduli and Poisson's ratios of the aggregate base used in the study are summarized in Table C-4. The resilient modulus of the asphalt surfacing used in the sensitivity study was 250,000 psi (1700 MN/m^2). The corresponding Poisson's ratio was 0.35. The resilient moduli of the subgrade included in the sensitivity analyses were 2000, 3500, 6000 and 12,500 psi (14, 24, 41, 86 MN/m^2).

The ratio of the resilient modulus of the base to that of the subgrade has a significant influence on the tensile strain developed in the base for a given value of subgrade resilient modulus. In turn, the level of tensile

Table C-4

Aggregate Base Properties Used in
Cross-Anisotropic Model for Sensitivity Study

Location in Base	Resilient Modulus		Poisson's Ratio	
	Vertical	Horizontal	Vertical	Horizontal
Top	1.375E	0.925E	0.43	0.15
Middle	1.0E	0.138E	0.43	0.15
Bottom	0.825E	0.0458E	0.45	0.10

Table C-5

Nonlinear Material Properties Used in Sensitivity Study

1. **Asphalt Surfacing:**   Isotropic, $E_r = 250,000$ psi, $\nu = 0.35$

2. **Granular Base:**

Position in Base	K1	G1	Y
Very Good Crushed Stone Base			
Upper 2/3	14,100	7,950	0.14
Lower 1/3	5,640	3,180	0.14
Poor Quality Gravel/Stone Base			
Upper 2/3	3,300	4,050	0.12
Lower 1/3	1,320	1,620	0.12

3. **Subgrade:** Typical Subgrade E_s (psi) given below (see Fig. C-1).[1]

Point	Resilient Moduli			σ_3 (psi)
	Top	Middle	Bottom	
1	1300	16,000	16,000	0
2	750	4,000	4,000	1.5
3	800	4,300	4,300	30.0

1. Average Subgrade E_s = 6,000 psi (isotropic)

2. $\nu = 0.4$

strain in the aggregate base determines to a great extent the force

developed in the geosynthetic. Since the force in the geosynthetic

significantly influences the improvement in behavior of the reinforced

pavement system, using a modular ratio comparable to that actually developed

in the field is very important.

For this study the cross-anisotropic modular ratio was defined as the

vertical resilient modulus of the center of the base divided by the uniform

(or average) resilient modulus of the subgrade. For the primary sensitivity

study the modular ratio used was 2.5. This was approximately the value

back calculated from the measured response of the test pavement on the very

soft subgrade having an average resilient modulus of about 2000 psi (14

MN/m^2) as shown in Table C-3. Supplementary sensitivity studies were also

carried out using modular ratios of 1.5 and 4.5. The modular ratio of 4.5

was about that observed for the full-scale test sections having the better

subgrade; the average resilient modulus of the subgrade was about 8000 psi

(55 MN/m^2) as shown in Table C-1.

Nonlinear Properties

The material properties used in the nonlinear finite element analyses

were developed by modifying typical nonlinear properties evaluated in the

past from laboratory studies using the measured response of the two test

pavement studies previously described. The resilient properties of the

asphalt surfacing were the same as used in the cross-anisotropic model.

Both studies comparing predicted and measured pavement response

indicate the base performs as a cross anisotropic material. For example,

the small vertical strain and large lateral tensile strain in the aggregate

base could only be obtained using the cross anisotropic model. The

nonlinear options in the GAPPS7 program, however, only permit the use of

C-17

isotropic properties. Therefore, some compromises were made in selecting the simplified contour model resilient properties of the aggregate base. The radial tensile strain in the bottom of the granular base could be increased by

1. Decreasing the resilient modulus of the top of the subgrade. However, if the resilient modulus of the entire subgrade was reduced calculated surface deflections were too large.

2. Decreasing the resilient modulus of the lower part of the base. Reducing this resilient modulus caused the calculated vertical strain in the layer to be much greater than observed.

The compromise selected gave weight to increasing the radial tensile strain in the granular base as much as practical.

The nonlinear material properties used in the upper two-thirds of the aggregate base are essentially the best and worst of the material properties given by Jouve et al. [C-6] multiplied by 1.5. Increasing the stiffness by 1.5 gave better values of vertical strain in the base. The resilient properties used in the lower third of the base were obtained by multiplying the properties used in the upper portion by 0.4. The nonlinear material properties employed in the simplified contour model are given in Table C-5.

The nonlinear subgrade material properties used in the study are also summarized in Table C-5. The subgrade properties, as well as the aggregate base properties, were developed from the trial and error procedure used to match the measured response variables with those calculated.

A considerable amount of effort was required to develop the reasonably good comparisons with measured responses shown in Table C-1 and C-3 for both the cross-anisotropic and nonlinear models. A better match of calculated and measured response could probably be developed by further refinement of

the process. For this sensitivity study, only the relative response is required of pavements with and without geosynthetic reinforcement. For such relative comparisons the material properties developed are considered to be sufficiently accurate.

Estimation of Permanent Deformation

The presence of the geosynthetic in the granular base was found to cause small changes in vertical stresses and somewhat larger changes in lateral stresses (at least percentage-wise) within the granular layer and the upper portion of the subgrade. During the numerous preliminary nonlinear computer runs that were performed early in this study, it was found that the GAPPS7 program in its present form is not suitable for predicting the effects on rutting due to the relatively small changes in lateral stress. Therefore the layer strain method proposed by Barksdale [C-9] was selected as an appropriate alternate technique for estimating the relative effect on rutting of using different stiffnesses and locations of reinforcement within the aggregate layer.

In summary, the layer strain method consists of dividing the base and upper part of the subgrade into reasonably thin sublayers as illustrated in Figure C-2. The complete stress state on the representative element within each sublayer beneath the center of loading is then calculated using either the cross-anisotropic or the nonlinear pavement model. Residual compaction stresses must be included in estimating the total stress state on the element. The representative element is located beneath the center of the loading where the stresses are greatest. For this location, the principal stresses σ_1 and σ_3 are orientated vertically and horizontally, respectively. Shear stresses do not act on these planes which greatly simplifies the analysis.

C-19
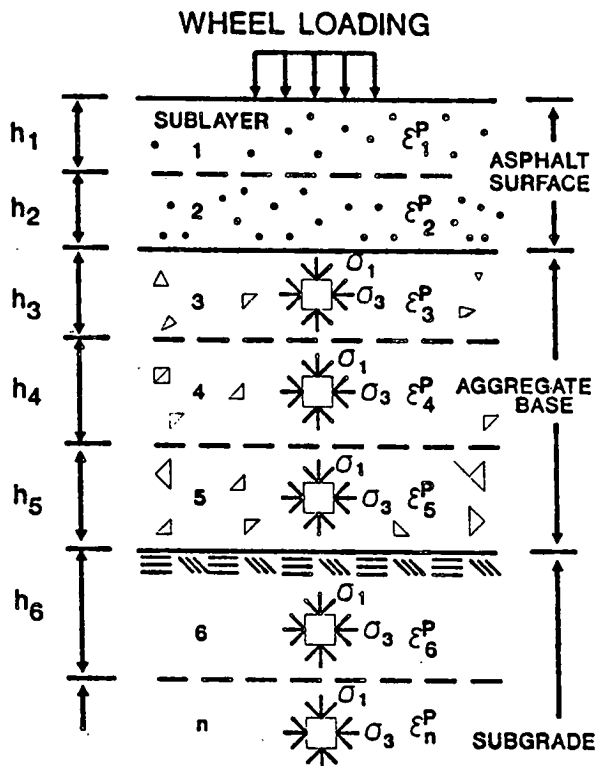
Figure C-2. Idealization of Layered Pavement Structure for Calculating
Rut Depth (After Barksdale, Ref. C-9).

Figure C-3. Comparison of Measured and Computed Permanent Deformation
Response of a High Quality Crushed Stone Base: 100,000
Load Repetitions.

The vertical permanent strain, ε, is then calculated in each element knowing an accurate relationship between the permanent strain ε_p and the existing stress state acting on the element. Total permanent deformation (rutting) is calculated for each sublayer by multiplying the permanent strain within each representative element by the corresponding sublayer thickness. The sum of the permanent deformations in each sublayer gives an estimation of the level of rutting within the layers analyzed.

Placement of even a stiff geosynthetic within the aggregate base causes only small changes in confining pressure on the soil and also small vertical stress changes. To predict accurately the effects of these small changes in stress on rutting, the permanent strain ε_p must be expressed as a continuous function of the deviator stress (q) and confining stress σ_3:

$$\varepsilon_p = f(q, \sigma_3) \tag{C-7}$$

where:

ε_p = vertical permanent strain which the element would undergo when subjected to the stress state σ_3 and $\sigma_1 - \sigma_3$

σ_1 = major principal stress acting vertically on the specimen below the center of the load

σ_3 = lateral confining pressure acting on the specimen below the center of the load

q = deviator stress, $\sigma_1 - \sigma_3$

Although the changes in confining stress are relatively small, these changes, when the element is highly stressed, can greatly reduce permanent deformations under certain conditions.

The hyperbolic permanent strain model proposed by Barksdale [C-9] for permanent deformation estimation gives the required sensitivity to changes in both confining pressure and deviator stress. The hyperbolic expression for the permanent axial strain for a given number of load repetitions is

C-21

$$\varepsilon_p = \cfrac{(\sigma_1 - \sigma_3)/K\,\sigma_3{}^n}{1 - \cfrac{(\sigma_1 - \sigma_3) \cdot R_f}{\cfrac{2(c \cdot \cos\phi + \sigma_3\sin\phi)}{1 - \sin\phi}}} \qquad (C\text{-}8)$$

where:

ϕ and c = quasi angle of internal friction ϕ and cohesion c determined from cyclic loading testing

R_f, k and n = material constants determined from cyclic load testing

All of the material constants (c, ϕ, K, n and R_f) used in the expression must be determined from at least three stress-permanent strain relationships obtained from at least nine cyclic load triaxial tests. Three different confining pressures are used in these tests. The resulting stress-permanent strain curves are then treated similarly to static stress-strain curves.

Two different quality crushed stone bases were modeled for use in the sensitivity studies [C-9]: (1) an excellent crushed granite gneiss base having 3 percent fines and compacted to 100 percent of T-180 density and (2) a low quality soil-aggregate base consisting of 40 percent of a nonplastic, friable soil and 60 percent crushed stone compacted to 100 percent of T-180 density. The soil-aggregate blend was about three times more susceptible to rutting than the high quality crushed stone base. The silty sand subgrade used in the comparative study was compacted to 90 percent of T-99 density. The subgrade had a liquid limit of 22 percent and a plasticity index of 6 percent.

A comparison of the stress-permanent strain response predicted by the hyperbolic relationship given by equation C-8 and the actual measured response for the two bases and the subgrade are shown in Figures C-3 through C-5 for 100,000 cyclic load applications. The theoretical curve given by
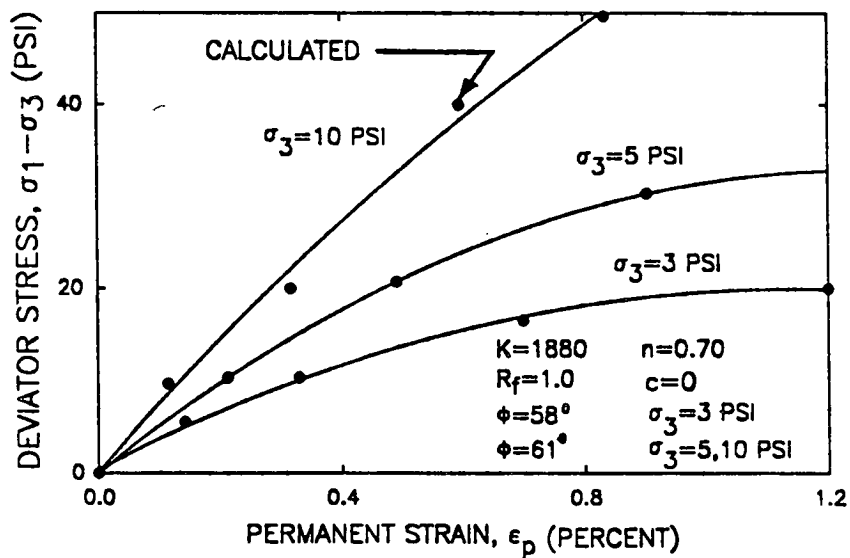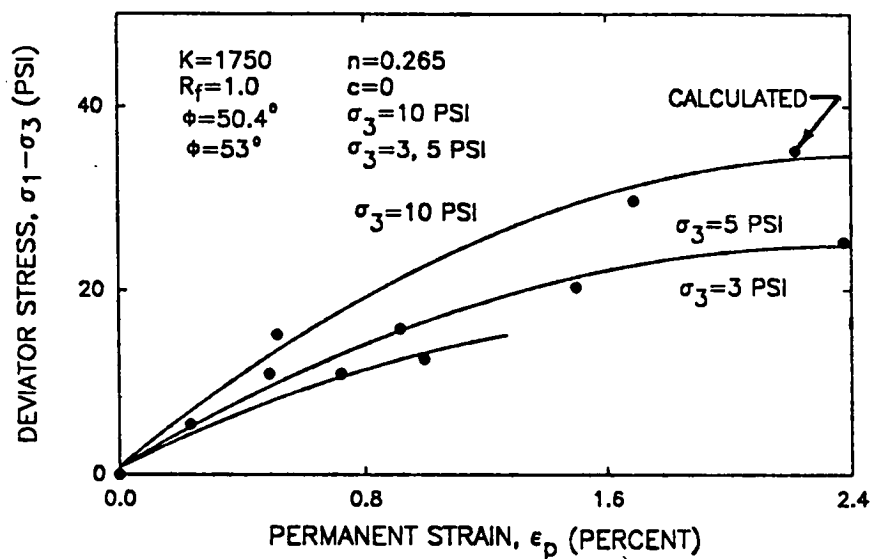
Figure C-4. Comparison of Measured and Computed Permanent Deformation
Response for a Low Quality Soil-Aggregate Base: 100,000
Load Repetitions.
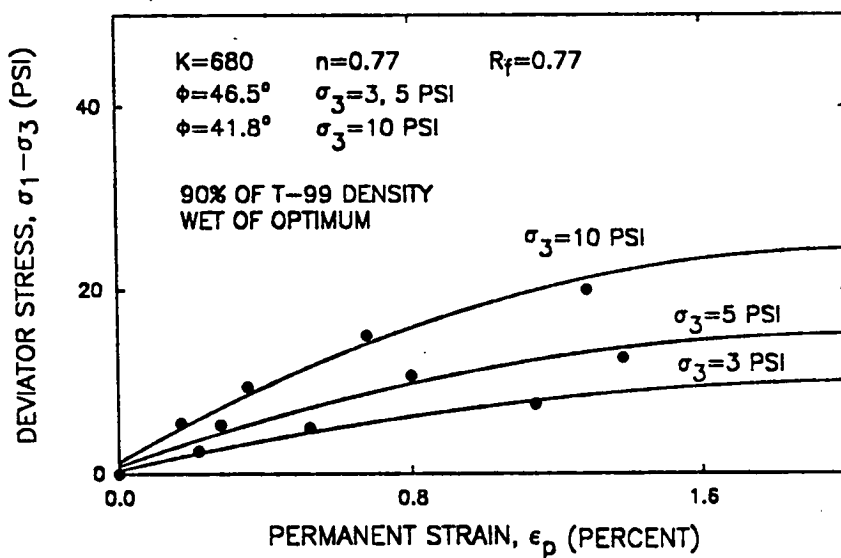
Figure C-5. Comparison of Measured and Computed Permanent Deformation
Response for a Silty Sand Subgrade: 100,000 Load Repetitions.

the hyperbolic model agrees quite nicely with the actual material response. The material parameters used in the hyperbolic model are given in Figures C-3 to C-5; Table C-6 summarizes the general material properties of the base and subgrade.

Table C-6

General Physical Characteristics of Good and Poor Bases
and Subgrade Soil Used in the Rutting Study[1]

| BASE | DESCRIPTION | GRADATION | | | | | COMPACTION T-180 | | $S^{(3)}$ (%) | LA WEAR (%) |
		$1\frac{1}{2}$	3/4	10	60	200	γ_{max} (pcf)	ω_{opt} (%)		
2	40-60 Soil/Crushed Granite Gneiss Blend[2]	99	85	42	25	13	138	5.5	73	45
6	Crushed Granite Gneiss	100	60	25	9	3	137	4.2	50	47
1	Slightly Clayey Silty Sand[4]	100	100	100	63	40	115.4	13.0	-	-

1. Data from Barksdale [C-9].
2. The granite gneiss crushed stone had 0% passing the No. 10 sieve; the soil was a gray, silty fine sand [SM; A-2-4(0)], nonplastic with 73% < No. 40 and 20% < No. 200 sieve.
3. Degree saturation in percent as tested.
4. Classification SM-ML and A-4(1); liquid limit 22%, plasticity index 6.

APPENDIX C

REFERENCES

C-1 Zeevaert, A.E., "Finite Element Formulations for the Analysis of Interfaces, Nonlinear and Large Displacement Problems in Geotechnical Engineering", PhD Thesis, School of Civil Engineering, Georgia Institute of Technology, Atlanta, 1980, 267 p.

C-2 Barksdale, R.D., Robnett, Q.L., Lai, J.S., and Zeevaert-Wolf, A., "Experimental and Theoretical Behavior of Geotextile Reinforced Aggregate Soils Systems", Proceedings, Second International Conference on Geotextiles, Vol. II, Las Vegas, 1982, pp. 375-380.

C-3 Brown, S.F., and Pappin, J.W., "The Modeling of Granular Materials in Pavements", Transportation Research Board, Transportation Research Record 810, 1981, pp. 17-22.

C-4 Brown, S.F., and Pappin, J.W., "Analysis of Pavements with Granular Bases", Transportation Research Board, Transportation Research Record 810, 1981, pp. 17-22.

C-5 Mayhew, H.C., "Resilient Properties of Unbound Roadbase Under Repeated Loading", Transport and Road Research Lab, Report LR 1088, 1983.

C-6 Jouve, P., Martinez, J., Paute, J.S., and Ragneau, E., "Rational Model for the Flexible Pavements Deformations", Proceedings, Sixth International Conference on the Structural Design of Asphalt Pavements, Ann Arbor, August, 1987, pp. 50-64.

C-7 Barksdale, R.D., and Todres, H.A., "A Study of Factors Affecting Crushed Stone Base Performance", School of Civil Engineering, Georgia Institute of Technology, Atlanta, Ga., 1982, 169 p.

C-8 Barksdale, R.D., "Crushed Stone Base Performance", Transportation Research Board, Transportation Research Record 954, 1984, pp. 78-87.

C-9 Barksdale, R.D.., "Laboratory Evaluation of Rutting in Base Course Materials", Proceedings, 3rd International Conference on Structural Design of Asphalt Pavements, 1972, pp. 161-174.

C-10 Barksdale, R.D., Greene, R., Bush, A.D., and Machemehl, C.M., "Performance of a Thin-Surfaced Crushed Stone Base Pavement", ASTM Symposium on the Implications of Aggregate, New Orleans (submitted for publication), 1987.

APPENDIX D

TEST SECTION MATERIALS, INSTRUMENTATION AND CONSTRUCTION

APPENDIX D

TEST SECTION MATERIALS, INSTRUMENTATION AND CONSTRUCTION

Materials

All materials were carefully prepared, placed and tested to insure as uniform construction as possible. The properties of the pavement materials used in construction of the test pavements were thoroughly evaluated in an extensive laboratory testing program, described in detail in Appendix E. For quality control during construction, some of the readily measurable material properties such as density, water content and cone penetration resistance were frequently determined during and after the construction of the test sections. These quality control tests are fully described subsequently.

Two different asphalt surfacings, aggregate bases and geosynthetic reinforcement materials were used in the tests. The same soft silty clay subgrade was employed throughout the entire project. A brief description of the materials used in the experiments is given in the following subsections.

Asphalt Surfacing. During the first series of tests, a gap-graded, Hot Rolled Asphalt (HRA) mix was used, prepared in accordance with the British Standard 594 [D-1]. An asphaltic concrete mix was employed for the remaining three series of tests. The asphaltic concrete mix was prepared in accordance with the Marshall design results given in Appendix E, Figure E-11. The granite aggregate gradation used in each bituminous mix is shown in Figure D-1, and the specifications of both mixes are summarized in Table D-1.

Aggregate Base. To enhance the benefit of a geosynthetic inclusion in the pavement structure, a weak granular base was used during the first series of
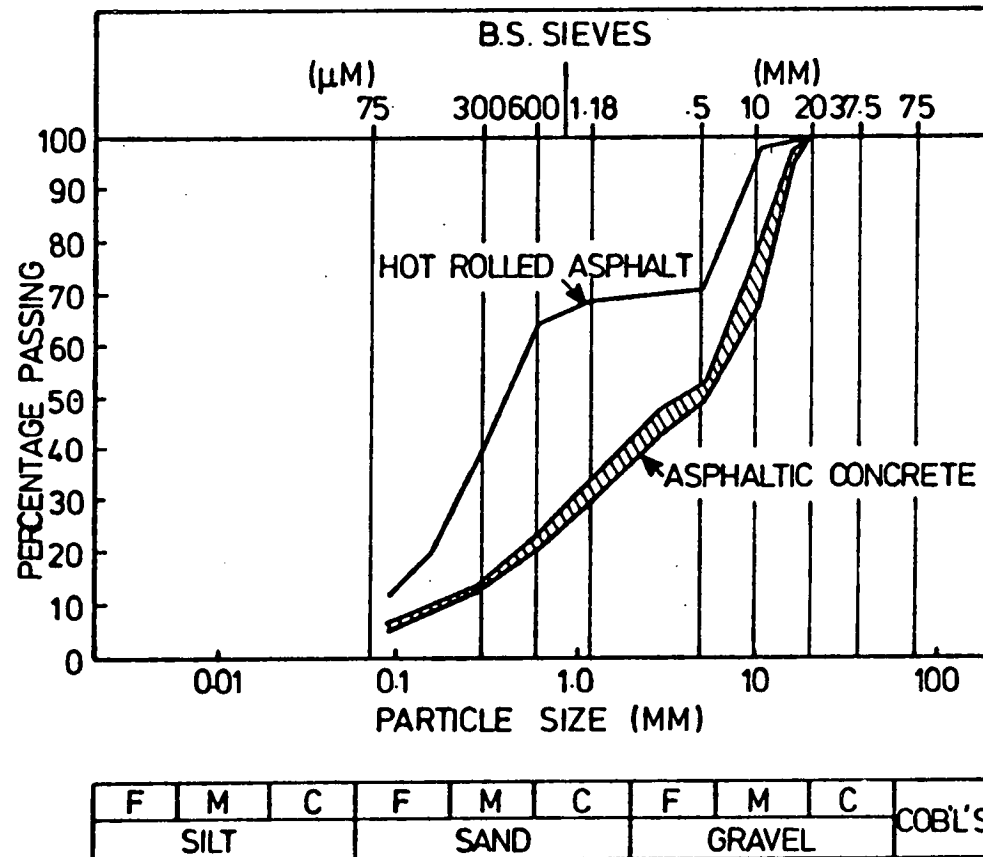
Figure D-1. Gradation Curve for Aggregates Used in Asphaltic Mixes.

Table D-1

Specification of Hot Rolled Asphalt and Asphaltic Concrete

	Hot Rolled Asphalt	Asphaltic Concrete
Binder Penetration	100	50
Binder Content (% by weight)	8	6.5
Maximum Aggregate Size (in.)	0.75	0.75
Delivery Temperature	110 °C	160 °C
Rolling Temperature	80°C	120 °C

tests. This base consisted of rounded sand and gravel, with a maximum particle size of about 3/4 in. (20 mm), and about 3 percent passing the 75 micron sieve. The grading of the granular material, as shown in Figure D-2, conforms with the British Standard Type 2 subbase specification [D-2]. The gravel base sections used in Test Series 1 exhibited extremely poor performance as evidenced by a very early failure at 1690 repetitions of wheel load. As a result, the gravel was replaced for the remaining three test series by a crushed dolomitic limestone.

The dolomitic limestone had a maximum particle size of 1.5 in. (38 mm) and about 7 percent fines passing the 75 micron sieve. The limestone aggregate was slightly angular and non-flaky. The grading, as shown in Figure D-2, lay within the British Standard Type 1 subbase specification. This latter type of granular material is widely used in British highway construction.

Both granular materials were compacted in the test facility at optimum moisture content to generally between 96 and 100 percent of the maximum dry density as determined by the laboratory compaction tests described in Appendix E.

Subgrade. The subgrade was an inorganic, low plasticity, silty clay known locally as Keuper Marl. The clay subgrade was transported to the test facility in the form of unfired wet bricks from a local quarry. An 18 in. (450 mm) thick layer of this soft clay was placed over an existing 3.5 ft. (1.1 m) layer of drier and hence stiffer silty clay subgrade obtained previously from the same quarry. The upper 18 in. (450 mm) of the soft subgrade had an in-place CBR value of about 2.6 percent, and a moisture content of 18 percent. The CBR of the underlying stiffer subgrade was found to be about 8 to 10 percent.
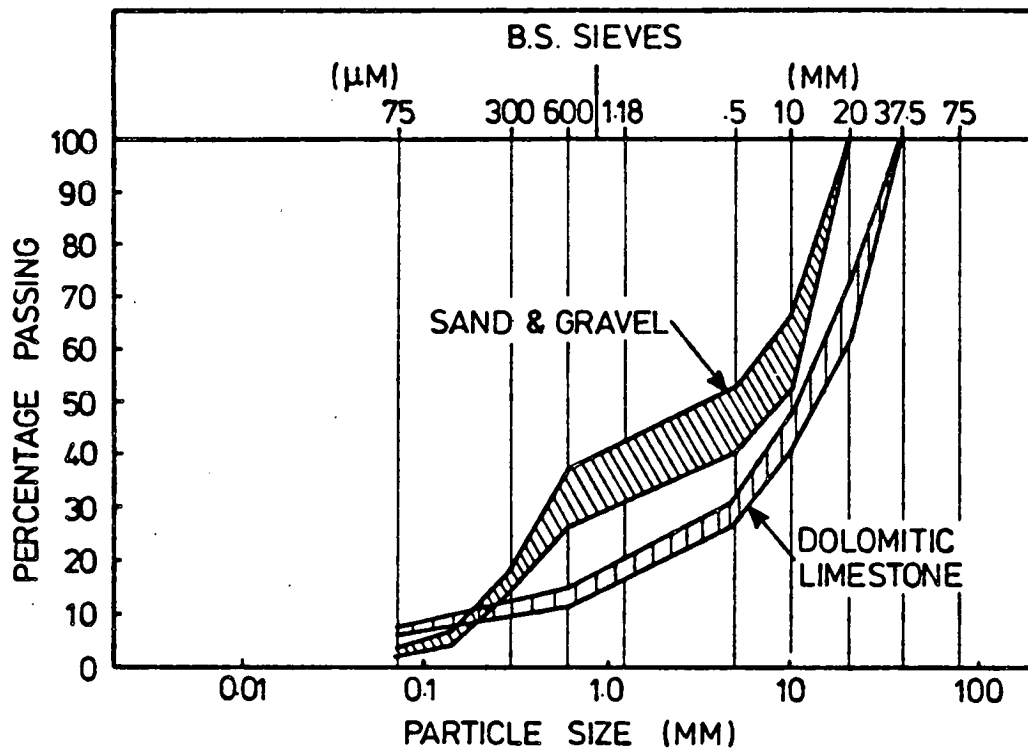
Figure D-2. Gradation Curves for Granular Base Materials.

Geosynthetic Reinforcement.   Two types of geosynthetics were used in the study (Table D-2).   Both geosynthetics were manufactured from polypropylene. One was a very stiff, woven geotextile having a stiffness, S_g = 4300 lbs/in. (750 kN/m) and a weight of 28.5 oz/yd^2 (970 gm/m^2).   The other was a medium to high stiffness biaxial geogrid having a stiffness S_g = 1600 lbs/in. (280 kN/m) and a weight of 6 oz/yd^2 (203 gm/m^2).   Both stiffnesses were measured at 5 percent strain.

Instrumentation

All the sections were instrumented using diaphragm pressure cells [D-3].   Bison type inductance strain coils [D-4], and copper-constantan thermocouples.   Details of instrument calibration have been described in the literature [D-5].   The arrangement of instrumentation installed in each pavement section was similar.   The instrumentation used in one test section is shown in Figure D-3.   Beginning with the third series of tests, additional pressure cells and strain coils were installed in both the top and bottom of the aggregate base.   This additional instrumentation assisted in validating the analytical results.   All the instruments were placed directly beneath the center line of each test section in the direction of wheel travel.

Instrumentation was installed to measure the following parameters:

1.   The magnitude and distribution with depth of the transient and permanent vertical strains in both the granular base and the subgrade.

2.   Transient and permanent longitudinal strain at the bottom of the asphaltic layer; beginning with Test Series 3 longitudinal strain was also determined at both the top and bottom of the granular base layer.

D-7

Table D-2

Properties of Geosynthetics Used.

	Geotextile	Geogrid
Polymer Composition	Polypropylene	Polypropylene
Weight/ area (oz/yd2)	28.5	5.99
Tensile Strength (lb/in)	886	119
Stiffness at 5% Strain (lb/in)	4300	1600
% Open Area	2 - 8	n/a
Grid Size (in. X in.)	n/a	1.22 X 1.56
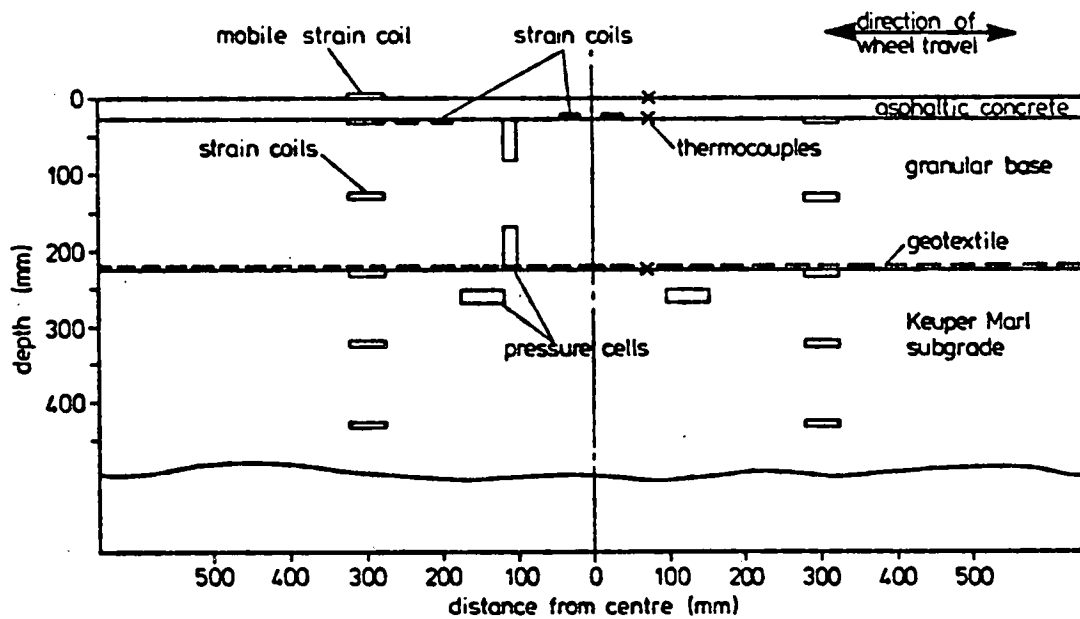
Figure D-3. Typical Layout of Instrumentation Used in Test Track Study.

3. Transient and permanent lateral strain in the geosynthetic, and at the complimentary location in the control section.

4. Transient stress near the top of the subgrade. Beginning with the Third Test Series the transient longitudinal stress was measured at both the top and bottom of the granular layer.

5. Temperature in each pavement layer.

In addition to the instrumentation installed within the pavement, a profilometer (Figure D-4) consisting of a linear potentiometer mounted on a roller carriage, was used to measure the surface profile.

Pavement Construction

Subgrade. During the construction of the first series of pavement sections, 18 in. (450 mm) of fresh silty clay was placed after the same thickness of existing stiff subgrade material was removed. The silty clay subgrade (Keuper Marl) was installed as 7 layers of wet bricks. Each layer was compacted by using a triple legged pneumatic tamper (Figure D-5) which had sufficient energy to destroy the joints in the bricks. The final subgrade surface was then leveled with a single legged pneumatic compactor (Figure D-6) before the aggregate material was placed over it. The surface elevation of the subgrade was established by measuring the distance from a reference beam to various locations on the subgrade surface.

The fresh silty clay subgrade employed in the first series of tests was reused for all subsequent tests. However, since the design thickness for both the aggregate base and asphalt surfacing was increased after the first test series, an additional 2.5 in. (64 mm) of the newly installed silty clay was removed before construction of the Second Series pavement sections.

Chain Support structure Electric motor

Pavement surface

LVDT Core Return spring

LVDT Body Moving carriage

Roller wheel
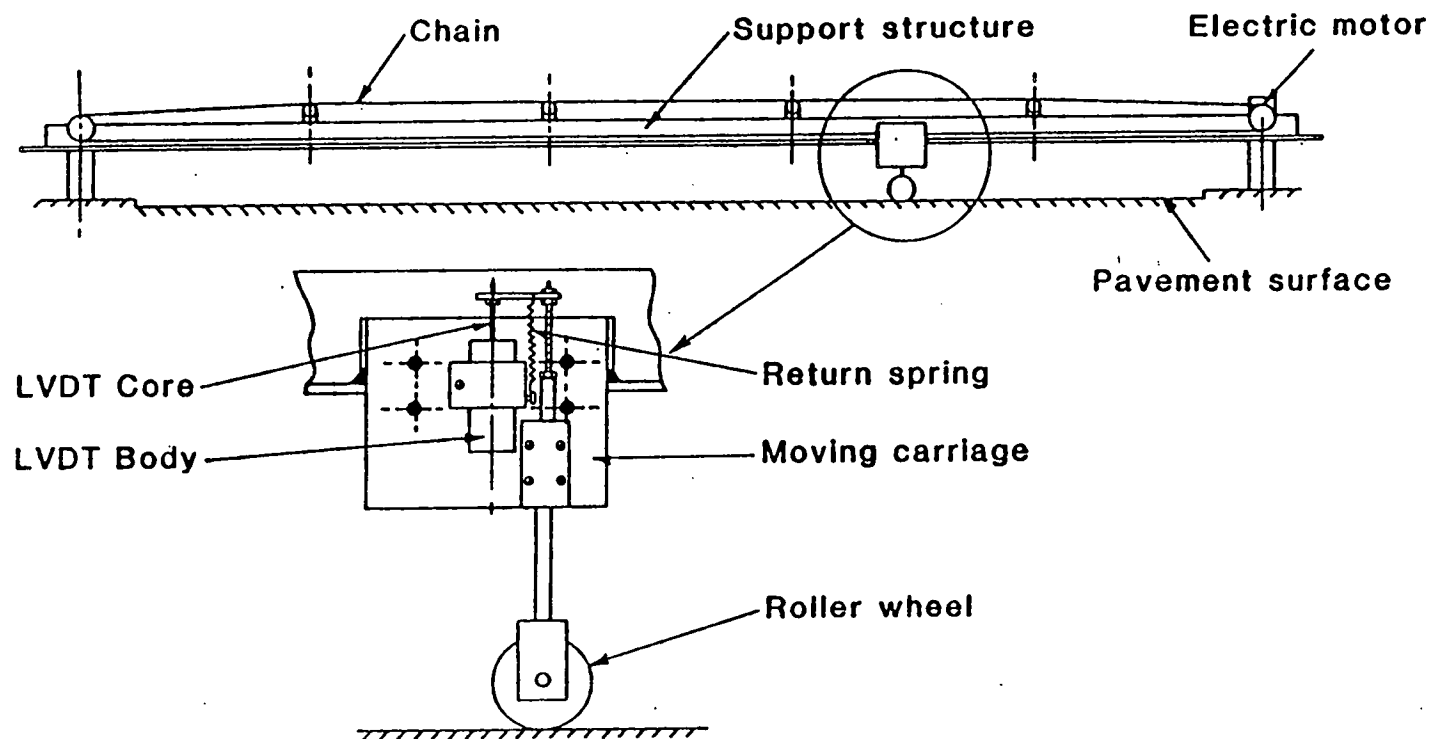
Figure D-4. Profilometer Used to Measure Transverse Profiles on Pavement.
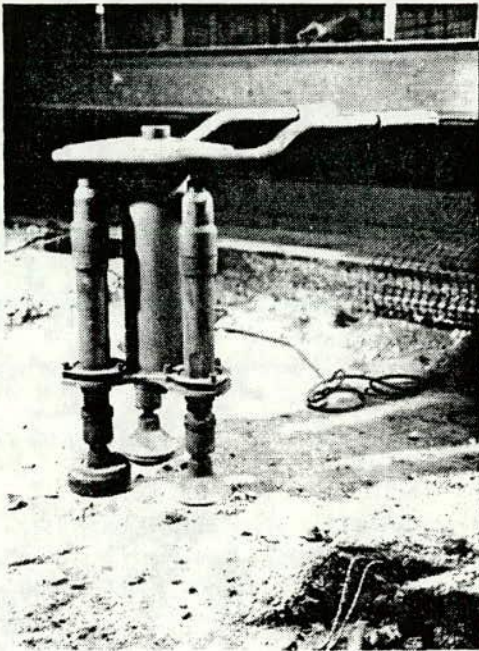
Figure D-5. Triple Legged Pneumatic
Tamper Used on Subgrade.
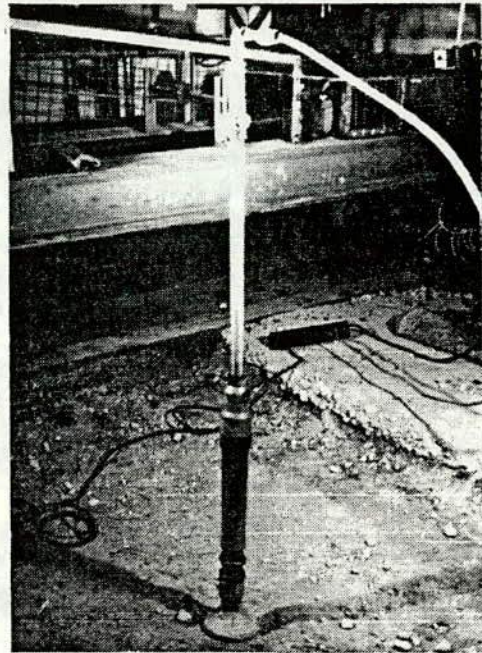
Figure D-6. Single Legged Pneumatic
Compactor Used on Subgrade.
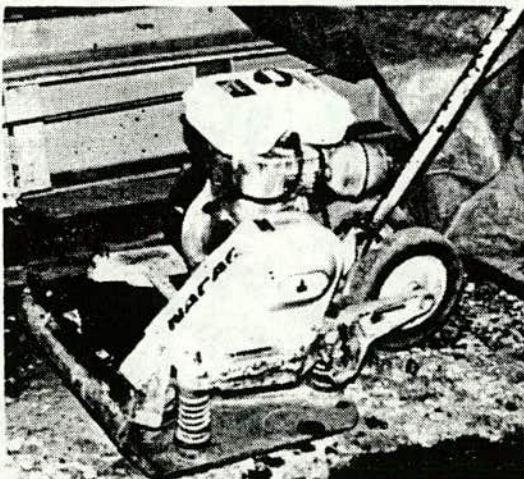
Figure D-7. Vibrating Plate
Compactor.

Figure D-8. Vibrating Roller.

In general, the condition of the subgrade remained constant throughout the study. This was partly due to the fact that it was covered most of the time with a moist aggregate base, preventing drying out and stiffening of the subgrade. The finished subgrade had an average CBR of 2.3 percent after it was first placed. This value increased slightly to 3.2 percent at the end of the last series of tests. The moisture content and dry density remained relatively constant throughout, at about 18 percent and 111 pcf (1778 kg/m^3), respectively. The subgrade density of 111 pcf (1778 kg/m^2) corresponds to about 95 percent of the maximum dry density of this subgrade material as obtained in the British Standard compaction test [D-6].

Pressure cells and strain coils in the subgrade were placed in holes which were cut with special tools designed to ensure minimum disturbance around the instruments [D-7]. All holes and horizontal layer surfaces were scarified as installation proceeded to give good bonding of materials.

Aggregate Base Material.   The aggregates used in the base were brought up to their optimum moisture content prior to placing and compacting. The 6 in. (150 mm) thick layer of sand and gravel base employed in the first test series was compacted in three 2-in. (50 mm) layers at a moisture content of 7 percent by means of a vibrating plate compactor (Figure D-7). The first two layers each received 5 passes of the compactor. The last layer was continuously compacted until no further densification was apparent.

For the 8 in. (200 mm) layer of crushed limestone base used after the first test series, compaction was performed on the two 4 in. (100 mm) layers. Compaction was performed at a moisture content of 7 percent by using an 840 lb. (380 kg) hand operated vibrating roller (Figure D-8). Compaction of the two layers was continued until no rut was detected in the wheel path of the roller. Typical compacting time per layer was about 30

minutes. The dolomitic limestone employed in the second series of tests was reused in the third series after the bottom 2 in. (50 mm) of material contaminated by the subgrade was replaced. In the last series all 8 in. (200 mm) of base was replaced with fresh limestone aggregate.

To install pressure cells and strain coils in the aggregate base, holes were excavated after compaction of the layer was completed. To prevent large aggregate particles from damaging or influencing the output of the cells, a fine sand passing the B.S. No. 7 sieve (212 micron) was placed and carefully tamped around the instruments. The vertically oriented pressure cells were placed in the excavated hole in a prepacked condition, with the fine sand backfill held in position over the diaphragm with a thin plastic film. A similar installation procedure was used during pressure cell calibration in a large triaxial specimen.

Geosynthetic Reinforcement. For each pavement section, the geosynthetic was placed after all pressure cells and strain coils were installed in the subgrade, or within the aggregate base below the level of geosynthetic. The geotextile was stretched tight by hand-pulling at the edges while the granular base material was being placed. The geogrid was held in place by small U-shaped steel anchors after it was stretched tight by hand.

The induction strain coils were attached to the underside of the woven geotextile. To do this, a set of plastic nuts and bolts were used. The plastic bolt, which passed through the central hole of the strain coil and between the filaments of the geotextile, was tightened against a small nut located on the upper side of the geotextile (Figure D-9). Plastic was used to prevent interference with the induction coil magnetic flux field. For the geogrid, a very small hole was drilled through the thick junction of the grid before the coil was attached using the plastic nut and bolt (Figure D-
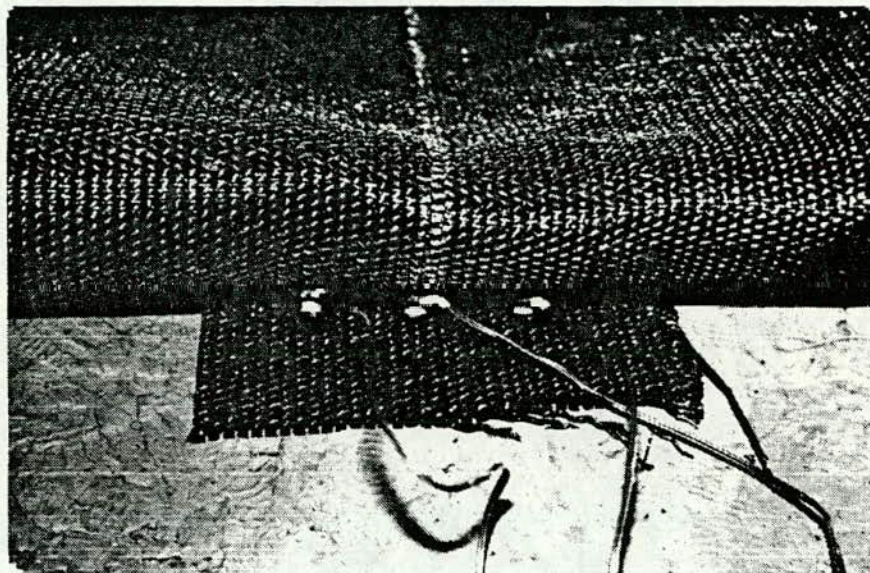
Figure D-9. Woven Geotextile with 1 in. Diameter Induction Strain Coils.
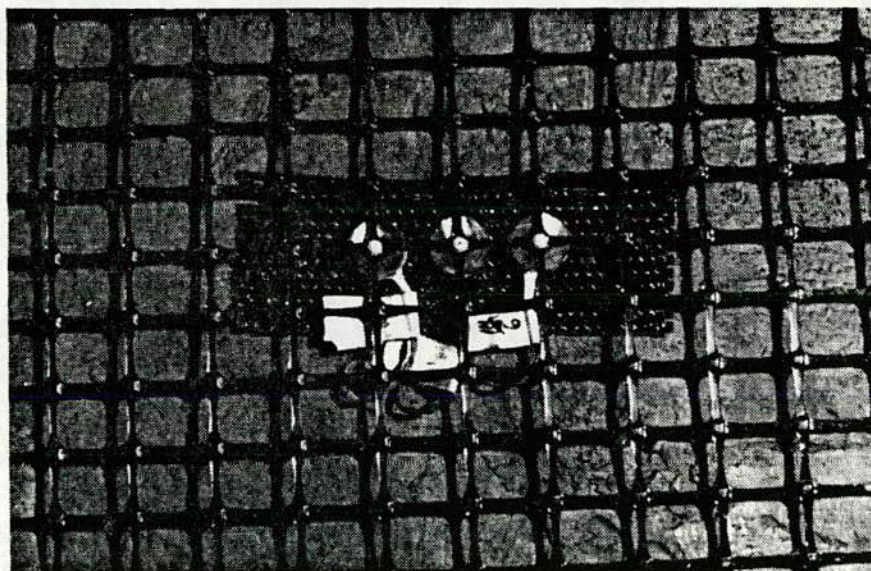
Figure D-10. Geogrid with 1 in. Diameter Induction Strain Coils.

10). To prevent the strain coils from interlocking with the surrounding soil or granular material, they were covered on the underside by a small piece of geotextile. The geosynthetic used in each test section was carefully examined and stored after each series of tests were completed; no geosynthetic materials were reused.

Prerutting.   Prerutting was carried out in every series of tests after the aggregate base was placed, but prior to the construction of the asphalt surfacing. The purpose of prerutting is to induce a tensile force in the geosynthetic, thereby potentially increasing its effectiveness as a reinforcing element. Sometimes prerutting was performed down the center of the pavement as a primary test variable. In other instances prerutting was carried out along the edge of the pavement as a supplementary study. To carry out prerutting, a moving wheel load from the Pavement Test Facility was applied directly onto the surface of the granular base layer of the pavement section. This simulated the traffic condition during construction when heavily loaded trucks pass over the aggregate base. The applied wheel loadings varied from 1.1 kips (5 kN) for the sand and gravel base (Test Series 1) to 2 kips (9 kN) for the crushed dolomitic limestone used in the remaining three test series. When prerutting was conducted along the center line of the section under which strain coils were installed, vertical permanent deformations were monitored during prerutting of both the aggregate surface and the subgrade. The wheel load was discontinued when a specified amount of rut was established at the surface of the subgrade.

When prerutting was carried out in areas away from the centerline of the pavement section, only the surface rut could be monitored. Criteria to discontinue the wheel load was then based on an accumulation of about 2 in. (50 mm) of rut at the surface of the aggregate layer. Very often during

prerutting, the rut created in the aggregate layer needed to be partially refilled because the ram used to force the tire against the pavement had a limited amount of travel. Upon completion of prerutting, the entire rut in the base was refilled and carefully compacted with aggregate preconditioned to the proper moisture content. With the exception of the sand-gravel base, prerutting generally resulted in local densification of the aggregate base.

Prestressing Geosynthetic. One section included in the Fourth Test Series had a prestressed aggregate base. Prestressing was accomplished using the stiff geogrid. A schematic diagram showing the prestressing arrangement used in the laboratory tests is given in Figure D-11. After the first layer of granular material was placed and compacted, the geogrid was clamped to the side wall of the pavement using the clamping system detailed in Figure D-11. The geogrid then went through a set of rollers and was connected, by way of a load transfer steel bar and steel cable, to a hydraulic jack. By jacking against a steel column which was firmly bolted to the concrete floor, a tension force was generated and transferred to the geogrid. As soon as the target force of 40 lb/in. (7 kN/m) was achieved, a second clamping bar was used to lock the geogrid in position thus maintaining its tensioned state. In performing the clamping operation, some additional tensile force may have been created in the geogrid. After the pretensioning force was "locked in" the geogrid, the second layer of aggregate base was immediately placed and compacted; the load from the hydraulic jack was then released applying a prestress to the base and subgrade. The total period of stretching the geosynthetic (i.e., when the hydraulic jack was in action) was about one hour.
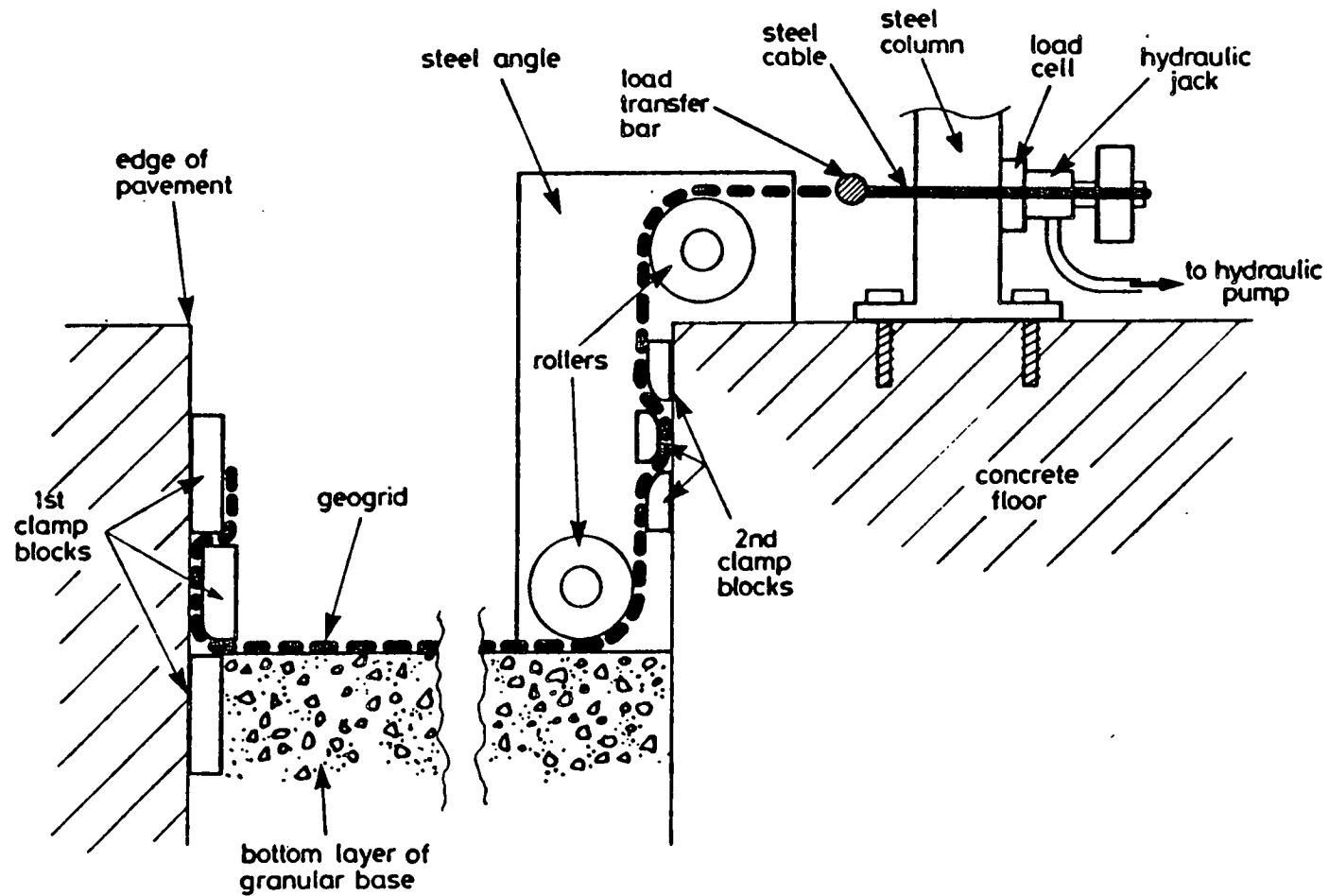
Figure D-11. Method Employed to Stretch Geogrid Used to Prestress the Aggregate Base - Test Series 4.

Asphalt Surfacing.   Both asphalt surface mixes used in this project were transported by truck from the same plant located about 22 miles (35 km) from the test facility. Three tons (2730 kg) of material were delivered for each test series. This quantity of asphalt is about three times the amount required for the single lift construction. The excess material helped to prevent rapid loss of heat during transportation. Upon arrival at the test facility, the material was transferred to the test sections by using preheated wheelbarrows. The temperature of the hot rolled asphalt (HRA) mix employed in the first series, which used 100 Pen binder, was about 230°F (110°C) when it was being placed. The temperature for the AC mix, which used 50 Pen binder, was about 320°F (160°C) at the time of placement.

Compaction of the single layer was performed using the same vibrating roller that was employed for the aggregate base. The first pass was made without using vibration to avoid creating large distortions. Compaction was carried out in both the longitudinal and transverse directions of the pavement area. Rolling was continued until no further movement or indentation was observed on the surface. The whole sequence of construction of the asphalt layer took about 35 minutes.

To protect the strain coils placed on top of the aggregate layer, they were covered with a fine asphalt mix before placement of the main bulk of material. All exposed cables were also protected when the mix arrived by covering them with carefully selected material from which relatively large aggregate particles were removed.

Pavement Surface Profile

Despite great care during construction, the thickness of the layers of the completed pavement were not exactly as specified. This was probably due to difficulties in judging the quantity of material required for a specified

compacted thickness. However, variations between sections within one series of tests were within acceptable tolerances, generally less than 10 percent. The finished profiles for all 12 sections are summarized in Table D-3. The thickness of individual layers was obtained by several technique including: (1) core samples of the asphalt surfacing, (2) strain coil readings, (3) measurements from a reference beam to points on the top and bottom of each layer, and (4) cross sections taken during trench excavation at the end of each test series.

Construction Quality Control

Construction of the subgrade during each series of tests was closely monitored. For the first test series, static cone penetrometer tests (Figure D-12) were performed to determine the corresponding CBR values after compaction of each layer of fresh silty clay. The moisture content was also measured at a number of locations for each layer of subgrade. After placement of the subgrade, four insitu CBR tests (ASTM D4429) and two dynamic cone penetrometer tests (Figure D-13) were performed at the surface. In addition, the nuclear density meter (Figure D-14) was used to determine the density and moisture content at various locations. The nuclear density tests were complimented by regular laboratory moisture and density tests using four 2.5 in. (64 mm) diameter tube samples. After the first test series, with the exception of the insitu CBR tests, all of the tests described above were repeated on the subgrade surface both before and after the wheel loading tests.

Gradation tests were performed on the aggregate base when they were delivered, after compaction, and at the end of the wheel loading test. In general, no significant change in grading was noticed as a result of the various operations. At least two dynamic cone penetrometer tests, nine

Table D-3

Layer Thickness of Pavement Sections and Depth of Geosynthetics
From Pavement Surface

Test Series	Pavement Section*	Thickness of Layer (in.)			Depth of Geosynthetic from Surface (in.)
		A.C.	Base	Soft Subgd	
1	PR-GX-B	1.2	6.3	17.5	7.5
	CONTROL	1.35	5.8	17.9	n/a
	GX-B	1.3	6.1	17.6	7.4
2	PR-GD-B	1.2	8.5	15.3	9.7
	CONTROL	1.2	8.3	15.5	n/a
	GD-B	1.1	8.1	15.8	9.2
3	GX-B	1.2	8.1	15.7	9.3
	CONTROL	1.2	8.3	15.5	n/a
	GX-M	1.3	7.7	16.0	5.1
4	GX-M	1.5	8.3	15.2	5.4
	GD-M	1.35	8.5	15.2	5.6
	PS-GD-M	1.6	8.6	14.8	5.8

* PR= Prerutted   GX= Geotextile   M= Middle of Base
  PS= Prestressed   GD= Geogrid   B= Bottom of Base

Figure D-12. Static Cone Penetrometer Test on Subgrade.
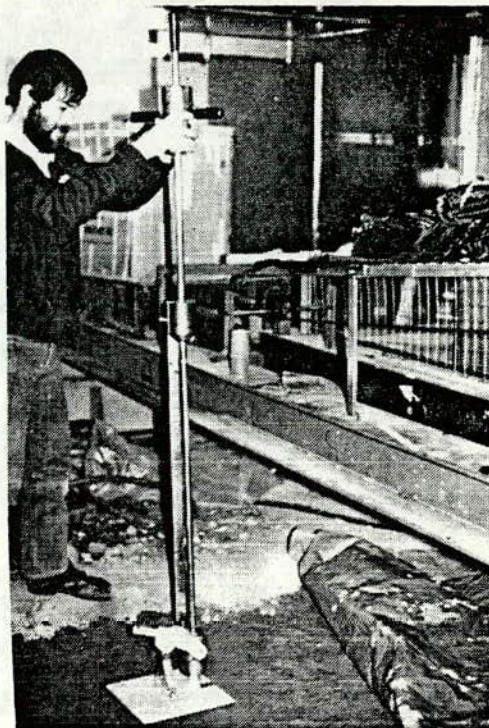
Figure D-13. Dynamic Cone Penetrometer Test on Subgrade.

Figure D-14. Nuclear Density Meter.
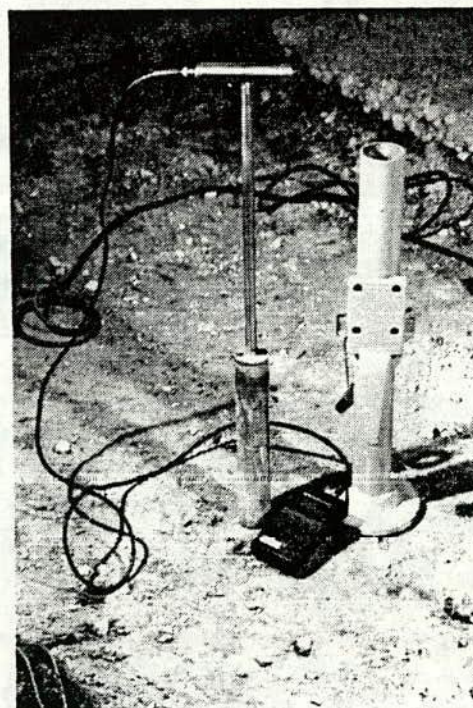
Figure D-15. Clegg Hammer Used on Aggregate Base.

Clegg Hammer tests (Figure D-15), and nine nuclear moisture-density tests were performed on the aggregate base before and after each test series.

On delivery of the asphalt surfacing, six samples were taken to determine the aggregate gradation and binder content. Density of the asphalt surfacing immediately after compaction was measured by the nuclear density meter. At the end of each test series, at least ten core samples were taken to determine the compaction, void ratio and density.

A summary of the results obtained from the various quality control tests just described is given in Table D-4. In addition, Falling Weight Deflectometer (FWD) tests were carried out on the test sections. Tests were performed directly on the aggregate base as well as on the asphalt surfacing. The results of these tests, however, appeared to be unsatisfactory due to the fact that very high deflections were obtained from the impact load of the FWD, as shown in Table D-5. The high deflections created difficulties in reliably back-calculating the stiffness of individual layers; in most cases, convergence of the analysis was not possible. Interpretation of the test results was further complicated by the fact that the test facility was constructed on and surrounded by thick concrete which reflected abnormal signals to the geophones of the FWD. As a result, the shape of the recorded deflection bowl was different from those encountered outside the Pavement Test Facility (PTF).

Table D-4

Summary of Construction Quality Control Test Results for all Test Series

Pavement Layer	Type of Quality Control Test		Test Series 1	2	3	4
Asphaltic	Binder Content (%)		8	6.5	6.5	6.5
	Max. Aggregate Size (mm)		14	14	14	14
	Ave. Compacted Density (pcf)	Before	132	141	141	144
		After[1]	144	145	149	149
	Ave. Air Void[2] (%)	Before	8.8	6.4	7.0	4.4
Granular	Material type		Sand & Gravel	Crushed Limestone	Crushed Limestone	Crushed Limestone
	Max. Aggregate Size (mm)		20	37.5	37.5	37.5
	% Finer than .075mm		3	7	7	7
	Ave. Dry Density (psf)	Before	132	141	136	138
		After[3]	124	140	133	136
	Ave Moisture Content (%)	Before	8.3	6.0	8.0	7.0
		After	4.8	4.5	4.4	5.5
	Ave.Clegg Hammer Reading	Before	14	46	32	40
		After	23	78	75	70
	Ave.Dynamic Cone Reading (No of Blows/10cm)	Before	10	40	35	40
		After	8	100	80	85
Subgrade	Ave. Dry Density (pcf)	Before	112	111	111	111
		After	111	111	111	113
	Ave. Moisture Content (%)	Before	17.3	17.9	17.8	17.2
		After	18.7	18.4	18.4	17.3
	Ave.Static Cone Reading[4]	Before	286	262	282	330
		After	204	288	319	384
	Ave.CBR (ASTM D4429)	Before	2.9	/	/	/

Notes: 1) Measured from core samples.
2) Based on the average initial density and binder content.
3) Values may be too low because a lot of fine sand had to be use to provide a flat surface for the nuclear density meter to operate on.
4) CBR value can be obtained approximately by dividing the reading by 110.

Table D-5

Summary of Results from Falling Weight Deflectometer Tests Performed
on Laboratory Test Sections

Test Series	1		2		3		4	
Section Designation*	PR-GX-B	CONTROL	PR-GD-B	CONTROL	CONTROL	GX-B	GX-M	GD-M
Data on Unsurfaced Pavement Contact Stress (kPa) Deflection** (micron)	117 2999	118 2730	377 2646	344 2589	163 2050	160 2222	166 1980	172 1950
Data on Surfaced Pavement Contact Stress (kPa) Deflection**(micron)	126 3109	125 2871	377 2470	335 2473	164 2004	165 2207	170 1953	178 1880

Notes: * PR = Prerutted GX = Geotextile M = Middle of Base
GD = Geogrid   B = Bottom of Base
** Deflection directly underneath the loading platen.

D-25

APPENDIX D

REFERENCES

D-1 BRITISH STANDARDS INSTITUTION, "Specification for Rolled Asphalt (hot process) for Roads and Other Paved Areas", BS594, 1973.

D-2 DEPARTMENT OF TRANSPORT, "Specification for Road and Bridge Works", London, HMSO, 1976.

D-3 Brown, S.F., and Brodrick, B.V., "The Performance of Stress and Strain Transducers for Use in Pavement Research", University of Nottingham, Research Report to Scientific Research Council, United Kingdom, 1973.

D-4 BISON INSTRUMENT INC., "Instructions Manual; Bison Instrument, Soil Strain Gage Model 410A".

D-5 Brown, S.F., and Brodrick, B.V., "Stress and Strain Measurements in Flexible Pavements", Proceedings, Conference on Measurements in Civil Engineering, Newcastle, England, 1977.

D-6 BRITISH STANDARDS INSTITUTION, "Methods of Testing Soils for Civil Engineering Purposes", BS1377, 1975.

D-7 Brown, S.F., Brodrick, B.V., and Pappin, J.W., "Permanent Deformation of Flexible Pavements", University of Nottingham, Final Technical Report to ERO U.S. Army, 1980.

APPENDIX E

PROPERTIES OF MATERIALS USED IN LARGE-SCALE
PAVEMENT TEST FACILITY

APPENDIX E

LABORATORY TESTING OF MATERIALS

An extensive laboratory testing program was carried out to characterize all the pavement material used in this project. The tests were carried out in accordance with either (1) existing ASTM and British Standards, (2) tentative standards and procedure in their proposal stage (for the geosynthetics), or (3) established and published testing procedures adopted by individual laboratories (for the cyclic load triaxial test).

Tests on Silty Clay Subgrade

The silty clay, known as Keuper Marl, has been used extensively at Nottingham in earlier research projects on repeated load triaxial testing (E-1,E-2) and also as the subgrade in the PTF (E-3). The work carried out by Loach (E-4) on compacted samples of Keuper Marl was of most relevance to the current project. One result obtained from Loach's tests is shown in Fig. E-1. This indicates the relationship between resilient modulus and CBR for compacted samples of Keuper Marl and clearly shows the influence of shear stress on the relationship (i.e., the nonlinear stiffness characteristic of the soil).

Despite the large amount of data accumulated from previous tests on Keuper Marl, a few index tests and four repeated load triaxial tests were carried out on samples of material used during the project in order to characterize the particular index and mechanical properties. The basic material properties of Keuper Marl used in the current project is given in Table E-1.
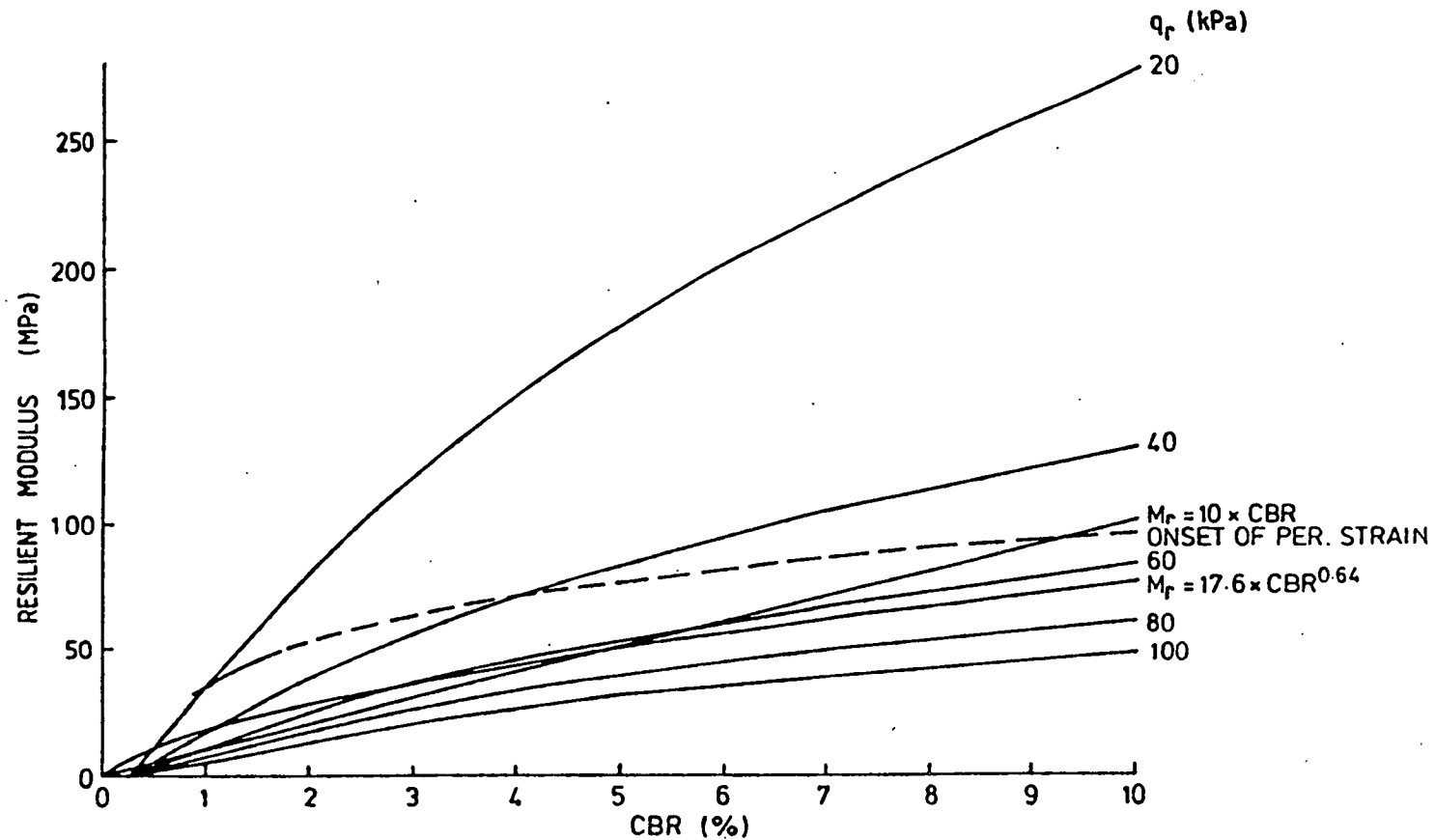
Figure E-1. The Relationship Between Stiffness and CBR for Compacted Samples of Keuper Marl for a Range of Stress Pulse Amplitudes (After Loach).

Table E-1. Results of classification tests for Keuper Marl.

Unified Soil Classification	CL
Specific Gravity	2.69
% Clay	33
Plastic Limit (%)	18
Liquid Limit (%)	37
Plasticity Index	19
Maximum Dry Density* (pcf)	117
Optimum Moisture Content* (%)	15.5

* According to British Standard 1377 (E-8).

Cyclic Load Triaxial Test.   It has been found (E-5,E-6,E-7) that relationships exist between soil suction and elastic stiffness for saturated and near saturated clay. Therefore, in order to determine the general resilient properties of Keuper Marl, a series of soil suction and cyclic load triaxial tests are required. Loach (E-4) carried out some soil suction tests on samples of compacted Keuper Marl at their original moisture contents using the Rapid Suction Apparatus developed at the Transport and Road Research Laboratory (E-9). The results of his tests are shown in Fig. E-2. Loach also carried out repeated load triaxial tests on compacted 3 in. (76 mm) diameter cylindrical samples of Keuper Marl. The ranges of cell pressure and repeated deviator stress he used during these tests were 0 to 4.35 psi (0 to 30 kPa) and 0 to 10.15 psi (0 to 70 kPa), respectively. Using a similar procedure to that adopted by Loach and with the aid of a computer-controlled servo-hydraulic testing system, four additional tests were performed on recompacted samples obtained from the pavement test sections. The results of these tests generally conformed with those obtained by Loach who suggested the following equation to model the elastic stiffness of compacted Keuper Marl:

$$E_r = \frac{q_r}{A} \left(\frac{u + \alpha p}{q_r}\right)^B$$

where: u = suction in kPa

p = cell pressure in kPa

α = 0.3 (suggested by Croney)

E_r = Elastic Stiffness in kPa

q_r = Repeated deviator stress in kPa

A = 2740

B = 2.1
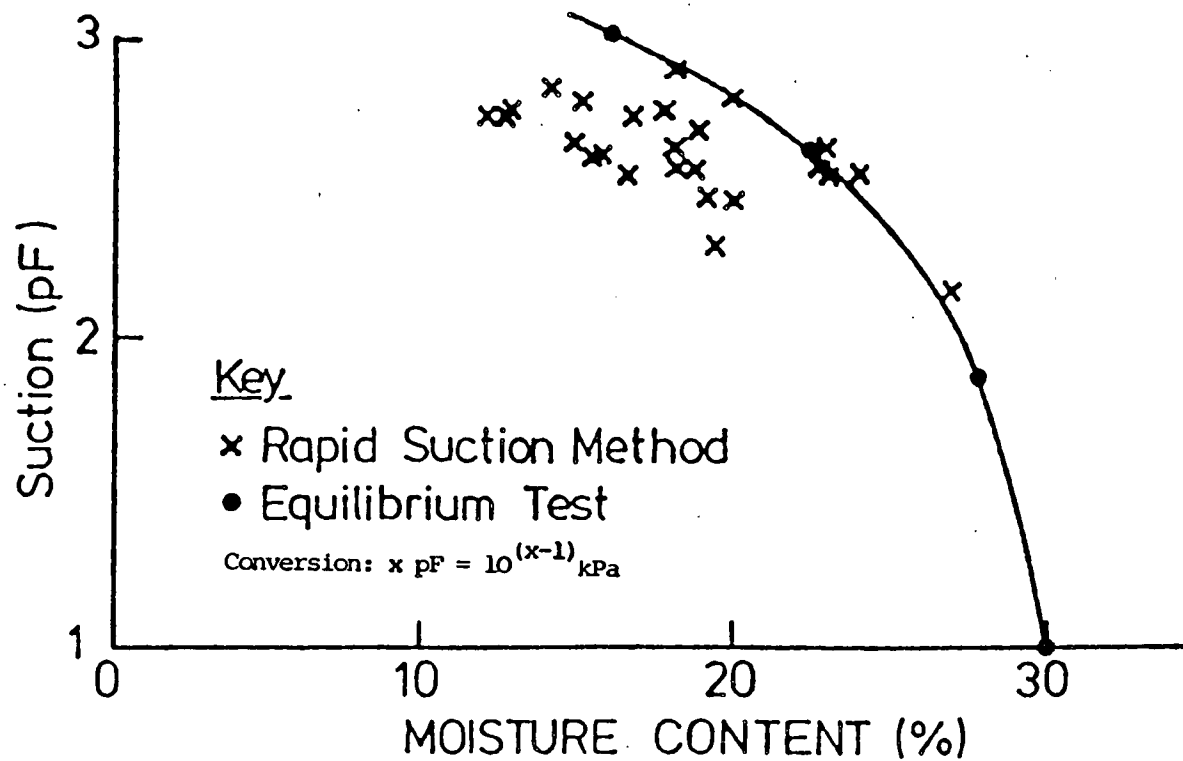
Figure E-2. Results from Suction-Moisture Content Tests on Keuper Marl (After Loach).

Both A and B are constants derived from experiments.

For the permanent strain behavior of Keuper Marl, the results obtained by Bell (E-3) was found to be the most applicable. Comparison of the index properties between Bell's soil and the one used in the current project showed them to be similar. The permanent strain tests were carried out at a frequency of 4 Hz and with a 2 second rest period. A cell pressure of 0.26 psi (1.8 kPa) and repeated deviator stresses in the range of 2.2 to 10.2 psi (15 to 70 kPa) were used. The increase of permanent axial and radial strains with number of cycles for the tests are summarized in Fig. E-3.

Tests on Granular Base Material

Laboratory tests performed on the granular materials consisted mainly of cyclic load triaxial tests, compaction tests, sieve analyses and other index tests.

Cyclic Load Triaxial Test.   Details of procedure and equipment for carrying out cyclic load triaxial tests on granular material were described by Pappin (E-10) and Thom (E-11). Each cyclic load triaxial test was subdivided into:

1) A resilient strain test where the stress paths were far away from failure with the resulting strain essentially recovered during unloading and,

2) A permanent strain test where the stress path was considerably closer to the failure condition, hence allowing permanent strain to accumulate.

A total of six tests were carried out on recompacted 6 in. (150 mm) diameter samples of the two types of material at various moisture contents. The results of earlier testing showed that resilient behavior of a granular material under repeated loading was very stress dependent and, therefore,
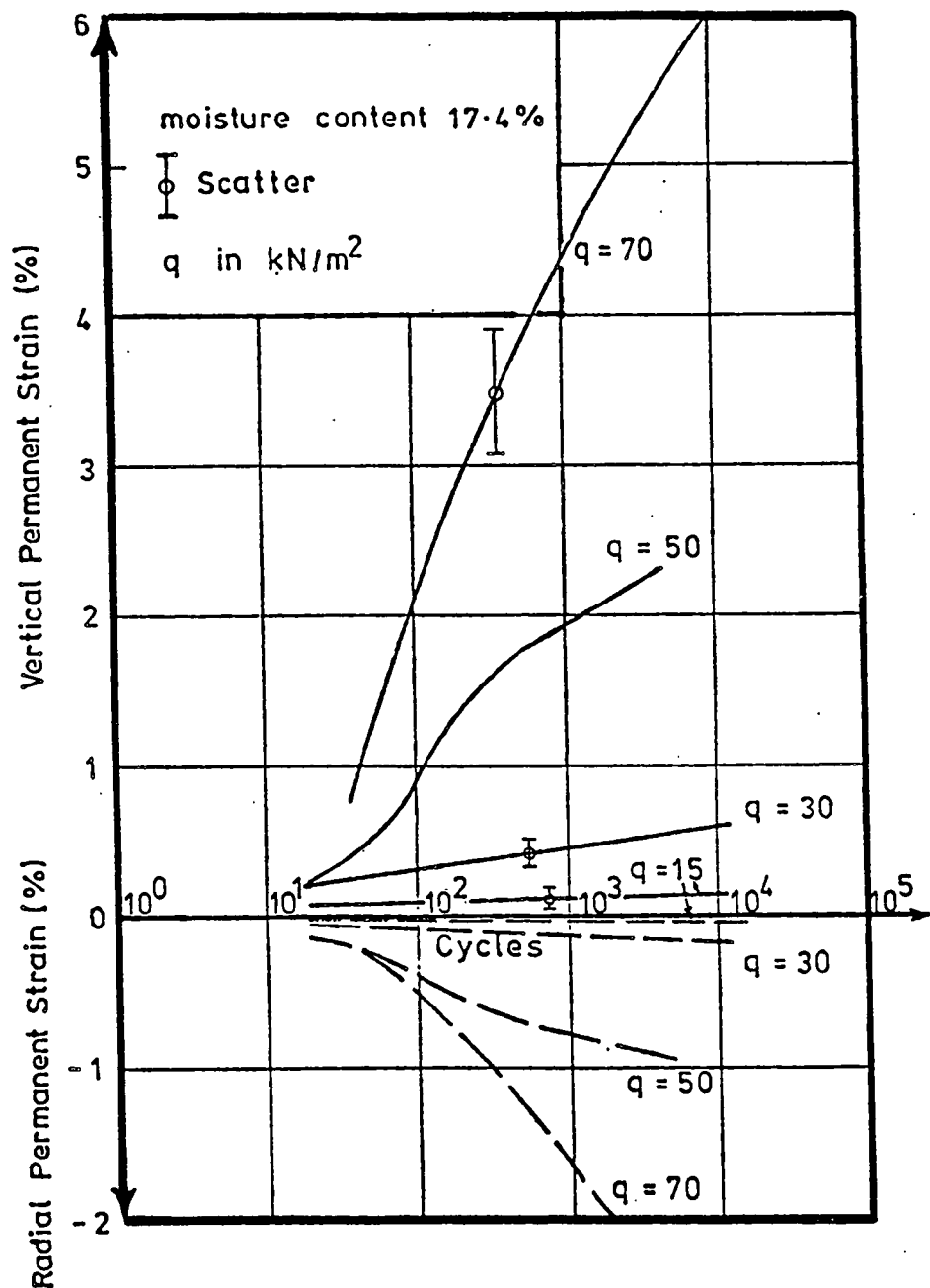
Figure E-3. Permanent Axial and Radial Strain Response of Keuper Marl for a Range of Stress Pulse Amplitudes (After Bell).

nonlinear. Hence, each of the six tests used 20 stress paths, as shown in Fig. E-4, to characterize resilient strain. The ranges of repeated cell pressure and repeated deviator stress used in the tests were 0 to 36 psi (0 to 250 kPa) and 0 to 29 psi (0 to 200 kPa), respectively. For permanent strain tests, a cell pressure of 7.3 psi (50 kPa) and a repeated deviator stress of 0 to 29 psi (0 to 200 kPa) were used. Up to 2000 stress cycles at a frequency of about 1 hz were applied to the test samples.

The results of the resilient strain tests were interpreted by means of Boyce's model (E-12) which expressed the bulk modulus, K, and the shear modulus, G, as a function of both p', the mean normal effective stress, and q, the deviator stress. The equations which Boyce used in the interpretation of results are as follows:

$$G = G_1 p'^{(1-n)}$$

$$K = K_1 p'^{(1-n)} / \{1 - \beta(q/p')^2\}$$

where

$$p' = 1/3 \ (\sigma_a + 2\sigma_c) \qquad q = 1/2(\sigma_a - \sigma_c)$$

and K_1, G_1, n and β are constants to be determined by experiments.

Based on the above equations, the results of the resilient tests are summarized in Table E-2.

The results for the permanent strain tests for the two types of granular material are shown in Figs. E-5 and E-6. The dry densities of the test samples are shown in Table E-2. The results are presented in the form of change of permanent axial and radial strains with the number of stress cycles. Figure E-5 indicates that the sand and gravel has a rather low resistance to permanent deformation. For the dolomitic limestone, Fig. E-6 indicates that the rate of development of permanent deformation varies with

E-9

Table E-2. Summary of resilient parameters for granular materials obtained from cyclic load triaxial tests.

E-10

Test No	Type of Material	Dry Density (pcf)	Moisture Content (%)	Volumetric Strain Coefficients			Shear Strain Coefficients	
				Kl	n	β	Gl	n
1	Sand & Gravel	129	3.7	3040	.33	.110	2530	.33
2	Crushed Limestone	133	4.0	4785	.33	.108	3975	.33
3	Crushed Limestone	127	3.3	4900	.33	.127	3720	.33
4	Crushed Limestone	128	6.0	4130	.33	.142	3010	.33
5	Crushed Limestone	131	6.7	2975	.33	.136	3540	.33
6	Crushed Limestone	136	8.4	3800	.33	.398	1650	.33

Notes: 1) The strain coefficients are deduced from Boyce's model.
2) Kl and Gl are measured in kPa and the corresponding strain calculated is in με.
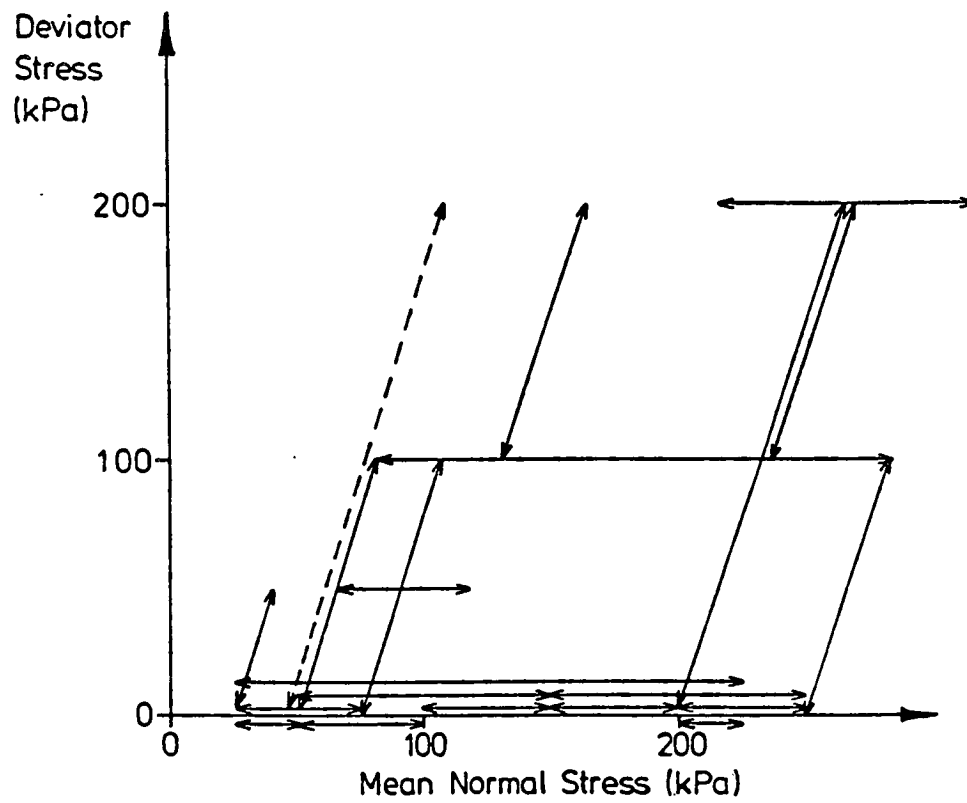
Figure E-4. Stress Paths Used in Cyclic Load Triaxial Tests for Granular Materials.
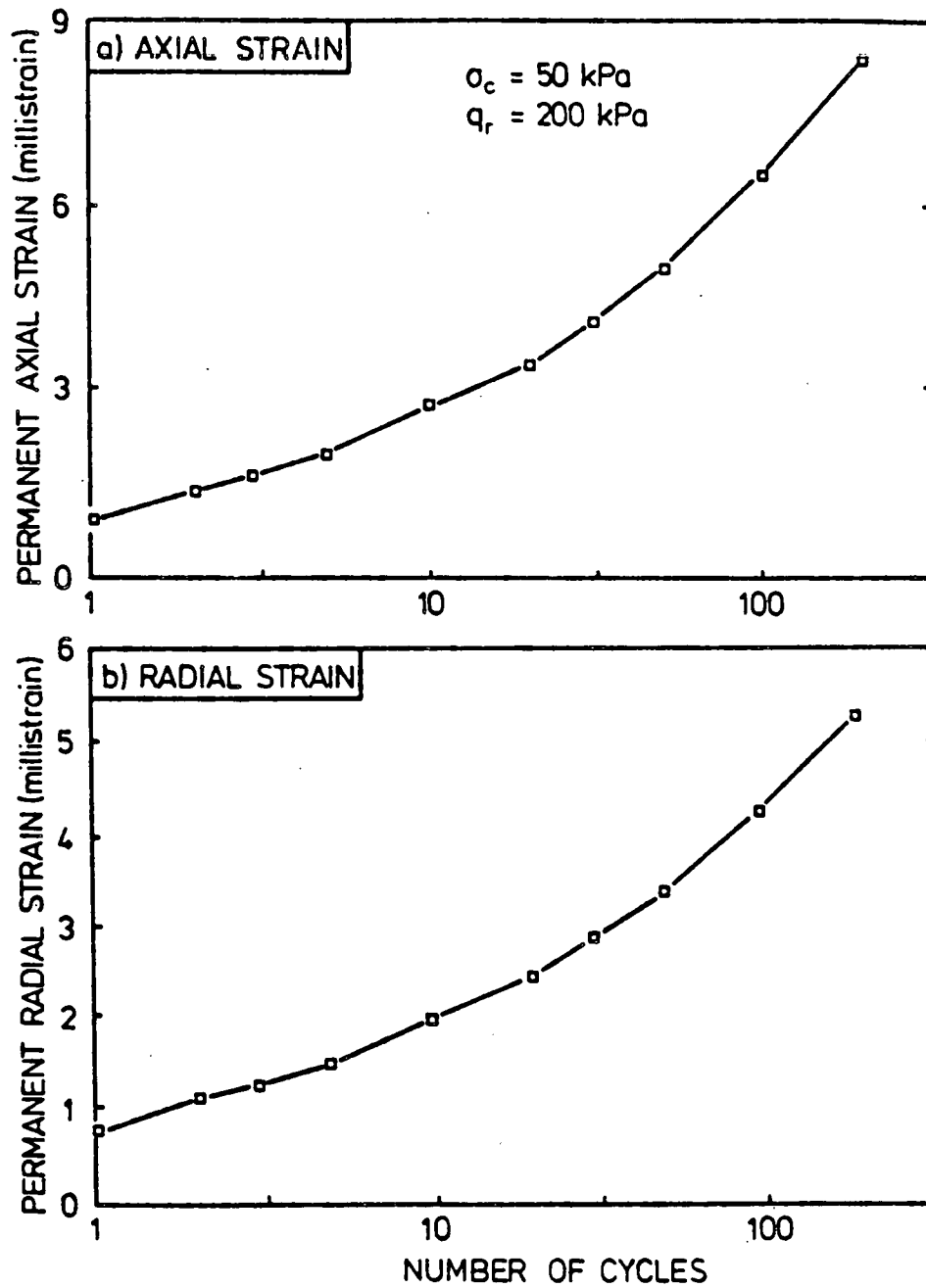
Figure E-5. Permanent Axial and Radial Strains Response of Sand and Gravel During Repeated Load Triaxial Test.
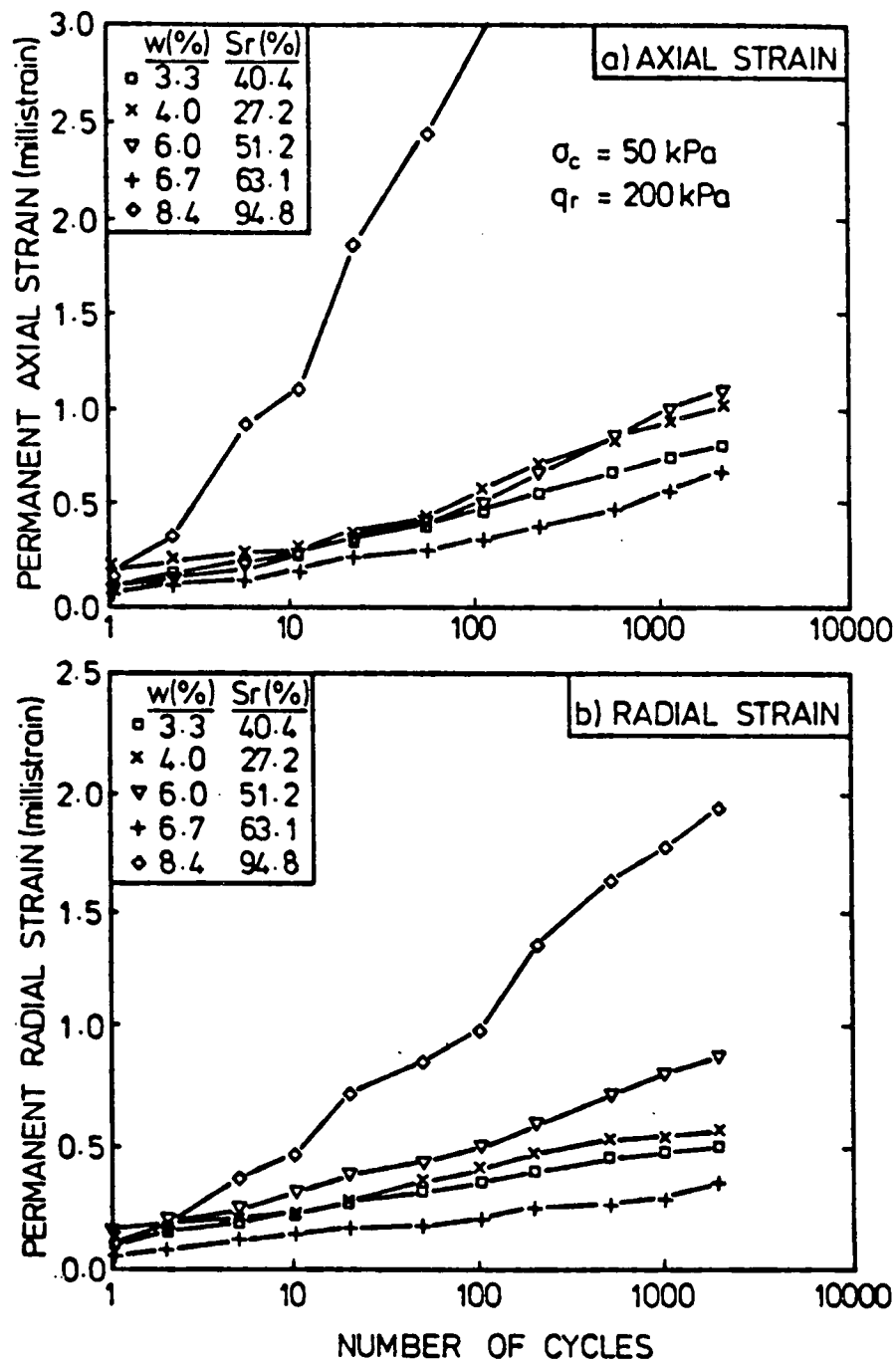
Figure E-6. Permanent Axial and Radial Strain Response of Dolomitic Limestone During Repeated Load Triaxial Test at Various Moisture Contents (w) and Degree of Saturation (Sr).

E-13

moisture content and as the material approaches saturation, very rapid increase in the rate of deformation will occur.

Compaction Tests.   A series of compaction tests were carried out in order to determine the optimum moisture content and maximum dry density of the compacted material. For the sand and gravel, the test was carried out according to the ASTM D-1557 test method (E-13) while for the dolomitic limestone, the British Standard Vibrating Hammer method (E-8) was adopted. The results of the tests for the two materials are shown in Fig. E-7.

Index Tests.   Two plasticity index tests were carried out for the fines (less than 425 micron) of each of the two granular materials. The fines for the sand and gravel were found to be non-plastic, while the PI of the fines for the dolomitic limestone was found to be 3 percent. One flakiness index test BS812 (E-14) was performed on the crushed dolomitic limestone used in the third series of tests. The result of the test indicated an index of 9 percent overall while for individual size fractions, the index varied from 3.8 to 16.1 percent.

Tests on Geosynthetics

Large Direct Shear Box Tests.   Twenty-four large direct shear box tests were performed on the two geosynthetic materials in conjunction with the soil and granular materials. The shear box used for these tests measured 11.8 in. (300 mm) square by 6.7 in. (170 mm) high. In each test, the same material was used in both the upper and lower half of the shear box. Compaction was carried out by using a hand-held vibrating hammer. In general, the moisture content and dry density of the material at the time of the large scale pavement test were simulated. Details of the tests and the results are shown in Table E-3 and Fig. E-8, respectively. For most of the
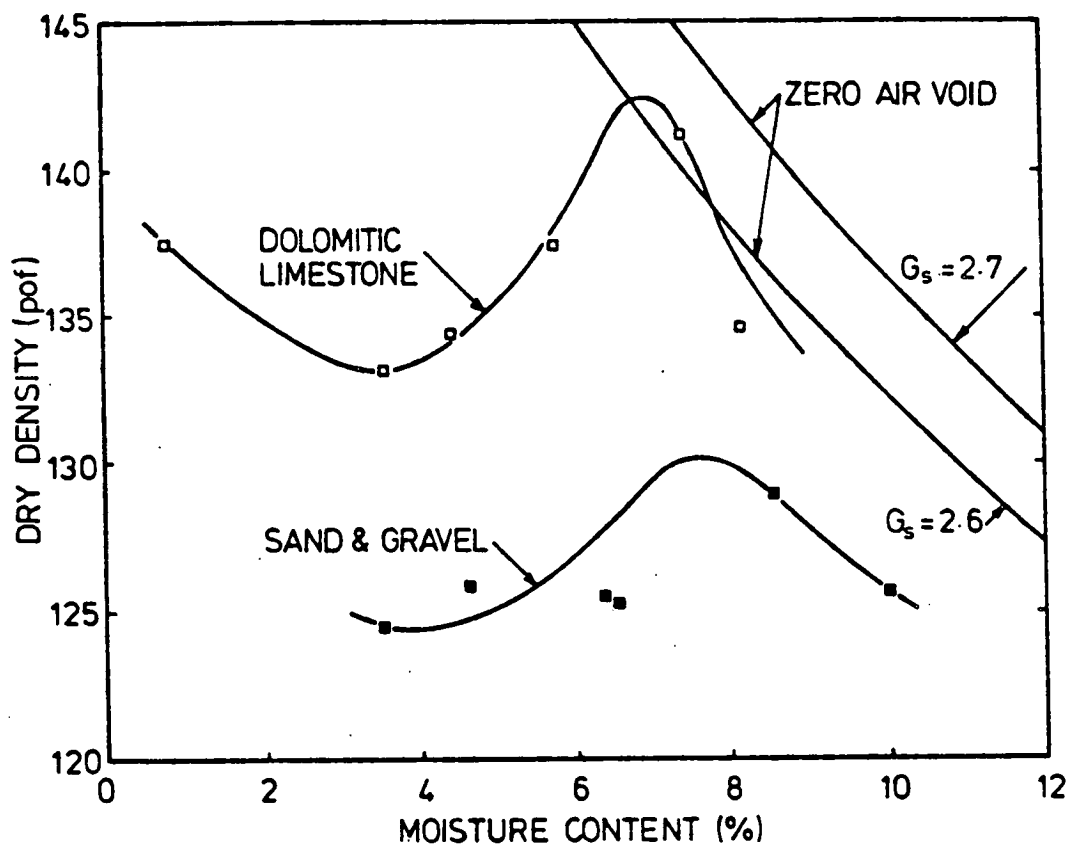
Note: Sand and gravel are compacted according to ASTM D-1557 test method [E-13] while dolomitic limestone uses the British Standard vibrating hammer test method [E-8].

Figure E-7. Results of Standard Compaction Tests for the Granular Materials.

Table E-3. Summary of Large Shear
Box Tests.

Test No	Type of Geosynthetic/Soil	Dry Density (pcf)	Moisture Content (%)	Normal Stress (tsf)	Shear Stress (tsf)	Shear Rate (mm/min)
1	Nicolon/Sand&Gravel	140	3.2	0.55	0.36	.06
2		138	3.8	1.10	0.75	.06
3		138	3.4	2.18	1.46	.06
4	Sand & Gravel	138	3.2	0.54	0.57	.30
5		136	3.4	1.22	1.15	.30
6		136	3.4	2.35	2.14	.30
7	Nicolon/Limestone	138	5.0	0.54	0.46	.06
8		137	4.7	1.06	0.99	.06
9		138	4.9	2.18	1.75	.06
10	Tensar SS1/Limestone	139	5.7	0.55	0.62	.06
11		139	5.6	1.10	1.10	.06
12		141	5.0	2.18	2.00	.06
13	Crushed Limestone	138	5.0	0.65	0.70	.30
14		140	4.9	1.29	1.27	.30
15		138	5.2	2.21	2.30	.30
16	Nicolon/Keuper Marl	107	16.6	0.55	0.38	.06
17		109	16.3	1.12	0.75	.30
18		110	16.6	2.18	1.39	.30
19	Tensar/Keuper Marl	106	16.5	0.55	0.48	.30
20		109	16.2	1.10	0.95	.30
21		111	16.3	2.10	1.48	.30
22	Keuper Marl	105	16.8	0.54	0.47	.30
23		107	16.9	1.07	0.75	.30
24		108	16.4	2.20	1.30	.30
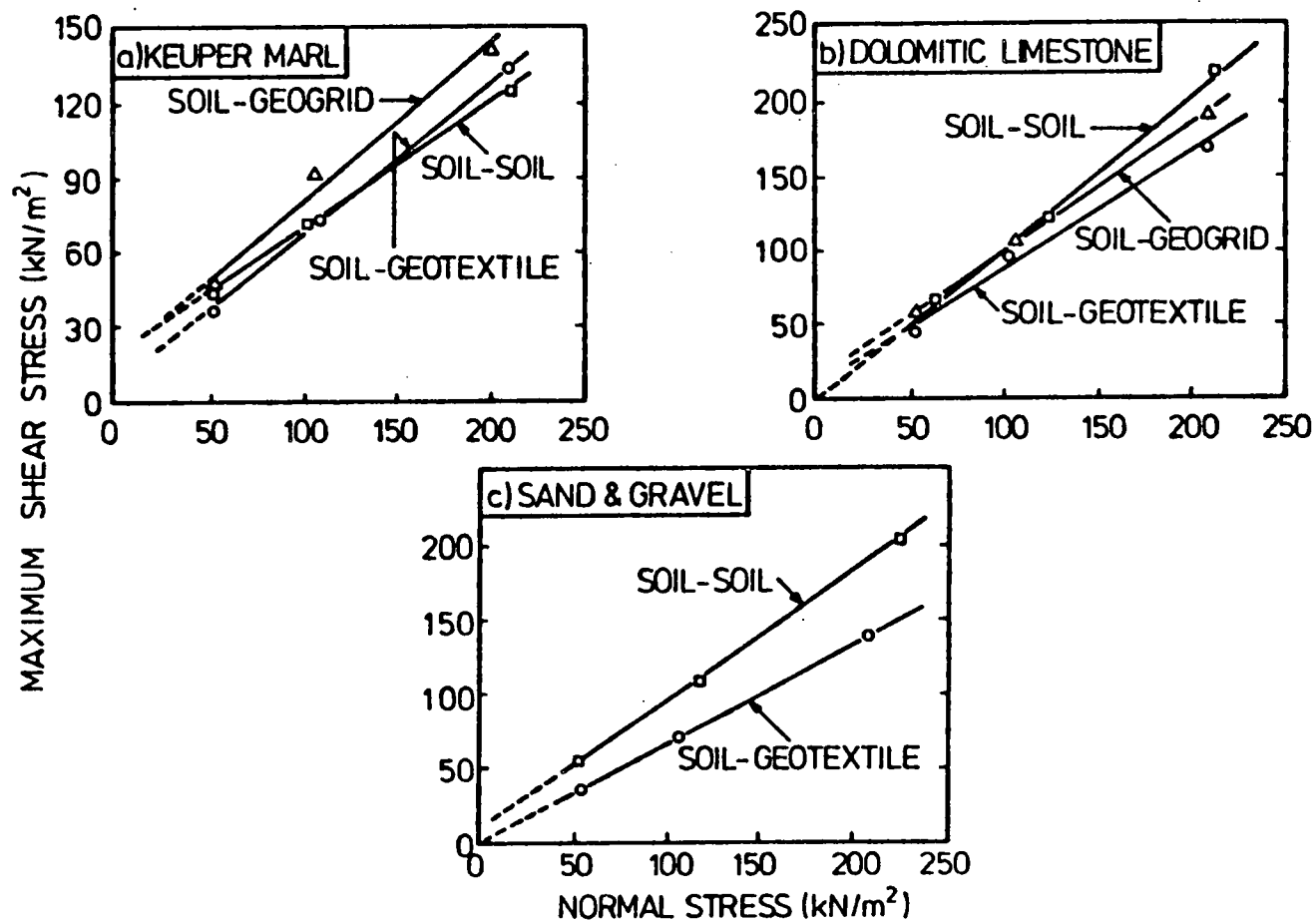
Figure E-8. Relationship Between Normal and Maximum Shear Stress in Large Shear Box Tests.

tests involving granular material, maximum shear stress was obtained at a horizontal displacement of less than 0.4 in. (10 mm). However, for tests with Keuper Marl, a horizontal displacement of up to 1.2 in. (30 mm) was required to achieve maximum shear stress.

Wide Width Tensile Test.   These tests were carried out at the University of Strathclyde where specialist apparatus was available (E-15). All tests were conducted at a standard test temperature of $68^{\circ}F$ ($20^{\circ}C$) and were continued until rupture occurred. A standard shearing rate of 2 percent per minute was used for the geogrid but for the stiff geotextile, because of the requirement of a much higher failure load, the use of a faster rate of 7.5 percent per minute was necessary. The results of the tests for both materials are shown in Fig. E-9.

Creep Test.   Background and details of the test was reported by Murray and McGown (E-16). All creep tests were carried out in isolation with no confining media. For each geosynthetic material, up to five separate tests, each with a different sustained load, were performed. For the geogrid, the maximum sustained load corresponded to 60 percent of the tensile strength of the material. All tests were carried out at $68^{\circ}F$ ($20^{\circ}C$) and, in most cases, lasted for 1000 hours. The results of the two sets of tests during the first 10 hours are shown in Fig. E-10.

Tests on Asphaltic Materials

Marshall Tests.   One series of Marshall tests (ASTM D1559) was carried out for the design of the asphaltic concrete mix. The result of the test is summarized in Fig. E-11. The aggregate used in the design mix had a maximum particle size of 0.5 in. (12 mm) with grading as shown in Fig. E-12. A grade 50 Pen binder was used. For the Hot Rolled Asphalt, a recipe grading

Figure E-9. Variation of Axial Strain with Load in Wide-Width
Tensile Tests.

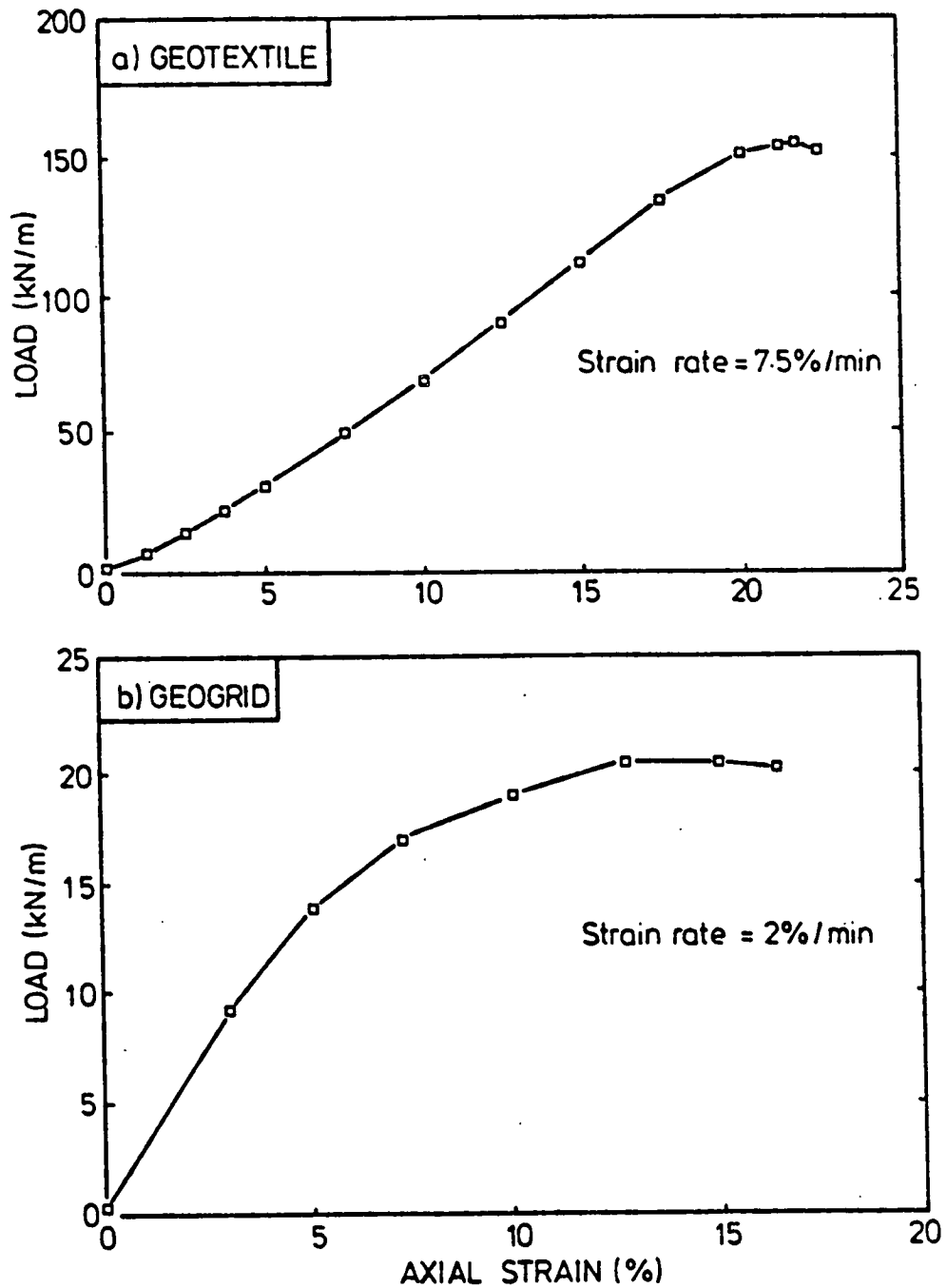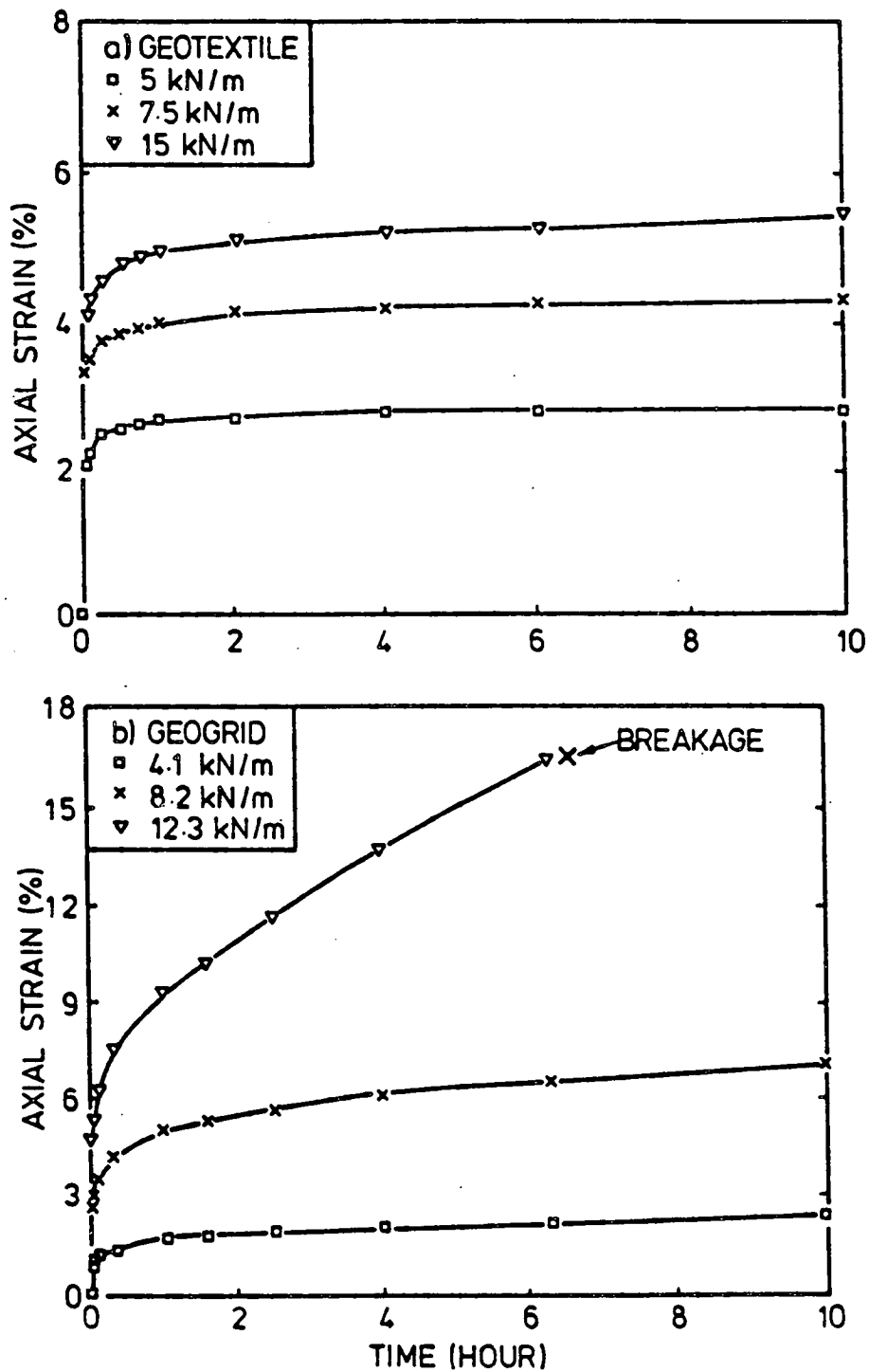Figure E-10. Results of Creep Tests at Various Sustained Loads
for the Geosynthetics During the First 10 Hours.
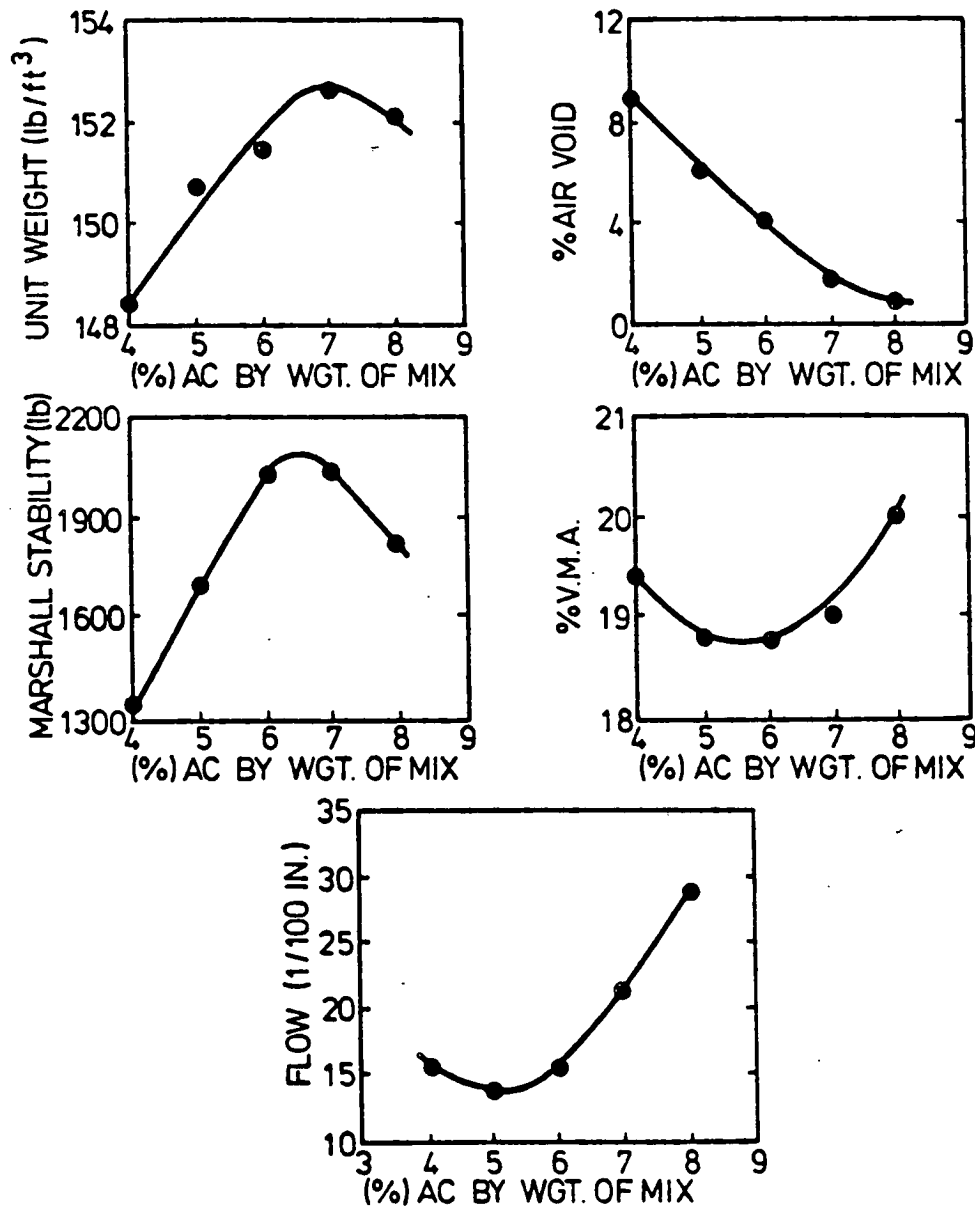
Figure E-11. Summary of Hot-mix Design Data by the Marshall Method.
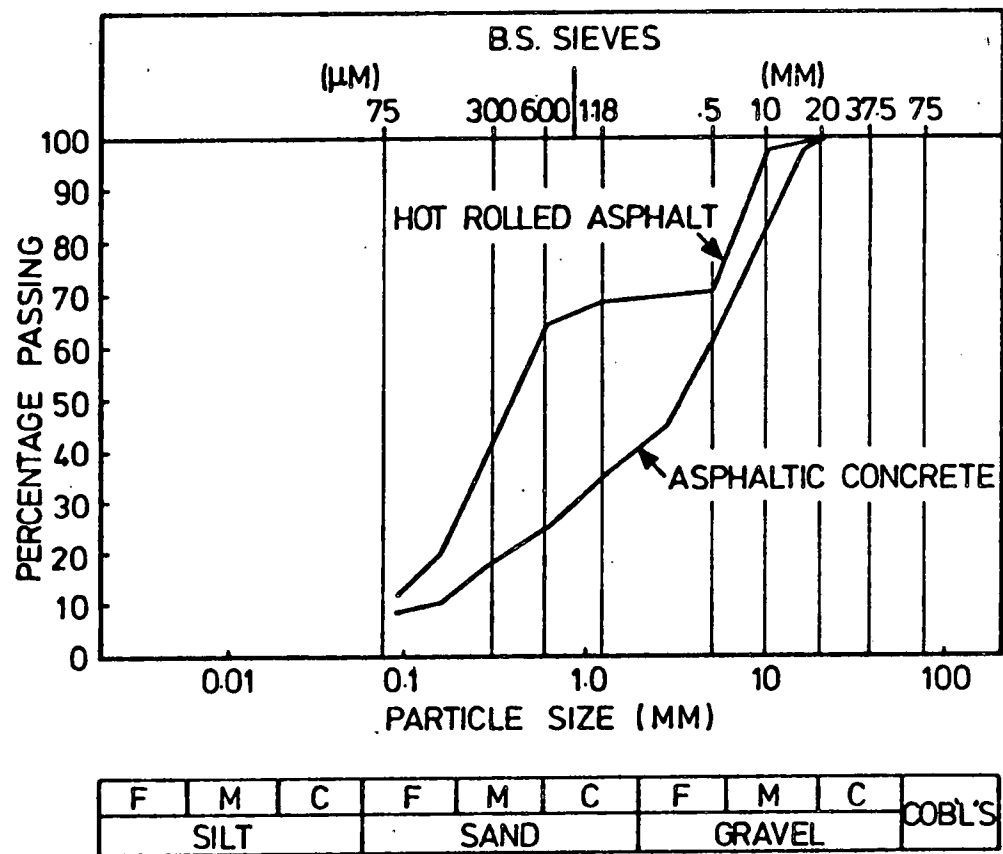
Figure E-12.   Gradation Curves for Aggregates Used in Marshall Tests.

as shown in Fig. E-12 with 8 percent of 100 Pen binder was used. For comparison purposes, six Marshall samples, made out of the HRA used in the first series were tested. The average test results of the six samples are shown in Table E-4. Also shown in the table are the test results obtained from an asphaltic concrete sample with a binder content of 6.5 percent, a specification which was used for the last three series of tests.

Viscosity Test. Two viscosity tests were carried out by the Georgia Department of Transportation on the 50 Pen binder used for the asphaltic concrete mix. The viscosity at $140^\circ F$ ($60^\circ C$) was found to be about 4600 poises.

APPENDIX E

REFERENCES

E-1 Hyde, A.F.L., "Repeated Load Testing of Soils", PhD Thesis, University of Nottingham, 1982.

E-2 Overy, R.F., "The Behavior of Anisotropically Consolidated Silty Clay Under Cyclic Loading", PhD Thesis, University of Nottingham, 1982.

E-3 Bell, C.A., "The Prediction of Permanent Deformation in Flexible Pavements", PhD Thesis, University of Nottingham, 1987.

E-4 Loach, S.C., "Repeated Loading of Fine Grained Soils for Pavement Design", PhD Thesis, University of Nottingham, 1987.

E-5 Croney, D., "The Design and Performance of Road Pavements", HMSO, 1977.

E-6 Finn, F.N., Nair, K., and Monismith, C.L., "Application of Theory in the Design of Asphalt Pavements", Proc. of 3rd Int. Conf. on the Structural Design of Asphalt Pavements, Vol. 1, London, 1972.

E-7 Brown, S.F., Lashine, A.K.F., and Hyde, A.F.L., "Repeated Load Triaxial Testing of a Silty Clay", The Journal of Geotechniques, Vol. 25, London, 1972.

E-8 British Standards Institution, "Methods of Testing Soils for Civil Engineering Purposes", BS1377, 1975.

Table E-4. Comparison of Marshall test data for two asphaltic mixes.

	Hot Roller Asphalt	Asphaltic Concrete
Binder Content (% by weight)	8	6.5
Mix Density (pcf)	144	152
Air Void (%)	6	2.5
VMA (%)	23.6	19
Corrected Stability (lb)	2028	2150
Flow (1/100 in.)	16.5	18

E-9   Dumbleton, M.J., and West, G., "Soil Suction by the Rapid Method on Apparatus with Extended Range", The Journal of Soil Science, Vol. 19, No. 1, 1975.

E-10   Pappin, J.W., "Characteristics of a Granular Material for Pavements Analysis", PhD Thesis, University of Nottingham, 1979.

E-11   Thom, N.H., and Brown, S.F., "Design of Road Foundations", Interim Report to SCRC, University of Nottingham, 1985.

E-12   Boyce, J.R., "The Behavior of a Granular Material Under Repeated Loading", PhD Thesis, University of Nottingham, 1976.

E-13   ASTM Standard, Vol. 04.08, "Soil and Rock; Building Stones; Geotextiles", Standard D-1557, 1987.

E-14   British Standards Institution, "Methods for Determining the Flakiness Index of Coarse Aggregate", BS 812, Sections 105.1, 1985.

E-15   Yeo, K.L., "The Behavior of Polymeric Grid Used for Soil Reinforcement", PhD Thesis, University of Strathclyde, 1985.

E-16   Murray, R.T., and McGown, A., "Geotextile Test Procedures Background and Sustained Load Testing", TRRL Application Guide 5, 1987.

APPENDIX F

SEPARATION AND FILTRATION

APPENDIX F

SEPARATION AND FILTRATION

INTRODUCTION

In recent years, considerable interest has been shown in using open-graded aggregate layers as bases, subbases and drainage layers in pavements. A well-designed drainage system has the potential for increasing the life of a flexible pavement by a factor of forty or more [F-1]. If, however, an open graded layer (and, in many cases even a more densely graded layer) is placed directly on the subgrade, silt and clay may with time contaminate the lower portion of the drainage layer.

The intrusion of fines into an aggregate base or subbase results in (1) Loss of stiffness, (2) Loss of shear strength, (3) Increased susceptibility to frost action and rutting, and (4) Reduction in permeability. Figure F-1 shows that an increase in fines of up to 6 percent can have a minor effect upon the resilient modulus [F-2]. Other work, however, indicates contamination of a portion of an aggregate layer with 2 to 6 percent clay can cause reductions in shear strength on the order of 20 to 40 percent [F-3]. In either case, when the level of contamination becomes sufficiently great, the effective thickness and strength of the aggregate layer is reduced.

Contamination due to the intrusion of fines into the base or subbase can be caused by the following two mechanisms:

1. <u>Separation</u> - A poor physical separation of the base/subbase and subgrade can result in mechanical mixing at the boundary when subjected to load.

2. <u>Filtration</u> - A slurry of water and fines (primarily silt, clay and fine sand size particles) may form at the

F-2
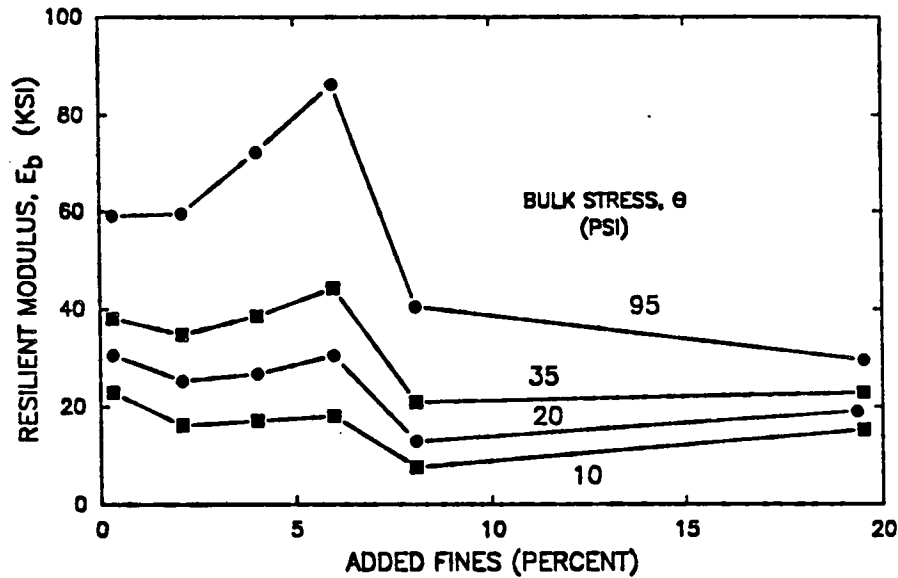
Figure F-1. Influence of Added Fines on Resilient Modulus of Base (After Jorenby, Ref. F-2).
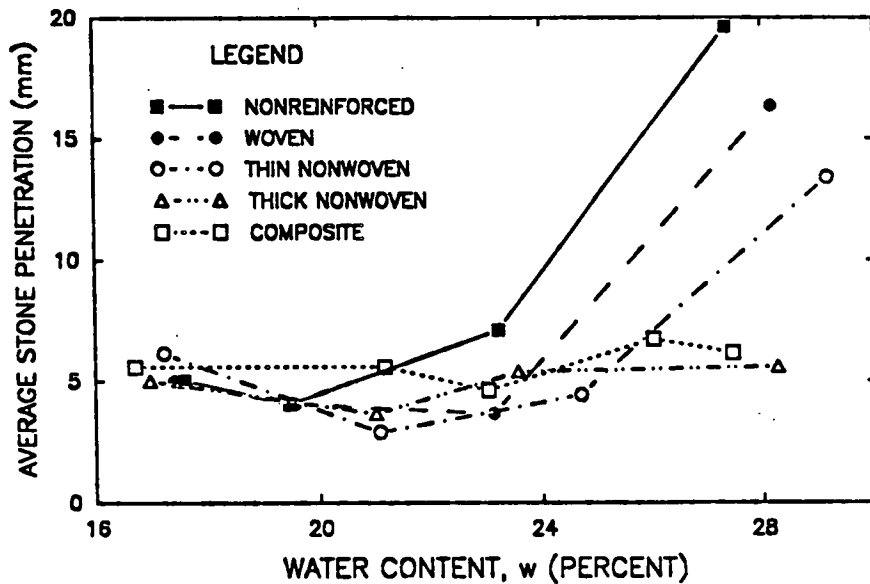
Figure F-2. Influence of Subgrade Water Content and Geosynthetic on Stone Penetration (After Glynn & Cochrane, Ref. F-31).

top of the subgrade when water is present and under

pressure due to repeated traffic loading. If the

filtration capacity of the layer above the subgrade is

not sufficiently great, the slurry will move upward

under pressure into the aggregate layer and result in

contamination.

Comprehensive state-of-the-art summaries of the separation and

filtration problem have been given by Dawson and Brown [F-4], Jorenby [F-2]

and more recently by Dawson [F-5].

FILTER CRITERIA FOR PAVEMENTS

To perform properly for an extended period, the filtration/

separation aggregate filter or geotextile must: (1) Maintain a distinct

separation boundary between the subgrade and overlying base or subbase, (2)

Limit the amount of fines passing through the separator so as not to

significantly change the physical properties of the overlying layer, (3)

Must not become sufficiently clogged with fines so as to result in a

permeability less than that of the underlying subgrade, and (4) Because of

the relatively harsh environment which can exist beneath a pavement, the

geotextile must be sufficiently strong, ductile and abrasion resistant to

survive construction and in service loading. In harsh environments some

clogging and loss of fines through the geosynthetic will occur.

Unfortunately, the classical Terzaghi filter criteria used for steady

state filter design are not applicable for severe levels of pulsating

loading, such as occur beneath pavements where the flow may be turbulent and

also reversing. For these conditions, a filter cake probably does not

develop in the soil adjacent to the filter [F-6 through F-8]. Formal filter

criteria, however, have not yet been developed for aggregate or geotextile filters placed at the interface between the base and subgrade of a pavement.

The classical Terzaghi criteria were developed for uniform, cohesionless soils in contact with an aggregate filter. These criteria, which assumes steady state flow conditions, are summarized in Part III of Table F-1, which was taken from Christopher and Holtz [F-9]. Christopher and Holtz give a good general discussion of the engineering utilization of geotextiles, including filter criteria and infiltration. The geotextile selection criteria given by Christopher and Holtz is also summarized in Table F-1 for both steady state and cyclic flow conditions.

SEPARATION

Maintaining a clean separation between the subgrade and overlying aggregate layer is the first level of protection that can be provided to the base. Most serious separation problems have developed when relatively open-graded aggregates have been placed on very soft to soft subgrades [F-3,F-10,F-11].

Separation Failure Mechanisms

Contamination of the base occurs as a result of the aggregate being mechanically pushed into the subgrade, with the subgrade squeezing upward into the pores of an open-graded stone as it penetrates downward. A separation type failure can occur either during construction or later after the pavement has been placed in service. This type problem is described in the report as a separation failure. Contamination due to washing of fines into the base from seepage is referred to as filtration.

The total thickness of this contaminated zone as a result of separation problems (as opposed to filtraton) is typically up to about 2 times the

Table F-1

Design Criteria for Geosynthetic and Aggregate Filters
(Adapted Christopher and Holtz, Ref. F-9)

I. GEOSYNTHETIC FILTERS
   I. SOIL RETENTION (PIPING RESISTANCE CRITERIA)[1]

Soils	Steady State Flow	Dynamic, Pulsating, and Cyclic Flow
≤50% Passing[2] U.S. No. 200 sieve	AOS -- $O_{95} \leq B\ D_{85}$	$O_{95} \leq D_{15}$ (If soil can move beneath fabric) or
	$C_u \leq 2$ or ≥ 8 B=1	$O_{50} \leq 0.5\ D_{85}$
	$2 \leq C_u \leq 4$ B=0.5 C_u	
	$4 \leq C_u \leq 8$ B=8/C_u	
≥50% Passing U.S. No. 200 Sieve	Woven: $O_{95} \leq D_{85}$ Nonwoven: $O_{95} \leq 1.8\ D_{85}$ AOS No. (fabric) ≥ No. 50 sieve	$O_{50} \leq 0.5\ D_{85}$

1. When the protected soil contains particles from 1 inch size to those passing the U.S. No. 200 sieve, use only the gradation of soil passing the U.S. No. 4 sieve in selecting the fabric.
2. Select fabric on the basis of largest opening value required (smallest AOS)

II. PERMEABILITY CRITERIA[(1)]
  A. Critical/Severe Applications: k (fabric) ≥ 10 k (soil)
  B. Less Critical/Less Severe and (with Clean Medium to Coarse Sands and Gravels): k (fabric) ≥ k (soil)
    1. Permeability should be based on the actual fabric open area available for flow. For example, if 50% of fabric area to be covered by flat concrete blocks, the effective flow area is reduced by 50%.

III. CLOGGING CRITERIA
  A. Critical/Severe Applications[1]
    Select fabric meeting I, II, IIIB, and perform soil/fabric filtration tests before specification, prequalifying the fabric, or after selection before bid closing. Alternative: use approved list specification for filtration applications. Suggested performance test method: Gradient Ratio ≤ 3
  B. Less Critical/Non-Severe Applicatons
    1. Whenever possible, fabric with maximum opening size possible (lowest AOS No.) from retention criteria should be specified.
    2. Effective Open Area Qualifiers[2]:
    Woven fabrics: Percent Open Area: ≥ 4%
    Nonwoven fabrics: Porosity[3] ≥ 30%
    3. Additional Qualifier (Optional): $O_{95} \geq 3D_{15}$
    4. Additional Qualifier (Optional): $O_{15} \geq 3D_{15}$
  Note: 1. Filtration tests are performance tests and cannot be performed by the manufacturer as they depend on specific soil and design conditions. Tests to be performed by specifying agency or his representative. Note: experience required to obtain reproducible results in gradient ratio test.
    2. Qualifiers in potential clogging condition situations (e.g. gap-graded soils and silty type soils) where filtration is of concern.
    3. Porosity requirement based on graded granular filter porosity

II. AGGREGATE FILTERS - TERZAGHI CRITERIA FOR STEADY FLOW
Piping Requirement:	D_{15} (filter) $\leq 5\ D_{85}$ (soil)
Permeability Requirement:	D_{15} (filter) $\geq 5\ D_{15}$ (soil)
Uniformity Requirement:	D_{50} (filter) $\leq 25\ D_{50}$ (soil)
Well screens/slotted pipe criteria:	D_{85} (filter) $\geq$ (1.2 to 1.4) x slot width
	D_{85} (filter) $\geq$ (1.0 to 1.2) x hole diameter

where: D_{15}, D_{50}, and D_{85} = the diameter of soil particles, D of which 15%, 50%, and 85%, respectively, of the soil particles are, by dry weight, finer than that grain size.

diameter of the aggregate which overlies the subgrade [F-3,F-12,F-13].
Under unfavorable conditions such as a heavy loading and a very weak
subgrade, the depth of contamination could be even more. Bell, et al. [F-3]
found for a very large, 4.5 in. (110 mm) diameter aggregate, the stone
penetration to be about equal to the radius of the aggregate. A similar
amount of squeezing of the subgrade was also observed, giving a total
contamination depth of approximately one aggregate particle diameter.

The subgrade strength, and as a result the subgrade moisture content,
are both important factors affecting stone penetration. As the moisture
content of the subgrade increases above the optimum value, the tendency for
aggregate to penetrate into it greatly increases as illustrated in Figure F-
2.

Construction Stresses

The critical time for mixing of the subgrade with the aggregate layer
is when the vertical stress applied to the subgrade is greatest. The
largest vertical subgrade stresses usually occurs during construction of the
first lift of aggregate base. It might also occur later as construction
traffic passes over the base before the surfacing has been placed.

The common practice is to compact an aggregate layer with a moderate to
heavy, smooth wheel vibratory roller. Even a reasonably light roller
applies relatively large stresses to the top of the subgrade when an initial
construction lift is used of even moderate thickness.

Smooth drum vibratory rollers develop dynamic vertical forces varying
from 4 tons (or less) for a small, light roller to as much as 15 to 20 tons
for very large rollers. Figure F-3 summarizes the vertical stress caused at
the subgrade interface by a typical 4, 8 and 17.5 ton, smooth drum vibratory
roller for initial lift thicknesses up to 18 in. (460 mm). Linear elastic
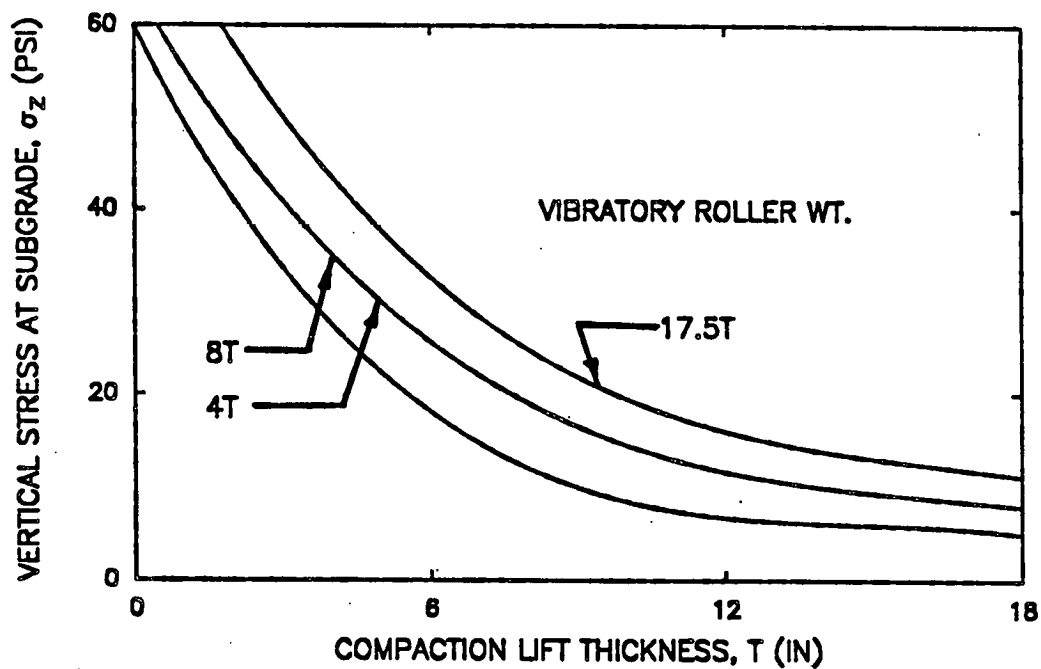
Figure F-3. Variation of Vertical Stress on Subgrade with Initial
Compaction Lift Thickness and Roller Force.
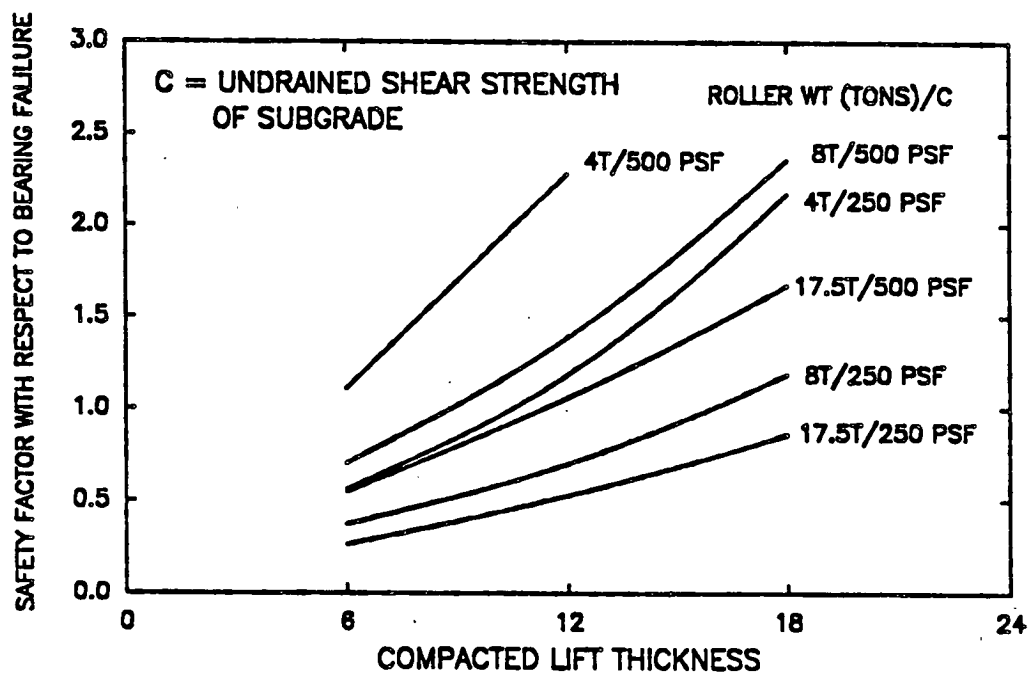
Figure F-4. Bearing Capacity Failure Safety Factor of Subgrade During
Construction of First Lift.

layered theory was used in developing these relationships. Because of the presence of the soft subgrade, the modulus of elasticity of the first 6 in. (150 mm) thickness of the initial lift was assumed to be 1.5 times the modulus of elasticity of the subgrade. Each successive 6 in.(150 mm) thickness within the lift was assigned an elastic modulus equal to 1.5 times that of the material underlying it.

Bearing Capacity Analysis

For a separation problem to develop, the externally applied stress level must be near the ultimate bearing capacity of the subgrade. The ultimate bearing capacity of a cohesive subgrade can be expressed as [F-14]:

$$q_{ult} = 5.2c \tag{F-1}$$

where: q_{ult} = ultimate bearing capacity of the subgrade
c = undrained shear strength of a cohesive subgrade

The above equation is for plane strain conditions such as would exist beneath a long vibratory roller. When the load is applied over a circular area, which is approximately the case for a wheel loading, the ultimate bearing capacity is about 20 percent greater than given by equation (F-1).

The vertical stress at the subgrade interface predicted by conventional layered theory requires continuous contact on a horizontal plane between the two layers. Large pore openings are, however, present in coarse, open-graded granular materials. As a result, the actual average vertical stress developed on large stone particles at the subgrade interface is greater than the average stress predicted by conventional stress distribution theories. Hence, a local bearing failure occurs below the tips of the aggregate, and the soil squeezes upward between the aggregate into the open pores.

The actual average vertical stress $\sigma_z{}^*$ for an open-graded base is approximately equal to:

$$\sigma_z{}^* = \sigma_z/(1-n) \tag{F-2}$$

where: $\sigma_z{}^*$ = actual average stress developed on the stone particles

σ_n = theoretically calculated vertical stress

n = porosity of the granular layer

The problem is further complicated by the fact that the aggregate particles are both three-dimensional and irregular in shape. Therefore, until penetration of the aggregate particles into the subgrade occurs, contact stresses between the aggregate and subgrade will be even higher than the average stress given by Equation (F-2).

For conditions of a wet, weak soil, the irregular-shaped aggregates will be readily pushed into the subgrade, usually during the construction phase. When stone penetration equals about the effective radius of the stone, the average contract stress between the stone and soil becomes close to that given by equation (F-2). The bearing capacity is probably somewhat greater than obtained from applying equation (F-1) which does not consider the resistance to flow of soil through the pores of the stone.

Several additional factors further complicate the aggregate penetration problem. Under dynamic loading, the strength of a cohesive subgrade is greater than under slow loading. However, several passes of the roller may result in reduction in strength due to the build-up of pore pressures in the subgrade. The possibility exists that the pores in the lower, tensile portion of the aggregate layer open slightly as the external load moves over [F-5]. Because of the overall complexity of the problem, a rigorous theoretical prediction of soil intrusion is quite difficult. Therefore, until more research is performed in this area, a simplified approach can be

taken using equation (F-1) for performing a general assessment of the severity of the aggregate penetration problem.

Construction Lift Thickness

For an initial lift thickness of 6 in. (150 mm), the average vertical stress at the top of the subgrade varies from about 16 to 32 psi (110-220 kN/m^2) as the dynamic vibratory roller force increases from 4 to 17.5 tons (Figure F-3). These stress levels are sufficient, based on equation (F-1), to cause a general bearing capacity failure of a very soft to soft subgrade having undrained shear strength less than about 400 to 800 psf (19-38 kN/m^2), respectively. Aggregate penetration and excessive permanent deformations during construction can occur at even lower stress levels.

Where very soft subgrades are present, frequently the first lift to be constructed is placed at a greater thickness than used for succeeding lifts because of subgrade instability problems caused by the construction equipment. A lift thickness of 12 in. (300 mm) is probably reasonably typical. For this lift thickness, the average vertical subgrade stress varies from about 8 to 16 psi (55-110 kN/m^2) as the dynamic roller force increases from 4 to 17.5 tons. For these conditions a general bearing capacity failure, as predicted by equation (F-1), could occur for undrained shear strengths less than about 200 to 400 psf (10-20 kN/m^2).

Permanent Deformation

Under repeated loading at a stress level below failure, as predicted by equation (F-1), the permanent deformations in the subgrade increases with each load repetition. These permanent deformations are due to accumulation of permanent strains at stress levels below failure but above the permanent strain yield stress of the material.

Equation (F-1) predicts the required load to cause a general bearing failure under the application of a single load. Jurgenson [F-21] has shown, however, that the soil beneath the load first starts to fail locally at an applied loading of 3.14c. Yielding of the soil occurs at even lower stresses and is greatly influenced by the initial stress state in the soil (i.e., the over-consolidation ratio). Bender and Barenberg [F-33] found for non-reinforced aggregate bases if $\sigma_z/c \geq 3.3$, large permanent strains rapidly develop under the application of repeated loadings. By using a light fabric, the threshold stress (σ_z/c) was found by Bender and Barenberg to increase above this level.

These results indicate that a suitable safety factor must be used with equation (F-1) to avoid accumulation of excessive permanent deformations. The safety factor during construction should be a minimum of 1.5 to 2 for a relatively few number of loadings and an unreinforced aggregate layer. With reinforcement the safety can decrease somewhat. After construction the stress on the subgrade would, in general, be much smaller and conventional pavement design theory can be used to avoid problems with permanent deformations.

Separation Case Histories

Mixing of the subgrade with an aggregate base has been reported at several sites where geosynthetics have not been used. At one site well-graded aggregate with about a 1.25 to 1.5 in.(30-38 mm) top size and 5 percent fines was observed during construction to intrude up to a depth of about 1 to 2 in. (25-50 mm) into a soft subgrade [F-12,F-13]. For the conditions existing at the site, the calculated safety factor for a general bearing capacity type failure varied from about 0.8 to 1.4.

At two sites where intrusion occurred, the ratio D_{15}/d_{85} varied from 17 to 20. For comparison, the Terzaghi filter criteria for steady seepage requires $D_{15}/d_{85} \leq 5$. Hence, conventional static filter criteria was significantly exceeded at these two sites. Under severe conditions of loading, intrusion may also occur even if conventional Terzaghi filter criteria are satisfied [F-16,F-17].

Separation Design Recommendations

The following tentative design criteria are proposed to minimize problems with separation between an aggregate layer and the underlying subgrade and to avoid excessive permanent deformation during construction. Most problems involving separation will occur where soft to very soft cohesive subgrades are encountered typically having undrained shear strengths less than about 500 psf (24 kN/m^2). Problems such as excessive permanent subgrade deformations during construction or aggregate penetration would also occur on firm subgrades under more severe loading conditions.

1. If the safety factor with respect to a general bearing capacity failure is greater than 2.0, no special precaution is needed with respect to separation or excessive permanent deformations during construction. For very open-graded granular bases or subbases, a limited amount of punching of the aggregate into the subgrade will occur for a safety factor of 2. The depth of punching should approach the radius of the maximum aggregate size.

2. For a bearing capacity safety factor between about 1.4 and 2.0, either conventional Terzaghi filter criteria should be satisfied or a geotextile should be used as a

separator. This criteria should also avoid permanent deformation problems from compacting the first lift. If a small to modest amount of construction traffic is to use the initial construction lift, then a safety factor of at least 2.0 to 2.5 should be provided to avoid excessive deformations. Specific recommendations concerning the selection of a geotextile are given in a later section.

3. If the safety factor is less than about 1.4, use of a geotextile is recommended regardless of whether filter criteria are satisfied. Consideration should also be given to satisfying filter criteria, particularly if a very open-graded stone is to be used for drainage applications. If the granular filter material satisfies filter criteria, the geotextile will serve primarily as a construction aid. Construction traffic should not be permitted for this condition.

The above recommendations are given to avoid contamination of the granular layer due to intrusion and subsequent mixing and also prevent excessive permanent deformations from construction traffic on the unsurfaced aggregate layer. Drainage applications where filtration is important are discussed in the next section.

Figure F-4 gives the bearing capacity safety factor as a function of construction lift thickness for selected vibratory rollers and undrained subgrade shear strengths. This figure shows for a moderate vibratory roller weight of 8 tons and lift thicknesses of 12 in. (300 mm), separation could become a problem for subgrades having undrained shear strengths less than

about 500 psf (24 kN/m^2). This subgrade strength corresponds to a standard penetration resistance (SPT-value) of approximately 4 blows/ft.(13 b/m). Heavy construction traffic on this thickness would, for the existing soil conditions, be even more critical and in general unacceptable.

A very substantial increase in shear strength of a soft to very soft subgrade will, in most cases, occur reasonably rapidly after placement of the pavement structure [F-18]. This increase in strength should be considered in estimating the bearing capacity safety factor for long-term traffic loading conditions. The initial undrained shear strength of the subgrade can be estimated from vane shear tests, undrained triaxial shear tests, or from the results of cone penetrometer tests. For preliminary design purposes, Table F-2 can be used when reliable estimates of the shear strength based on testing are not available.

Selection of an actual geosynthetic or aggregate filter to use as a separator is considered later in the section on Filter Selection.

FILTRATION

Some general requirements for intrusion of a slurry of subgrade fines into an open-graded aggregate layer can be summarized from the early work of Chamberlin and Yoder [F-19]:

1.   A saturated subgrade having a source of water.

2.   A base more permeable than the subgrade with large
     enough pores to allow movement of fines.

3.   An erodable subgrade material. Early laboratory work by
     Havers and Yoder [F-20] indicate a moderate plasticity
     clay to be more susceptible to erosion than a high
     plasticity clay. Silts, fine sands and high plasticity

F-15

Table F-2

Preliminary Subgrade Strength Estimation

Subgrade Description	Field Condition	Standard Penetration Resistance,N (blows/ft.)	Approximate Undrained Shear Strength,C (psf)
Very Soft	Squeezes between fingers	0-1	0-250
Soft	Easily molded by fingers	2-4	250-500
Firm	Molded by strong pressure of fingers	5-8	500-1000
Stiff	Dented by strong pressure of fingers	9-15	1000-1500
Very Stiff	Dented slightly by finger pressure	15-30	1500-2000
Hard	Dented slightly by pencil point	>30	>2000

Table F-3

Vertical Stress on Top of Subgrade for Selected Pavement Sections

Section	A.C. Surface (in.)	Granular Base (in.)	Vertical Subgrade Stress (psi)
Very Light	1.5	6	21
Light	3.5	8	10
Medium	6	8	6
Heavy	8	14	3

Notes: 1. Dual wheel loading of 4.5 kips/wheel at 100 psi tire pressure.

2. Moduli/Poisson's Ratio: AC - 200,000 psi/$\nu = 0.2$; Granular Base - 10,000 psi/$\nu = 0.35$; Subgrade - 4000 psi/$\nu = 0.4$.

3. Analysis - Linear elastic; linear elastic vertical subgrade stress increased by 12 percent to give good agreement with measured test section subgrade stress.

clays that undergo deflocculation are also very

susceptible to erosion.

4. The applied stress level must be large enough to cause a pore pressure build-up resulting in the upward movement of the soil slurry.

Although the work of Chamberlin and Yoder [F-19] was primarily for concrete pavements, similar mechanisms associated with the formation and movement of slurry also occurs for flexible pavements.

Filtration Mechanisms

Repeated wheel load applications cause relatively large stresses to be developed at the points of contact between the aggregate and the subgrade. As loading continues, the moisture content in the vicinity of the projecting aggregate points, for at least some soils, increases from about the plastic limit to the liquid limit [F-7]. The moisture content does not, however, significantly increase in the open space between aggregates (Figure F-5). As a result the shear strength of the subgrade in the vicinity of the point contacts becomes quite small. Hoare [F-7] postulates the increase in moisture content may be due to local shearing and the development of soil suction. When a geotextile is used, soil suction appears to be caused under low stress levels by small gaps which open up upon loading [F-25]. The gaps apparently develop because the geotextile rebounds from the load more rapidly than the underlying soil. Remolding may also play a role in the loss of subgrade strength.

Due to the application of wheel loadings, relatively large pore pressures may build up in the vicinity of the base-subgrade interface [F-22,F-23,F-24]. As a result, in the unloaded state the effective stress between particles of subgrade soil become negligible because of the high
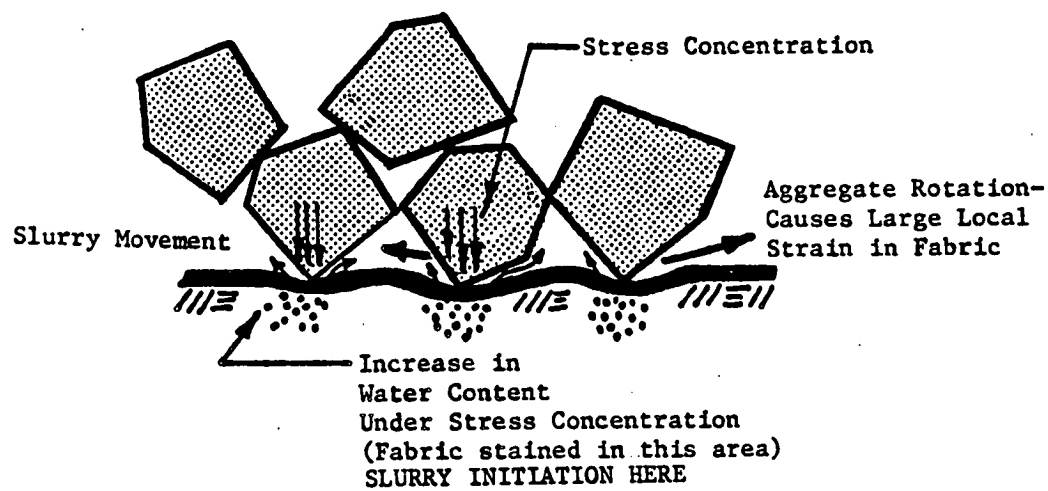
F-17

Figure F-5. Mechanisms of Slurry Formation and Strain in Geosynthetic.

residual pore water pressures. These pore pressures in the subgrade result in the flow of water upward into the more permeable aggregate layer. The subgrade, in its weakened condition, is eroded by the scouring action of the water which forms a slurry of silt, clay and even very fine sand particles. The slurry of fines probably initiates in the vicinity where the aggregate tips press against the soil [F-3]. This location of slurry initiation is indicated by staining of geotextiles in the immediate vicinity of where the aggregates contact the fabric.

The upward distance which fines are carried depends upon (1) the magnitude of induced pore pressure which acts as the driving force, (2) the viscosity of the slurry, and (3) the resistance encountered to flow due to both the size and arrangement of pores. Fine particles settle out in the filter or the aggregate layer as the velocity of flow decreases either locally because of obstructions, or as the average flow velocity becomes less as the length of flow increases. Some additional movement of material within, or even out of, the base may occur as the moisture and loading conditions change with time [F-19].

Geotextile Filters

Geotextile filters have different inherent structural characteristics compared to aggregate filters. Also, a considerable difference can exist between geotextiles falling within the same broad classification of woven or nonwoven materials due to different fiber characteristics. Nonwoven geotextiles have a relatively open structure with the diameter of the pore channels generally being much larger than the diameter of the fibers. In contrast, aggregate filters have grain diameters which are greater than the diameter of the pores [F-8]. Also, the porosity of a nonwoven geotextile is larger than for an aggregate filter.

F-19

Electron microscope pictures showing the internal structure of several non-woven geosynthetics are given in Figure F-6. None of these geosynthetics were considered to fail due to clogging during 10 years of use in edge drains [F-26]. The approximate order of ranking with respect to clogging from best to worst is from (a) to (d) for similar geotextiles. The following review of factors influencing geotextile filtration performance are primarily taken from work involving cyclic type loading.

Thickness. The challenging part of modifying granular filter criteria for use with fabrics is relating soil retention characteristics on a geotextile with those of a true three-dimensional granular filter. Heerten and Whittmann [F-8] recommend classifying geotextiles as follows:

1. Thin: thickness t<2 mm and geotextile weights up to 9 oz./yd^2 (300 g/m^2).

2. Thick: single layer, needle punched: thickness t>2 mm and geotextile weights up to 18 oz./yd^2 (600 g/m^2).

3. Thick multi-layer, needle punched geotextiles.

Earlier work by Schober and Teindl [F-6] found wovens and non-wovens less than 1 mm in thickness to perform different than non-wovens greater than 2 mm, which gives support to the above classifcation scheme.

As the thickness of a nonwoven, needle punched geotextile increases, the effective opening size decreases up to a limiting thickness which is also true for an aggregate filter [F-8]. Thick needle punched geotextiles have been found to provide a three-dimensional structure that can approach that of an aggregate filter; thin geotextiles do not. Also, soil grains which enter the geotextile pores reduce the amount of compression which occurs in a nonwoven, needle punched geotextile subjected to loading.
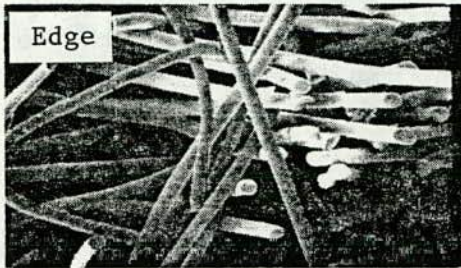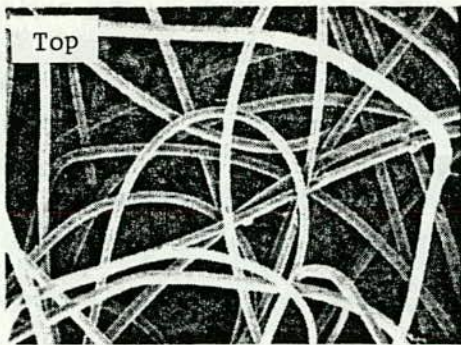
(a) Nonwoven, Needle 4.5 oz/yd^2, 75 mil.
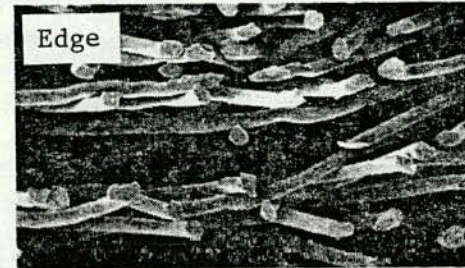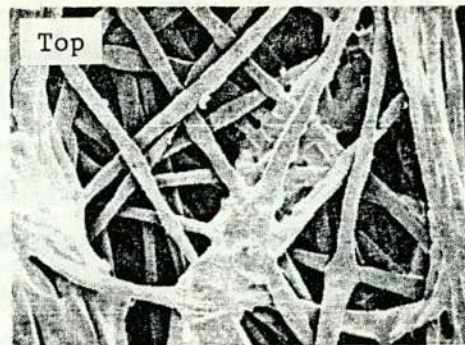
(b) Nonwoven, Needle 5.3 oz/yd^2, Heat Bonded, 60 mil.
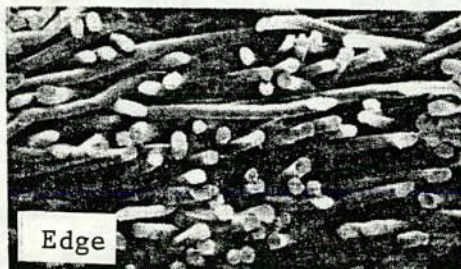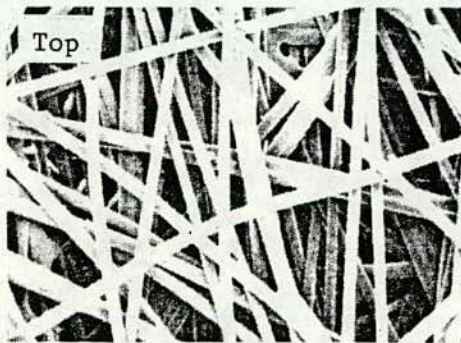
(c) Nonwoven 4.5 oz/yd^2, 30 mil.
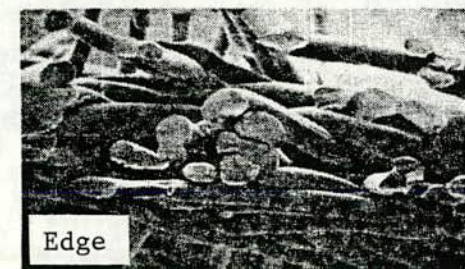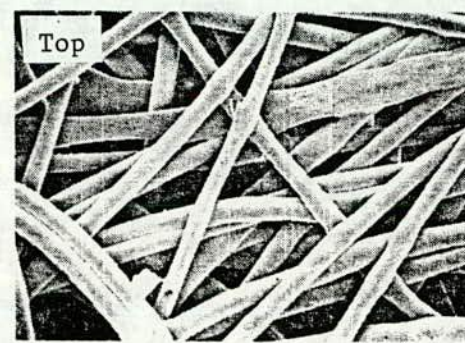
(d) Spun-Bonded, 15 mil.

Figure F-6.   Electron Microscope Pictures of Selected Geotextiles: Plan and Edge Views (84x).

As the thickness of the geotextile increases, the effective opening size decreases and fines in suspension have a harder time passing through because of the three-dimensional structure [F-7,F-25,F-27]. The fines which do pass through the geotextile may be deposited on the upstream side of the fabric in a thin layer that can significantly reduce effective permeability. A layer of fines forming a cake on the downstream side of the geotextile has also been observed. When open-graded granular materials are located above the geotextile, the fines passing through would probably be pumped into the voids of the stone resulting in stone contamination. The load on the aggregates in contact with the geotextile can result in a significant amount of stretching of the fabric and a temporary increase in pore diameter, which allows more fines to pass through. If, however, the geotextile has pores which are too small in diameter or the porosity is too small, clogging can occur, and the geotextile is not self-cleaning.

Self-Cleaning Action. Laboratory tests have shown a change in the direction of flow through a geotextile can cause an increase in its permeability [F-25,F-28]. Hence, partial flushing of fines from a geotextile is apparently possible under conditions of reversing flow. The permeability, however, does not go back to its original value upon flow reversal. Flushing was found by Saxena and Hsu [F-25] to be more effective for heavier, nonwoven geotextiles. Whether self-cleansing can actually occur in the field has not been demonstrated.

Load Repetitions. The quantity of fines migrating upward through a geotextile filter is directly related to the log of the number of load applications [F-7,F-25] as illustrated in Figure F-7. The Soil
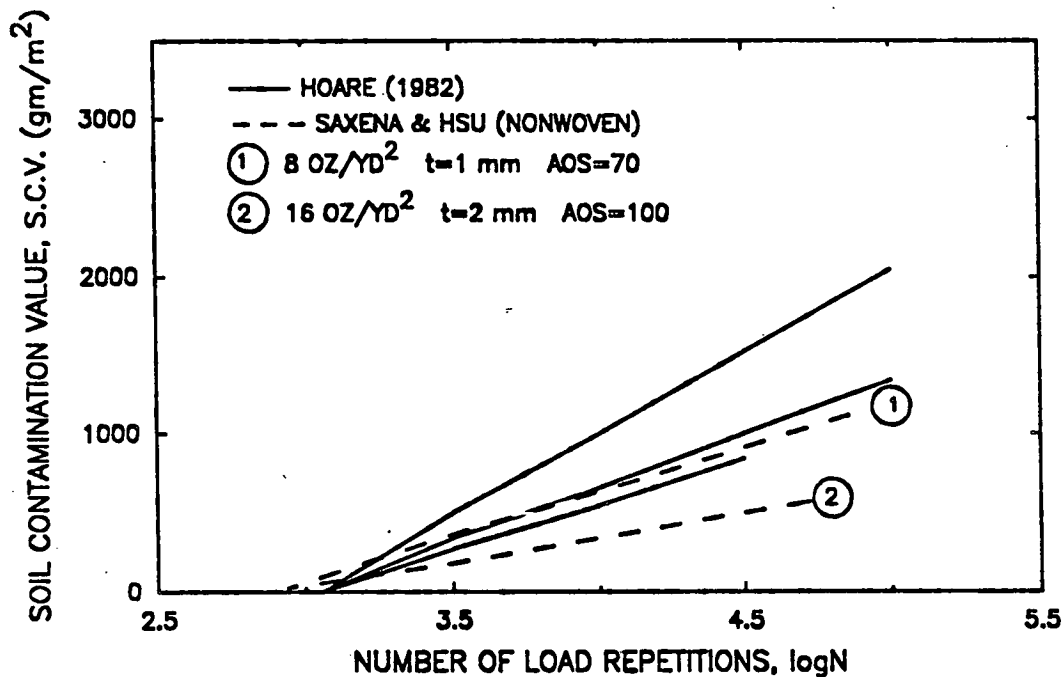
Figure F-7. Variation of Geosynthetic Contamination with Number of
Load Repetitions (After Saxena and Hsu, Ref. F-25).
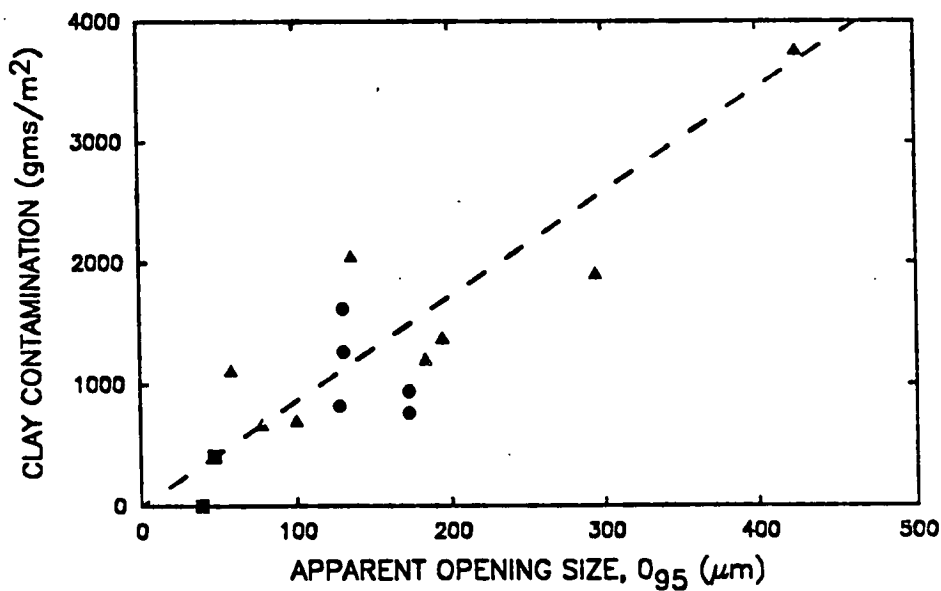
Figure F-8. Variation of Geosynthetic Contamination with Geosynthetic
Apparent Opening Size, O_{95} (After Bell, et al., Ref. F-10).

Contamination Value (SCV) quantifies soil loss through a geotextile. SCV is the weight of soil per unit area passing through the geotextile [F-7].

Apparent Opening Size. The Apparent Opening Size (AOS) quantifies at least approximately the effective pore opening size of a geosynthetic. The apparent opening size (AOS) of a geotextile is defined as the minimum uniform, spherical particle size of a uniform shape that allows 5 percent or less of the particles to pass through the geotextile [F-9]. For a given weight, geotextiles having a small fiber size, and as a result a smaller effective opening, allow less material to be washed through [F-8]. Some general findings by Carroll [F-29] involving AOS as related to geotextile filtration are as follows:

1. The apparent opening size (AOS) of the geotextile cannot be used alone to directly compare the retention ability of a nonwoven and woven geotextile.

2. The AOS measures the maximum "straight through" openings in a woven geotextile. Fabric pore size, pore structure and filtration capacity are not accurately defined by AOS.

3. AOS values can be related to the retention ability of geotextiles provided proper consideration is given to the other significant factors.

4. The uniformity coefficient of the soil being protected has an important influence on the filter criteria.

Also, the AOS of woven monofilaments and nonwoven geotextiles should not in general be compared since they will not have the same filtration efficiency [F-29].

The quantity of fines trapped by the filter layer when subject to cyclic loading generally increases with increasing apparent opening size (AOS) of the filtering media (expressed in units of length and not sieve size) (Figure F-8). In the laboratory tests performed by Bell, et al. [F-10], the least amount of contamination was observed when a thin sand layer was employed compared to the geotextiles tested. The sand layer also had the smallest apparent opening size, as estimated using the method of Schober and Teindl [F-6].

Soil contamination of geotextiles removed from beneath railroad tracks has been reported by Raymond [F-11]. This extensive field study also indicates increasing soil contamination of the geotextile occurs with increasing apparent opening size (AOS) as shown in Figure F-9. As defined in this figure, soil contamination is the percent of soil trapped within the geotextile compared to the uncontaminated dry geotextile weight. Undoubtedly the scatter in data in Figure F-9 is at least partly because soil contamination is not only related to AOS but also to a number of other factors as previously discussed.

Figure F-9 shows results for an alternate definition of AOS based on 95 percent of the uniform particles being retained on the surface of the geotextile [F-30]. As pointed out by Raymond [F-11], this alternate definition is more closely related to classical filter criteria that limits the amount of soil which can enter the filter.

Stress Level. As the applied stress level on the geosynthetic increases, so does the quantity of fines migrating through the geotextile (Figure F-10) and the amount of contamination. Data obtained from field studies (Figure F-11) show that the level of contamination rapidly decreases below a railroad track structure with increasing depth [F-10]. Since the applied

F-25
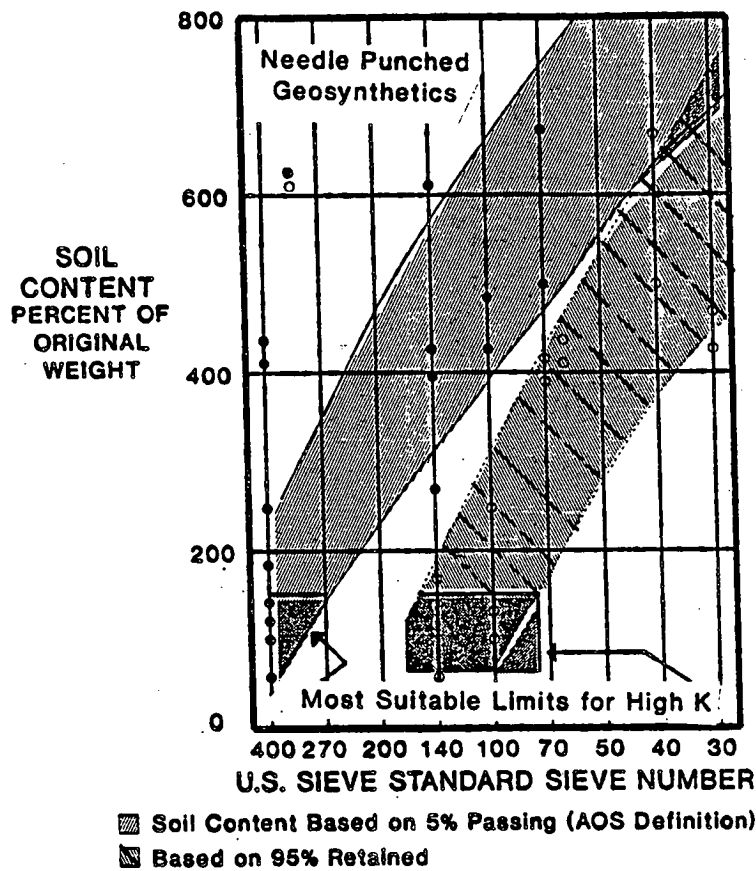
Figure F-9. Variation of Geosynthetic Contamination Approximately 8 in. Below Railroad Ties with Geosynthetic Opening Size (After Raymond, Ref. F-11).
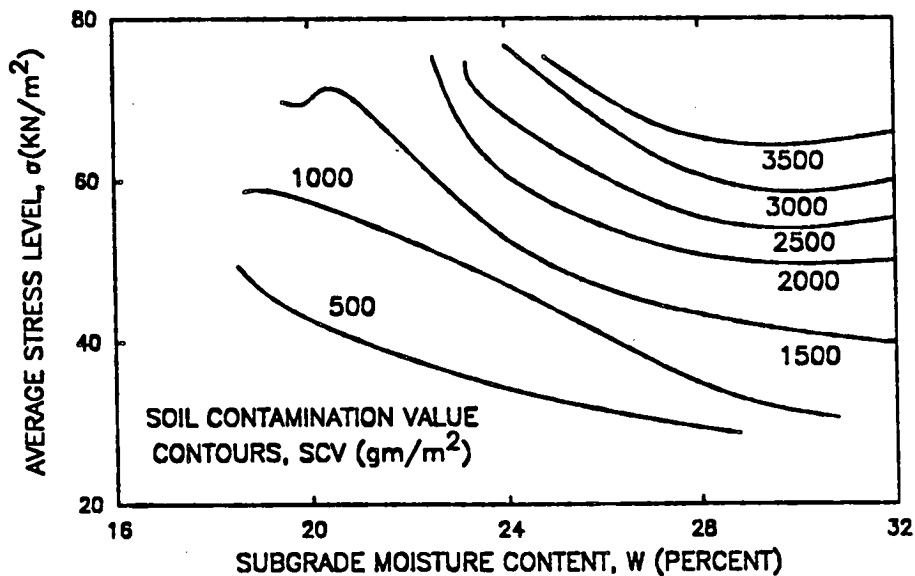
Figure F-10. Variation of Geosynthetic Contamination with Stress Level and Subgrade Moisture (After Glynn & Cochrane, Ref. F-31).

vertical stress also decreases with increasing depth, contamination of a geotextile in the field is indeed dependent upon stress level. The curve relating variation of soil content with depth (Figure F-11) is similar in general shape to a typical vertical stress distribution curve. Loss of integrity of the geotextile due to abrasion and also breakdown of the aggregate may also play an important role in aggregate contamination.

To approximately translate the extensive findings of Raymond [F-10] for geotextiles placed below railroad track installations to pavements, a comparison was made of the vertical stress developed beneath a heavily loaded railroad track with the stress developed at the top of the subgrade for typical pavement sections. Assume 4.5 kip (20 kN) dual wheel loads are applied to the surface of the pavement, and the tires are inflated to 100 psi (0.7 MN/m^2). Let the critical railroad loading be simulated by a fully loaded cement hopper car.

Figure F-12 shows the approximate equivalent depths below the railroad cross-ties that corresponds to the vertical stress at the top of the subgrade for a typical light, medium and heavy highway pavement section. A heavy train loading causes large vertical stresses which spread out slowly with depth. In contrast, vertical stresses from pavement type loadings spread out relatively quickly because of the small diameter of the loaded area.

For railroad track rehabilitation, geotextiles are generally placed at a depth of about 8 to 12 in. (200-300 mm) beneath the tie which corresponds to a vertical stress level on the order of 14 psi (96 kN/m^2). For comparison, typical very light, light, medium and heavy pavement sections (Table F-3) have maximum vertical stresses at the base-subgrade interface on the order of 21, 10, 6 and 3 psi (138, 69, 41, 21 kN/m^2), respectively.
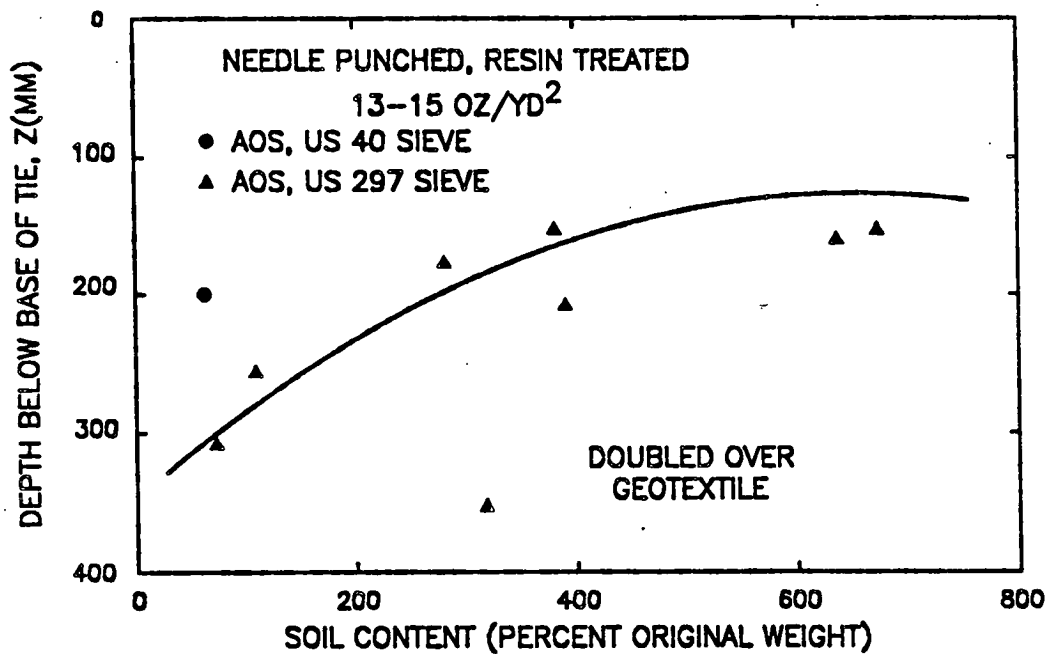
Figure F-11. Observed Variation of Geosynthetic Contamination with Depth Below Railway Ties (After Raymond, Ref. F-11).
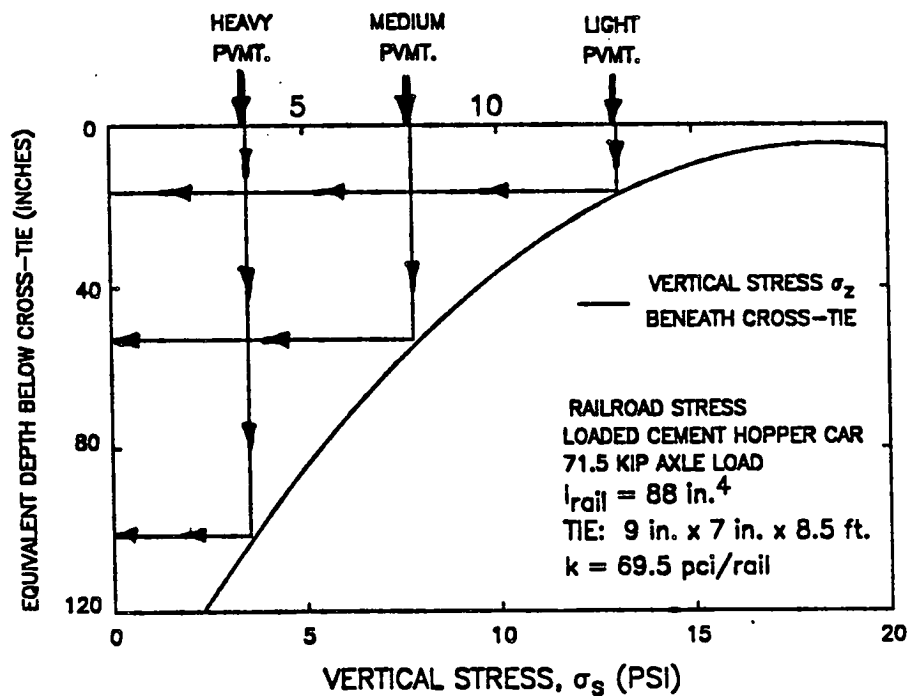
Figure F-12. Variation of Vertical Stress with Depth Beneath Railroad Track and Highway Pavement.

The practical implications of these findings are that (1) the railroad type loading is considerably more severe compared to most structural sections used for pavements, and (2) a highway type pavement should exhibit a wide variation in performance with respect to filtration depending, among other things, upon the thickness and strength of the structural section. Very thin pavement sections are probably subjected to an even more severe vertical stress, and hence more severe infiltration condition, than for a typical railroad ballast installation. In contrast, a heavy structural pavement section would be subjected to a much less severe stress condition.

Laboratory Testing Methods

Laboratory studies to observe the migration of fines through both granular filter layers and geotextile filters have most commonly employed a constant gradient test which simulates steady state, unidirectional seepage conditions [F-7,F-29]. The results obtained from constant gradient tests, which do not use a cyclic load, serve as an upper, possibly unsafe, bound for establishing design criteria for pavement infiltration applications.

Most frequently dynamic testing to simulate pavement conditions has been carried out in cylindrically shaped, rigid cells which may consist of either a steel mold [F-3,F-31,F-32] or a plexiglass cylinder [F-33]. The subgrade soil is generally placed in the bottom of the mold, with the filter layer and base material above. A cyclic loading is then applied to the top of the specimen through a rigid loading platen.

An improved test [F-28] has been developed by Dempsey and Janssen for evaluating the relative effectiveness of different geotextiles (Figure F-13). The test is performed in a triaxial cell at a realistic confining pressure. In contrast to other tests, the subgrade soil is placed on top of the geotextile filter. Water is continuously passed downward through the

F-29
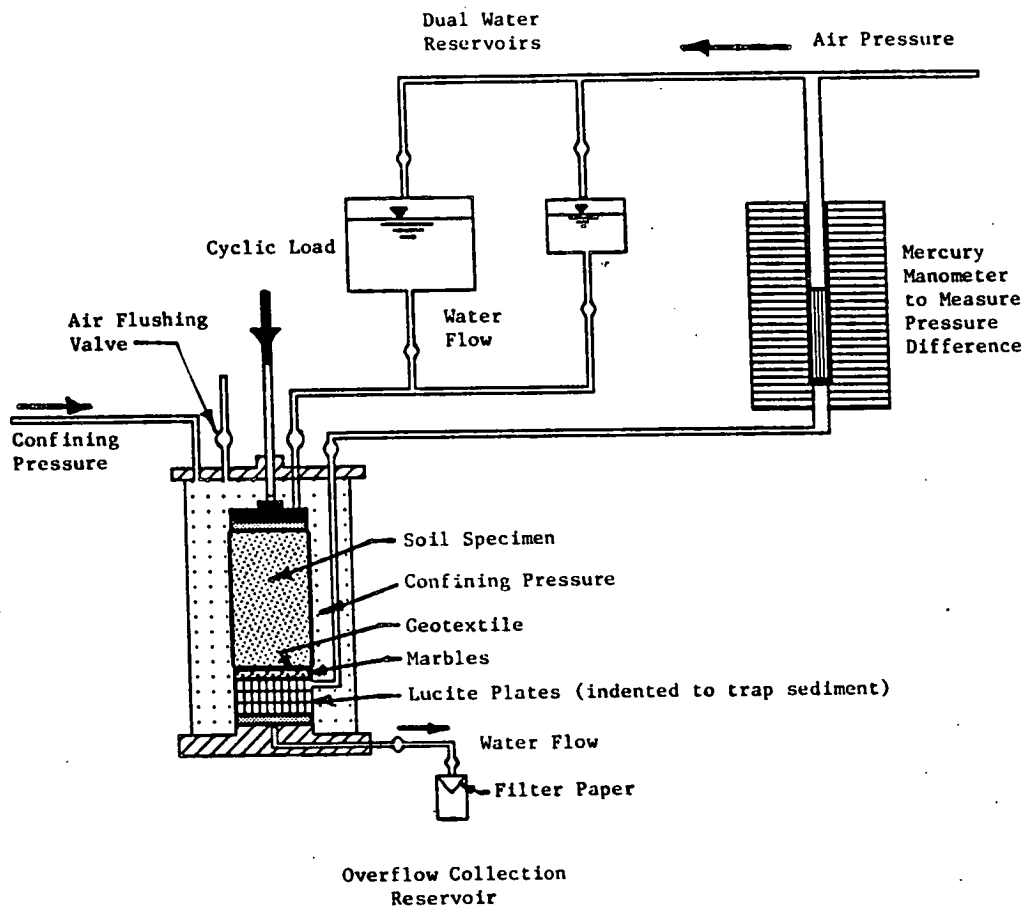
Figure F-13. Cyclic Load Triaxial Apparatus for Performing Filtration Tests (Adapted from Janssen, Ref.F-28).
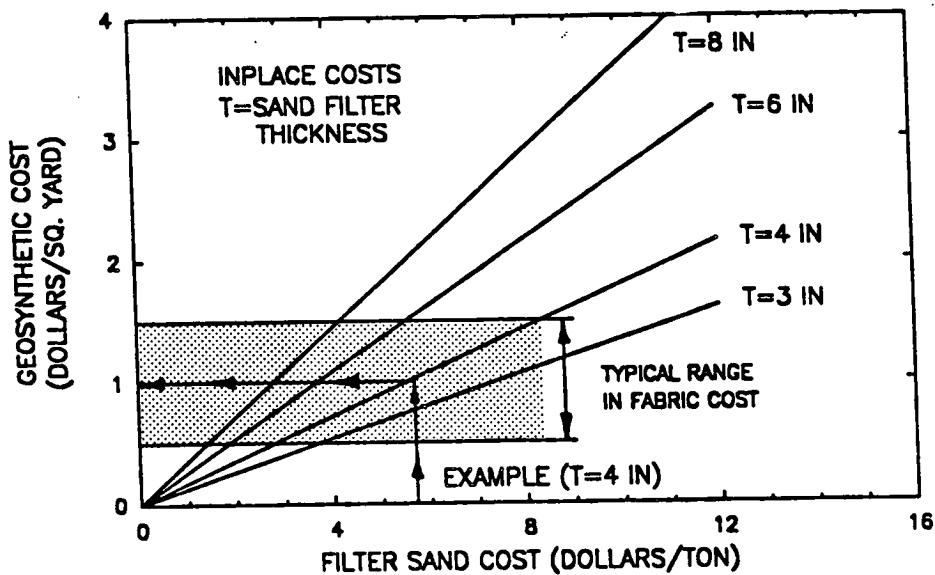
Figure F-14. Economic Comparison of Sand and Geosynthetic Filters for Varying Sand Filter Thickness.

specimen at a constant hydraulic gradient as a repeated loading is applied. The quantity of fines washed through the geotextile is measured, as well as the permeability of the geotextile as a function of load repetitions. To evaluate long-term performance, one million load repetitions are applied.

Dawson [F-5] has pointed out the important need for performing tests at realistic vertical stress levels comparable to those existing in pavements. He also shows that three dimensional pavement tests are more appropriate than the conventional one-dimensional test.

Selected Practices

Task Force 25 Criteria. Over about the last five years Task Force 25 has developed comprehensive specification guidelines for drainage geotextiles. Task Force 25 has representatives from a number of organizations including AASHTO, AGC, ARTBA, universities and the geotextile industry. As a result this task force has a wide range of experience and backgrounds.

Intended applications for the Task Force 25 criteria are as follows: edge of pavement drains, interceptor drains, wall drains, recharge basins, and relief wells. The current version of the Task Force 25 criteria requires that:

> "Fibers used in the manufacture of geotextile, and the
> threads used in joining geotextiles by sewing, shall
> consist of long chain synthetic polymers composed of at
> least 85% by weight polyolefins, polyesters, or
> polyamides. They shall be formed into a network such
> that the filaments or yarns retain dimensional stability
> relative to each other, including selvedges".

Task Force 25 geotextile criteria are summarized in Table F-4.

Corps of Engineers Filter Criteria. For unidirectional, non-turbulent conditions of flow, the Corps of Engineers recommends the criteria show in Table F-5. The Corps [F-34] cautions about using filter materials in inaccessible areas indicating that their use "must be considered carefully."

For fine grained soils having 50 or more percent passing the number 200 sieve, this criteria requires that the AOS generally be between the No. 70 and No. 120 U.S. Standard Sieve. Both woven and non-woven geotextiles are allowed. To permit adequate drainage and to resist clogging, non-woven geotextiles must have a permability greater than 5 times that of the soil. For similar reasons, wovens must have a percent open area greater than 4 percent for soils having 5 to 85 percent passing the number 200 sieve, and greater than 10 percent for soils having less than 5 percent fines.

Pennsylvania DOT Filtration/Separation Practices. The Pennsylvania DOT uses as a standard design an open graded subbase (OGS) to act as a blanket drain (Table F-6). To maintain separation a more densely graded Class 2A stone separation layer is placed beneath the open graded drainage course. If a 6 in (150 mm) thick subbase is used, the two layers are each 3 in. (75 mm) in thickness; if a 12 in. (300 mm) subbase is used the two layers are each 6 in. (150 mm) thick.

An approved geotextile may be substituted for the separation layer. If a geotextile is used, the open graded aggregate drainage layer is placed directly on the geotextile, and is equal in thickness to the full depth of the subbase. The geotextile separator used typically has a weight of about

Table F-4

Recommended Minimum [1] Engineering Fabric Selection Criteria
in Drainage and Filtration Applications – AASHTO–AGG–ARTBA Task Force 25
(After Christopher and Holtz, Ref. F-9)

I. PIPING RESISTANCE (soil retention - all applications)

    A. Soils with 50% or less particles by weight passing U.S. No. 200 Sieve:

          EOS No. (fabric) $\geq$ 30 sieve

    B. Soils with more than 50% particles by weight passing U.S. No. 200 Sieve:

          EOS No. (fabric) $\geq$ 50 sieve

Note:

1. Whenever possible, fabric with the lowest possible EOS No. should be specified.

2. When the protected soil contains particles from 1 inch size to those passing the U.S. No. 200 Sieve, use only the gradation of soil passing the U.S. No. 4 Sieve in selecting the fabric.

II. PERMEABILITY

Critical/Severe Applications*	Normal Applications
k(fabric) $\geq$ 10 k (soil)	k(fabric) $\geq$ k (soil)

* Woven monofilament fabrics only; percent open area > 4.0 and EOS No. $\leq$ 100 sieve.

III. CHEMICAL COMPOSITION REQUIREMENTS/CONSIDERATIONS

    A. Fibers used in the manufacture of civil engineering fabrics shall consist of long chain synthetic polymers, composed of at least 85% by weight of polyolephins, polyesters, or polyamides. These fabrics shall resist deterioration from ultraviolet exposure.

    B. The engineering fabric shall be exposed to ultraviolet radiation (sunlight) for no more than 30 days total in the period of time following manufacture until the fabric is covered with soil, rock, concrete, etc.

IV. PHYSICAL PROPERTY REQUIREMENTS (all fabrics)

	Fabric Unprotected	Fabric Protected [4]
Grab Strength (ASTM D-1682) (Minimum in either principal direction)	180 lbs.	80 lbs.
Puncture Strength (ASTM-D-751-68) [2]	80 lbs.	25 lbs.
Burst Strength (ASTM D-751-68) [3]	290 psi	130 psi
Trapezoid Test (ASTM D-1117) (Any direction)	50 lbs.	25 lbs.

---

[1] All numerical values represent minimum average roll values (i.e., any roll in a lot should meet or exceed the minimum values in the table). Note: these values are normally 20% less than manufacturers typically reported values.

[2] Tension Testing Machines with Ring Clamp, Steel ball replaced with a 5/16 inch diameter solid steel cylinder with hemispherical tip centered within the ring clamp.

[3] Diaphram Test Method

[4] Fabric is said to be protected when used in drainage trenches or beneath/ behind concrete (Portland or asphalt cement) slabs. All other conditions are said to be unprotected. Examples of each condition are:
Protected: highway edge drains, blanket drains, smooth stable trenches < 10 feet in depth. In trenches, in which the aggregate is extra sharp additional puncture resistance may be necessary.
Unprotected: stabilization trenches, interceptor drains on cut slopes, rocky or caving trenches or smooth stable trenches > 10 feet in depth.

Table F-5

U.S. Army Corps of Engineers Geosynthetic Filter Criteria
(Ref.F-34)

Protected Soil (Percent Passing No. 200 Sieve)	Piping [1]	Permeability	
		Woven	Non-Woven
Less than 5% [2]	EOS(mm) $\leq D_{85}$ (mm) [3]	POA $\geq$ 10%	$k_G \geq 5k_S$ [4]
5% to 50% [2]	EOS(mm) $\leq D_{85}$ (mm)	POA $\geq$ 4%	$k_G \geq 5k_S$
50% to 85%	(a) EOS(mm) $\leq D_{85}$ (mm) (b) Upper Limit on EOS is EOS (mm) $\leq$ .212 mm (No. 70 U. S. Standard Sieve)	POA $\geq$ 4%	$k_G \geq 5k_S$
>85%	(a) EOS(mm) $\leq D_{85}$ (mm) (b) Lower Limit on EOS is EOS (mm) $\geq$ .125 mm (No. 120 U. S. Standard Sieve)		$k_G \geq 5k_S$

(1) When the protected soil contains appreciable quantities of material retained on the No. 4 sieve use only the soil passing the No. 4 sieve in selecting the EOS of the geotextile.

(2) These protected soils may have a large permeability and thus the POA or k_G may be a critical design factor.

(3) D_{85} is the grain size in millimeters for which 85 percent of the sample by weight has smaller grains.

(4) k_G is the permeability of the non-woven geotextile and k_S is the permeability of the protected soil.

Table F-6

Aggregate Gradations Used by Pennsylvania DOT For Open-Graded
Drainage Layer (OGS) and Filter Layer (2A)

AASHTO SIEVE	SEPARATION LAYER (2A)	DRAINAGE LAYER (OGS)	
		New Proposal[1]	Old
2	100	100	100
3/4	52-100	52-100	52-100
3/8	36-70	36-65	36-65
#4	24-50	20-40	8-40
#8	16-38	-	-
#16	30-70	3-10	0-12
#30	-	0-5	0-8
#50	-	0-2	-
#200	<10	0-2	<5

Note: 1. Tests indicate the proposed gradation should have
a permeability of about 200 to 400 ft/day.

Table F-7

Separation Number and Severity Classification Based
on Separation/Survivability

BEARING CAPACITY SAFETY FACTOR	GEOTEXTILE SEVERITY CLASSIFICATION			
	Low	Moderate	Severe	Very Severe
1.4 ≤ SF < 2	3,4	2	1	-
1.4 ≤ SF < 1.0	4	3	2	1
SF < 1.0	-	3,4	-	1,2

SEPARATION NUMBER[1], N			
2-4 in. Top Size Aggr., Angular, Uniform (no fines N = 1)	1-2 in. Top Size Aggr., Angular, Uniform (No Fines) N=2	1/2-4 in. Top Size Angular, 1-5% Fines; Well-graded N=3	1/2-2 in. Top Size >5% Fines N=4

1. Rounded gravels can be given a separation number one less than indicated, if desired.

16 oz/yd^2 (380 gm/m^2). It also has the additional mechanical properties: AOS smaller than the No. 70 U.S. Sieve; grab tensile strength $\geq$ 270 lbs (0.3 kN); grab elongation $\geq$ 15 percent; puncture > 110 lbs (0.5 kN); trapezoidal tear strength > 75 lbs (0.3 kN); and an abrasion resistance $\geq$ 40 lbs (0.3 kN).

To exhibit some stability during construction, the open graded base is required to have a minimum of 75 percent crushed particles with at least two faces resulting from fracture. The open graded base must be well graded, and have a uniformity coefficient $C_u = D_{60}/D_{10} \geq 4$. The open graded base is placed using a spreader to minimize segregation.

California DOT. The California DOT allows the use of geotextiles below open graded blanket drains for pavements and also for edge drains. They require for blanket drains a nonwoven geotextile having a minimum weight of 4 oz./yd^2 (95 gm/m^2). In addition, the grab tensile strength must be $\geq$ 100 lbs. (0.4 kN), grab tensile test elongation $\geq$ 30 percent, and the toughness (percent grab elongation times the grab tensile strength) $\geq$ 4000 lbs (18 kN). These geotextile material requirements are in general much less stringent than those used by the Pennsylvania DOT.

New Jersey/University of Illinois. Barenberg, et al. [F-35,F-17,F-36] have performed a comprehensive study of open graded aggregate and bituminous stabilized drainage layers. These studies involved wetting the pavement sections and observing their performance in a circular test track. The subgrade used was a low plasticity silty clay.

These studies indicated good performance can be achieved by placing an open-graded aggregate base over a sand filter, dense-graded aggregate subbase or lime-flyash treated base. In one instance, although the open-

graded drainage layer/sand filter used met conventional static filter
criteria, about 0.5 to 0.75 in. (12-19 mm) of intrusion of sand occurred
into the open-graded base. A significant amount of intrusion of subgrade
soil also occurred into an open-graded control section which was placed
directly on the subgrade. An open-graded bituminous stabilized layer was
found to be an effective drainage layer, but rutted more than the non-
stabilized drainage material.

Lime modifications of the subgrade was also found to give relatively
good performance, particularly with an open-graded base having a finer
gradation. Stone penetration into the lime modified subgrade was
approximately equal to the diameter of the drainage layer stone.

As a result of this study, the New Jersey DOT now uses as standard
practice a non-stabilized, open-graded drainage layer placed over a dense
graded aggregate filter [F-37]. The drainage layer/filter interface is
designed to meet conventional Terzaghi type static filter criteria.

Harsh Railroad Track Environment. The extensive work of Raymond [F-11]
was for geotextiles placed at a shallow depth (typical about 8 to 12 in.;
200-300 mm) below a railroad track structure. This condition constitutes a
very harsh environment including high cyclic stresses and the use of large,
uniformly graded angular aggregate above the geotextile. The findings of
Raymond translates to a very severe condition for the problem of filtration
below a pavement including a thin pavement section.

Well needle punched, resin treated, nonwoven geotextiles were found by
Raymond to perform better than thin heat bonded geotextiles which behaved
similarly to non-wovens. Also, these nonwovens did better than spun bonded
geotextiles having little needling. Abrasion of thick spun bonded
geotextiles caused them not to perform properly either as a separator or as

a filter. Raymond also found the best performing geotextile to be multi-layered, having large tex fibers on the inside and low tex fibers on the outside. Wehr [F-16] concluded that only non-woven, needle bonded geotextiles with loose filament crossings have a sufficiently high elongation to withstand heavy railroad loadings without puncturing.

For the reversible, non-steady flow conditions existing beneath a railway track, heavy, non-woven geotextiles having a low AOS less than 55 μm (U.S. No. 270 sieve size) were found to provide the best resistance to fouling and clogging. Use of a low AOS was also found to insure a large inplane permeability, which provides important lateral drainage.

Raymond [F-11] recommends that at a depth below a railway tie of 12 in. (300 mm) a needle punched geotextile should have a weight of at least 20 oz./yd^2 (480 gm/m^2), and preferably more, for continuous welded rail. A depth of 12 in. (300 mm) in a track structure corresponds approximately to a geosynthetic placed at the subgrade of a pavement having an AASHTO structural number of about 2.75 based on vertical stress considerations (Figure F-12). Approximately extrapolating Raymond's work based on vertical stress indicates for structural numbers greater than about 4 to 4.5, a geosynthetic having a U.S. Sieve No. of about 100 to 140 should result in roughly the same level of contamination and clogging when a large uniformly graded aggregate is placed directly above.

FILTER SELECTION

INTRODUCTION

Factors of particular significance in the use of geotextiles for filtration purposes below a pavement can be summarized as follows [F-6,F-10,F-11,F-29,F-37,F-38]:

1. Pavement Section Strength. The strength of the pavement section placed over the filter/separator determines the applied stresses and resulting pore pressures generated in the subgrade.

2. Subgrade. The type subgrade, existing moisture conditions and undrained shear strength are all important. Low cohesion silts, dispersive clays, and low plasticity clays should be most susceptible to erosion and filtration problems. Full scale field tests by Wehr [F-16] indicate for low plasticity clays and highly compressible silts, that primarily sand and silt erodes into the geotextile.

3. Aggregate Base/Subbase. The top size, angularity and uniformity of the aggregate placed directly over the filter all affect performance. A large, angular uniform drainage layer, for example, constitutes a particularly severe condition when placed over a subgrade.

4. Aggregate Filters. Properly designed sand aggregate filters are superior to geotextiles, particularly under severe conditions of erosion below the pavement [F-3,F-11,F-17,F-31]. Granular filters are thicker than geosynthetics and hence have more three dimensional structural effect.

5. Non-Wovens. Most studies conclude that needle punched, non-woven geotextiles perform better than wovens.

6. Geosynthetic Thickness. Thin (t < 1 mm) non-woven geotextiles do not perform as well as thicker, needle punched non-wovens (t ≥ 2 mm).

7. Apparent Opening Size (AOS). The apparent opening size (AOS) is at least approximately related to the level of base contamination and clogging of the geotextile. Fiber size, fiber structure and also internal pore size are all important.

8. Clogging. In providing filtration protection particularly for silts and clays some contamination and filter clogging is likely to occur. Reductions in permeability of 1/2 to 1/5 are common, and greater reductions occur [F-5,F-8,F-11,F-26,F-39].

9. Strain. For conditions of a very soft to soft subgrade, large strains are locally induced in a geosynthetic when big, uniformly graded aggregates are placed directly above. Wehr [F-16], for example, found strains up to 53 percent were locally developed due to the spreading action of the aggregate when subjected to railroad loads.

GEOTEXTILE

Where possible cyclic laboratory filtration tests should be performed as previously described to evaluate the filtering/clogging potential of

geosynthetic or aggregate filters to be used in specific applications. The filter criteria given in Table F-1 can serve as a preliminary guide in selecting suitable filters for further evaluation. A preliminary classification method is presented for selecting a geosynthetic based on the separation/survivability and filtration functions for use as drainage blankets beneath pavements. Survivability is defined as the ability of the geotextile to maintain its integrity by resisting abrasion and other similar mechanical forces during and after construction.

Separation. The steps for selection of a geosynthetic for separation and survivability are as follows:

1. Estimate from the bottom of Table F-7 the SEPARATION NUMBER N based on the size, gradation and angularity of the aggregate to be placed above the filter.

2. Select from the upper part of Table F-7 the appropriate column which the Separation Number N falls in based on the bearing capacity of the subgrade. Read the SEVERITY CLASSIFICATION from the top of the appropriate column. Figure F-5 provides a simple method for estimating subgrade bearing capacity.

3. Enter Table F-8 with the appropriate geotextile SEVERITY CLASSIFICATION and read off the required minimum geotextile properties.

Where filtration is not of great concern, the requirements on apparent opening size (AOS) can be relaxed to permit the use of geotextiles with U.S. Sieve sizes smaller than the No. 70 (i.e., larger opening size). A layer to maintain a clean interface (separation layer) is not required if the bearing capacity safety factor is greater than 2.0. Also for a Separation Number of 4, an intermediate layer is probably not required if the bearing capacity safety factor is greater than 1.4; and for a SEPARATION NUMBER of 3 or more it is probably not required if the safety factor is greater than about 1.7.

Table F-8

Guide for the Selection of Geotextiles for Separation and Filtration Applications Beneath Pavements

PROPERTY BEING EVALUATED	GEOTEXTILE SEVERITY CLASSIFICATION			
	Low[2]	Moderate[2]	Severe	Very Severe
Geotextile Weight (oz/yd²)	4	6-8	12-16[1]	16-32[1]
Grab Tensile (lbs) ASTM D-1682	100	150	275	400
Grab Tensile Elongation (%) ASTM D-1682	25	40	50	60
Burst Strength (psi) ASTM D3786	140	240	350	500
Puncture (lbs) - ASTM D-751 (Ball Burst) modified using 5/16 in. flat rod	50	75	90	150
Trapezoidal Tear Strength (lbs) ASTM D-1117	40	60	75	80
Abrasion Resistance (lb) ASTM D-1175 and D-1682	40	45	50	55
Apparent Opening Size (AOS) - U.S. Sieve Size [3] Soils with more than 50% passing No. 200 sieve	<70[4]	<100-140[4]	<100-200[4]	<120-400[4]
Permeability (cm/sec) ASTM D-4491-85	$k_g > 10 \ k_{soil}$			
Ultraviolet Degradation at 150 hrs. ASTM D-4355	70% strength retained for all classes			

Notes:
1. Only needle-punched, nonwoven geotextiles should be used for severe and very severe applications.

2. If a woven geotextile is used, the percent open area (POA) should be greater than 3 to 4% for all soils having more than 5% passing the No. 200 sieve. The POA should be greater than 8 to 10%.

3. For coarse grained soils, use the filter criteria given in Table F-1 for reversible flow conditions.

4. Less than U.S. 70 sieve means a similar opening size and hence a larger sieve number.

Both sand filter layers and geotextiles can effectively maintain a clean separation between an open-graded aggregate layer and the subgrade. The choice therefore becomes primarily a matter of economics.

A wide range of both nonwoven and woven geotextiles have been found to work well as just separators [F-3,F-4,F-13,F-16,F-17]. Most geosynthetics when used as a separator will reduce stone penetration and plastic flow [F-31]. The reduction in penetration has, however, been found by Glynn and Cochran [F-31] to be considerably greater for thicker, compressible geotextiles than for thinner ones.

More care is perhaps required for the design of an intermediate aggregate layer to maintain separation than is necessary for the successful use of a geotextile. An intermediate granular layer between the subgrade and base or subbase having a minimum thickness of 3 to 4 in. (75-100 mm) is recommended. Bell, et al. [F-3] found that large 4.5 in. (114 mm) diameter aggregates can punch through a thin, uncompacted 2 in. (50 mm) sand layer into a soft cohesive subgrade.

Finally, excessive permanent subgrade deformations may occur during construction of the aggregate base as a result of loads applied by construction traffic. This potentially important aspect must be considered separately as discussed in the separation section.

Filtration. The geotextile selected based on filtration considerations (i.e., washing of fines from the subgrade into the base or subbase) should also satisfy the previously given requirements for separation/survivability. The suggested steps for selection of a geosynthetic for filtration considerations are as follows:

1. Estimate the pavement structural strength category from Table F-9 based on its AASHTO structural number.

Table F-9

Pavement Structural Strength Categories Based on Vertical
Stress at Top of Subgrade

Category	Approximate Structural Number (SN)	Approximate Vertical Subgrade Stress (psi)
Very Light	<2.5	>14
Light	2.5-3.25	14-9.5
Medium	3.25-4.5	9.5-5
Heavy	>4.5	<5

Table F-10

Partial Filtration Severity Indexes

Pavement Structure		Subgrade Moisture Condition: Partial Index				Susceptibility to Erosion	
Description (1)	SN (2)	Wet Entire Year (3)	Frequently Wet, Wet More Than 3 mo. of Year (4)	Periodically Wet (5)	Rarely Wet (6)	Description[1] (7)	Partial Index (8)
Very Light	<2.5	25	17	9	5	Dispersive clays; very uniform fine cohesion-less sands (PI<6); Micaceous Silty Sands and Sandy Silts	20
Light	2.5-3.25	18	13	7	4	Well-graded cohesion-less gravel-sand-silt mixtures (PI<6); Medium plasticity; Clay binder may be present; Low PI clays	12
Medium	3.25-4.5	13	9	6	3		
Heavy	>4.5	10	7	4	2	Nondispersive clays of high plasticity (PI>25); Coarse sands; Gravels	3

Note: 1. See for example References F-2, F-15, F-20, F-31 for indications of susceptibility to erosion.

2. Add the appropriate Partial Filtration Severity Indexes given in Table F-10 given for the appropriate subgrade moisture condition and pavement structural strength (Add one number from one of columns (3) through (6) to the partial index (one number) given in column (8) corresponding to the subgrade soil present). The addition of these two numbers gives the FILTRATION SEVERITY INDEX.

3. Estimate the filtration SEVERITY CLASSIFICATION as follows:

FILTRATION SEVERITY CLASSIFICATION	FILTRATION INDEX
Very Severe	> 36
Severe	28-35
Moderate	18-27
Low	≤ 17

4. Enter Table F-8 (third row from bottom) with the appropriate FILTRATION SEVERITY CLASSIFICATION , and determine the required filtration characteristics of the geotextile. In making a final geotextile selection good judgment and experience should always be taken into consideration.

The proposed procedures for considering separation, filtration and permanent subgrade deformations during construction are intended to illustrate some of the fundamental parameters of great importance in selecting geotextiles for separation/filtration applications. For example, it has been shown earlier that filtration and contamination levels are significantly influenced by the magnitude of the subgrade stress, number of load repetitions, and subgrade moisture content. Stress level in turn is determined by the strength of the structural section placed above the subgrade. In separation problems important variables include (1) size, gradation and angularity of the aggregate, and (2) subgrade strength and applied stress level at the subgrade. It would seem illogical not to consider these important parameters in selecting a geotextile for use beneath a pavement.

The primary purpose of presenting the proposed procedure for geotextile selection was, hopefully, to encourage engineers to begin thinking in terms of the variables that are known to be significant. The procedures presented were developed during this study using presently available data. For example, the previously presented effects of stress level, number of load repetitions (both of which are related to structural number) and moisture content were used in developing the semi-rational procedures presented here. The interaction between some variables such as stress level and number of load repetitions was through necessity estimated. Nevertheless, it is felt that the proposed procedure, when good judgement and experience is applied, offers a reasonable approach to semi-rationally select a suitable geotextile.

Economics. Figure F-14 can be employed to quickly determine whether a geosynthetic is cheaper to use as a filter or separator than a sand filter layer.

APPENDIX F

REFERENCES

F-1 Cedergren, H.R., and Godfrey, K.A., "Water: Key Cause of Pavement Failure", Civil Engineering, Vol. 44, No. 9, Sept. 1974, pp. 78-82.

F-2 Jorenby, B.N., "Geotextile Use as a Separation Mechanism", Oregon State University, Civil Engineering, TRR84-4, April, 1984, 175 pp.

F-3 Bell, A.I., McCullough, L.M., and Gregory, J., "Clay Contamination in Crushed Rock Highway Subbases", Proceedings, Session Conference on Engineering Materials, NSW, Australia, 1981, pp. 355-365.

F-4 Dawson, A.R., and Brown, S.F., "Geotextiles in Road Foundations", University of Nottingham, Research Report to ICI Fibres Geotextiles Group, September, 1984, 77 p.

F-5 Dawson, A., "The Role of Geotextiles in Controlling Subbase Contamination", Third International Conference on Geotextiles, Vienna, Austria, 1986, pp. 593-598.

F-6 Schober, W., and Teindl, H., "Filter Criteria for Geotextiles", Proceedings, International Conference on Design Parameters in Geotechnical Engineering, Brighton, England, 1979.

F-7 Hoare, D.J., Discussion of "An Experimental Comparison of the Filtration Characteristics of Construction Fabrics Under Dynamic Loading", Geotechnique, Vol. 34, No. 1, 1984, pp. 134-135.

F-8 Heerten, G., and Wittmann, L., "Filtration Properties of Geotextile and Mineral Fillers Related to River and Canal Bank Protection", Geotextiles and Geomembranes, Vol. 2, 1985, pp. 47-63.

F-9 Christopher, B.R., and Holtz, R.D., "Geotextile Engineering Manual", Federal Highway Administration, 1985.

F-10 Bell, A.L., McCullough, L.M., Snaith, M.S., "An Experimental Investigation of Subbase Protection Using Geotextiles", Proceedings, Second International Conference on Geotextiles, Las Vegas, 1978, p. 435-440.

F-11 Raymond, G.P., "Research on Geotextiles for Heavy Haul Railroads", Canadian Geotechnical Journal, Volume 21, 1984, pp. 259-276.

F-12 Ruddock, E.C., Potter, J.F., and McAvoy, A.R., "Report on the Construction and Performance of a Full-Scale Experimental Road at Sandleheath, Hants, CIRCIA, Project Record 245, London, 1982.

F-13 Potter, J.F., and Currer, E.W.H., "The Effect of a Fabric Membrane on the Structural Behavior of a Granular Road", Pavement, Transport and Road Research Laboratory, TRRL Report 996, 1981.

F-14 Sowers, G.F., INTRODUCTORY SOIL MECHANICS AND FOUNDATIONS, MacMillan, New York, 1979 (4th Edition).

F-15 Sherard, J.L., Woodward, R.J., Gizienski, S.F., Clevenger, W.A., "Earth and Earth-Rock Dams", John Wiley, New York, 1963.

F-16 Wehr, H., "Separation Function of Non-Woven Geotextiles in Railway Construction", Proceedings, Third International Conference on Geotextiles, Vienna, Austria, 1986, p. 967-971.

F-17 Barenberg, E.J., and Tayabji, S.D., "Evaluation of Typical Pavement Drainage Systems Using Open-Graded Bituminous Aggregate Mixture Drainage Layers", University of Illinois, Transp. Engr. Series 10, UILU-ENG-74-2009, 1974, 75 p.

F-18 Barksdale, R.D., and Prendergast, J.E., "A Field Study of the Performance of a Tensar Reinforced Haul Road", Final Report, School of Civil Engineering, Georgia Institute of Technology, 1985, 173 p.

F-19 Chamberlain, W.P., and Yoder, E.J., "Effect of Base Course Gradations on Results of Laboratory Pumping Tests", Proceedings, Highway Research Board, 1958.

F-20 Havers, J.A., and Yoder, E.J., "A Study of Interactions of Selected Combinations of Subgrade and Base Course Subjected to Repeated Loading", Proceedings, Highway Research Board, Vol. 36, 1957, pp. 443-478.

F-21 Jurgenson, L., "The Application of Theories of Elasticity and Plasticity to Foundation Engineering", Contributions to Soil Mechanics 1925-194, Boston Society of Civil Engineers, Boston, Mass., pp. 148-183.

F-22 Dempsey, B.J., "Laboratory Investigation and Field Studies of Channeling and Pumping", Transportation Research Board, Transportation Research Record 849, 1982, pp. 1-12.

F-23 Barber, E.S., and Stiffens, G.T., "Pore Pressures in Base Courses", Proceedings, Highway Research Board, Vol. 37, 1958, pp. 468-492.

F-24 Haynes, J.H., and Yoder, E.J., "Effects of Repeated Loading on Gravel and Crushed Stone Base Course Materials Used in AASHO Road Test", Highway Research Board, Research Record 39, 1963, pp. 693-721.

F-25 Saxena, S.K., and Hsu, T.S., "Permeability of Geotextile-Included Railroad Bed Under Repeated Load", Geotextiles and Geomembranes, Vol. 4, 1986, p. 31-51.

F-26 Hoffman, G.L., and Turgeon, R., "Long-Term In Situ Properties of Geotextiles", Transportation Research Board, Transportation Research Record 916, 1983, pp. 89-93.

F-27 Dawson, A.R., and Brown, S.F., "The Effects of Groundwater on Pavement Foundations", 9th European Conf. on Soil Mechanics and Foundation Engineering, Vol. 2, 1987, pp. 657-660.

F-28 Janssen, D.J., "Dynamic Test to Predict Field Behavior of Filter Fabrics Used in Pavement Subdrains", Transportation Research Board, Transportation Research Record 916, Washington, D.C., 1983, pp. 32-37.

F-29 Carroll, R.G., "Geotextile Filter Criteria", Transportation Research Board, Transportation Research Record 916, 1983.

F-30 Gerry, B.S., and Raymond, G.P., "Equivalent Opening Size of Geotextiles", Geotechnical Testing Journal, GTJODJ, Vol. 6, No. 2, June, 1983, pp. 53-63.

F-31 Glynn, D.T., and Cochrane, S.R., "The Behavior of Geotextiles as Separating Membrane on Glacial Till Subgrades", Proceedings, Geosynthetics, 1987, New Orleans, La., February.

F-32 Snaith, M.S., and Bell, A.L., "The Filtration Behavior of Construction Fabrics Under Conditions of Dynamic Loading", Geotechnique, Vol. 28, No. 4, pp. 466-468.

F-33 Bender, D.A., and Barenberg, E.J., "Design and Behavior of Soil-Fabric-Aggregate Systems", Transportation Research Board, Research Record No. 671, 1978, pp. 64-75.

F-34 Office of the Chief, Department of the Army, "Civil Works Construction Guide Specifications for Geotextiles Used as Filters", Civil Works Construction Guide Specification, CW-02215, March, 1986.

F-35 Barenberg, E.J., and Brown, D., "Modeling of Effects of Moisture and Drainage of NJDOT Flexible Pavement Systems", University of Illinois, Dept. of Civil Engineering, Research Report, April, 1981.

F-36 Barenberg, E.J., "Effects of Moisture and Drainage on Behavior and Performance of NJDOT Rigid Pavements", University of Illinois, Dept. of Civil Engineering, Research Report, July, 1982.

F-37 Kozlov, G.S., "Improved Drainage and Frost Action Criteria for New Jersey Pavement Design", Vol. III, New Jersey Dept. of Transportation Report No. 84-015-7740, March, 1984, 150 p.

F-38 Sherard, J.L., Dunnigan, L.P., and Decker, R.S., "Identification and Nature of Dispersive Soils", Proceedings, ASCE, Vol. 102, GT4, April, 1976, pp. 287-301.

F-39 Christopher, B.R., "Evaluation of Two Geotextile Installations in Excess of a Decade Old", Transportation Research Board, Transportation Research Record 916, 1983, pp. 79-88.

APPENDIX G

DURABILITY

APPENDIX G

DURABILITY

PAVEMENT APPLICATIONS

The commonly used geosynthetics can be divided into two general groups:
(1) the polyolefins, which are known primarily as polypropylenes and
polyethylenes, and (2) the polyesters. Their observed long-term durabiilty
performance when buried in the field is summarized in this section.

Most flexible pavements are designed for a life of about 20 to 25
years. Considering possible future pavement rehabilitation, the overall
life may be as great as 40 years or more. When a geosynthetic is used as
reinforcement for a permanent pavement, a high level of stiffness must be
maintained over a large number of environmental cycles and load repetitions.
The geosynthetic, except when used for moderate and severe separation
applications, is subjected to forces that should not in general exceed about
40 to 60 lb/in. (7-10 kN/m); usually these forces will be less. The
strength of a stiff to very stiff geosynthetic, which should be used for
pavement reinforcement applications, is generally significantly greater than
required. Therefore, maintaining a high strength over a period of time for
reinforcement would appear not to be as important as retaining the stiffness
of the geosynthetic. For severe separation applications, maintaining
strength and ductility would be more important than for most pavement
reinforcement applications.

Most mechanical properties of geosynthetics such as grab strength,
burst strength and tenacity will gradually decrease with time when buried
beneath a pavement. The rate at which the loss occurs, however, can vary
greatly between the various polymer groups or even within a group depending

upon the specific polymer characteristics such as molecular weight, chainbranching, additives, and the specific manufacturing process employed. Also, the durability properties of the individual fibers may be significantly different than the durability of the geosynthetic manufactured from the fibers.

Stiffness in some instances has been observed by Hoffman and Turgeon [G-1] and Christopher [G-2] to become greater as the geosynthetic becomes more brittle with age. As a result, the ability of the geosynthetic to act as a reinforcement might improve with time for some polymer groups, as long as a safe working stress of the geosynthetic is not exceeded as the strength decreases. Whether some geosynthetics actually become a more effective reinforcement with time has not been shown.

Changes in mechanical properties with time occur through very complex interactions between the soil, geosynthetic and its environment and are caused by a number of factors including:

1. Chemical reactions resulting from chemicals in the soil
    - in which it is buried, or from chemicals having an
    external origin such as diesel fuel, chemical pollutants
    or fertilizers from agricultural applications.

2. Sustained stress acting on the geosynthetic which
    through the mechanism of environmental stress cracking
    can significantly accelerate degradation due to chemical
    micro-organisms and light mechanisms.

3. Micro-organisms.

4. Aging by ultraviolet light before installation.

Some general characteristics of polymers are summarized in Table G-1 and some specific advantages and disadvantages are given in Table G-2.

General Environmental Characteristics of Selected Polymers

Polymer (Thermoplastic composition)	Environmental factor												
	Dry heat (melting)	Steam	Moisture absorption	Acids	Alkalis	Fungus Vermin Insects	Brine	Mineral oil	Aviation fuel	Glycol	Detergents	UV Light Un-stabilized	UV Light Stabilized
Polyester													
Polyamide													
Polyethylene													
Polypropylene													

Resistance to factor specified: Low [ ] Moderate [////] High [XXXX] Very high [████]

Summary of Mechanisms of Deterioration, Advantages and Disadvantages of Polyethylene, Polypropylene and Polyester Polymers[1]

POLYMER TYPE	MECHANISMS OF DETERIORATION	GENERAL ADVANTAGES	IMPORTANT DISADVANTAGES
Polyethylene	Environmental stress cracking catalized by an oxidizing environment; Oxidation Adsorption of Liquid Anti-oxidants usually added	Good resistance to low pH environments Good resistance to fuels	Susceptible to creep and stress relaxation; environmental stress Degradation due to oxidation catalized by heavy metals - iron, copper, zinc, manganese Degradation in strong alkaline environment such as concrete, lime and fertilizers
Polypropylene	Environmental stress cracking catalized by (2) an oxidizing environment; Oxidation; Adsorption of Liquid; Anti-oxidants usually added	Good resistance to low and high pH environments	Susceptible to creep and stress relaxation; Environmental stress cracking Degradation due to oxidation catalized by heavy metals - iron, copper, zinc, manganese, etc. May be attacked by hydrocarbons such as fuels with time
Polyester	Hydrolysis - takes on water	Good creep and stress relaxation properties	Attacked by strong alkaline environment

Notes: 1. Physical properties in general should be evaluated of the geosynthetic which can have different properties than the fibers.
2. Environmental stress cracking is adversely affected by the presence of stress risers and residual stress.

SOIL BURIAL

Full validation of the ability of a geosynthetic used as a reinforcement to withstand the detrimental effects of a soil environment can only be obtained by placing a geosynthetic in the ground for at least three to five years and preferably ten years or more. One study has indicated that the strength of some geosynthetics might increase after about the first year of burial [G-1], but gradually decrease thereafter. The geosynthetic should be stressed to a level comparable to that which would exist in the actual installation.

Relatively little of this type data presently exists. Translation of durability performance data from one environment to another, and from one geosynthetic to another is almost impossible due to the very complex interaction of polymer structure and environment. Different environments including pH, wet-dry cycles, heavy metals present, and chemical pollutants will have significantly different effects on various geosynthetics. In evaluating a geosynthetic for use in a particular environment, the basic mechanisms affecting degradation for each material under consideration must be understood.

Long-term burial tests should be performed on the actual geosynthetic rather than the individual fibers from which it is made. The reduction in fiber tensile strength in one series of burial tests was found by Sotten [G-3] to be less than ten percent. The overall strength loss of the geotextile was up to 30 percent. Hence, geosynthetic structure and bonding can have an important effect on overall geosynthetic durability which has also been observed in other studies [G-4].

Hoffman and Turgeon [G-1] have reported the change in grab strength with time over 6 years. After six years the nonwoven polyester geotextile

G-5

studied exhibited no loss in strength in the machine direction (a 26 percent strength loss was observed in the cross-direction). The four polypropylenes exhibited losses of strength varying from 2 to 45 percent (machine direction). All geotextiles (except one nonwoven polypropylene) underwent a decrease in average elongation at failure varying up to 32 percent; hence these geotextiles became stiffer with time. Since the geosynthetics were used as edge drains, they were not subjected to any significant level of stress during the study.

After one year of burial in peat, no loss in strength was observed for a polypropylene, but polyester and nylon 6.6 geotextiles lost about 30 percent of their strength [G-5]. In apparent contradiction to this study, geosynthetics exposed for at least seven years showed average tenacity losses of 5 percent for polyethylene, 15 percent for nylon 6.6, and 30 percent for polypropylene. Slit tape polypropylenes placed in aerated, moving seawater were found to undergo a leaching out of anti-oxidants if the tape is less than about eight microns thick [G-6]. Table G-3 shows for these conditions the important effects that anti-oxidants, metals and condition of submergence can have on the life of a polypropylene. Alternating cycles of wetting and drying were found to be particularly severe compared to other conditions.

Burial tests for up to seven years on spunbonded, needle-punched nonwoven geotextiles were conducted by Colin, et al. [G-7]. The test specimens consisted of monofilaments of polypropylene, polyethylene and a mixture of polypropylene and polyamide-coated polypropylene filaments. The geotextiles were buried in a highly organic, moist soil having a pH of 6.7. Temperature was held constant at 20°C. A statistically significant decrease in burst strength was not observed over the seven year period for any of the

Table G-3. Effect of Environment on the Life of a Polypropylene
(After Wrigley, Ref. G-6).

Polypropylene Fabric at an Average Temperature of 10°C		Minimum Expected Lifetime in Maritime Applications, Including Some Steep in Lye	
		Normal Anti-Oxidant	'Low Leach' Anti-Oxidant
Total Under Water	With Metal Influence	60-100 yrs.	400-600 yrs.
	Without Metal Influence	200 yrs.	1200 yrs.
Half Wet/ Half Dry	With Metal Influence	30-50 yrs.	200-300 yrs.
	Without Metal Influence	100 yrs.	600 yrs.

samples. One polypropylene geotextile did indicate a nine percent average loss of burst strength.

When exposed to a combination of HCL, NaOH, sunlight and burial, polyester nonwovens were found to be quite susceptible to degradation, showing strength losses of 43 to 67 percent for the polyesters compared to 12 percent for polypropylene [G-8]. Polyester and polyproylene, when buried for up to 32 months, did not undergo any significant loss of mechanical properties [G-9]. Both low and high density polyethylene, however, became embrittled during this time. Stabilizers were not used, however, in any of these materials.

Schneider [G-8] indicates geotextiles buried in one study for between four months and seven years, when subjected to stress in the field, underwent from five to as much as seventy percent loss in mechanical properties. The loss of tenacity of a number of geotextiles buried under varying conditions for up to ten years in France and Austria has been summarized by Schneider [G-8]. Typically the better performing geotextiles lost about 15 percent of their strength after five years, and about 30 percent after ten years of burial.

Summary of Test Results. Scatter diagrams showing observed long-term loss of strength as a function time are given in Figure G-1 primarily for polyproylene and polyester geotextiles. This data was obtained from numerous sources including [G-1,G-2,G-7,G-8,G-10]. The level of significance of the data was generally very low except for the nonwoven polypropylene geotextiles where it was 73 percent. Confidence limits, which admittedly are rather crude for this data, are given on the figures for the 80 and 95 percent levels.
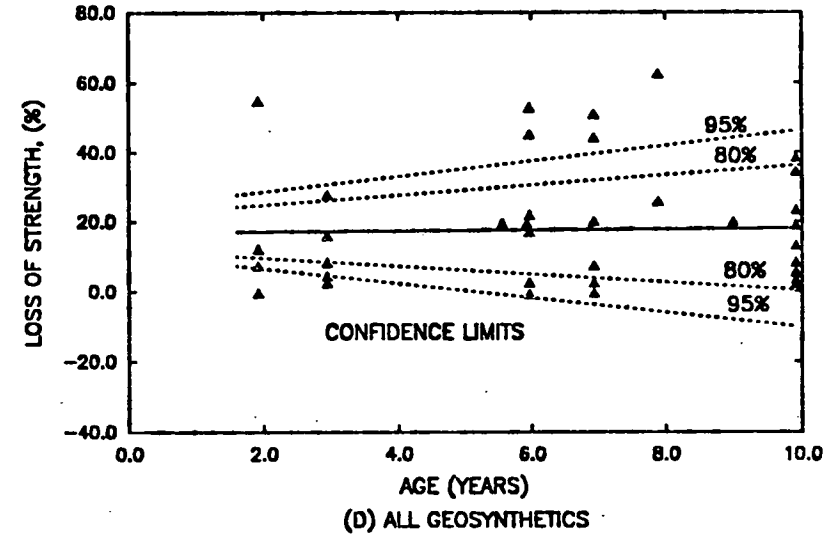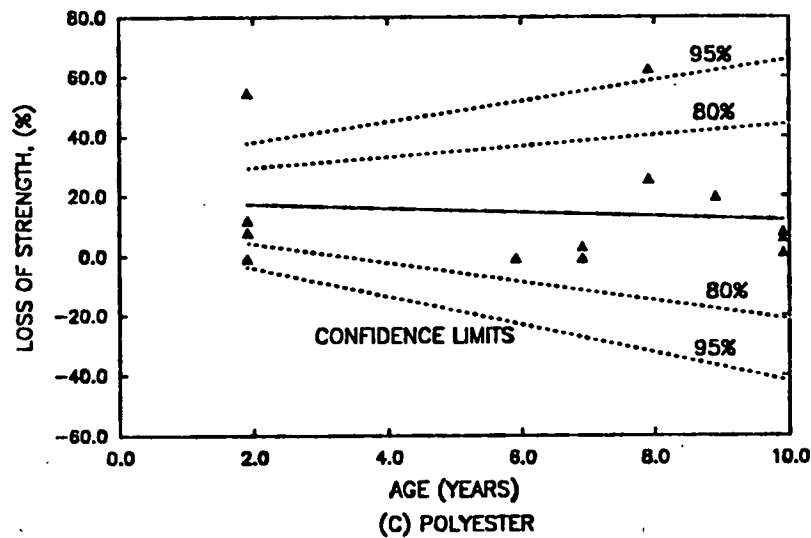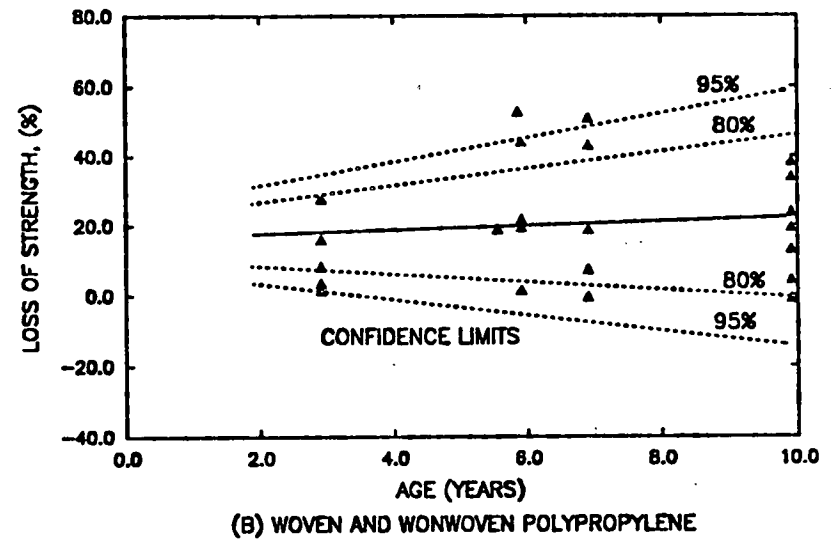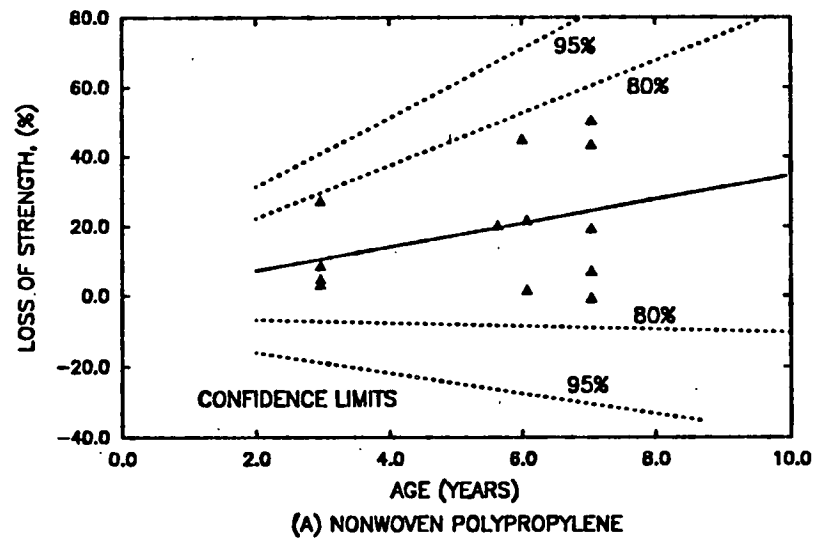
Figure G-1. Observed Strength Loss of Geosynthetics with Time.

In these comparisons, loss of strength was measured by a number of different tests including burst strength, grab strength and tenacity. The wide range of geosynthetics, test methods and environments included in this data undoubtedly account for at least some of the large scatter and poor statistical correlations found. As a result, only general trends should be observed from the data. The results indicate after 10 years the typical reduction in strength of a polypropylene or polyester geotextile should be about 20 percent; the 80 percent confidence limit indicates a strength loss of about 30 percent. With two exceptions, the polyester geosynthetics showed long-term performance behavior comparable to the polypropylenes.

APPENDIX G

REFERENCES

G-1 Hoffman, G.L., and Turgeon, R., "Long-Term In Situ Properties of Geotextiles", Transportation Research Board, Transportation Research Record 916, 1983, pp. 89-93.

G-2 Christopher, B.R., "Evaluation of Two Geotextile Installations in Excess of a Decade Old", Transportation Research Board, Transportation Research Record 916, 1983, pp. 79-88.

G-3 Sotton, M., "Long-Term Durability", Nonwovens for Technical Applications (EDANA), Index 81, Congress Papers, Brussels, 1981, 16,19.

G-4 Strobeck, G.W., Correspondence and Unpublished Report, Phillips Fibers Corp., Seneca, S.C., August, 1986.

G-5 Barsvary, A.K., and McLean, M.D., "Instrumented Case Histories of Fabric Reinforced Embankments over Peat Deposits", Proceedings, Second International Conference on Geotextiles, Vol. III, Las Vegas, 1982, pp. 647-652.

G-6 Wrigley, N.E., "The Durability of Tensar Geogrids", Netlon Limited, Draft Report, England, May, 1986.

G-7 Colin, G., Mitton, M.T., Carlsson, D.J., and Wiles, D.M., "The Effect of Soil Burial Exposure on Some Geotechnical Fabrics", Geotextiles and Geomembranes, Vol. 3, 1986, pp. 77-84.

G-8 Schneider, H., "Durability of Geotextiles", Proceedings, Conference on Geotextiles, Singapore, May, 1985, pp. 60-75.

G-9 Colin, G., Cooney, J.D., Carlsson, D.J., and Wiles, D.M., Journal of Applied Polymer Science, Vol. 26, 1981, p. 509.

G-10 Sotton, M., LeClerc, B., Paute, J.L., and Fayoux, D., "Some Answers Components on Durability Problem of Geotextiles", Proceedings, Second International Conference on Geotextiles, Vol. III, Las Vegas, August, 1982, pp. 553-558.

APPENDIX H

PRELIMINARY EXPERIMENTAL PLAN FOR FULL-SCALE FIELD TEST SECTIONS

APPENDIX H

PRELIMINARY EXPERIMENTAL PLAN FOR FULL-SCALE FIELD TEST SECTIONS

INTRODUCTION

An experimental plan is presented for evaluating in the field the improvement in pavement performance that can be achieved from the more promising techniques identified during the NCHRP 10-33 project. These methods of improvement are as follows:

1. <u>Prerutting</u> the unstabilized aggregate base without reinforcement.

2. <u>Geogrid Reinforcement</u> of the unstabilized aggregate base. The minimum stiffness of the geogrid should be $S_g = 1500$ lbs/in. (260 kN/m).

Prestressing was also found to give similar reductions in permanent deformations of the base and subgrade as prerutting. Because of the high cost of prestressing, however, a prestressed test section was not directly included in the proposed experiment. If desired, it could be readily added to the test program as pointed out in the discussion. The inclusion of a non-woven geosynthetic reinforced section would be a possibility if sufficient funds and space are available to compare its performance with the geogrid reinforcement proposed. The stiffness of the geotextile should be at least 1500 lbs/in. (260 kN/m) and preferably 3000 to 4000 lbs/in. (500-700 kN/m).

TEST SECTIONS

The layout of the ten test sections proposed for the experiment are shown in Figure H-1. The experiment is divided into two parts involving (1) five test sections constructed using a high quality aggregate base, and (2)

10 Sections @ 100 ft. Each (not including transitions)

Low Quality Aggregate Base | High Quality Aggregate Base

⑩	⑨	⑧	⑦	⑥	⑤	④	③	②	①
PR	R	C	PR	PR	PR	C	R	R	PR

4.5 in.

8 in.

2.5 in.

10 in.

Soft Subgrade CBR ≅ 2.5
(CBR of 3 maximum)

Notation: PR = prerutted section
          C = control section
          R = geogrid reinforced section
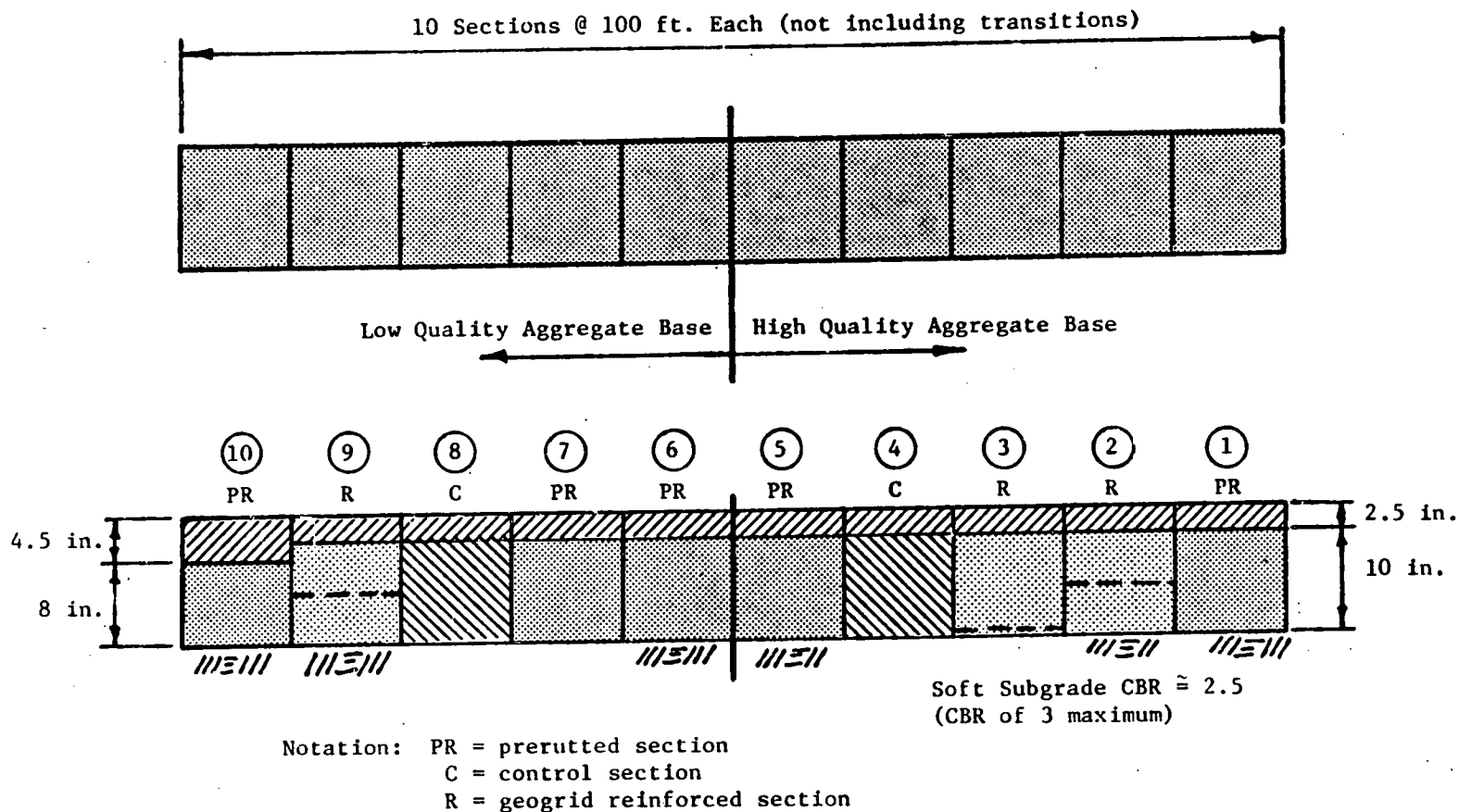
Figure H-1. Tentative Layout of Proposed Experimental Plan –
            Use of Longer Sections and More Variables are
            Encouraged.

five test sections constructed using a low quality aggregate base susceptible to rutting. A control section is included as one of the test sections for each base type.

All test sections, except Section 10, are to be constructed using a 2.5 in. (64 mm) asphalt concrete surfacing and a 10 in. (250 mm) unstabilized aggregate base. Test Section 10, which is to be prerutted, is to have a 4.5 in. (114 mm) thick asphalt surfacing and an 8 in. (200 mm) low quality aggregate base. Although not shown, it would be quite desirable to include a companion control section. An even stronger structural section might be included in the experiment if sufficient space and funds are available. Also, use of a geogrid and nonwoven fabric together could be studied to provide reinforcement, separation and filtration capability.

Test Sections 1 to 5 should be placed over a soft subgrade having a CBR of about 2.5 to 3.0 percent. Extensive vane shear, cone penetrometer or standard penetration resistance tests should be conducted within the subgrade at close intervals in each wheel track of the test sections. The purpose of these tests is to establish the variability of the subgrade between each section.

The test sections should be a minimum of 100 ft. (32 m) in length with a transition at least 25 ft. (8 m) in length between each section. Longer test sections are encouraged. The high quality base experiment could be placed on one side of the pavement and the low quality base experiment on the other to conserve space.

A careful quality control program should be conducted to insure uniform, high quality construction is achieved for each test section. Measurements should also be made to establish as-constructed thicknesses of each layer of the test sections. A Falling Weight Deflectometer (FWD),

device, should be used to evaluate the as-constructed stiffness of each section. The reinforced sections should have similar stiffnesses to the control sections. The FWD tests will serve as an important indicator of any variation in pavement strength between test sections.

High Quality Base Sections. Two prerutted sections and two reinforced sections are included in the high quality base experiment. The high quality base section study is designed to investigate the best pattern to use for prerutting, number of passes required, and the optimum position for geosynthetic reinforcement. Prerutting would be carried out for an aggregate base thickness of about 7 in. (180 mm). After prerutting, additional aggregate would be added to bring the base to final grade, and then densified again by a vibratory roller. Prerutting would be accomplished in Test Section 1 by forming two wheel ruts in each side of the single lane test section. The ruts would be about 12 in. (200-300 mm) apart. A heavy vehicle having single tires on each axle should be used. In Section 5, which is also prerutted, a single rut should be formed in each side of the lane. In each test section, prerutting should be continued until a rut depth of approximately 2 in. (50 mm) is developed. Optimum depth of prerutting is studied in the low quality base experiment; it could also be included in this study.

Sections 2 and 3 have geogrid reinforcement at the center and bottom of the base, respectively. The minimum stiffness of the geogrid should be $S_g = 1500$ lbs/in. (260 kN/m). If desired, Section 2 could be prestressed.

Low Quality Base Section. This experiment is included in the study to establish, in the field, the improvement in performance that can be obtained by either prerutting or reinforcing a low quality base. A good subgrade

could be used rather than a weak one for this experiment.

Two prerutted sections are included in the study to allow determination of the influence of prerut depth on performance. Section 6 should be prerutted to a depth of about 1.5-2 in. (37-50 mm), while Section 7 should be prerutted to a depth of about 3 in. (90 mm).

In Section 9 a geogrid reinforcement (S_g > 1500 lbs/in.; 260 kN/m) would be placed at the center of the base. Section 10 is included in the experiment to determine whether or not improved performance due to prerutting is obtained for heavier pavement sections.

MEASUREMENTS

The primary indicators of pavement test section performance are surface rutting and fatigue cracking. Both of these variables should be carefully measured periodically throughout the study. Use of a surface profilometer, similar to the one described in Appendix D, is recommended in addition to the manual measurement of rut depth.

Much valuable information can be gained through a carefully designed instrumentation program demonstrated during the experiments conducted as a part of this study. Such a program is therefore recommended. The instrumentation layout for one test section should be similar to that shown in Figure H-2. In general, a duplicate set of instruments is provided to allow for instrumentation loss during installation and instrument malfunction.

The following instrumentation should be used for each test section. Inductance Bison strain coils should be employed to measure both permanent and resilient deformations in each layer (Figure H-2). At least one pair of strain coils (preferably two) should be placed in the bottom of the aggregate base to measure lateral tensile strain. Two pressure cells should
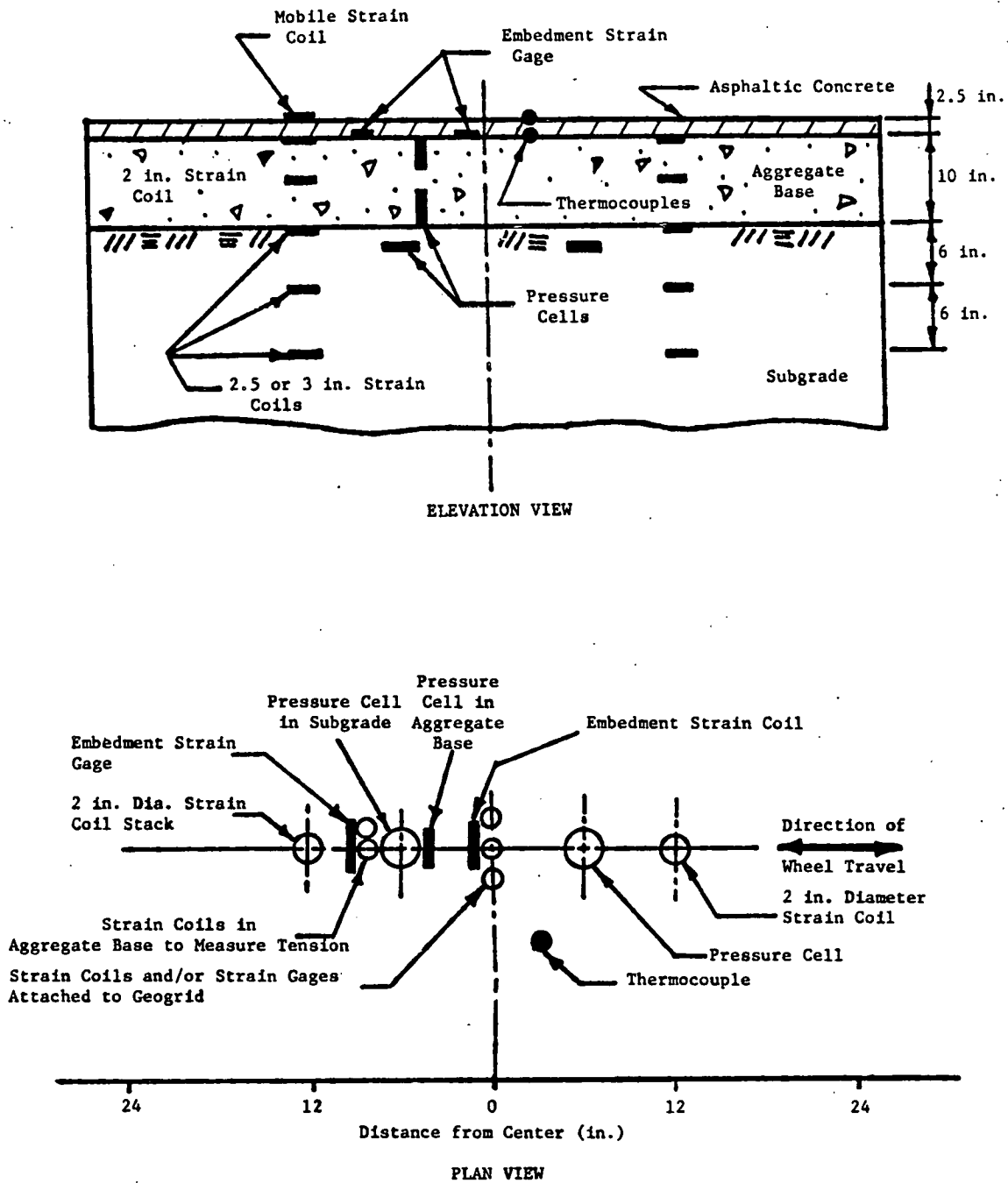
ELEVATION VIEW

Mobile Strain Coil
Embedment Strain Gage
Asphaltic Concrete — 2.5 in.
2 in. Strain Coil
10 in.
Aggregate Base
Thermocouples
6 in.
Pressure Cells
6 in.
2.5 or 3 in. Strain Coils
Subgrade

Pressure Cell in Subgrade
Pressure Cell in Aggregate Base
Embedment Strain Coil
Embedment Strain Gage
2 in. Dia. Strain Coil Stack
Direction of Wheel Travel
2 in. Diameter Strain Coil
Strain Coils in Aggregate Base to Measure Tension
Pressure Cell
Strain Coils and/or Strain Gages Attached to Geogrid
Thermocouple

| 24 | 12 | 0 | 12 | 24 |

Distance from Center (in.)

PLAN VIEW

Figure H-2. Preliminary Instrument Plan for Each Test Section.

H-7

be used to measure vertical stress on top of the subgrade. Although quite desirable, the two vertically oriented pressure cells in the base shown in Figure H-2 could be omitted for reasons of economy. In addition to using strain coils, wire resistance strain gages should also be employed to directly measure strain in the geogrid reinforcement.

Tensile strain in the bottom of the asphalt concrete should be measured using embedment type wire resistance strain gages. The embedment gages should be oriented perpendicular to the direction of the traffic.

Thermocouples for measuring temperature should be placed in each section, and measurements made each time readings are taken. Placement of moisture gages in the subgrade would also be desirable.

MATERIAL PROPERTIES

The following laboratory material properties should as a minimum be evaluated as a part of the materials evaluation program:

1. Mix design characteristics of the asphalt concrete surfacing.

2. Resilient and permanent deformation characteristics of the low and high quality aggregate base and also of the subgrade.

3. Shear strength and water content of the subgrade beneath each test sections.

4. Stress-strain and strength of the geogrid reinforcement as determined by a wide width tension test.

5. Friction characteristics of the geogrid reinforcement as determined by a direct shear test.